FERMILAB-CONF-xx
SLAC-PUB-xx

The Future of US Particle Physics

Report of the 2021 US Community Study on the Future of Particle Physics organized by the APS Division of Particles and Fields

Study Conveners: M. Artuso, K. Assamagan, P. Barbeau, L. Baudis, R. Berstein, A. Chou, N. Craig, C. Csaki, A. El-Khadra, S. Gourlay, S. Gottlieb, O. Gutsche, J. Hall, P. Huber, K. Lesko, P. Merkel, M. Narain, B. Nachman, J. Orrell, A. Petrov, B. Quinn, T. Raubenheimer, L. Reina, K. Scholberg, V. Shiltsev, M. Soares-Santos, T. M. P. Tait, A. Tricoli, E. Worcester, J. Zhang

Division of Particles and Fields Chairs during the study: P. Cushman (2019 chair), Y.-K. Kim (2020 chair), T. Han (2021 chair), J. Butler (2022 chair), Sekhar Chivukula (2023 chair)

Editorial Committee: R. H. Bernstein, S. Chekanov, M. E. Peskin, (others to be added)

Contents

1 Summary of the 2021 US Community Study on the Future of Particle Physics 1

2 Energy Frontier v2.3.6 (July 22, 2022) 5

2.1 Big Questions in the Energy Frontier . . . 5

2.2 How to Connect Fundamental Questions to Energy Frontier Colliders: Energy & Precision . 9

2.3 Electroweak Sector of the Standard Model . . . 14

2.3.1 Higgs and BSM physics . . . 14

2.3.1.1 Higgs present and future . . . 16

2.3.1.2 What can we learn about BSM physics from Higgs physics . . . 25

2.3.2 Heavy-flavor and top quark production . . . 28

2.3.2.1 Top-quark mass . . . 29

2.3.2.2 Top-quark production processes . . . 30

2.3.2.3 Angular correlations . . . 32

2.3.2.4 BSM physics from top physics . . . 33

2.3.2.5 Heavy-flavor and top quark production summary . . . 34

2.3.3 Electroweak precision physics and new physics constraints . . . 36

2.3.3.1 Electroweak precision physics . . . 36

2.3.4 EFT and new physics . . . 40

2.3.4.1 Multi-boson processes . . . 40

2.3.4.2 SMEFT global fits . . . 40

2.4 QCD and Strong Interactions . . . 45

2.4.1 Perturbative QCD . . . 46

2.4.1.1 Precision Calculations . . . 46

2.4.1.2 Strong Coupling . . . 48

2.4.1.3 Jet Substructure . . . 49

2.4.1.4 New Observables . . . 49

2.4.2 Non-perturbative QCD . . . 50
2.4.2.1 Parton distribution functions in the nucleon . . . 50
2.4.2.2 Predicting hadron structure in lattice QCD . . . 52
2.4.2.3 Hadronization and Fragmentation Functions . . . 53
2.4.3 Forward Physics . . . 54
2.4.3.1 Diffraction . . . 54
2.4.3.2 Physics opportunities at the CERN Forward Physics Facility . . . 55
2.4.3.3 Neutrino-Induced Deep Inelastic Scattering . . . 55
2.4.4 Heavy Ions . . . 56
2.4.4.1 Hard Probes . . . 56
2.4.4.2 Hadronic Structure . . . 57
2.4.4.3 Collective Phenomena . . . 57
2.4.4.4 Photon-Nuclear Collisions . . . 58
2.4.5 Cross-Cutting QCD . . . 58
2.4.5.1 Comprehensive uncertainty estimates . . . 59
2.4.5.2 QCD in new physics searches and SM EFT fits . . . 59
2.4.5.3 Photon–Photon Scattering . . . 60
2.4.5.4 Detectors and QCD theory for FCC-hh . . . 60
2.5 The physics beyond the Standard Model . . . 62
2.5.1 Composite Higgs . . . 63
2.5.2 SUSY . . . 64
2.5.3 New Bosons, Heavy Resonances, and New Fermions . . . 66
2.5.4 Long Lived Particles . . . 70
2.5.5 Dark Matter . . . 72
2.5.5.1 Testing the traditional WIMP paradigm . . . 73
2.5.5.2 Beyond WIMP dark matter . . . 78
2.6 Detectors, reconstruction, simulation and data analysis . . . 81
2.6.1 Detectors . . . 82
2.6.2 Monte Carlo Event Generators . . . 85
2.6.3 Computational resources . . . 86

2.6.4 Artificial Intelligence and Machine Learning 88
2.6.5 Analysis reinterpretation, preservation and Open Data 89
2.7 Enabling the Energy Frontier research 90
2.7.1 Goals 90
2.7.2 Context 90
2.7.3 Collaboration 91
2.7.3.1 Interdependence between Frontiers 91
2.7.3.2 Interdependence between US and international communities 91
2.7.3.3 Cross-fertilization between Energy Frontier and other domains of physics 92
2.7.4 Building a diverse Energy Frontier community 92
2.7.4.1 Continue to innovate and empower 92
2.7.4.2 Training the next generation of scientists 93
2.7.5 Investments essential to the progress of the Energy Frontier 93
2.8 The Energy Frontier vision 95
2.8.1 Community input 95
2.8.2 Vision overview 95
2.8.3 The immediate-future Energy Frontier collider 96
2.8.4 The intermediate-future Energy Frontier collider 98
2.8.5 The long-term-future Energy Frontier collider 100
2.8.6 Opportunity for US as a site for a future Energy Frontier Collider 101
2.8.7 Resource needs and timelines 102
2.8.8 Vision Summary 103

13 Glossary **139**

1 Higgs Boson Properties **159**

2 Higgs Boson as a Portal to New Physics **161**

3 Heavy Flavor and Top Quark Physics **163**

4 Electroweak Precision Physics **165**

5 QCD and Strong Interactions: Precision QCD 167

6 QCD and Strong Interactions: Hadronic Structure and Forward Reactions 169

7 QCD and Strong Interactions: Heavy Ions 171

8 Beyond the Standard Model: Model-Specific Explorations 173

9 Beyond the Standard Model: General Explorations 175

10 Beyond the Standard Model: Dark Matter at Colliders 177

2

Energy Frontier v2.3.6 (July 22, 2022)

Meenakshi Narain, Laura Reina, Alessandro Tricoli

M. Begel, A. Belloni, T. Bose, A. Boveia, S. Dawson, C. Doglioni, A. Freitas, J. Hirschauer, S. Hoeche, A. Korytov, Y.-J. Lee, H.-W. Lin, E. Lipeles, Z. Liu, P. Meade, S. Mukherjee, P. Nadolsky, I. Ojalvo, S. Pagan Griso, C. Royon, M. Schmitt, R. Schwienhorst, N. Shah, J. Tian, C. Vernieri, D. Wackeroth, L.-T. Wang

2.1 Big Questions in the Energy Frontier

After decades of pioneering explorations and milestone discoveries, particle physics is facing a unparalleled time defined by the possibility of explaining fundamental components of the physical world from the interactions of all elementary particles up to the history and dynamics of our universe. The Standard Model (SM) of particle physics has been confirmed as the theory that describes electroweak and strong interactions up to energies of a few hundreds GeV with great accuracy but also leaves other fundamental questions unexplained. The Energy Frontier aims at advancing the investigation of still open fundamental questions such as

- The origin of the electroweak scale
- The evolution of the early universe
- The matter-antimatter asymmetry of the universe
- The nature of dark matter
- The origin of flavor dynamics
- The origin of neutrino masses

with a broad and strongly motivated physics program that will push the exploration of particle physics to the TeV energy scale and beyond. Our sharply focused agenda includes in-depth studies of the SM as well as the exploration of physics beyond the SM to discover new particles and interactions. The vision of the Energy Frontier (EF) must keep its focus on these *big questions*, and must provide opportunities to examine them from as many angles as possible, while also continuing to pursue the *exploration of the unknown*, a leading driver of the Energy Frontier physics program. This is the core of the EF program as pictorially illustrated in Fig. 2-1.

Collider Physics offers a unique opportunity to study a huge number of phenomena and explore the connections between many of the fundamental questions we want to answer. The plethora of measurements, together with the development in theoretical insights, have established the SM of particle physics to a very

Figure 2-1. *The Big Questions in the Energy Frontier.*

high level of precision. The *big questions* outlined in Figure 2-1 unambiguously require new concepts beyond the standard model (BSM) of particle physics to be answered. Each of those questions is likely to manifest in a variety of processes, that can be used as *probes* to discover and then characterize the nature of the BSM physics at play, as schematically shown in Figure 2-2. Colliders at the energy frontier are key to investigating such phenomena via numerous distinct *signatures*, that probe the new physics that lies behind the big questions, as depicted in Figure 2-3, The multi-probe characteristic of high-energy colliders makes them a unique tool in the fundamental quest for answers to the core unknowns of particle physics. With a combined strategy of precision measurements and high-energy exploration, future lepton colliders starting at energies as low as a few hundreds GeV up to a few TeV can shed substantial light on some of these key questions. Ultimately, it will be crucial to find a way to carry out experiments at higher energy scales, probing new physics at the 10 TeV energy scale and beyond.

The activities of the Snowmass 2021 EF group has been structured around three main areas broadly defined as Electroweak Physics (Higgs-boson physics, top-quark and heavy-flavor physics, electroweak gauge bosons physics), Strong Interactions, and BSM (model-specific explorations, general explorations, dark matter at colliders). As illustrated in Fig. 2-2 they are the *probes* of many EF investigations. The EF program focuses on three main key questions:

1. What is the origin of the electroweak scale and of the EW phase transition?

   The 10^{th} anniversary of the discovery of the Higgs boson, a tremendous achievement for our field, is being celebrated this year, 2022. This discovery provides the last piece of the SM puzzle and at the same time gives a unique connection to new physics beyond the SM that we need to exploit. The plethora of studies relating to precision Higgs-boson measurements (mass, width, couplings) may help uncover the nature of physics above the EW scale. Together with the full spectrum of electroweak, top-quark, and flavor physics precision measurements, these studies will greatly improve the constraining power of global fits. The large number of Higgs boson events may lead to measurements of the shape of the Higgs potential. The study of the Higgs boson, may also give us insight into flavor physics and vice versa. Last but not least this study may lead us to understand the implications for naturalness.

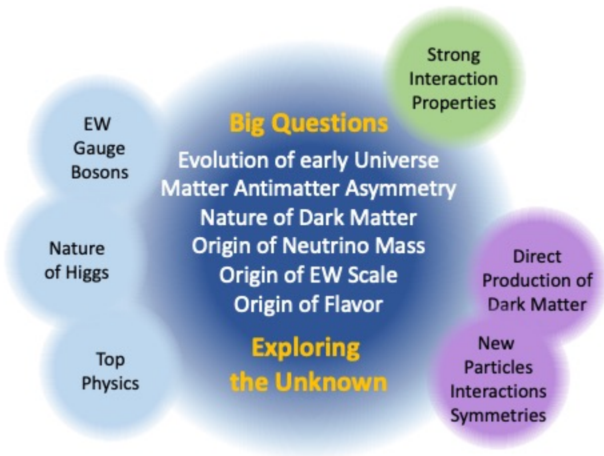

Figure 2-2. *The probes available in the energy frontier to address the Big Questions and Exploring the Unknown.*

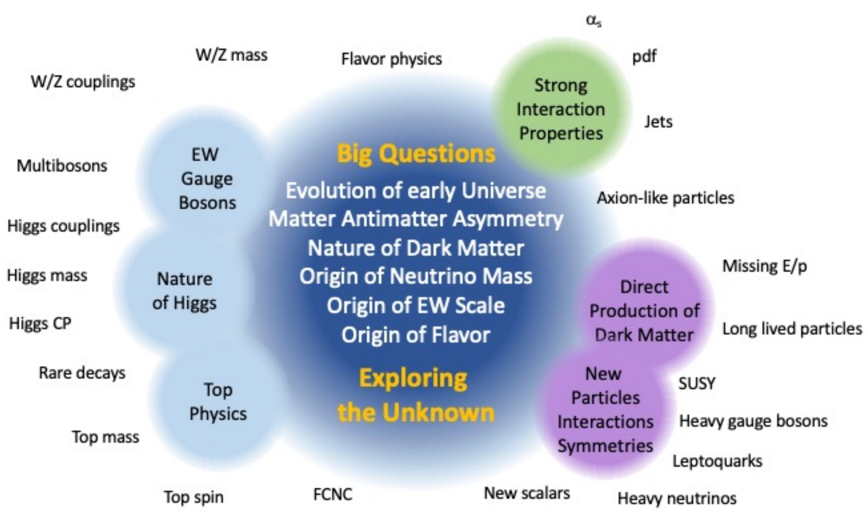

Figure 2-3. *The signatures that probe the new physics that lies behind the big questions in the energy frontier.*

2. What can we learn of the nature of strong interactions in different regimes?

Strong interactions pervade the studies of experimental signatures at the HL-LHC, and will do so at future hadron colliders as well as at future lepton colliders. Despite the great improvement in the understanding of QCD and its modeling at the LHC, several theoretical and experimental challenges are faced in the quest for a more fundamental understanding of the complex phenomenology of strong interactions in different regimes. Recent revolutionary progress in perturbative QCD calculations promises to allow sub-precent precision in QCD predictions and poses the challenge to control other QCD effects to a similar level of precision, and the following outstanding questions emerge. Are systematic uncertainty in Monte Carlo event generations controlled at the same level?

What precision in α_S can be reached by each future experiments? What is the evolution of jets as a function of energy? To what extent are jets universal? How do we deal with non-universality in our hadronization models? What dynamics drives the internal jet structure? Should the estimate of the accuracy on Parton Distribution Functions (PDFs) be revisited and improved vis à vis of new Lattice QCD results?

3. How is a complete program of BSM searches built that includes both model-specific and model-independent explorations?

   Models connect the high-level unanswered questions in particle physics (dark matter, electroweak naturalness, CP violation, etc) to specific phenomena, in a self-consistent way. They can be very predictive but model-dependent studies may fail to consider a broad range of new phenomena and search avenues. Many important questions needs to be critically addressed. Which models should be considered and how can model parameter spaces be compared in a consistent way? Can searches be conducted and interpreted in a model agnostic way? How can results from different experiments be compared in a model-independent way to ensure complementarity and avoid gaps in coverage? Can future colliders charter new regions of model parameter space and also fill in gaps left by existing colliders? What is the complementarity between precision measurement and direct searches?

Finding answers generates more specific questions that will be considered in the studies presented in this report and will be an important factor in building a concrete vision for the future of particle physics exploration at the Energy Frontier. Among others, the following aspects have emerged as most relevant in determining future directions for the energy frontier.

- What is the potential of each future collider proposal to provide substantial new insights in answering the key questions identified as the focus of the Energy Frontier physics program? What is the breadth of the physics program of future proposals, what is the complementarity of these proposals?
- What collider and detector developments are necessary to fully pursue the desired physics program of both precision measurements and searches for new physics?
- What theory calculations are needed? Where does theoretical accuracy matter, and how can it be implemented in numerical simulations to be used by the experiments? How can we reduce the theoretical systematic errors that, unless improved, are bound to limit the accuracy attainable in future collider measurement?
- What theoretically motivated new directions and signatures should be explored?
- Where do new approaches in searches or data analysis matter most? What progress in computing and data acquisition and handling will enable the desired physics program?

2.2 How to Connect Fundamental Questions to Energy Frontier Colliders: Energy & Precision

While all colliders offer a multifaceted approach to the search for new physics, different types offer different strengths and features. For example some colliders focus on extending the energy reach, some on reaching the highest precision possible. For the Snowmass 2021 exercise, we will focus on two main classes of colliders identified as *Higgs factories* and *multi-TeV colliders* respectively. We define *Higgs factories* as lepton colliders with center-of-mass energy up to 1 TeV that will substantially improve the Higgs-boson precision physics program beyond the HL-LHC reach. On the other hand lepton and hadron colliders with center-of-mass energies beyond 1 TeV will be labeled as *multi-TeV colliders* and will primarily be identified by the potential of allowing for the direct exploration of energy scales beyond the reach of the HL-LHC. Of course, any such separation is intrinsically arbitrary. Higgs factories can also complement the discovery reach of the HL-LHC in the low-mass region, and will provide a wealth of precision measurements beyond Higgs-physics alone. At the same time, multi-TeV colliders will produce huge numbers of Higgs-bosons and continue to indirectly test new physics via SM precision measurements. The labeling of *Higgs factories* versus *multi-TeV colliders* is only meant to organize the possible benchmark scenarios considered in the EF report, as illustrated in Tables 2-1 and 2-2. The reach of different scenarios in terms of *energy* and *precision* and their complementarity is crucial to connect the big questions discussed in Sec. 2.1 to colliders and will be discussed in the rest of this section.

Table 2-1. *Benchmark scenarios for Snowmass 2021 Higgs factory studies.*

Collider	Type	$\sqrt{s}$	$\mathcal{P}[\%]$ e^-/e^+	$\mathcal{L}_{\text{int}}$ ab^{-1} /IP
HL-LHC	pp	14 TeV		3
ILC & C^3	ee	250 GeV	$\pm80/\pm30$	2
		350 GeV	$\pm80/\pm30$	0.2
		500 GeV	$\pm80/\pm30$	4
		1 TeV	$\pm80/\pm20$	8
CLIC	ee	380 GeV	$\pm80/0$	1
CEPC	ee	M_Z		50
		$2M_W$		3
		240 GeV		10
		360 GeV		0.5
FCC-ee	ee	M_Z		75
		$2M_W$		5
		240 GeV		2.5
		$2\ M_{top}$		0.8
μ-collider	$\mu\mu$	125 GeV		0.02

While the existence of BSM physics is well established by observational phenomena, and heavily suggested by theoretical considerations, the energy scale at which it will manifest and its characteristics, e.g. the couplings to known SM particles, are only indirectly constrained. For example Dark Matter may be a

Table 2-2. *Benchmark scenarios for Snowmass 2021 energy frontier multi-TeV collider studies.*

Collider	Type	$\sqrt{s}$	$\mathcal{P}[\%]$. e^-/e^+	$\mathcal{L}_{\mathrm{int}}$ $\mathrm{ab}^{-1}/\mathrm{IP}$
HE-LHC	pp	27 TeV		15
FCC-hh	pp	100 TeV		30
SPPC	pp	75-125 TeV		10-20
LHeC	ep	1.3 TeV		1
FCC-eh		3.5 TeV		2
CLIC	ee	1.5 TeV	±80/0	2.5
		3.0 TeV	±80/0	5
μ-collider	$\mu\mu$	3 TeV		1
		10 TeV		10

thermal WIMP with possible extensions to the multi-TeV range, or it might have an extraordinarily low mass. Naturalness in principle points to as close to the Electroweak scale as possible, but in concrete scenarios, such as supersymmetry, it can easily point to the 10 TeV scale or higher given the measured Higgs mass. Furthermore it is quite possible that phenomena could show up unexpectedly at unpredicted scales as we have seen historically in our field.

Depending on the mass scale of new physics and the type of collider, the primary method for discovery new physics can vary. Investigation at the energy frontier allows one to combine direct BSM searches with precision measurements of observables sensitive to scales above the available center-of-mass energy. Furthermore, the type of collider employed directly influences what signatures are possible to probe within the foreseeable accelerator parameters, detector technology and physics backgrounds.

The fundamental lessons learned from the LHC thus far, are that a Higgs-like particle exists at 125 GeV and there is no other obvious and unambiguous signal of BSM physics. This means that either there is generically a gap to the scale of new physics, or it must be more weakly coupled to the SM or hidden in backgrounds at the LHC. The HL-LHC will either strengthen these conclusions further or potentially point us in a particular direction for discovery.

To understand how future colliders have complementary potential to unlock the mysteries around these fundamental questions beyond what the LHC and HL-LHC physics program can probe, it is illustrative to use a simplified picture depicted in Figure 2-4. In Figure 2-4 we can imagine that generic new physics lives in a 2D parameter space governed by the coupling of these new states to the SM and its mass scale. This is of course an enormous simplification of how BSM physics can manifest, but nevertheless is useful to depict the types of future colliders being proposed. Obviously if the energy scale of a collider is pushed beyond the LHC it can *directly* search for new states to a higher mass scale. Higgs factories have a smaller energy scale than the LHC, and therefore don't extend the *direct* mass reach beyond the LHC typically. However, by colliding leptons they offer significantly reduced backgrounds and the ability for triggerless readout, therefore they are able to probe potentially new physics that is coupled more weakly to the SM. Additionally, even in the "overlap" region of Higgs factories with the LHC, they can potentially find physics that would be too difficult to discriminate from backgrounds at the LHC. This categorization is also similar to how the Rare Processes and Precision Measurement Frontier is differentiated from the Energy Frontier, but here we

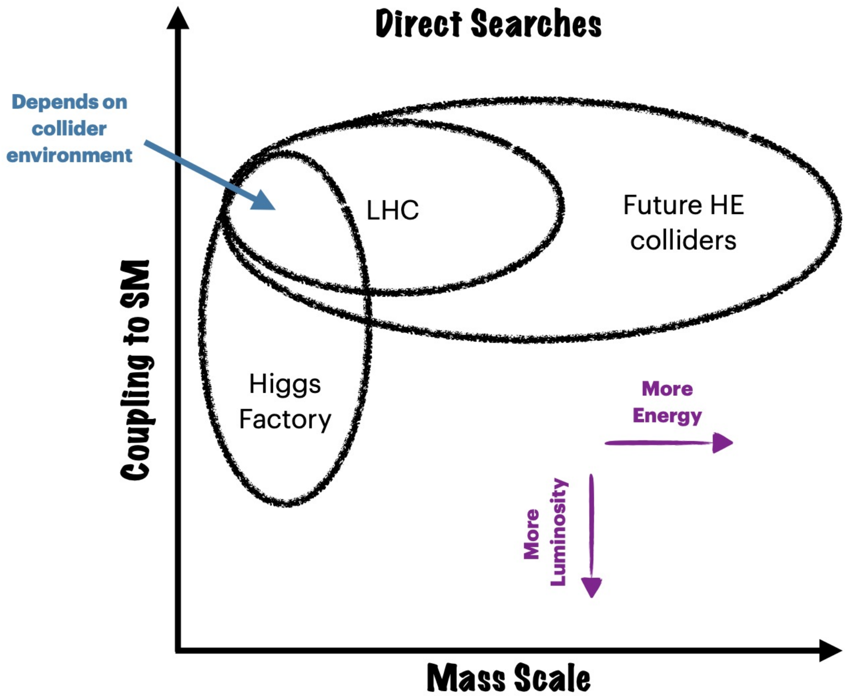

Figure 2-4. *The direct coverage of various colliders in the schematic space of coupling to the SM versus mass scale of BSM physics. HE refers to high-energy/multi-TeV colliders as listed in Table 2-2. Higgs factory corresponds to a generic option as listed in Table 2-1.*

emphasize in Figure 2-4, that even *within* the Energy Frontier there are multiple approaches in the search for new physics depending on the type of collider considered.

Beyond the direct search for new physics, a key program for the Energy Frontier is the precision measurement of SM predictions and parameters. If measurements can be made sufficiently precise, it in principle allows one to probe scales above the kinematic limit for direct searches at colliders. This can be captured through Effective Field Theory (EFT) techniques when there is a gap between the energy scale probed and the scale of new physics. In the Energy Frontier, typically this is done by employing the specific EFTs, the SMEFT or more general HEFT. However, without going into the details, we can understand the scaling very simply. If M is the mass scale of new physics and g_{BSM} is the coupling of the state to the SM then often deviations in SM parameters, η_{SM}, which occur from integrating heavy particles out at tree-level, scale at the leading order as

$$\delta\eta_{SM} \sim g_{BSM}^2 \frac{v^2}{M^2}, \tag{2.1}$$

for Higgs related parameters, where v is the VEV of the Higgs, or

$$\delta\eta_{SM} \sim g_{BSM}^2 \frac{E^2}{M^2}, \tag{2.2}$$

where the energy scale $E \ll M$ for the framework to be most applicable. If new physics only creates loop level deviations in a SM observable, then one can insert a loop factor$\sim 1/16\pi^2$ into Eqns. 2.1 and 2.2. Therefore depending on the precision achievable, as seen in Eqns. 2.1 and 2.2, mass scales larger than the direct reach can be probed. We can then overlay these types of indirect collider searches, particularly relevant for Higgs factories in Table 2-1 on our schematic space of BSM physics shown in Figure 2-4. In Figure 2-5, we show this explicitly where the solid lines illustrate direct search limits while the dashed lines represent indirect limits. As can be seen in this Figure 2-5 the energy versus precision trade-off *crucially* depends on the precision attainable. Suggestively, we have shown a 1% number often associated with Higgs parameter measurements (except for e.g. the hZZ coupling at Higgs factories), where the scaling typically does not extend beyond the LHC without invoking strong coupling. However, for quantities that are measured significantly more precise, e.g. $\lesssim .1\%$, at future Higgs factory programs, such as M_W, the reach can extend much further. This exact scaling in mass reach depends of course on the type of BSM physics, and both Higgs parameters and EW observables measured at Higgs factories are important for understanding complementary measurements available at future High Energy colliders. The precision that can ultimately be reached and in what types of observables strongly motivates detector technology, increases in luminosity, polarization, and improved theoretical calculations. Moreover depending on the type of collider, for example in a high-energy/multi-TeV collider, the dichotomy between precision reach and energy reach can potentially be bridged with the availability of large statistics for processes as e.g. Higgs production *if* the environment can be fully controlled, as discussed in Section 2.8.

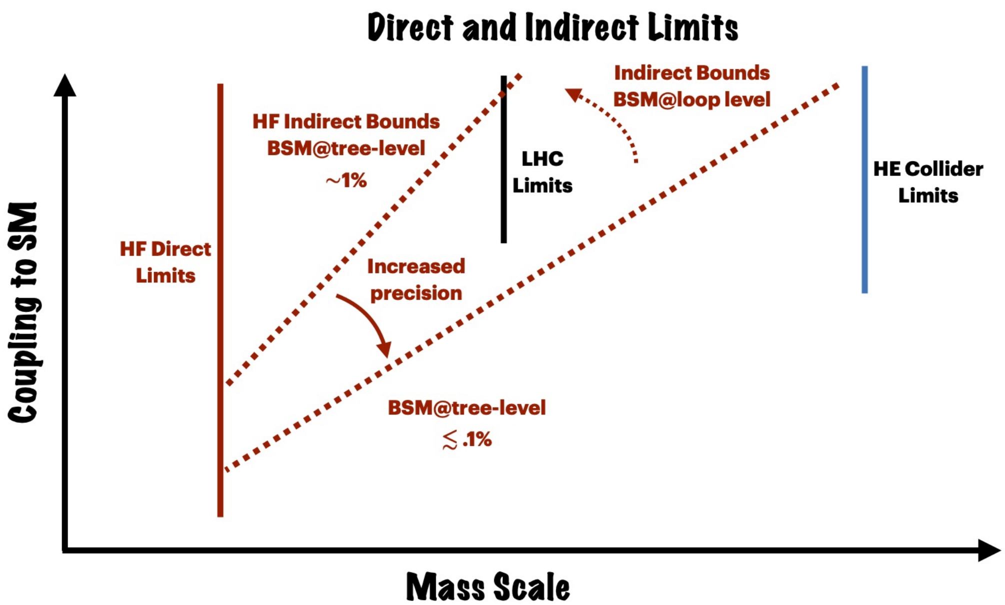

Figure 2-5. *Lepton colliders such as the Higgs Factory options (HF) can provide increased reach in the schematic coupling vs mass plane through indirect searches benefiting from increased precision. However, the level of precision reached is ultimately a function of our technology and control of systematic uncertainties. As shown in the plot, a 1% precision measurement suggests a scale probed of up to a few TeV in perturbative UV completions if BSM physics couples at tree-level to the observables of interest. This is of course potentially within reach of the LHC, and the type of UV physics determines whether or not this results in additional reach beyond the LHC or complementary probes. If new physics couples at loop-level then the scale probed indirectly is lower. However the ultimate precision, and what scale the High Energy (HE), i.e. multi-TeV, colliders can probe is ultimately a collider specific question.*

It is important to understand the types of scalings discussed so as to understand the reach of various types of colliders at high mass and how they are complementary. However, it should be stressed again that this direct versus indirect approach is not the only way to compare colliders. As discussed for Figure 2-4, there can still be a multitude of phenomena studied at low masses, incompatible with the EFT framework at those energies, that benefit from a reduced background environment at a e^+e^- Higgs factory. Additionally, even *within* one collider, precision measurements and direct searches coexist and offer multiple complementary probes. To move beyond scaling it is useful to give a few examples of how direct and indirect complementarity play out within the Energy Frontier, as well as what are potential BSM features at low energy that the LHC in principle is missing. The remaining of Energy Frontier report and Topical Group reports will provide examples and more details, but we list a few illustrative ones below:

- Higgs couplings and mass reach: the Higgs boson as the primary target for all future EF colliders has many examples of the interplay of direct and indirect searches. For example in Two-Higgs doublet models, indirect Higgs precision can be overlaid with direct resonance searches, EW precision, flavor physics and beyond. Numerous cases are discussed in Section 2.3 and in the corresponding topical group report.

- Supersymmetry is still a leading example of BSM physics, and while it is a canonical example of direct searches it also can be tested indirectly in numerous ways. However as shown in Section 2.5.2 for pMSSM parameter scans, indirect searches at Higgs factories do not exceed the typical region covered by the HL-LHC. Further examples can be found in several of the topical group reports.

- The search for anomalous Trilinear Gauge Couplings (aTGC) and anomalous Quartic Gauge Couplings (aQGC) offer a particularly interesting example of the interplay of several search strategies and measurements. At lowest dimension in the SMEFT expansion, deviations are only possible from BSM physics at loop level from new EW charged states. Therefore on top of indirect multiboson measurements, direct searches for charged particle which generate the effects are powerful. These can include long-lived particle searches in the degenerate mass limit, or more canonical direct searches that can also be overlaid with Higgs precision when the splitting becomes larger. Furthermore there are multiple ways to search for vector boson scattering such as in ultraperiphreal collisions as discussed in Section 2.4.5.3.

- Higgs to invisible decays is an example of where there can be "holes" in the LHC coverage even at low mass. It is particularly interesting as it does not fit into the standard precision EFT arguments for Higgs factories and represents a "direct" search. Similar arguments can be made for Higgs precision measurements into light quark flavors which are difficult at the LHC but produced copiously. These are both further discussed in Section 2.3 and in the corresponding topical group report.

As shown in the few examples above, as well as by the representative list of the vast physics program uniquely available, energy-frontier colliders are the ultimate tool we possess to clarify the fundamental nature of deviations observed either at colliders themselves or at low-energy experiments. The current landscape also provides notable examples of deviations in precision measurements of SM parameters that are currently under scrutiny by the particle physics community, and that can provide targets for direct BSM searches. Most notably, anomalies in (semi)leptonic B-hadrons decay, including hints of lepton flavor universality violations, the muon anomalous magnetic moment ($g_\mu - 2$) and the recent W mass measurement might develop to unambiguous BSM signals that call for direct exploration to clarify their nature. Regardless the nature of the present and future anomalies, such occurrences call for a flexible energy frontier program that can develop and deploy an energy-frontier collider able to directly and unambiguously probe energy scales of the order of several TeV.

2.3 Electroweak Sector of the Standard Model

2.3.1 Higgs and BSM physics

Over the past decade the LHC has fundamentally changed the landscape of high energy particle physics through the discovery of the Higgs boson and the first measurements of many of its properties. As a result of this, and no other "discoveries" at the LHC, the questions surrounding the Higgs have only become sharper and more pressing for planning the future of particle physics.

The Standard Model (SM) is an extremely successful description of nature, with a basic structure dictated by symmetry. However, symmetry alone is not sufficient to fully describe the microscopic world we explore, and even after specifying the gauge and space-time symmetries, and number of generations, there are still 19 parameters undetermined by the SM (not including neutrino masses). Out of these parameters 4 are intrinsic to the gauge theory description, the gauge couplings and QCD theta angle. The other 15 parameters are intrinsic to the Higgs sector or how other SM particles couple to the Higgs, illustrating its paramount importance in the SM. In particular, the masses of all fundamental particles, their mixing, CP violation, and the basic vacuum structure are all undetermined and derived from experimental data. Therefore, as simply a test of the validity of the SM, all these couplings must be measured experimentally. However, the centrality of the Higgs boson goes far beyond just dictating the parameters of the SM.

The Higgs boson is connected to some of our most fundamental questions about the Universe. Its most basic role in the SM is to provide a source of Electroweak Symmetry Breaking (EWSB). However, while the Higgs can describe EWSB, it is simply put in by hand in the Higgs potential.

$$V(H) = -\mu^2 H^2 + \lambda H^4 \tag{2.3}$$

If the mass parameter in the potential (the term quadratic in H) simply had a positive sign rather than negative, there would be no EWSB and our universe would not exist in its current form. The explanations of *why* EWSB occurs and the presence of such a minus sign are outside the realm of the SM Higgs boson. However, in other examples of spontaneous symmetry breaking that we have see manifest in our universe described by quantum field theory (QFT), there has been a dynamic origin. In principle the Higgs could be a composite of some other strongly coupled dynamics, as we have seen before. However, the Higgs also could be a fundamental scalar and EWSB could arise dynamically through its interactions with other BSM fields. It's even possible that there could dynamical connections to cosmology or the anthropic principle. Nevertheless, whatever is the origin of EWSB it will leave imprints on the properties of the SM Higgs itself. Moreover, answers to the questions such as is the Higgs composite or fundamental can have ramifications far beyond just the origin of EWSB.

If the Higgs boson is a fundamental particle, it represents the first fundamental scalar particle discovered in nature. This has profound consequences both theoretically and experimentally. From our modern understanding of QFT, fundamental scalars should not exist in the low energy spectrum without an UV sensitive fine tuning if the SM is an Effective Field Theory(EFT) of some more fundamental theory. This is known as the naturalness or hierarchy problem. From studying properties of the Higgs boson, one can hope to learn whether there is some larger symmetry principle at work stabilizing the spectrum. For example supersymmetry, neutral naturalness, or if the correct theory is a composite Higgs model, the Higgs could be a pseudo-Goldstone boson.

Experimentally there are also a number of intriguing directions that open up if the Higgs boson is a fundamental particle. The most straightforward question is whether the Higgs boson is a unique scalar field in our universe, or is it just the first of many? Additional scalars can always couple to the Higgs at the renormalizable level, and depending on their symmetry properties they can couple to gauge bosons or fermions as well (e.g. the more commonly known Two Higgs Doublet models). What this implies is that if the Higgs is not unique, there are two complementary methods for investigating this: searching directly for these new scalar states, or their indirect effects on the SM Higgs properties. Also related to the fact that new scalars can always leave imprints on the Higgs is that a fundamental Higgs particle is special in QFT. Using only the SM Higgs field, one can construct the lowest dimension gauge and Lorentz invariant operator in the SM. This means that generically if there are other "Hidden" sectors beyond the SM (perhaps related to Dark Matter), the Higgs is the most relevant portal to these sectors, often referred to as the "Higgs Portal". Whether these new sectors have a mass scale well below or above the scale of EWSB implies drastically different experimental observables. For light new sectors of the universe, this can manifests itself as exotic Higgs decays, invisible Higgs decays, and shifts in the Higgs total width, and as can be probed well at e^+e- colliders. For heavier hidden sectors, the observables are different and the highest energy collider options are needed.

Another aspect of determining if the Higgs is a fundamental scalar particle concerns whether the minimal Higgs potential is correct. If there are new BSM particles that couple to the Higgs, the potential itself can receive modifications. This isn't just solely a question about the potential, because its form has repercussions for both our understanding of the early universe and its ultimate fate. For the early universe, the SM predicts that the electroweak symmetry should be restored at high temperatures. However, depending on the actual form of the potential the question remains as to whether there even was a phase transition let alone its strength. Additionally, depending on the form of the Higgs potential, it controls the future of our universe as our vacuum may only be metastable. Furthermore a strong EW first order phase transition can have implications for Baryogenesis as well.

Finally, the Higgs boson is connected to some of the most puzzling questions in the universe: flavor, mass and CP violation. There are effectively two types of interactions in the SM, gauge interactions and Higgs interactions. Gauge interactions are tightly constrained and do not fundamentally differentiate flavor. Higgs interactions govern all the important quantities for flavor, mass, and CP violdation in the SM. In particular, all problems connected with flavor and CP – the origin of the fermion masses, the origin of neutrino masses, the origin of the PMNS and CKM angles, ultimately require knowledge of the fundamental nature of the Higgs sector. Otherwise, we are just fitting parameters without an understanding. The full information that we need is only available at high energy by studying the Higgs.

The fact that understanding the properties of the SM Higgs boson connects to so many fundamental questions illustrates how central it is to the HEP program. The connections briefly reviewed so far obviously can each be expanded in greater detail, but to collect the various themes in a simple to digest manner this is illustrated in Figure 2-6. The generality of the concepts and questions posed in Figure 2-6 could even belie connections to additional fundamental mysteries. For example, the Higgs portal could specifically connect to Dark Matter or other cosmological mysteries.

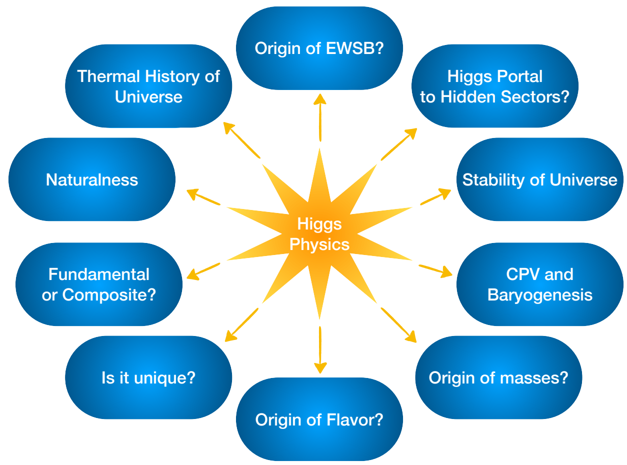

Figure 2-6. *The Higgs boson as the keystone of the Standard Model is connected to numerous fundamental questions that can be investigated by studying it in detail.*

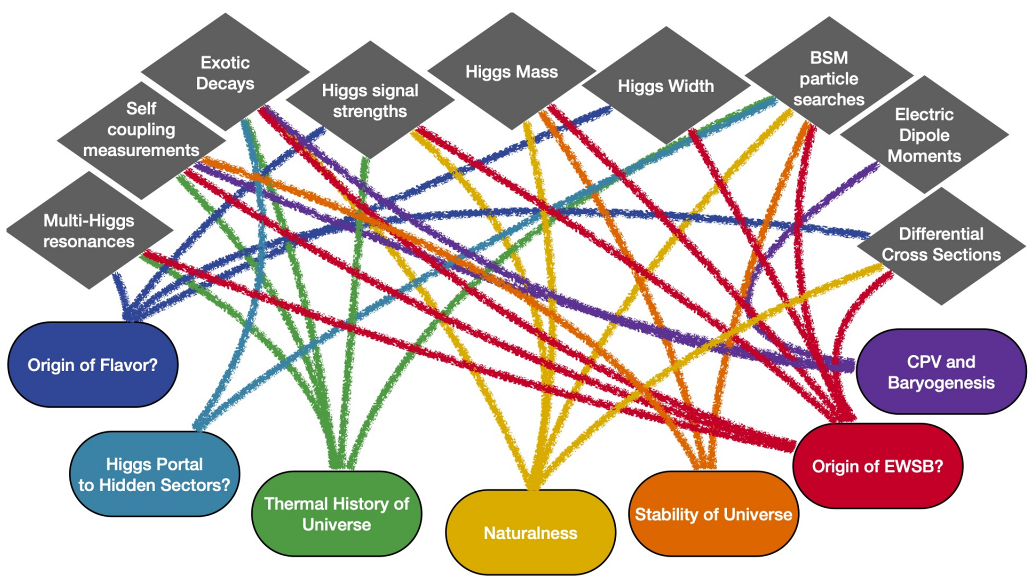

Figure 2-7. *Examples of the interplay between experimental observables and fundamental questions connected to the Higgs boson.*

2.3.1.1 Higgs present and future

LHC Run 2 with about 140 fb^{-1} of data analyzed is providing a wealth of new measurements for the Higgs sector. The most recent Higgs boson mass measurements, from CMS and ATLAS set its value to be 125.38±0.14 GeV [1] and 124.92±0.21 GeV [2] respectively, using both the diphoton and ZZ decay channels. The mass is a free parameter in the SM and it is now known to per-mille accuracy. We are entering the era of precision Higgs physics, with some of the Higgs boson couplings measurements approaching $\mathcal{O}$(5-10)% precision. All the major production mechanisms of the Higgs boson have been observed at the LHC: gluon fusion (ggF), vector-boson fusion (VBF), the associated production with a W or Z boson (Wh, Zh), and the associated production with top quarks (tt$h$, th), as shown in Figure 2-8. All of these channels are precisely measured, with the experimental sensitivity of some modes nearing the precision of state-of-the-art theory predictions. The most updated measurements of Higgs decay modes are shown in Figure 2-9.

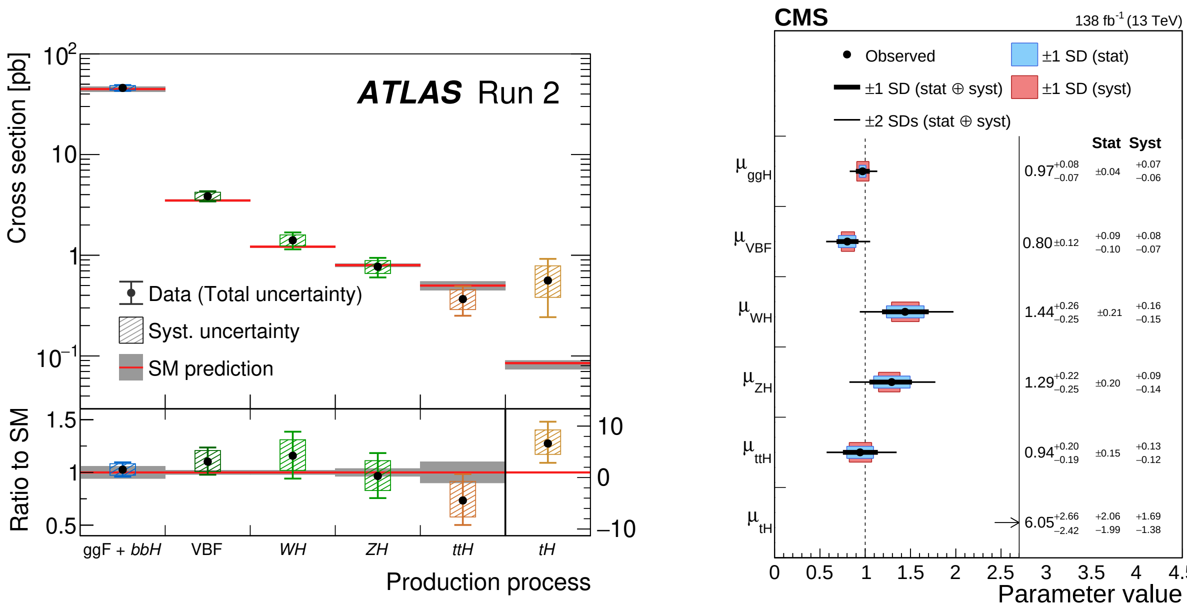

Figure 2-8. *Measured cross sections for ggF, VBF, $Wh_{\rm SM}$, $Zh_{\rm SM}$, $t\bar{t}h_{\rm SM}$, and $th_{\rm SM}$ normalized to their SM predictions, assuming SM values for the decay branching fractions for ATLAS (left) and CMS (right) [3, 4].*

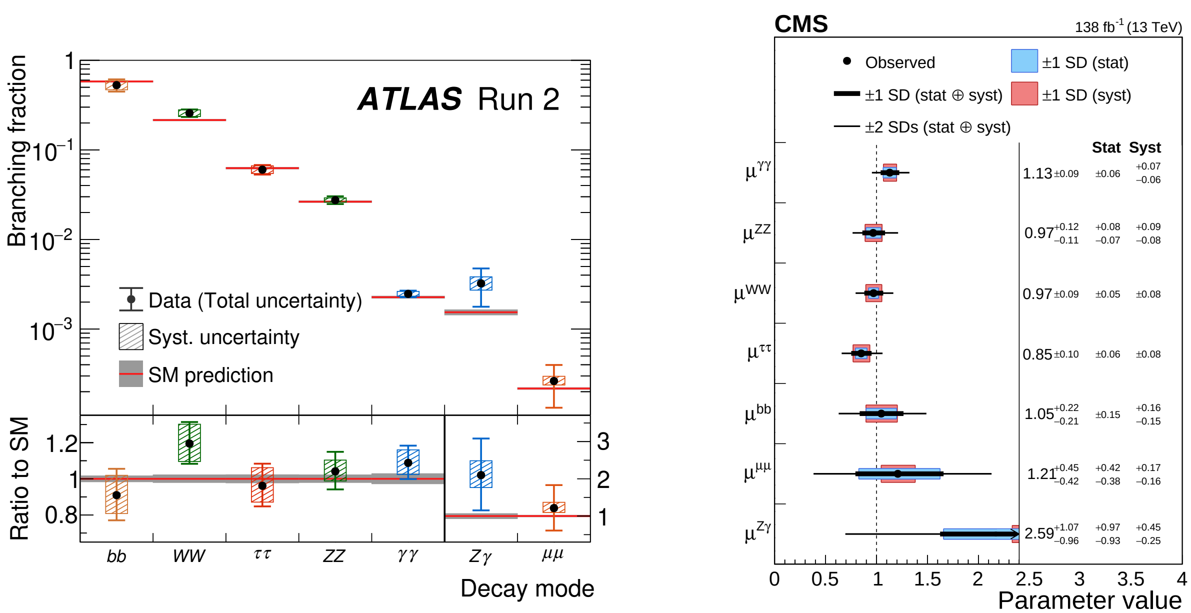

Figure 2-9. *Left, observed and predicted Higgs boson branching fractions for different Higgs boson decay modes [3]. Right, CMS signal strength modifiers for the various decay modes [4].*

The extraction of the Higgs couplings to gauge bosons and to the third generation fermions is shown in Figure 2-10. Probing the charm Yukawa at the LHC is very challenging. Novel jet reconstruction and identification tools and analysis techniques have been developed to look for $h \to c\bar{c}$ in the Vh production mode, leveraging also the expertise developed for $h \to b\bar{b}$ in the same topology. The most stringent constraint to date is set by CMS using 138 fb^{-1} Run 2 data. The observed 95% CL interval (expected upper limit) is $1.1 < |\kappa_c| < 5.5$ ($|\kappa_c| < 3.4$) [5] [1]. This should be compared to indirect bounds on the charm Yukawa, since if $\kappa_c \sim 5$, one would already be ruled out by contributions to the Higgs width if κ_c were the only parameter that was modified in the SM (see for example Refs. [6, 7]). CMS has reported the first evidence of Higgs decay to muons with 137 fb^{-1} at 13 TeV [8], but the measurement of Higgs coupling to the muon will require the additional dataset of HL-LHC. In the SM, the branching fraction to invisible final states, B(h→ invisible), is only about 0.1%, from the decay of the Higgs boson via $ZZ^* \to 4\nu$. The strongest constraint is set by CMS exploring the VBF topology and using 108 fb^{-1} at 13 TeV. The observed (expected) upper limit on the invisible branching fraction of the Higgs boson is found to be 18% (10%) at the 95% CL, assuming the SM production cross section [9].

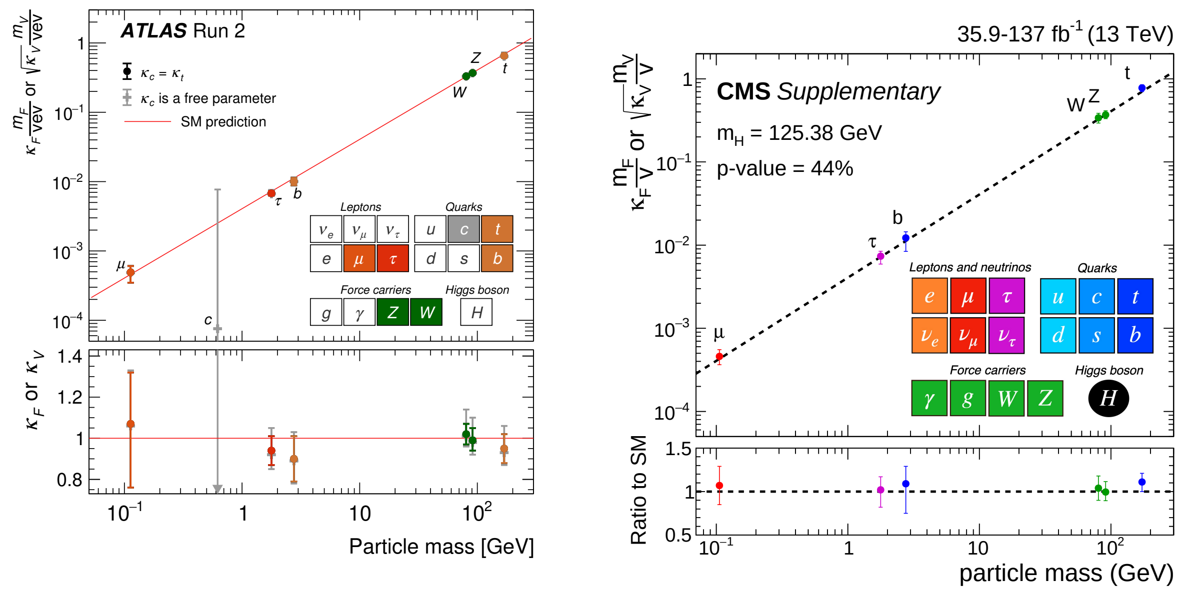

Figure 2-10. *The best-fit estimates for the reduced coupling modifiers extracted for fermions and weak bosons compared to their corresponding predictions from the SM. The associated error bars represent 68% CL intervals for the measured parameters for ATLAS (right) [3] and CMS (left) [8]. ATLAS considers two fit scenarios with $\kappa_c = \kappa_t$ (coloured circle markers) and κ_c left free-floating in the fit (grey cross markers).*

A simultaneous fit of many individual production times branching fraction measurements is performed to determine the values of the Higgs boson coupling strength. The κ-framework defines a set of parameters that affect the Higgs boson coupling strengths without altering any kinematic distributions of a given process. SM values are assumed for the coupling strength modifiers of first-generation fermions, the other coupling strength modifiers are treated independently. The results are shown in Figure 2-11 for ATLAS and CMS. In this particular fit, the presence of non-SM particles in the loop-induced processes is parameterized by introducing additional modifiers for the effective coupling of the Higgs boson to gluons, photons and $Z\gamma$, instead of propagating modifications of the SM particle couplings through the loop calculations. In these results, it also assumed that any potential effect beyond the SM does not substantially affect the kinematic properties of the Higgs boson decay products. The coupling modifiers are probed at a level of uncertainty of 10%, except for κ_b and κ_μ ($\approx 20\%$), and $\kappa_{Z\gamma}$ ($\approx 40\%$).

[1] The κ's are defined as the ratio of the measured Higgs couplings to the SM predictions.

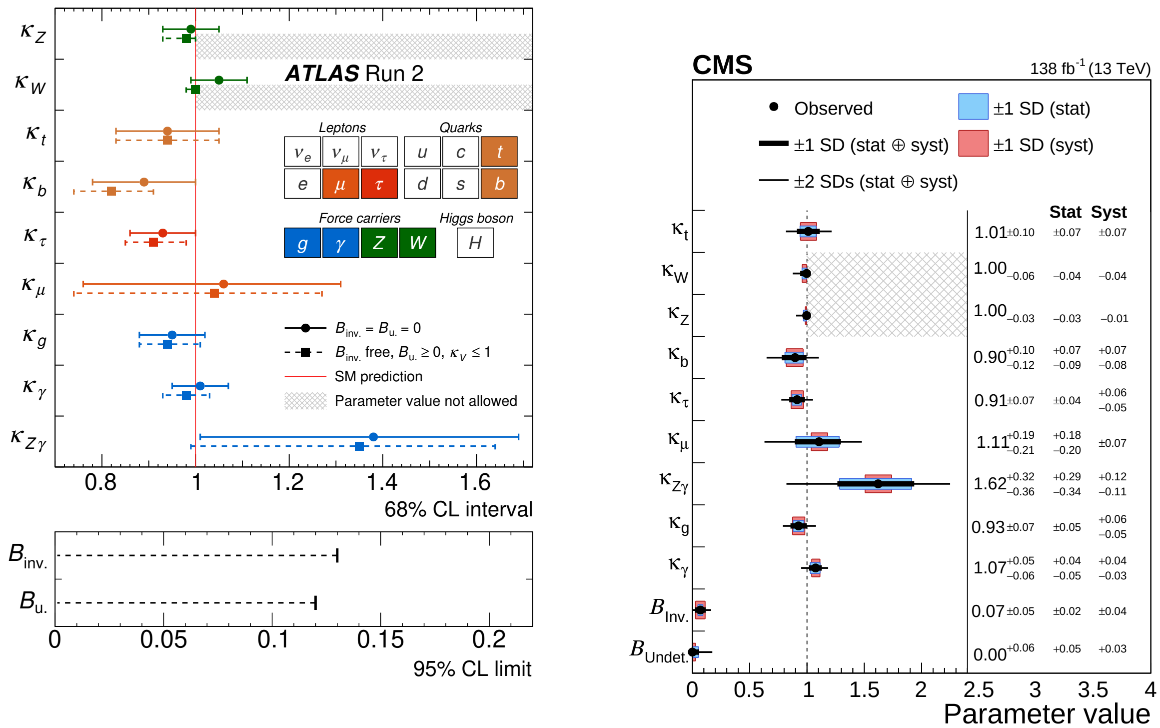

Figure 2-11. *Left, ATLAS best-fit values and uncertainties for Higgs boson coupling modifiers per particle type with effective photon and gluon couplings and the branching fraction to invisible (B_i) and undetected decays (B_u) included as free parameters and the measurement of the Higgs boson decay rate into invisible final states included in the combination [10]. Right, CMS summary of the couplings modifiers κ. The thick (thin) black lines report the 1σ (2σ) confidence intervals[4].*

The scalar potential of the Higgs boson field, responsible for the EWSB mechanism, is currently still very far from being probed. After EWSB, the Higgs boson potential gives rise to cubic and quartic terms in the Higgs boson field, inducing a self-coupling term. The Higgs boson self-coupling, within the SM, is fully predicted in terms of the Fermi coupling constant and the Higgs boson mass, which has been measured at per-mille level accuracy by the ATLAS and CMS experiments [2, 1]. The Higgs self-coupling is accessible through Higgs boson pair production (hh) and inferred from radiative corrections to single Higgs measurements. Measuring this coupling is essential to shed light on the structure of the Higgs potential, whose exact shape can have deep theoretical consequences.

The maximum value of the acceptance for the $gg \to hh$ process is obtained for $\kappa_\lambda \sim 2$, where the cross section is at a minimum. κ_λ is the ratio of the measured value to the predicted Standard Model value of the Higgs self coupling and must be unity if the Standard Model is a complete theory. A different measurement than 1 would unambiguously imply that there is some new physics beyond the Standard Model. The corresponding intervals where κ_λ is observed (expected) to be constrained at 95% CL are listed in Table 2-3 for the main channels.

The planned High Luminosity era of the LHC (HL-LHC), starting in 2029[2] will extend the LHC dataset by a factor of $\mathcal{O}(10)$, and produce about 170 million Higgs bosons and 120 thousand Higgs boson pairs. This would allow an increase in the precision for most of the Higgs boson couplings measurements. HL-LHC will

[2]This refers to the updated schedule presented in January 2022 [17]

Final state	Collaboration	allowed κ_λ interval at 95% CL	
		observed	expected
$b\bar{b}b\bar{b}$	ATLAS	-3.5 – 11.3	-5.4 – 11.4
	CMS	-2.3 – 9.4	-5.0 – 12.0
$b\bar{b}\tau\tau$	ATLAS	-2.4 – 9.2	-2.0 – 9.0
	CMS	-1.7 – 8.7	-2.9 – 9.8
$b\bar{b}\gamma\gamma$	ATLAS	-1.6 – 6.7	-2.4 – 7.7
	CMS	-3.3 – 8.5	-2.5 – 8.2
comb	ATLAS	-0.6 – 6.6	-2.1 – 7.8
	CMS	-1.2 – 6.8	-0.9 – 7.1

Table 2-3. *The observed and expected 95% CL intervals on κ_λ for the most sensitive individual final states analyzed for non-resonant hh production at 13 TeV with about 126-139 fb^{-1}. All other Higgs boson couplings are set to their SM values [11, 12, 13, 14, 15, 16, 4].*

dramatically expand the physics reach for Higgs physics. Current projections are based on the Run 2 results and some basic assumptions that systematic uncertainties will scale with luminosity and that improved reconstruction and analysis techniques will be able to mitigate pileup effects. The studies also assume that the theory uncertainty is reduced by a factor of 2 relative to current values. Studies based on the 3000 fb^{-1} HL-LHC dataset estimate that we could achieve $\mathcal{O}(2-4\%)$ precision on the couplings to W, Z and third generation fermions. But the couplings to u, d and s quarks will still not be accessible at the LHC directly, while the charm Yukawa is projected to be directly constrained to $\kappa_c < 1.75$ at the 95% CL [18]. The Higgs self coupling is a prime target of the HL-LHC and current rough projections claim the trilinear self-coupling will be probed with $\mathcal{O}(50\%)$ precision. We will be able to exclude the hypothesis corresponding to the absence of self-coupling at the 95% CL in these projections for HL-LHC, but not to test the SM prediction [18].

Future colliders are charged with the challenging tasks of testing the SM predictions of the Higgs boson Yukawa couplings to light flavor quarks, and improving the precision on the LHC Higgs coupling measurements. An e^+e^- Higgs factory or muon collider can measure these couplings with smaller uncertainties than the HL-LHC due to a combination of knowing the momentum of the incoming particles more precisely, smaller background environments and better detector resolutions. Tagging of charm and strange quarks, as previously demonstrated at SLC/LEP, gives effective probes for precision measurements of charm and strange quark Yukawa couplings. The cleaner e^+e^- environment aided by beam polarization could become a sensitive probe to reveal more subtle phenomena [19]. For high energy muon colliders, the primary driver is the cleaner environment plus increased statistics [20]. The measurement of the Higgs self-coupling demands access to high energy center-of-mass collisions to benefit from the larger dataset of hh pairs and is a major goal of all future colliders.

While all future colliders give strong contributions to the Higgs precision program, the first stages of e^+e^- Higgs factories are particularly compelling since they can all be constructed in the near future if funding is available, while other collider options require significantly more R&D. Studies for the five current e^+e^- Higgs factory proposals—ILC [22], C^3[19], CEPC [23], CLIC [24], and FCC-ee [25]—demonstrate that experiments at these facilities can achieve high precision. Despite their different strategies, all these proposals lead to very similar projected uncertainties on the Higgs boson couplings when the colliders are run at the same energies. The higher luminosity proposed for circular e^+e^- colliders is compensated by the advantages of polarization at linear colliders, yielding very similar projected sensitivity for the precision of Higgs couplings [26, 27].

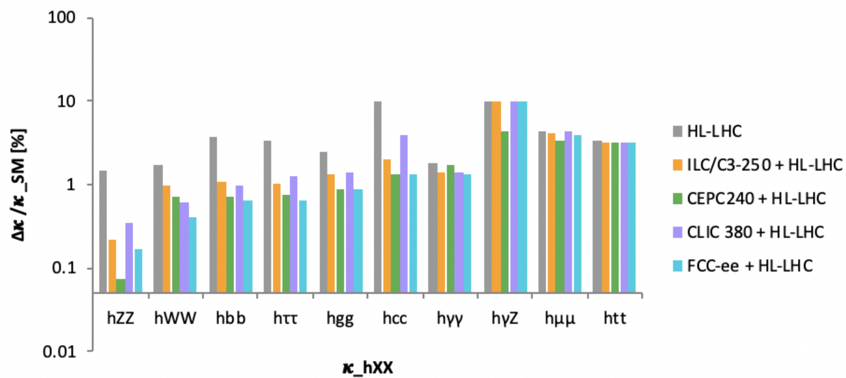

Figure 2-12. *Projected relative Higgs coupling measurements in % when combined with HL-LHC results. All values assume no beyond the Standard Model decay modes. In addition, only the following collider stages are shown: 3 ab^{-1} and two interaction points (IPs), ATLAS and CMS, for the HL-LHC at 14 TeV, 2 ab^{-1} and 1 IP at 250 GeV for ILC/C^3, 20 ab^{-1} and 2 IP at 240 GeV for CEPC, 1 ab^{-1} and 1 IP at 380 GeV for CLIC, and 5 ab^{-1} and 4 IPs at 240 GeV for FCC-ee. *Note the HL-LHC κ_{hcc} projection uses only the CMS detector and is an upper bound [21].*

We show the projected sensitivity for the first stages of possible lepton colliders combined with HL-LHC projections in Figure 2-12. These results are done in the so-called "kappa-0" framework and do not allow for beyond the Standard Model decays of the Higgs boson, and are then combined with projections for results from HL-LHC. It is clear that the dominant improvement from HL-LHC results is in the couplings to b's, c's, and $\tau's$, along with extremely precise measurements of the Higgs interactions with W and Z bosons. The future lepton colliders not only can significantly improve on the knowledge of the coupling to charm quarks, but potentially the coupling to strange quarks as well with possible future detector advances, depending on project, and even set relevant direct bounds on up and down quarks. A dedicated run at the Higgs pole by the FCC-ee has the possibility to measure the coupling of the Higgs to electrons, which would be an important verification of the SM. Therefore there are subtle differences in the various e^+e^- Higgs factories and in some cases further study is needed to understand how real the differences are.

Measuring the Higgs couplings can be viewed as part of a global program of fitting to beyond the Standard Model physics in the framework of effective field theory (EFT). In this approach, Higgs interactions are connected to processes without Higgs bosons through the EFT operators, the so-called Higgs without Higgs events. The κ framework, where the kinematic structure of the Higgs interactions is assumed to be identical to the Standard Model, can be seen as a simplified metric for understanding the capabilities of future colliders for Higgs studies alone. However, there are many possibilities for BSM physics that effects Higgs properties at scales not validly described by SM EFT. In these cases a combination of κ fits and other observables can be more useful. The dedicated EFT analysis shown in Section 2.3.4.2 combines information from the Higgs sector with information from precision electroweak measurements, diboson production, and top quark measurements, including kinematic information, to attempt to gain a deeper understanding of the underlying physics.

Beyond couplings to fermions and gauge bosons, the HL-LHC can constrain the Higgs boson width indirectly from the $ZZ \to 4$ lepton channel, with a projected measurement of $\Gamma_{h_{\rm SM}} = 4.1^{+.7}_{-.8}$ MeV, corresponding to roughly a 17% accuracy[18]. The indirect measurement of the Higgs width can be sensitive to the assumption that there is no new BSM physics contributing to the width. However, it is more akin to an absolute coupling normalization and can be vieweed as part of the larger "Higgs without Higgs" framework. BSM physics that invalidates these measurements are not generic, but further complementary information from other colliders is desired.

One distinct advantage of the lepton colliders is the possibility for obtaining extremely precise and relatively model independent measurements of the Higgs boson width. The measurement of the width not only confirms the Standard Model predictions, but is also extremely sensitive to high scale new physics. The fully reconstructed Z boson in the final state along with the well determined 4 momenta of the initial state leptons in the $Zh_{\rm SM}$ process allows for a clean determination of the Higgs boson kinematics regardless of the Higgs decay channel. The full FCC-ee program (combined with HL-LHC) allows for a 1% measurement of the Higgs width. Using a SMEFT fit, the ILC finds similar results for the full program, but with just the initial 250 GeV run, a 2% measurement on the total width can be obtained. A muon collider running at $\sqrt{s} = 125$ GeV can obtain a model independent measurement of the Higgs total width at the 68% level of 2.7% (1.7%) with 5 fb^{-1}(20 fb^{-1}) by using a line-shape measurement [28]. A high energy muon collider should obtain a similar order of magnitude precision using the indirect methods employed at the LHC with the same theoretical assumptions, and the FCC-hh could in principle also use these methods with further study.

collider	Indirect-$h_{\rm SM}$	$h_{\rm SM}h_{\rm SM}$	combined
HL-LHC [29]	100-200%	50%	50%
$\text{ILC}_{250}/\text{C}^3$-250 [22, 19]	49%	–	49%
$\text{ILC}_{500}/\text{C}^3$-550 [22, 19]	38%	20%	20%
$\text{ILC}_{100}/\text{C}^3$-1000 [22, 19]	36%	10%	10%
CLIC_{380} [24]	50%	–	50%
CLIC_{1500} [24]	49%	36%	29%
CLIC_{3000} [24]	49%	9%	9%
FCC-ee [25]	33%	–	33%
FCC-ee (4 IPs) [25]	24%	–	24%
FCC-hh [30]	-	3.4-7.8%	3.4-7.8%
μ(3 TeV) [28]	-	15-30%	15-30%
μ(10 TeV) [28]	-	4%	4%

Table 2-4. *Sensitivity at 68% probability on the Higgs cubic self-coupling at the various future colliders. Values for the indirect single Higgs determinations below the first line are taken from [31]. The values quoted here are combined with an independent determination of the self-coupling with uncertainty 50% from the HL-LHC.*

By the end of Run 3 in 2025, the LHC will have collected, by combining the ATLAS and CMS dataset, more than 600 fb^{-1} of integrated luminosity. A naive extrapolation of the most recent Run 2 results indicates that double Higgs production, as predicted by the SM, will not be observed even with the Run 3 dataset. Assuming current detector performance, it will be possible to set an upper limit on the di-Higgs production cross-section of 1-3 times the SM value at 95 % CL at best. A measurement of the Higgs self-coupling is thus out of reach of Run 3 and requires either a larger dataset, or/and a higher collision energy. The self coupling can be measured by the direct production of $h_{\rm SM}h_{\rm SM}$, or inferred indirectly through the contribution of the Higgs self-coupling to loop corrections to the single Higgs rate. However, for the indirect measurement to be relevant, it requires that new physics contributions dominate only the triple Higgs coupling shift. While this can naively be accounted for in a SMEFT fit, in realistic models this is much more difficult [32].

The projected sensitivities to the Higgs boson self-coupling at the various future colliders are presented in Table 2-4. These correspond to projections for a single experiment except for the 'combined' results which are HL-LHC projections. We see that this is an extremely challenging measurement at all colliders. Since the measurement is limited by the small number of $h_{\rm SM}h_{\rm SM}$ events, the measurement improves with the higher energy colliders. The indirect measurement improves with the luminosity of the lepton colliders since it is extracted from single Higgs production. In principle measurements at different center of mass energies can be used to disentangle the indirect effects of shifts in the triple Higgs couplings, however it also depends on the assumptions of what types of other operators can contribute.

The ATLAS and CMS experiments have determined that the Higgs boson quantum numbers are $j^{PC} = 0^{++}$ if the boson has definite CP. numbers. Small violations of CP symmetry in the $h_{\rm SM}VV$ and $h_{\rm SM}f\overline{f}$ couplings are still allowed and are an important target of future experimental measurements. Hadron colliders provide essentially the full spectrum of possible measurements sensitive to CP violation in the Higgs boson interactions. Most processes other than the Higgs gluon interactions could be studied at an e^+e^- collider, especially with the beam energy above the $t\bar{t}h_{\rm SM}$ threshold. Future e^+e^- colliders are expected to provide comparable sensitivity to HL-LHC in $h_{\rm SM}f\overline{f}$ couplings, and potentially higher sensitivity in hZZ couplings. A muon collider operating at the Higgs boson pole allows to measure the CP structure of the $h_{\rm SM}\mu\mu$ vertex with the beam polarization.

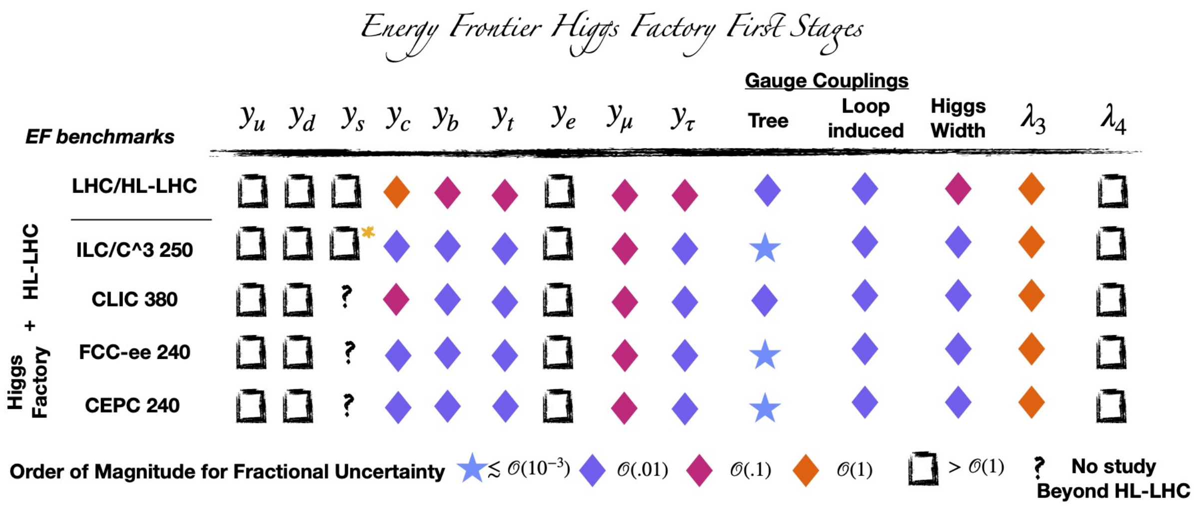

Figure 2-13. *A snapshot of future Higgs precision measurements of SM quantities based on the order of magnitude for the fractional uncertainties with the range defined through the geometric mean. In this figure the first states of each e^+e^- Higgs factory are shown in combination with the Hl-LHC, as well as the HL-LHC separately. The Higgs factories are defined as those listed in Section 2.2 of the Energy Frontier Report, excluding the 125 GeV muon collider whose timescale is in principle longer term. The specific precision associated to each coupling can be found in the corresponding Topical Group Report and references therein. A * is put on the ILC measurements for the strange Yukawa to single it out as a new measurement proposed during this Snowmass, and is shown in Fig 2-18. The ? symbol is used in the case where an official study has not yet been performed, for example in the case of strange tagging for CLIC, FCC-ee, and CEPC. This does not mean that they can't achieve a similar precision, but it is yet to be demonstrated whether based on their detector concepts the measurements is worse or can be improved.*

We have given an overview of the types of measurements that can be done at future colliders for Higgs precision, specific numbers for certain observables at all colliders have been shown, and general coupling fits in the case of the first stage $e+e^-$ Higgs factories were shown in Figure 2-12. However, it's important to understand that there are more observables than discussed so far, and also how high energy colliders fit into the Higgs precision program. All these numbers are in their exact form in the EF01/EF02 topical group report. However, instead of displaying all info as a large table or bar chart, we will conclude this section by displaying a quantitative coarse grained version of all Higgs precision results in Figure **??** and Figure 2-14.

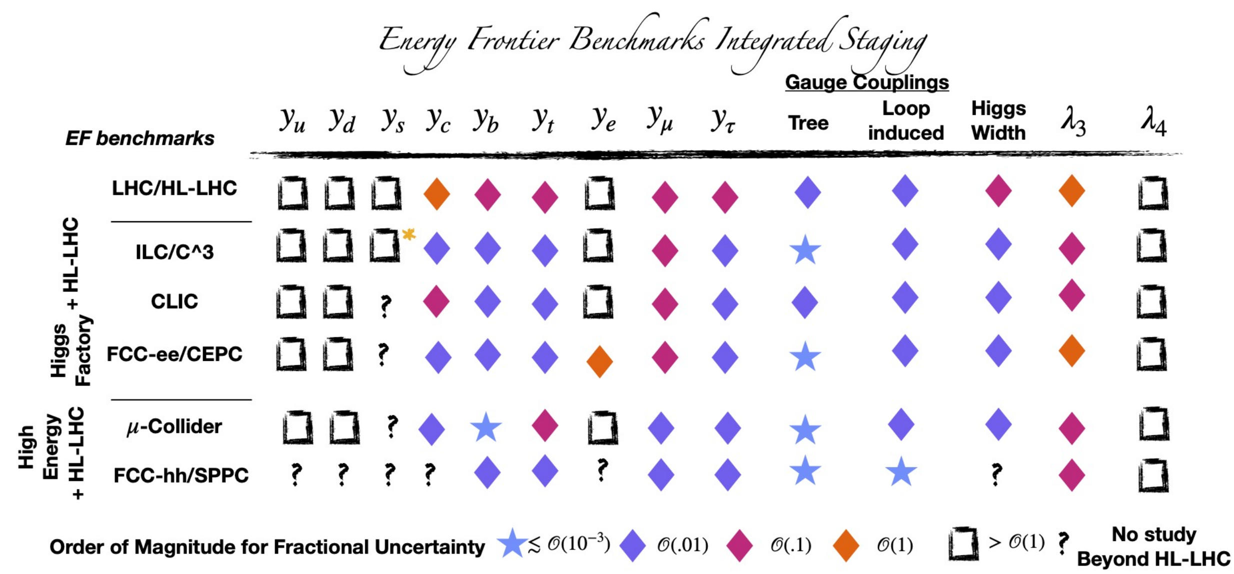

Figure 2-14. *A snapshot of future Higgs precision measurements of SM quantities based on the order of magnitude for the fractional uncertainties with the range defined through the geometric mean. In this figure the ultimate reach of states of all Higgs factories and High Energy colliders are shown in combination with the HL-LHC results, as well as the HL-LHC separately. All benchmarks and stages are defined in Section 2.2 of the Energy Frontier Report. The specific precision associated to each coupling can be found in the corresponding Topical Group Report and references therein. A * is put on the ILC measurements for the strange Yukawa to single it out as a new measurement proposed during this Snowmass, and shown in Fig 2-18. The ? symbol is used in the case where an official study has not yet been performed, but does not connotate that it should be worse than similar colliders, simply that whether it is better or worse based on detector design has not been demonstrated. Note that compare to Figure* **??**, *differences between Higgs Factories based on Linear Colliders and Circular colliders can be seen. Additionally for the High Energy Colliders such as FCC-hh and the Muon Collider, both offer extensions beyond the original Higgs factory proposals, of course on a longer timescale.*

As can be seen comparing Figure 2-12 and Figure **??**, Figure **??** shows more simply that all first stage Higgs factories are very similar. However, it also emphasizes that there are still a large number of missing pieces to the Higgs puzzle after only first stage Higgs factories. In Figure 2-14, all stages of future colliders that are discussed in Section 2.2, are combined that with the HL-LHC. As we see in this coarse graining, all colliders are compelling, and there is significant progress through Higgs factories and High Energy collider proposals compared to the HL-LHC program. In particular with the additional stages we start to see differences in the various proposed collider programs for the Higgs. Linear colliders beging to demonstrate advantages especially in the Higgs self coupling compared to circular e^+e^- colliders, whereas the circular colliders can potentially measure the electron Yukawa. Furthermore, High Energy colliders such as the muon Collider or FCC-hh extend the knowledge of the Higgs even further, albeit on different timecales. However, even if we ignore all BSM motivations for reaching a given precision, there clearly is a great deal of work to be done to completely test the SM Higgs sector beyond all colliders discussed thus far. In fact for certain couplings, they are well beyond the capability of any SM measurement at all proposed collider for this Snowmass. For example light quark Yukawas, or testing the quartic coupling of the Higgs boson directly. Therefore the study of the Higgs not only motivates the currently proposed colliders, but also R&D for the very far future if we ever want to finish testing the SM Higgs sector.

2.3.1.2 What can we learn about BSM physics from Higgs physics

The ultimate goal of precision Higgs physics is to learn about new physics at high scales, or to find portals to new physics that could be present at the EW scale or below. As discussed earlier from an EFT context, the generic scale associated with precision Higgs physics at future colliders typically extends up to a few TeV.

To go further requires the understanding of the interplay between UV models and Higgs physics. Given that the mapping of fundamental physics questions to Higgs direct and indirect observables is difficult to fully organize comprehensively, the topical report instead focused on specific types of models and observables: Higgs Singlets, Higgs Doublets (including Flavor), Loop-level deviations and Higgs Exotic Decays. Fundamental questions of course can be related to all of these types of models and is done so in the report. Other connections to fundamental questions are also emphasized in other parts of the EF report, for example whether the Higgs boson is an elementary or composite particle is investigated in Section 2.5.1.

Given that many of the model dependent topics have been covered extensively for years, we first wish to highlight some of the results that are new compared to the recent European Strategy Update:

- The phenomenology of a strong electroweak phase transition is significantly more nuanced than previously envisioned. It can manifest through shifts in the Higgs cubic coupling, but could still occur without any currently or far future measurable deviation in this coupling [33, 34, 35]. Deviations in all types of observables are also possibly correlated with the phase transition, including exotic Higgs decays [36]
- Flavored phenomenology is much richer than previously explored. Flavor violating decays have now richer possibilities and models [37, 38]. Flavor preserving deviations in light quarks Yukawas that are consistent now also exist [39, 40], and there are studies for direct probes of this at e^+e^- colliders and related resonance probes from the LHC and other colliders [41].
- Singlet phenomenology, a canonical example in beyond the Standard Model Higgs phenomenology can be quite a bit more varied, including the introduction of scalar resonance decaying to particles with different masses and these searches were explored more [42, 43, 44]
- There are now viable models of triple-Higgs production at the HL-LHC and beyond [43, 45, 40, 46]. The measurement of the quartic coupling should now be considered a standard part of beyond the Standard Model Higgs phenomenology and triple Higgs and quartic Higgs measurements should be pursued at future colliders.

We now give a sampling of results based on UV complete models, starting with the simplest extension of the Higgs sector of the SM with additional scalar singlet S. Despite the simplicity of this type of models, such results display a wide range of phenomenology and connections to fundamental physics questions. For example with a single degree of freedom from a real scalar, one can connect to the electroweak phase transition and thereby models of baryogenesis. This Higgs portal can then be connected to dark sectors and dark matter, or can be viewed as a proxy for models of neutral naturalness. The existence of a new scalar then also applies to the question of whether or not the Higgs is unique and modifies the Higgs potential. This can have implications for the stability of our universe. Thus, the rich phenomenology of the real singlet scalar is quite extensive. However, one can add additional scalar, i.e. a singlet complex scalar, or even more. The phenomenology can be further complicated and projections onto a two-dimensional plane aren't sufficient. In particular, because the masses of the various singlets can be varied thus resonance decays have a much wider range of phenomenology. Fig. 2-15 illustrates this possibility, where we see that a rate larger than that of $h_{\rm SM}h_{\rm SM}$ is possible[42].

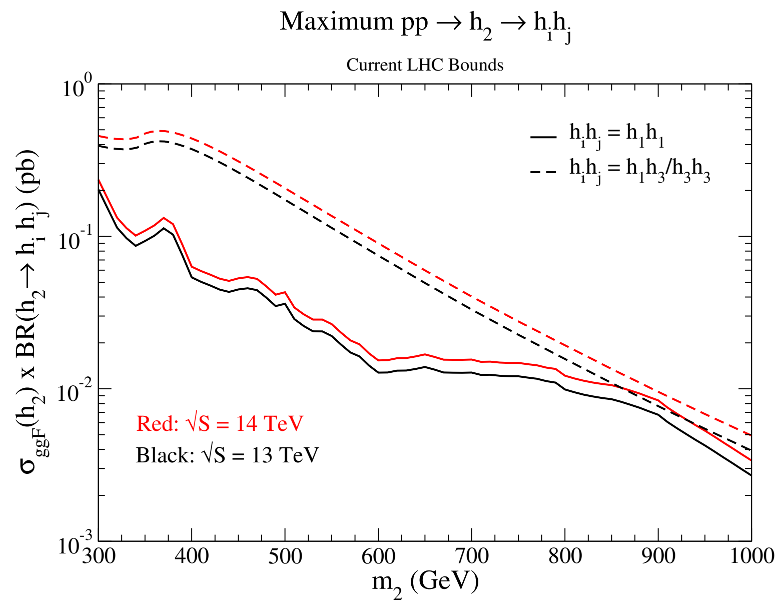

Figure 2-15. *Production of a pair of Higgs bosons in the complex singlet model. h_1 is the SM Higgs boson, and h_2, h_3 are new scalars. The maximum rates allowed by current LHC data are shown[42].*

Two Higgs doublet models (2HDMs) provide the next simplest extension after scalar singlets to the Higgs sector. They are particularly interesting because they allow for a new state with SM gauge charge that can also acquire a VEV while naturally allowing for small electroweak precision corrections. The new doublet allows for additional higgs bosons beyond the observed 125 GeV CP-even neutral scalar h, namely, an additional CP-even neutral scalar H, one CP-odd Higgs boson A, and a pair of charged Higgs bosons $H^{\pm}$. Restricting ourselves to the standard types of 2HDM still allows for an enormous range of phenomenology especially to those not fully familiar with the models. The standard parametrization of the physics is done in terms of a ratio of the VEVs of the 2HDM states, $\tan\beta$, and a mixing angle $\cos(\beta - \alpha)$ as well as the masses of the various eigenstates.

Precision Higgs measurements probe the model parameter space as demonstrated in Fig. 2-16 [47] and the improvement at lepton colliders for moderate $\tan\beta$ is apparent. The RHS of Fig. 2-16 demonstrates the ability of a high energy muon collider to probe the parameter space of the 2HDM models. We note that the region of moderate $\tan\beta$ is best probed by B decays. The direct search for the heavier Higgs bosons of the 2HDM is the provenance of the HL-LHC. For high $\tan\beta$, the decay of the heavier Higgs boson to $\tau^+\tau^-$ provides a stringent limit, as seen in Fig. 2-17.

Two Higgs doublet models have also allowed for a wider range of phenomenology. In particular 2HDMs do not have to be restricted to the usual 4 types of natural flavor conserving models. In Figure 2-18 an example of an SFV 2HDM exemplifies the wide range of phenomenology associated to direct and indirect searches, as well as the new techniques proposed at the ILC for tagging strange quarks directly. These models and measurements can also be further extended into relevant bounds on up and down quark yukawas as also shown in the ILC whitepaper [41].

There are of course numerous connections to deeper questions and additional models covered in the topical report, but at a general level even Figure 2-7 does provide important lessons. The first is that many observables map to fundamentally different questions related to the Higgs boson. It is, therefore, non-trivial to connect from observables related to Higgs physics with fundamental questions. This has been referred to

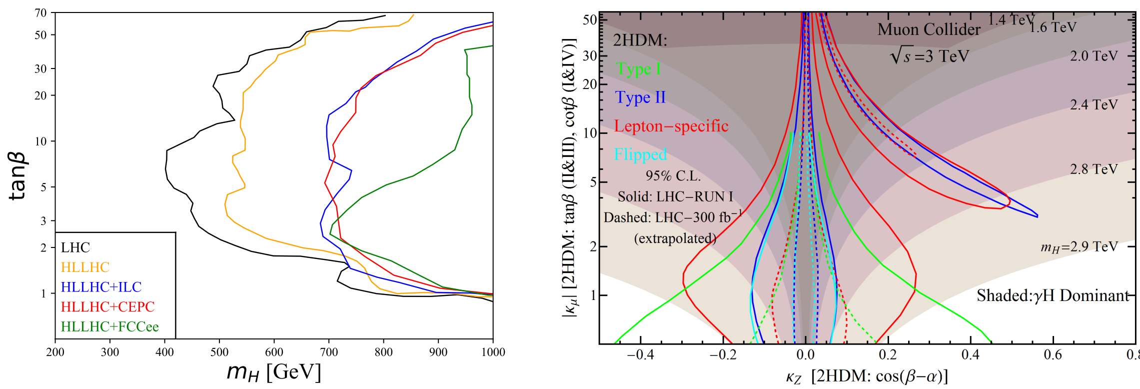

Figure 2-16. *Limits on the parameters of a 2HDM from precision Higgs couplings. LHS: Limits from future e^+e^- colliders [47]. RHS: Limits from a 3 TeV muon collider.*

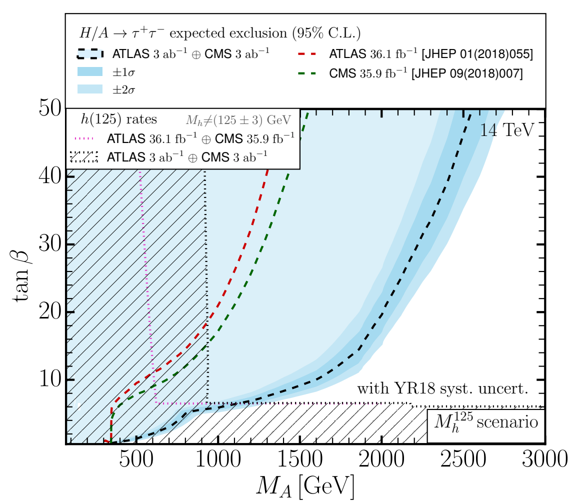

Figure 2-17. *Capability of HL-LHC to probe the scalar sector of the 2HDM.*

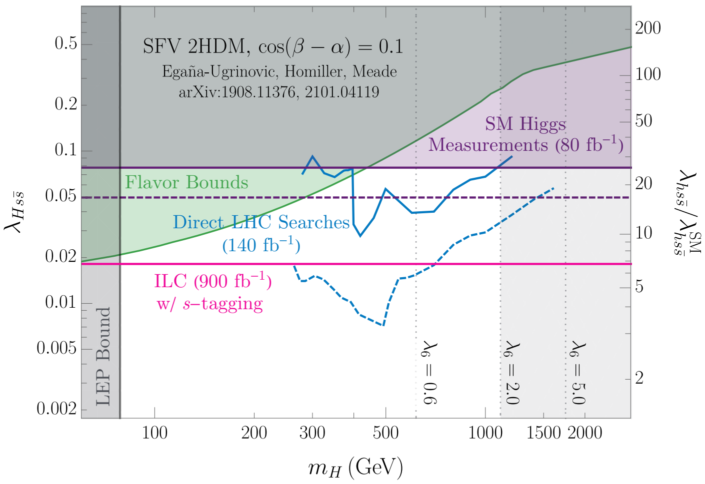

Figure 2-18. *A 2HDM with non standard Yukawa couplings, in this case an enhanced coupling to the strange quark. This can be probed through direct bounds on new di Higgs resonances, precision Yukawa measurements, as well as flavor physics and other single Higgs properties.*

as the "Higgs Inverse Problem", in analogy with the previously coined LHC inverse problem for BSM physics. Examples of this are given in the topical report as well as in the EF04 report. The second important lesson, alluded to in Figure 2-7, is that Higgs related observables do not just fall into the standard κ or effective field theory (EFT) fits. If there are any deviations in Higgs couplings, or differential measurements etc., there *must* be new physics that couples to the Higgs boson which gives origin to it. How it can be searched for is an ever expanding program and depends on the mass scale of new physics and collider energy. As mentioned earlier in the context of Higgs width measurements, there is an ever expanding program of "Higgs without Higgs" measurements and other types of differential probes being discovered. Suffice it to say, even 10 years after the Higgs discovery, we are still in the earliest stages of fully exploiting the potential connection of the Higgs to BSM physics.

2.3.2 Heavy-flavor and top quark production

The top quark plays a special role in the EW sector of the SM, with a Yukawa coupling (y_t) of order unity ($y_t = \sqrt{2}m_t/v \approx 1$, m_t is the top-quark mass and v is the vacuum expectation value of the Higgs field), introducing large quadratic corrections to the Higgs-boson mass, and affecting the stability of the EW vacuum [48]. The top-quark sector is therefore especially suitable for precision EW tests and to search for possible beyond-the-SM (BSM) physics. Figure 2-19 illustrates the different topics that are addressed through studying top quarks. As the heaviest of all elementary particles, the top quark is relevant for understanding the Higgs boson mass and quark masses. Precise measurements of the masses of the top quark (Section 2.3.2.1), the Higgs boson and the W boson provide a stringent test of the EW sector of the SM. The top quark decays before it can hadronize, making it the only bare quark that can be studied directly, including at high momenta, see Section 2.4.1.3. Top-quark production (Section 2.3.2.2) and decay kinematic information constrains top-quark EW couplings (Section 2.3.3) and the CKM element V_{tb}. Searches for FCNC and CP violation focus on the top quark couplings. Direct searches for new particles and interactions look for top-quark partners, SUSY, and high-mass resonances decaying to top quarks (Section 2.5). Studies of top-quark production at the highest energies (multi-TeV) probe models of compositeness, see Section 2.5.1.

The abundance of top quarks at the LHC makes them ideal for detector calibration of bottom-quark tagging and bottom- and light-quark jet energy calibration.

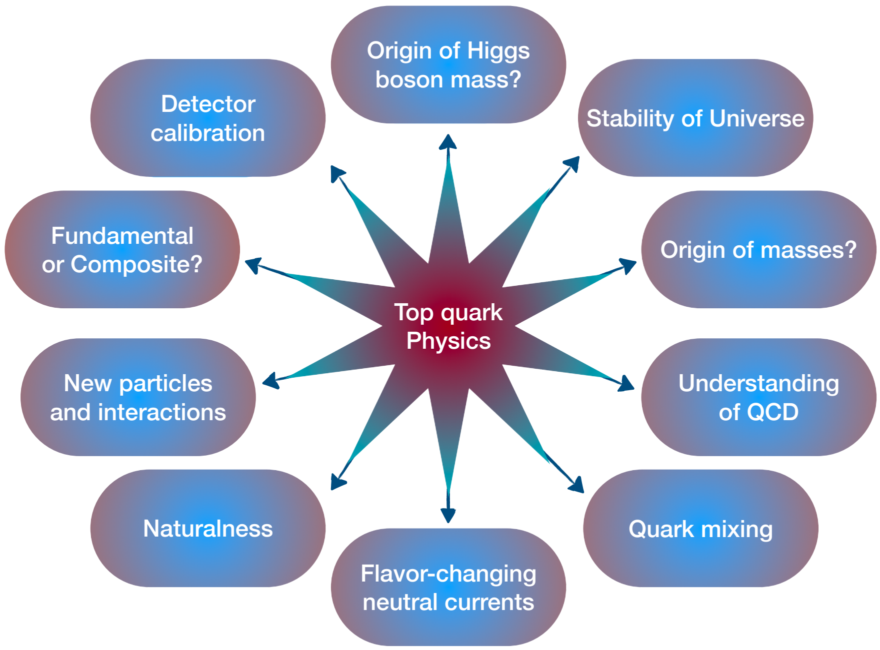

Figure 2-19. *Illustration of physics and studies that are studied with top quarks.*

Top-quark production processes contribute important backgrounds in many precision measurements and searches. Lepton colliders running at or above the top-quark production threshold provide significantly improved measurements of the top quark mass and its couplings. Precision measurements of top-quark and bottom-quark production at lepton colliders are the inputs needed to significantly improve the sensitivity of third generation and global EFT fits, see Section 2.3.3.

2.3.2.1 Top-quark mass

The top quark mass m_t is one of the most important parameters of the SM and relevant as an input for precise predictions and for the understanding of SM properties such as the stability of the spontaneously broken vacuum state. Top quark loop corrections impact the mass of the W boson, a top mass change of 100 MeV changes the S boson mass by 1 MeV [49]. Thus, a precision of better than 500 MeV is required for top mass measurement at the HL-LHC, and a precision of better than 50 MeV is required for a future lepton collider for precision EW fits [50, 51], see also Section 2.3.3.1. Since isolated quarks cannot be observed, the top quark mass is not physical, but a renormalization-scheme-dependent quantity. This scheme dependence can only be well-defined and controlled for mass-sensitive observables that are calculable in perturbation theory (at least at the NLO level). The currently most precise top-quark mass determinations at the LHC are obtained from the direct reconstruction of the top quark decay products (jets and leptons). Analytic QCD calculations are not available for the kinematic distribution of these objects, therefore the top-quark mass is extracted from comparisons to predictions by MC generators (mass from decay or MC mass). It is estimated that interpreting the mass from decay in a well-defined scheme (like the $\overline{\text{MS}}$ scheme) has an uncertainty of about 500 MeV [52, 53]. The current and expected precision for measurements of the mass from decay are compared to the projections from Snowmass 2013 in Figure 2-20. The recent measurements significantly improved on the projections from 2013. So far, only individual measurements at 13 TeV by ATLAS and CMS are available at the LHC. Significant improvements are expected when ATLAS and CMS combine multiple measurements at 13 TeV.

The top-quark pole mass by contrast is calculable in perturbation theory and is obtained from top-quark production measurements. A summary of the precision of the current and expected precision in top pole mass measurements is compared to the direct measurements in Figure 2-20. The pole mass precision has a large contribution from theoretical uncertainties, these mass measurements are currently limited by theory modeling and in particular the uncertainties in the parton distribution functions. The LHC Run 2 measurements at 13 TeV have not yet been combined between analysis channels and experiments, this combination is expected to reduce the uncertainty significantly. The projection for LHC Run 3 assumes that the experimental uncertainties will benefit from combinations, and that the theory uncertainties are halved. The HL-LHC projection assumes another halving of the theory uncertainties, including the interpretation uncertainty for the mass from decay [54].

δm_t^{pole} [GeV]	Tevatron	LHC Run 1	LHC Run 2	LHC Run 3	HL-LHC
$\sqrt{s}$ [TeV]	1.96	7/8	13	13.6	14
$\mathcal{L}[\text{fb}^{-1}]$	10	20	140	300	3,000
Experimental uncertainty	2.2	1.0	0.8	0.5	0.5
Theoretical uncertainty	1.4	0.7	1.0	0.5	0.25
Total uncertainty	2.5	1.2	1.3	0.71	0.56

Table 2-5. *Current (Tevatron [55], LHC Run 1 [56], and LHC Run 2 [57]) and anticipated (Run 3 and HL-LHC) experimental and theoretical uncertainties in the measurement of the pole mass, m_t^{pole} (indirect measurement) at hadron colliders [54].*

The ultimate precision in the top quark mass will be reached in a scan of the top-quark production threshold at a lepton collider. The corresponding expected precision for the different collider options is shown in Table 2-6. The overall uncertainty is expected to be limited by systematic uncertainties, in particular in the theoretical predictions, including the uncertainty on the strong coupling α_s. The top-quark width is similarly measured with the highest precision at a lepton collider, in combination with the top-quark mass in an energy scan of the top-production threshold. The Yukawa coupling of the top quark y_t can be measured in the same scan; the plateau above the top-production threshold is sensitive to y_t [58].

2.3.2.2 Top-quark production processes

Top quark are produced copiously at the hadron colliders in many different production modes, $t\bar{t}$, single top, and both modes in association with other quarks and bosons. Modeling the different processes requires precision high-order QCD calculations with heavy quarks. The cross-sections for the production of top quark pairs, as well as top quark pairs in association with various other particles are shown in Figure 2-21 [59]. Measuring all of these processes is possible with high precision at the HL-LHC. Even the process with the lowest production cross section, the production of four top quarks (lowest line in Figure 2-21), can be measured with an uncertainty of about 20% at the HL-LHC, and should be measurable to about a percent at higher-energy hadron colliders (including FCC-hh) [60, 61]. This production mode has the highest energy threshold of all top-quark-related SM processes studied at hadron colliders. It is sensitive to y_t and BSM interactions, for example contact interactions [60]. The production of top-quark pairs in association with vector bosons (W and Z) contributes backgrounds to many processes with vector-boson final states. Precision measurements of the processes shown in Figure 2-21 and the corresponding single top quark processes are

δm_t^{PS} [MeV]	ILC	CLIC	FCC-ee
$\mathcal{L}[\mathrm{fb}^{-1}]$	200	100 [200]	200
Statistical uncertainty	10	20 [13]	9
Theoretical uncertainty (QCD)	40 – 45		
Parametric uncertainty α_s	26	26	3.2
Parametric uncertainty y_t HL-LHC	5		
Non-resonant contributions	< 40		
Experimental systematic uncertainty	20 – 30		11 – 20
Total uncertainty	40 – 75		

Table 2-6. *Anticipated statistical and systematic uncertainties in the measurement of the threshold mass, m_t^{PS}, from a threshold scan around 350 GeV obtained with a one-dimensional fit of the top quark mass, keeping Γ_t, y_t, and α_s fixed. CLIC assumes a lower integrated luminosity than the other facilities. For comparison, the statistical precision achievable with 200 fb^{-1} for CLIC is also given. It should be noted that the results shown for ILC and FCC-ee assume a 8-point scan with a compressed energy range which improves sensitivity for m_t^{PS} at the expense of y_t sensitivity. For the standard 10-point scan assumed for CLIC the statistical uncertainties would be 12 and 10 MeV for ILC and FCC-ee, respectively. The uncertainty due to the current world average for α_S is shown for ILC and CLIC, while for FCC-ee, the run at the Z pole (Tera-Z) will reduce this uncertainty significantly. Concrete studies for CEPC are not yet available, but it can be assumed that uncertainties are similar as for FCC-ee. See text for further details.*

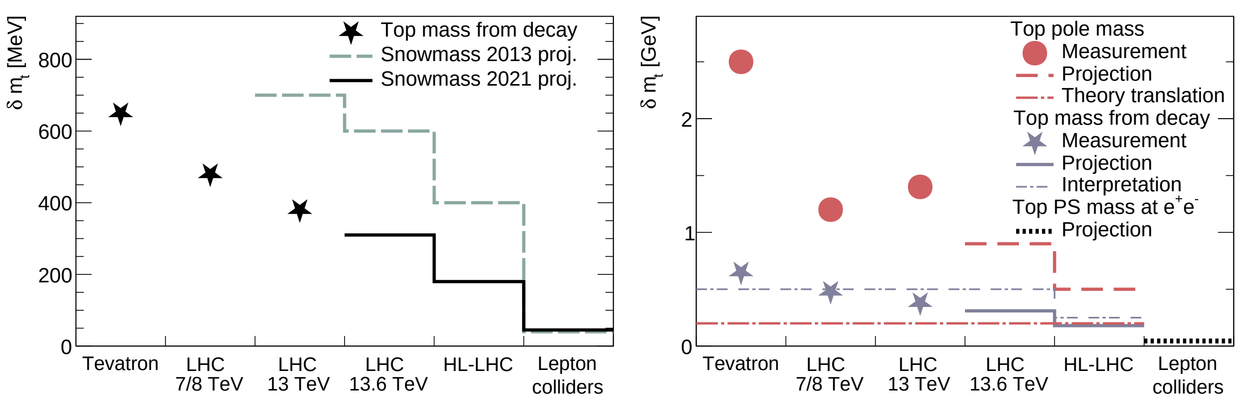

Figure 2-20. *(Left) Comparison of top-quark mass measurements from top decay (MC mass) at the Tevatron and the LHC, and projections for future LHC sensitivity and for future mass sensitivity from a top threshold scan at a lepton collider. (Right) Comparison of top-quark mass from decay and pole mass measurements at the Tevatron and the LHC and projections for future sensitivity, including the expected precision of mass measurements at lepton collider [54]. The dash-dotted lines show the approximate uncertainties in interpreting the mass from decay in and translating the pole mass to the $\overline{MS}$ scheme [52, 53].*

utilized in global EFT fits. It should be possible to reach a precision of O(1%) for $t\bar{t}$ production, higher for other processes. This requires careful calibration, improved modeling of top-quark and other processes, and theory calculations beyond N^{3}LO; currently the scale uncertainty on $\sigma(t\bar{t})$ is about 2% at N^{2}LO with NNLL resummation, while the PDF uncertainty is about 4% [62]. Extending the differential top quark measurements to high, multi-TeV transverse momenta gives sensitivity to 4-fermion interactions involving the third generation.

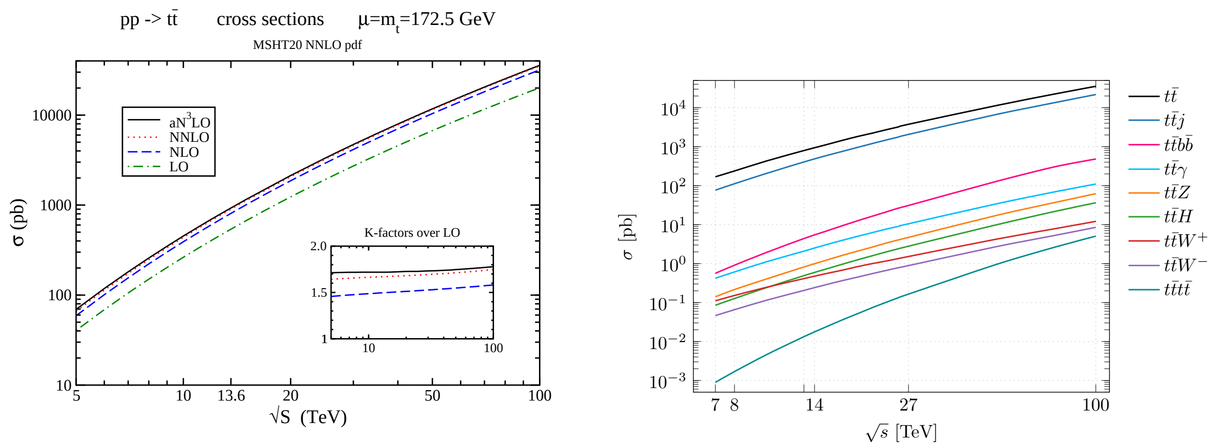

Figure 2-21. *Total cross sections as a function of the center-of-mass energy $\sqrt{s}$ at pp colliders for (left) $t\bar{t}$ production at LO, NLO, N^{2}LO and approximate N^{3}LO [59] and for (right) various $pp \to t\bar{t}X$ processes at NLO. The $pp \to t\bar{t}$ is also shown for reference. Light objects are subject to the following cuts $p_T > 25$ GeV, $|\eta| < 2.5$ and jets are clustered using the anti-k_T algorithm with $R = 0.4$.*

At lepton colliders running at or above the top-quark production threshold, $t\bar{t}$ production can be measured with high precision and the couplings of the top-quark to the Z boson measured precisely. These measurements, as well as the corresponding measurements of the production of bottom-quark pairs at similar precision, will allow to significantly extend the sensitivity of global EFT fits, see Figure 2-22. Producing $t\bar{t}$ in association with Higgs, W or Z requires significantly higher CM energies at a lepton collider.

2.3.2.3 Angular correlations

The measurements of cross-sections of top-quark production processes provide important inputs to global EFT fits [63]. Differential production measurements and studies of top quark decay and top-quark final state correlations provide further constraints [64]. At hadron colliders, these include top-quark pair and single top-quark production processes, and associated production, measured differentially. The precision of the measurements is limited by systematic uncertainties, the largest of which are due to jet energy calibration and QCD modeling of the top-quark final states. The largest uncertainties in the theory modeling are due to parton distribution functions.

At lepton colliders, the final state can be fully reconstructed, and most measurements have virtually no background, in contrast to hadron colliders. This means that despite the smaller sample sizes, lepton colliders can provides additional sensitivity to the top quark coupling to the W boson, typically through the use of optimal variables to be used in EFT fits, see Section 2.3.3.

Figure 2-22 shows the reach of the HL-LHC and the improvement that can be expected from adding lepton collider data to the Wilson coefficients relevant for top quark couplings in a global EFT fit. The fit uses cross-sections for various top-quark production processes (Section 2.3.2.2) and angular correlations at the HL-LHC, and optimal variables at the lepton collider.

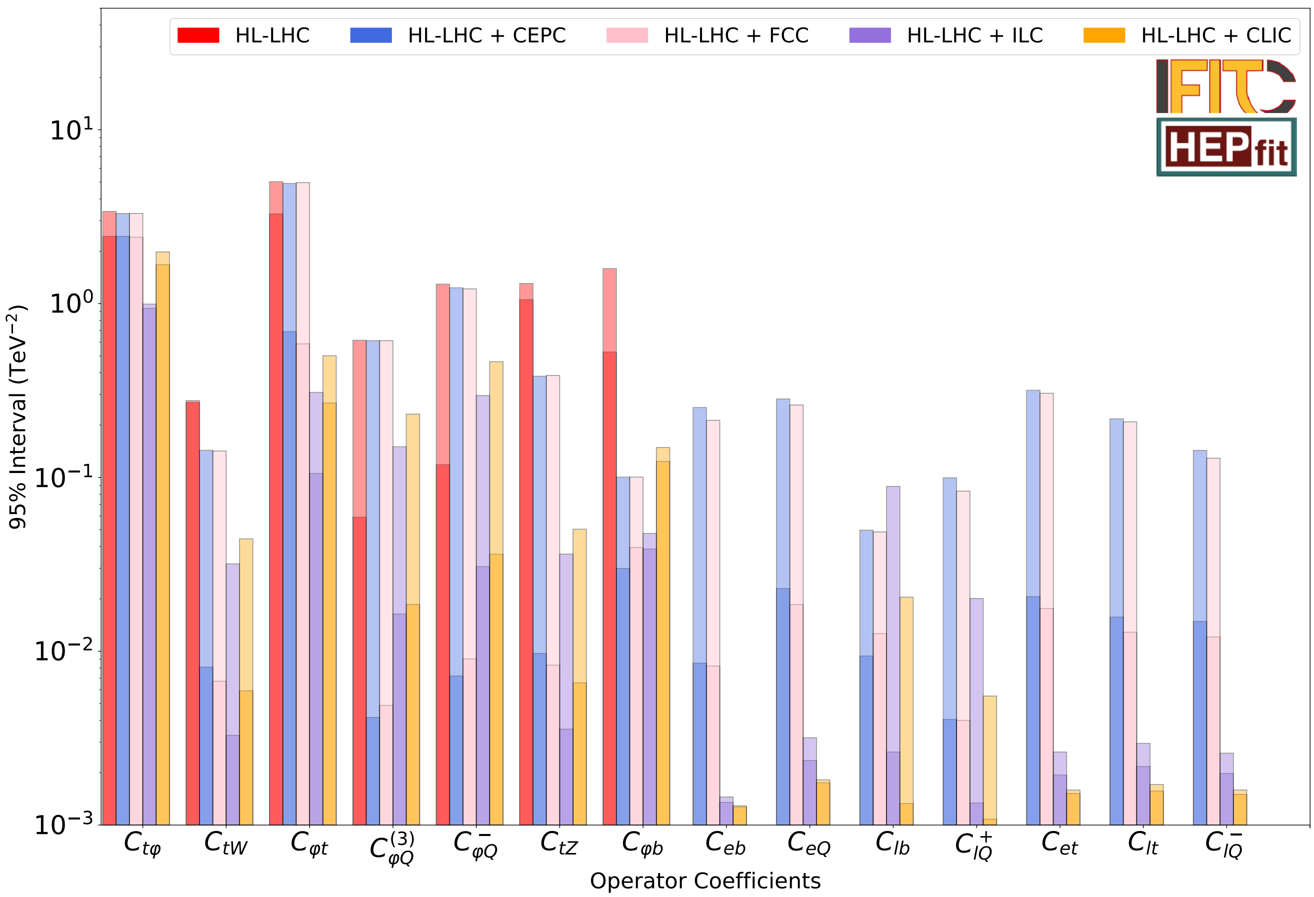

Figure 2-22. *Comparison of the constraints expected from a combination of HL-LHC and lepton collider data on Wilson coefficients for EFT operators relevant to top quark couplings, see Section 2.3.3. The solid bars provide the individual limits of the single-parameter fit and the shaded ones the marginalised limits of the global fit.*

2.3.2.4 BSM physics from top physics

The top quark is a sensitive probe in direct searches for new physics, described in Section 2.5 and indirectly in EFT fits, see Sections 2.3.2.3 and 2.3.3. At hadron colliders, precision measurements of top-pair production are sensitive to SUSY top squarks with masses close to the top-quark mass. At all colliders, flavor-changing neutral currents can be probed in the production and in the decay of top quarks.

The correlation of the spins of the two top quarks in $t\bar{t}$ production can be measured precisely. It is also a sensitive probe of BSM physics, in particular stop quarks in the compressed region (stop mass close to top mass and small neutralino mass). Figure 2-23 shows the projected limit for a 30 GeV-wide corridor in stop mass ($m(\tilde{t})$) and neutralino mass ($m(\chi_0)$) around the top quark mass ($m(\tilde{t}) - m(\chi_0) - m(t)| < 30$ GeV) [65].

The width of the corridor corresponds to the experimental resolution and the region where direct stop searches are not sensitive because of the large *tbart* background. The limits expected for the HL-LHC are a factor two (at low $m(\tilde{t})$) to ten (at high $m(\tilde{t})$) better than the Run 2 limits in this region. The predicted SUSY stop pair production cross-section in this region is between 10 pb and 100 pb, meaning the entire area will be excluded.

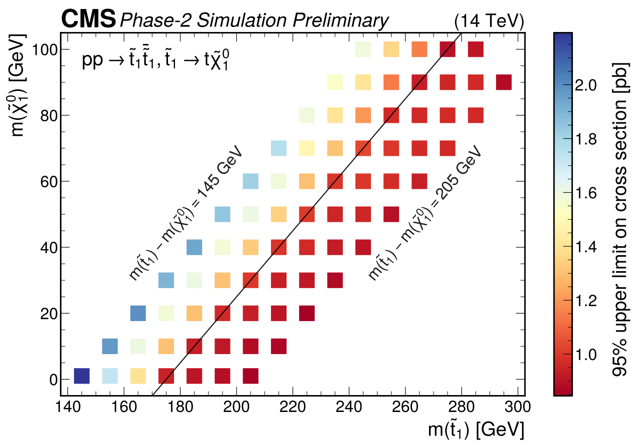

Figure 2-23. *Limit on the cross-section for SUSY stop production in the compressed region where the stop mass ($m(\tilde{t})$) is close to the neutralino mass ($m(\chi_0)$), $m(\tilde{t}) - m(\chi_0) = 175$ GeV [65]. Every point in this plot is excluded [65].*

Searches for flavor-changing neutral current interactions in single top-quark production at hadron colliders (sensitive to gluon FCNC interactions) and lepton colliders (sensitive to photon and Z boson FCNC interactions) take advantage of needing lower CM energy to produce one top quark rather than two. The large samples of top quarks collected at the LHC and expected at the HL-LHC allow for searches in the top-quark decay (sensitive to photon, Z boson, and Higgs FCNC interactions). The limits on the top decay branching ratios are around 10^{-4} with the Run 2 dataset, these will be improved to around 10^{-5} at the HL-LHC.

Lepton colliders are sensitive to FCNC couplings of the top quark to the photon and the Z boson, especially at energies below the $t\bar{t}$ production threshold [66, 58]. The production of a single top quark together with an up or charm quark provides a unique final state signature. Combining runs at multiple CM energies provides additional sensitivity, especially at the highest energies reached in e^+e- only by CLIC [67]. This is an area where a muon collider might also provide additional sensitivity.

As the heaviest fermion, it is also expected that the top quark plays a central role in models of compositeness, together with the Higgs boson [68]. Figure 2-24 compares the reach in the plane of mass scale and coupling $g*$ for a model of total right-handed top quark compositeness, giving rise to sizeable 4-top Wilson coefficients [69].

2.3.2.5 Heavy-flavor and top quark production summary

Table 2-7 compares a few top-quark measurements between different future collider options. Each of the measurements can be improved at future colliders beyond the precision at the HL-LHC. Significantly improving the precision of the top-quark Yukawa coupling beyond the 2-4% uncertainty expected at the HL-LHC [18] requires a high-energy lepton collider at a CM energy of 500 GeV or the FCC-hh. The precision of

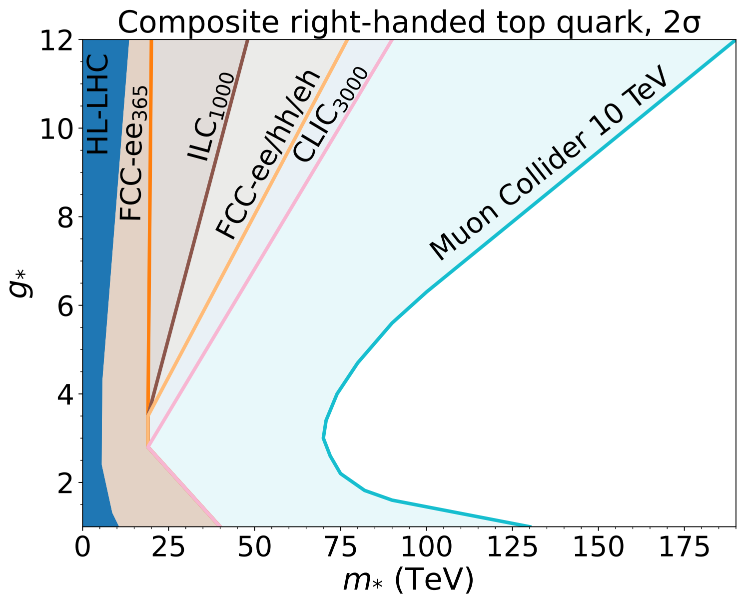

Figure 2-24. *Exclusion (2-σ) sensitivity projections for compositeness models for future colliders as labeled, for models where both the Higgs boson and the top quark with right-handed couplings are composite. Plot based on Refs. [68, 69].*

the coupling measurements to the SM bosons will all be significantly improved at a lepton collider running at or above the top-production threshold. The four-top coupling can be probed at hadron colliders, or at lepton colliders running at sufficiently high energies. Searches for flavor-changing neutral currents via the Z boson or photon are done in top-quark decays at hadron colliders, the sensitivity is significantly extended at lepton colliders running as a Higgs factory.

Parameter	HL-LHC	ILC 500	FCC-ee	FCC-hh
$\sqrt{s}$ [TeV]	14	0.5	0.36	100
Yukawa coupling y_t (%)	3.4	2.8	3.1	1.0
Top mass m_t (%)	0.10	0.031	0.025	–
Left-handed top-W coupling $C^3_{\phi Q}$ (TeV^{-2})	0.08	0.02	0.006	–
Right-handed top-W coupling C_{tW} (TeV^{-2})	0.3	0.003	0.007	–
Right-handed top-Z coupling C_{tZ} (TeV^{-2})	1	0.004	0.008	–
Top-Higgs coupling $C_{\phi t}$ (TeV^{-2})	3	0.1	0.6	
Four-top coupling c_{tt} (TeV^{-2})	0.6	0.06	–	0.024

Table 2-7. *Anticipated precision of top quark Yukawa coupling and mass measurements, and of example EFT Wilson coefficient for the top quark coupling to W, Z and Higgs bosons, as well as a four-top Wilson coefficient. The reach of the CEPC is expected to mirror that of the FCC-ee.*

Significant theoretical effort is required to exploit the full potential of future colliders. Some of the biggest challenges are:

- Calibration of the top quark MC mass to a well-defined scheme in perturbation theory with a precision comparable to the experimental uncertainty.
- Computing cross-sections, inclusively and differentially at higher orders in perturbation theory, going to N^3LO in QCD for top pair production plus resummation, going to N^2LO in QCD for associated production processes, and including EW higher order corrections, see also the Les Houches wishlist [70].
- Reducing the PDF uncertainties, which are already now the largest theory uncertainties for several processes, most importantly top-pair production. This requires close interconnections between theory and experiment and new differential measurements of top production processes.
- Improving the modeling of the full event at the LHC and future hadron and lepton colliders and reducing parton shower uncertainties.

For more details about the status and necessary advances in high-precision theory see the Theory Frontier Topical Group reports on *Theory Techniques for Precision Physics* (TF06) and *Theory of Collider Phenomena* (TF07).

2.3.3 Electroweak precision physics and new physics constraints

The precise measurement of physics observables and the test of their consistency within the standard model (SM) are an invaluable approach, complemented by direct searches for new physics, to determine the existence of physics beyond the standard model (BSM).

The indirect search for new physics, which exploits off-shell and loop contributions of new particles, allows one to explore a much wider range of energy scales than those probed by direct searches in specific BSM scenarios. Such indirect BSM effects are typically inversely proportional to some power of the mass scale of the new degrees of freedom, so that high precision is crucial for probing large energy scales. The achievable precision of an experiment is determined by the statistics of the collected data sample, the experimental and theoretical systematic uncertainties, and their correlations.

2.3.3.1 Electroweak precision physics

The current precision for a few selected electroweak precision pseudo-observables (EWPOs) is listed in Tab. 2-8. The HL-LHC with integrated luminosity of 3000 fb^{-1} can make improved measurements of certain EWPOs, as shown in Tab. 2-8. The effective weak mixing angle can be extracted from measurements of the forward-backward asymmetry in Drell-Yan production, $pp \to \ell^+\ell^-$ ($\ell = e, \mu$), while the W-boson mass can be extracted from measurements of $pp \to \ell\nu$. Both measurements crucially depend on precise knowledge of parton distribution functions (PDFs) and theory input for QCD and EW corrections, where the SM has to be assumed for the latter.

Future high-luminosity e^+e^- colliders can be used to study the masses and interactions of electroweak bosons to much higher precision than before. We here focus on four collider proposals: ILC [73, 74, 22], CLIC [75, 76], FCC-ee [77, 25], and CEPC [78, 79]. For ILC, CLIC and FCC-ee, we use the run scenarios and integrated luminosities in Tab. 2-1, where for CEPC the 50 MW upgrade is assumed, which corresponds to 100 ab^{-1} on the Z pole, 6 ab^{-1} at the WW threshold, and 1 ab^{-1} at the $t\bar{t}$ threshold [79]. For ILC also the GigaZ option with 100 fb^{-1} on the Z pole is considered. [Note that a Z-pole run is also considered as a possible option for CLIC [**?**].] Table 2-10 summarizes the achievable precision for a range of EWPOs.

EWPO Uncertainties	Current	HL-LHC
Δm_W (MeV)	12 / 9.4†	5
Δm_t (GeV)	0.6*	0.2
$\Delta \sin\theta^\ell_{\rm eff}$ ($\times 10^5$)	13	< 10

† The recent W mass measurement from CDF with 9.4 MeV precision [71] has not yet been included in the global average [72].

* This value includes an additional uncertainty due to ambiguities in the top mass definition (see **EF03 report** for more details).

Table 2-8. *The current precision of a few selected EWPOs, based on data from LEP, SLC, TeVatron and LHC [72], and expected improvements from the HL-LHC [18].* Δ (δ) *stands for absolute (relative) uncertainty.*

The table separately lists the expected statistical and experimental systematic uncertainties. Note that the latter are based on assumptions about future performance improvements that cannot be substantiated at this time. Uncertainties due to the physics modeling affect all collider proposals equally. As part of the Snowmass 2021 process, a consistent set of assumptions is being used and applied uniformly. **See EF04 report for more details.**

The impact of these estimated future precision measurements on the indirect determination of the Higgs-boson and top-quark mass is illustrated in Fig. 2-25. The dependence on m_H and m_t appears in loop corrections to the SM theory predictions for Z couplings parameters and the W mass, and their agreement with direct measurements of these masses is a highly non-trivial test of the SM.

For "canonical" electroweak precision measurements (Z-pole, WW threshold), circular e^+e^- colliders (FCC-ee, CEPC) have in general a higher sensitivity than linear colliders (ILC, CLIC) due to the high luminosity at center-of-mass energies below 200 GeV. Beam polarization at the linear colliders improves their sensitivity and can help to control systematics. In particular, for a linear collider run on the Z pole, beam polarization would enable measurements of the asymmetry parameters A_f with a precision that is only a factor of a few worse than for circular colliders, in spite of several orders of magnitude larger statistics for Z-pole physics at circular colliders.

For many of the most precisely measurable precision observables at linear colliders, the most significant source of experimental systematics stems from the polarization calibration. For the circular colliders, on the other hand, modeling uncertainties for hadronic final states appear to be the dominant systematic error source.

To exploit the full potential of the anticipated precision of any future e^+e^- collider, theory inputs are needed on multiple fronts. Accurate Monte-Carlo (MC) tools for the simulation of QED and QCD radiation are crucial for the evaluation of acceptance effects, and theory calculations including higher-order effects are needed for the prediction of irreducible backgrounds. For the interpretation of electroweak precision measurements, one needs to compare the measured values to their expectation within the SM, which requires multi-loop theory computations. For the anticipated experimental precision FCC-ee, CEPC, ILC or CLIC, the current state of the art of theory calculations needs to be extended by at least one order of perturbation theory, *i.e.* N^{2}LO/NLL contributions for MC tools and backgrounds, and N^{3}LO and partial N^{4}LO contributions for the SM predictions. **See EF04 report for more details.**

The SM predictions also rely on other SM parameters are inputs, such as the electromagnetic coupling at the weak scale, $\alpha(m_Z)$, the top-quark mass, m_t, and the strong coupling, α_s. The current uncertainties for these parameters would severely limit the possibility for future high-precision studies, and thus it is necessary to

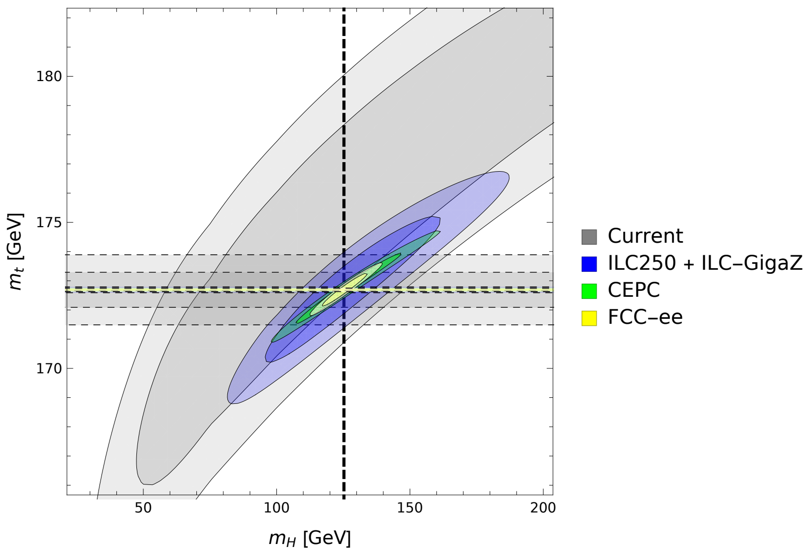

Figure 2-25. *Indirect sensitivity to m_H and m_t for a fit of SM theory predictions to current and projected future data for electroweak precision tests (W mass and Z-pole quantities). For comparison, the direct measurement precision is also shown (on the scale of the plot the width of the m_H band is not visible). The light (dark) shaded areas depict 95% (68%) confidence level regions. For the future collider scenarios it is assumed that the central values coincide with the SM expectations.*

perform improved measurements of these quantities at the future e^+e^- colliders. See sections 2.3.2.1 and 2.4.1.2 for more information.

The impact of the uncertainties of the SM input parameters on the interpretation of electroweak precision measurements is illustrated in Tab. 2-9. In addition to current measurement precision, two future scenarios are considered, where Scenario 1 assumes improvements from a Higgs factory with moderate luminosity spent on the Z pole and no $t\bar{t}$ running, whereas Scenario 2 displays the full potential of achievable precision at future e^+e^- colliders. Note that the dependence of the predictions for Γ_Z and R_ℓ on α_s are to a certain extent circular, since these quantities would be used for the extraction of the strong coupling constant at future e^+e^- colliders [81].

Experiments at lower-energy e^+e^- colliders, lepton-proton colliders, or neutrino scattering facilities can deliver complementary information about electroweak quantities, such as the running electroweak mixing angle at low scales, or the separate determination of up- and down-quark electroweak couplings.

A muon collider with center-of-mass energy $\sqrt{s} \approx 91$ GeV [82] would also be very interesting for electroweak precision measurements, but more studies are needed.

EWPO uncertainties	Current param. error	Projected param. error	
		Scenario 1	Scenario 2
Δm_W (MeV)	5	2.8	0.6
$\Delta\Gamma_Z$ (MeV)	0.5	0.3	0.1
$\Delta \sin^2\theta^\ell_{\rm eff}$ ($\times 10^5$)	4.2	3.7	1.1
ΔA_ℓ ($\times 10^5$)	30	25	7.5
δR_ℓ ($\times 10^3$)	6	3.2	1.3

Input par. uncertainties	Δm_t [GeV]	Δm_H [GeV]	Δm_Z [MeV]	$\Delta(\Delta\alpha)$	$\Delta\alpha_s$
Current	0.6	0.17	2.1	10^{-4}	9×10^{-4}
Scenario 1	0.3	0.02	0.8	10^{-4}	5×10^{-4}
Scenario 2	0.05	0.01	0.1	3×10^{-5}	2×10^{-4}

Table 2-9. *Impact of uncertainties of SM input parameters on the prediction of a few selected EWPOs (see Ref. [80]). Current uncertainties are compared to two future scenarios, see bottom table.*

Quantity	current	ILC250	ILC-GigaZ	FCC-ee	CEPC	CLIC380
$\Delta\alpha(m_Z)^{-1}$ ($\times 10^3$)	17.8*	17.8*		3.8 (1.2)	17.8*	
Δm_W (MeV)	12*	0.5 (2.4)		0.25 (0.3)	0.35 (0.3)	
Δm_Z (MeV)	2.1*	0.7 (0.2)	0.2	0.004 (0.1)	0.005 (0.1)	2.1*
Δm_H (MeV)	170*	14		2.5 (2)	5.9	78
$\Delta\Gamma_W$ (MeV)	42*	2		1.2 (0.3)	1.8 (0.9)	
$\Delta\Gamma_Z$ (MeV)	2.3*	1.5 (0.2)	0.12	0.004 (0.025)	0.005 (0.025)	2.3*
ΔA_e ($\times 10^5$)	190*	14 (4.5)	1.5 (8)	0.7 (2)	1.5 (**negl.?**)	64
ΔA_μ ($\times 10^5$)	1500*	82 (4.5)	3 (8)	2.3 (2.2)	3.0 (1.8)	400
ΔA_τ ($\times 10^5$)	400*	86 (4.5)	3 (8)	0.5 (**20**)	1.2 (**6.9**)	570
ΔA_b ($\times 10^5$)	2000*	53 (35)	9 (50)	2.4 (21)	3 (21)	380
ΔA_c ($\times 10^5$)	2700*	140 (25)	20 (37)	20 (15)	6 (**30**)	200
$\Delta\sigma^0_{\rm had}$ (pb)	37*			0.035 (4)	0.05 (2)	37*
δR_e ($\times 10^3$)	2.4*	0.5 (1.0)	0.2 (0.5)	0.004 (0.3)	0.003 (0.2)	2.7
δR_μ ($\times 10^3$)	1.6*	0.5 (1.0)	0.2 (0.2)	0.003 (0.05)	0.003 (0.1)	2.7
δR_τ ($\times 10^3$)	2.2*	0.6 (1.0)	0.2 (0.4)	0.003 (0.1)	0.003 (0.1)	6
δR_b ($\times 10^3$)	3.0*	0.4 (1.0)	0.04 (0.7)	0.0014 (< 0.3)	0.005 (0.2)	1.8
δR_c ($\times 10^3$)	17*	0.6 (5.0)	0.2 (3.0)	0.015 (1.5)	0.02 (1)	5.6

Table 2-10. *EWPOs at future e^+e^-: statistical error (estimated experimental systematic error). Δ (δ) stands for absolute (relative) uncertainty, while * indicates inputs taken from current data [**?**]. See Refs. [31, 83, 84, 85, 22, 79].*

2.3.4 EFT and new physics

2.3.4.1 Multi-boson processes

The SM predicts the existence of multi-boson interactions, which give rise to final states with two or three bosons. Anomalies in the rate and kinematic of these final states can be indicative of new physics not currently described in the SM. Such anomalies can be parametrized through modifications of the strength of form of the SM multi-boson vertices. A newer approach consists in using EFT operators of dimension six or above, where measurements of multi-boson processes can be recast as direct determinations of the Wilson coefficients of these operators.

It shall be noted that the sensitivity to BSM effects, or, in other terms, the upper limits to the Wilson coefficients of new operators, scale with a power of the c.o.m. energy, thus making multi-TeV colliders the ideal tools for studying these final states. At this time, the most promising avenues for reaching multi-TeV energies are proton-proton colliders or $\mu^+\mu^-$ colliders.

High-energy (> 1 TeV) lepton colliders are effectively boson colliders. The total cross-section for many production processes is dominated by vector-boson fusion (VBF) and/or vector-boson scattering (VBS) contributions. However, for studies of BSM effects at very high invariant masses, non-VBF processes become typically more dominant.

At multi-TeV lepton colliders, multiple electroweak gauge-boson production is ubiquitous, and new theoretical tools are needed for calculating and simulating these effects (e.g., theory modeling of EW PDF and fragmentation, ISR, FSR).

Plentiful experimental results with multi-boson final states are available. Both the ATLAS and CMS collaborations have measured di-boson [86, 87, 88, 89, 90, 91, 92, 93, 94], tri-boson processes [95, 96, 97, 98], as well as VBF/VBS processes [99, 100, 101, 102, 103, 104, 105, 106, 107, 108, 109], which are characterized by a $VVjj$ final state. Di-boson final states include W^+W^-, same-sign $W^\pm W^\pm$, WZ, ZZ, $Z\gamma$. Tri-boson final states include $W\gamma\gamma$, $Z\gamma\gamma$, $WV\gamma$ (where $V = W, Z$), and WVV' (where $V, V' = W, Z$).

Bounds on new physics have been determined in the language of anomalous gauge-boson couplings (aGCs) [86, 89, 90, 91, 94] and effective operators [87, 105, 106, 91, 107, 92, 93, 108, 98]. The latter is theoretically preferred since it provides a consistent power counting and allows one to implement theoretical consistency constraints. In these studies, only one or two aGCs/operators are allowed to be non-zero at the same time, i.e., no full aGC/SMEFT analysis has been performed.

The most up-to-date limits on gauge-coupling anomalies are available at Refs. [110, 111]. Expected limits at the end of the HL-LHC and HE-LHC runs are reported in Ref. [112].

2.3.4.2 SMEFT global fits

Assuming new physics scales are significantly higher than the EW scale, Effective Field Theories (EFT) provide a model-independent prescription that allows us to put generic constraints on new physics and to study and combine large sets of experimental data in a systematically improvable quantum field theory approach. All new physics effects are represented by a set of higher dimensional operators which consist of only the SM fields and respect the SM gauge symmetries.

The EFT approach has some features that are of particular interest for studying precision EW physics, for instance: it provides a well-defined theoretical framework that enables the inclusion of radiative corrections for both the SM and BSM parts; and the synergies between different precision EW measurements can be explored globally so that a comprehensive picture of the constraints on new physics can be drawn. However, the EFT approach also has some practical limitations since it has in principle an infinite number of degrees of freedoms, and it is only an adequate description if the new physics scales are larger than the experimentally reachable energies. In a realistic global EFT fit, various flavor assumptions and truncations to the lowest order of relevant operators often have to be applied.

A model-independent parametrization of the new-physics reach of different colliders is given by the SMEFT framework, where the SM is extended by higher-dimensional operators, with the leading contribution to most observables furnished by dimension-6 operators. Several subsets of such dimension-6 operators have been investigated in a set of global fits across a large number of observables: (a) operators contributing to electroweak gauge-boson interactions; (b) operators contributing to Higgs interactions; (c) operators contrbuting to top-quark interactions; and (d) operators contributing to four-fermion contact interactions.

For Snowmass 2021, the global EFT fit for European Study Group (ESG) [31] has been extended in a few directions [113]: consistent implementation of full EFT treatment in $e^+e^- \to WW$ using optimal observables; new inclusion of a large set of 4-fermion operators; more complete set of operators that are related to top-quarks. In all the fits, operators for third-generation fermions are treated independently, without assuming flavor universality, and in some cases even universality between the first two generations has been lifted. However, no flavor-changing operators were included in the analysis. The projections of the uncertainties of required input observables are provided by EF01 for Higgs related observables, EF03 for top-quark related observables, EF04 for W/Z related observables, and Rare Process and Precision Frontier (RF) for a set of low-energy measurements. Care has been taken to ensure that the various inputs are consistent and based on similar assumptions, *e.g.* by using extrapolations to compare inputs from two different e^+e^- colliders.

Fig. 2-26 displays the result of the global EFT fit for the subset of operators that affect Higgs and EW observables. Instead of showing the projected constraints on the Wilson coefficients of the operators, they have been translated into constraints on the effective Higgs and gauge-boson couplings. **See EWK report for details.**

Generally, future lepton colliders have the best reach for many of the aforementioned operators. Circular e^+e^- colliders have the best sensitivity to electroweak operators, due to the large statistical precision of Z pole and WW threshold measurements. All lepton colliders (e^+e^- and $\mu^+\mu^-$) are comparable in their reach for Higgs operators, although a multi-TeV muon collider cannot constrain exotic Higgs decays in a model-independent way, and the combination with a run on the s-channel Higgs resonance would be required for this purpose. Since some of the same operators contribute to Z-pole precision observables, as well as to HZ, WW and ZZ pair production cross sections, the operator constraints extracted from the latter can be improved by performing a combined fit with Z-pole data. This effect is more significant for circular e^+e^- colliders than for linear e^+e^- colliders, since for the latter beam polarization helps to disentangle the contributions of different operators in $HZ/WW/ZZ$ pair production processes.

Fig. 2-27 shows a selection of results for a fit that combines a set of Higgs and EW operators with 4-fermion operators. The latter are better constrained at linear e^+e^- than circular e^+e^- taking advantage of higher energy reach and beam polarizations[3]. A recent analysis of the sensitivity of muon colliders to new 4-fermion interactions can be found in Ref. [68]. Low-energy measurements (from fixed-target neutrino and electron scattering, tau and meson decays) are needed to close the fit for four-fermion operators. For complete results of the combined fit with 4-fermion operators, **see EWK report**.

Non only four-fermion operators, but also top-quark electroweak operators are best constrained at lepton colliders with $\sqrt{s} \geq 500$ GeV, and measurements at at least two values of $\sqrt{s}$ are crucial for breaking

[3] For now the global fit for 4-fermion operators did not include muon colliders.

degeneracies. Many constraints on top-quark operators are improved by combining e^+e^- and (HL-)LHC inputs and exploiting synergies between them. **See EWK report for more information.**

The results from global fits can be also interpreted in terms of constraints on BSM model parameters. Figure 2-28 is one example of the limits on new physics scales one can draw from the bounds on 4-fermion operators [114]. More examples on composite Higgs models and Z' models are also discussed in **the BSM report**.

More model interpretations are still work in progress.

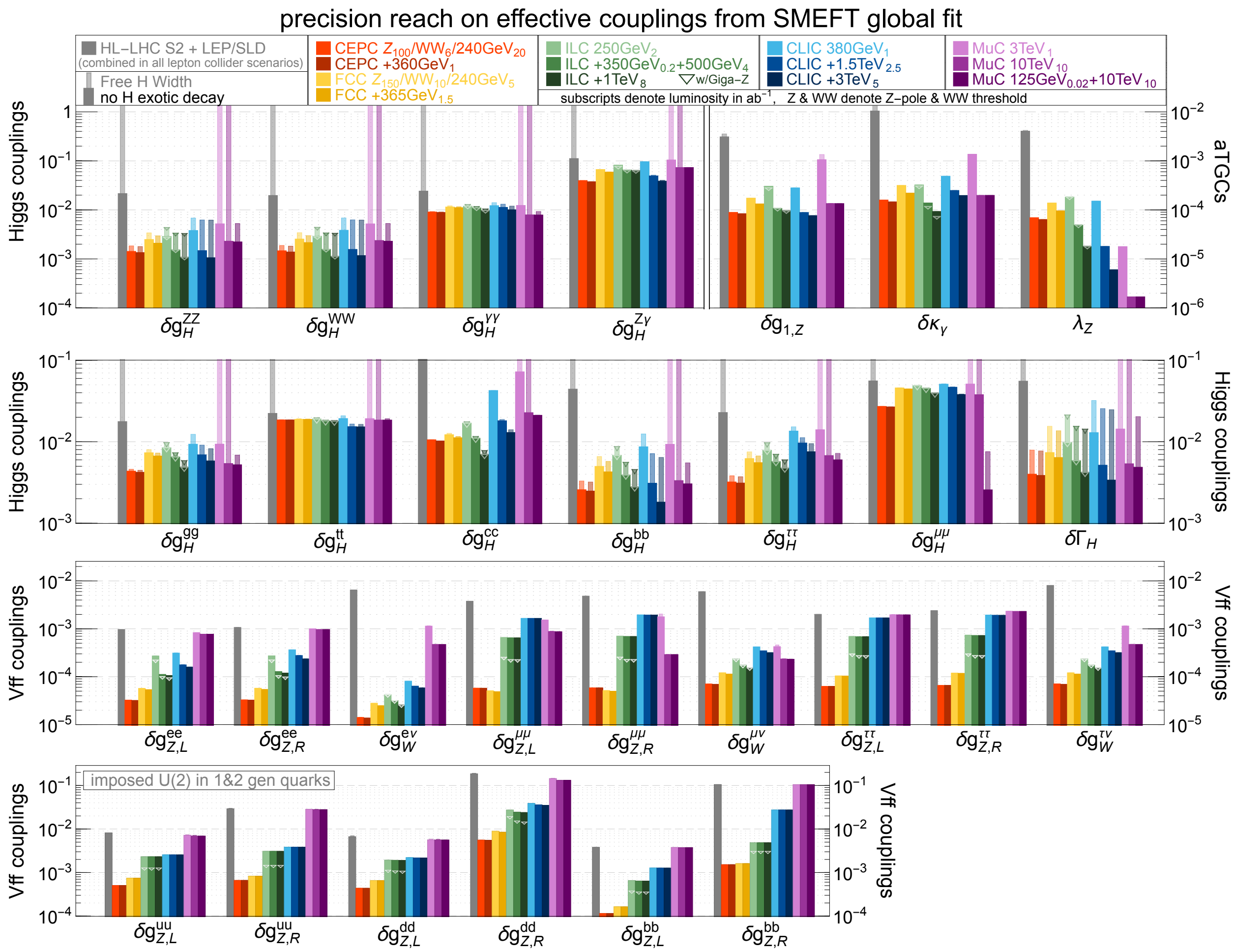

Figure 2-26. *Precision reach on Higgs and electroweak effective couplings from a SMEFT global analysis of the Higgs and EW measurements at various future colliders. The wide (narrow) bars correspond to the results from the constrained-Γ_H (free-Γ_H) fit. The HL-LHC and LEP/SLD measurements are combined with all future lepton collider scenarios. For e^+e^- colliders, the high-energy runs are always combined with the low energy ones. For the ILC, the (upper edge of the) triangle mark shows the results for which a Giga-Z run is also included. For the muon collider, three separate scenarios are considered. The subscripts in the collider scenarios denote the corresponding integrated luminosity of the run in* ab^{-1}.

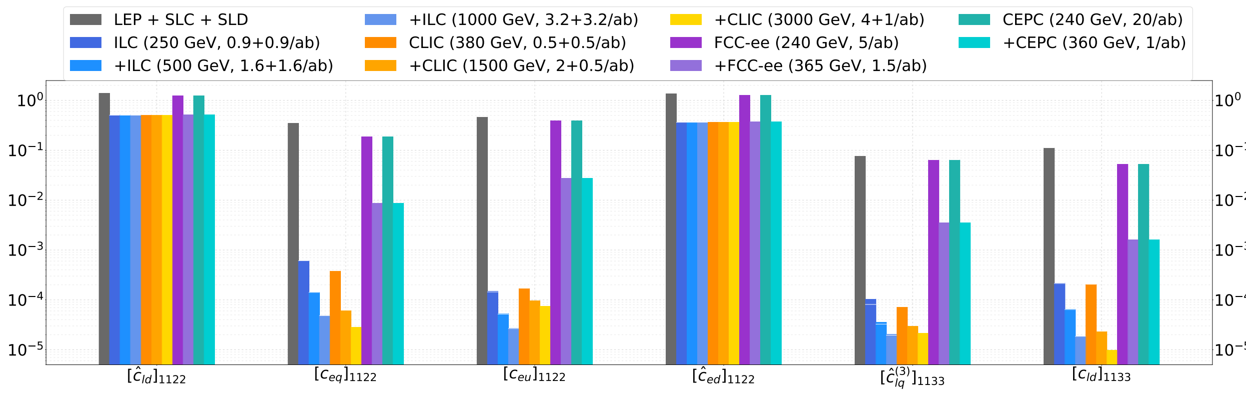

Figure 2-27. *Precision reach on a subset of 4-fermion operators from a SMEFT global fit at various future lepton colliders. "LEP+SLC+SLD" represents current measurements which are always combined in the future collider scenarios. The horizontal white line for ILC illustrates the global fit results when the pole observables from its Giga-Z option are included.*

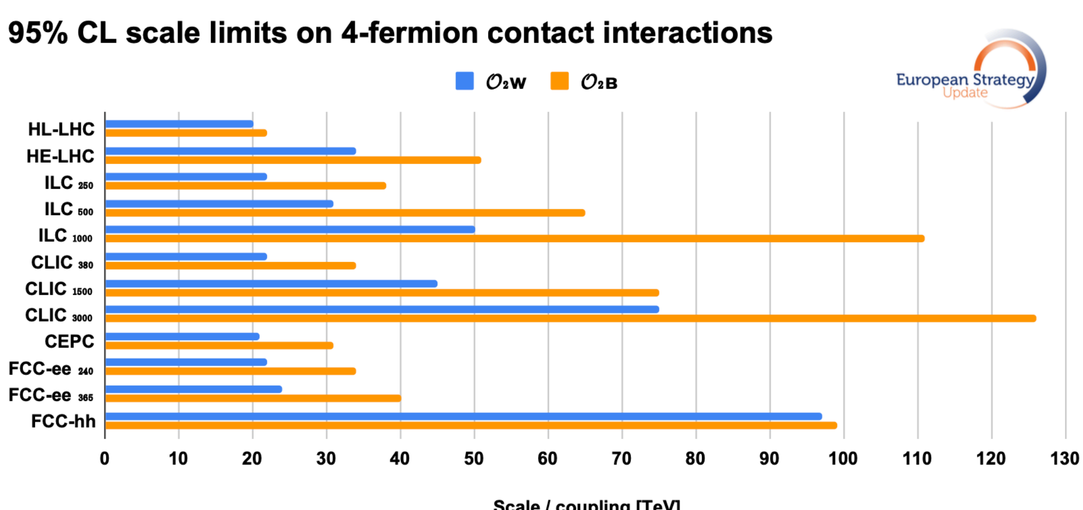

Figure 2-28. *Exclusion reach of different colliders on four-fermion contact interactions from the operators O_{2W} and O_{2B} (figure taken from Ref. [114]).*

2.4 QCD and Strong Interactions

Quantum Chromodynamics (QCD), the fundamental theory of strong interactions, plays a unique role in the Standard Model. Being a confining gauge theory, it is an interesting quantum field theory to study in its own right. It is also a crucial tool to enable discovery at virtually every high-energy collider. QCD predicts a rich panoply of phenomena associated with both perturbative and nonperturbative dynamics of the strong interactions. Continued success of the high-energy and nuclear physics research program hinges on an improved understanding of both regimes, as well as the dynamical transition between them.

Several research areas drive rapid developments in QCD at colliders. The ongoing revolution in high-order **perturbative** calculations provides precise predictions for short-distance matrix elements of many scattering processes (Sec. 2.4.1.1). Advanced determinations of the **QCD coupling strength** α_s (Sec. 2.4.1.2) and long-distance **nonperturbative** functions (Sec. 2.4.2.1) are made available by large-scale analyses of phenomenological data and increasingly from *ab initio* calculations in **lattice QCD**. Combined with all-order resummations and **multi-functional parton showering programs** (Sec. 2.6.2), perturbative cross sections are confronted by precise measurements available at the LHC and other facilities. Profound insights are being made about the universality, substructure, and energy dependence of **hadronic jets**, which play an outsized role in collider physics (Secs. 2.4.1.3 and 2.4.1.4). **Forward and diffractive scattering** at the LHC tests QCD in novel kinematic regimes that will be routine at future hadron colliders (Sec. 2.4.3). The **heavy-ion** program explores quark-gluon plasma and collective QCD phenomena (Sec. 2.4.4). In the age of the extensive LHC data and precision measurements, new opportunities emerge for **cross-cutting applications** in QCD and adjacent research directions (Sec. 2.4.5).

Future SM measurements and new physics searches will allow the exploration of new kinematic regions, such as very high transverse momentum and very forward rapidities, where large scale hierarchies may induce hitherto unseen QCD effects. The upcoming era — featuring the HL-LHC, Belle II, the EIC, new advances in theory including in lattice QCD, and potentially a Higgs factory — will be a new golden age for QCD easily rivaling the 1990's when the Tevatron, HERA, and LEP were all operating.

Measurements of jet, photon, and top-quark cross-sections at the HL-LHC will test perturbation theory to an unprecedented level, and constrain parton distribution functions (PDFs) and fragmentation functions [115] as well as the running of the strong coupling, α_s [81]. The accurate prediction of QCD radiative effects will remain a key factor in precision measurements of the W boson and top-quark mass, and weak mixing angle at hadron colliders, as discussed in Sec. 2.3. Knowledge about the substructure of QCD jets is now being widely used to minimize the impact of pileup, to probe fundamental and emergent properties of the strong force, to enhance the precision of measurements of highly-Lorentz-boosted SM particles, and to extend the sensitivity of searches for new particles (cf. Sec. 2.4.1.3) [116]. Detection of the decay products of far-forward hadrons at the proposed Forward Physics Facility (FPF) at the HL-LHC would offer an unprecedented opportunity for deeper tests of QCD in a novel high-energy regime (Sec. 2.4.3.2) [117, 118]. Neutrino production of all flavors as well as new particle production could be explored both by the FPF detectors alone and in coincidence with ATLAS, leading to improved understanding of small-x dynamics, forward heavy flavor – particularly charm – production, neutrino scattering in the TeV range, and hadronization inside nuclear matter.

Due to their QCD neutral initial state, e^+e^- colliders offer the cleanest environment in which to study QCD dynamics. Belle II will perform various measurements in the low and medium energy region [119], such as the cross section for $e^+e^- \to$ hadrons (in particular two pions), from which the leading-order hadronic contribution to the anomalous magnetic moment of the muon can be extracted. The low-background environment exploited at unprecedented statistical precision will also enable highly impactful tests of factorization and QCD evolution, as well as the determination of multidimensional correlation functions. The latter will help to constrain Monte-Carlo models of hadronization at levels that may be instrumental for the HL-LHC program.

There has been much progress since LEP in understanding hadronic final states at e^+e^- colliders, driven by the interest in jet substructure at the LHC, and the improved understanding of energy correlation functions. The techniques developed have enabled a variety of new ways of analyzing QCD dynamics with increasing sophistication [120, 121]. Precision determinations of event shapes have also enabled precision extractions of the strong coupling, α_s [122, 123]. A particular advantage of future lepton colliders is the availability of pure samples of gluon jets through the process $e^+e^- \to HZ$, with Z decaying to leptons and the Higgs boson decaying to gg [124]. Improved understanding of b-quark showering and hadronization, as well as b-quark production by secondary gluons, will also play an important role at these facilities; as they are leading sources of systematic uncertainty in the measurement of the b-fraction in hadronic decays (R_b) and of the b forward-backward asymmetry in Z decays.

Proposed muon colliders offer a physics reach for discoveries similar to that of proposed high-energy hadron colliders, while maintaining appealing experimental aspects of lepton collider environments such as a lack of pileup and underlying event. Advanced pileup mitigation techniques studied at the LHC could provide versatile handles to remove beam-induced background contamination during reconstruction [125, 126, 127, 128].

The EIC physics program [129], dedicated to exploration of hadronic matter, has significant synergies with exploration of QCD at the HL-LHC, FPF, and other experiments. The EIC is capable of obtaining new precise measurements of hadronic structure in deep inelastic scattering (DIS) through both neutral- and charged-current reactions in addition to performing spin-dependent three-dimensional tomography of nucleons and various ion species through highly-polarized beams for electrons and light ions. With its variable center-of-mass energy and excellent detection of final hadronic states, the EIC can precisely probe the unpolarized proton PDFs and their flavor composition in the kinematic region of relevance for BSM searches at the HL-LHC, but at QCD scales of only a few (tens of) GeV. The EIC program inspires in particular the development of new theoretical and numerical tools for QCD at the interface between particle and nuclear physics.

Proposed lepton-hadron colliders operating in the TeV energy range (Muon-Ion Collider [130], Large Hadron-Electron Collider [131, 132], FCC-eh [133]) would be both machines for subpercent-level measurements of α_s, nucleon structure, EW and Higgs couplings, as well as discovery machines to search for new physics such as compositeness and leptoquarks. Future hadron-hadron colliders, including the FCC-hh [30] operating at 100 TeV, would open unprecedented opportunities for precision measurements in perturbative and nonperturbative QCD. Their physics program would require innovative developments both in particle detection and QCD theory (Sec. 2.4.5.4), such as parton distributions for electroweak bosons, predictions for boosted final states inside jets, and new types of event generators.

2.4.1 Perturbative QCD

2.4.1.1 Precision Calculations

Perturbative precision calculations are crucial for measurements of SM parameters and a key ingredient for the reliable estimation of SM backgrounds to new physics searches. They also serve as an input to precision simulations in modern MC event generators for collider physics [135]. There has been significant recent progress in the computation of QCD radiative corrections [136, 137, 138, 134]. Several groups have used

Table 2-11. *Summary of the Les Houches precision wish-list for hadron colliders [134]. HTL stands for calculations in heavy top limit, VBF* stands for structure function approximation.*

process	known	desired
$pp \to H$	$\mathrm{N^3LO_{HTL}}$, $\mathrm{N^2LO^{(t)}_{QCD}}$, $\mathrm{N^{(1,1)}LO^{(HTL)}_{QCD\otimes EW}}$	$\mathrm{N^4LO_{HTL}}$ (incl.), $\mathrm{N^2LO^{(b,c)}_{QCD}}$
$pp \to H+j$	$\mathrm{N^2LO_{HTL}}$, $\mathrm{NLO_{QCD}}$, $\mathrm{N^{(1,1)}LO_{QCD\otimes EW}}$	$\mathrm{N^2LO_{HTL} \otimes NLO_{QCD} + NLO_{EW}}$
$pp \to H+2j$	$\mathrm{NLO_{HTL} \otimes LO_{QCD}}$ $\mathrm{N^3LO^{(VBF^*)}_{QCD}}$ (incl.), $\mathrm{N^2LO^{(VBF^*)}_{QCD}}$, $\mathrm{NLO^{(VBF)}_{EW}}$	$\mathrm{N^2LO_{HTL} \otimes NLO_{QCD} + NLO_{EW}}$, $\mathrm{N^2LO^{(VBF)}_{QCD}}$
$pp \to H+3j$	$\mathrm{NLO_{HTL}}$, $\mathrm{NLO^{(VBF)}_{QCD}}$	$\mathrm{NLO_{QCD} + NLO_{EW}}$
$pp \to VH$	$\mathrm{N^2LO_{QCD} + NLO_{EW}}$, $\mathrm{NLO^{(t,b)}_{gg\to HZ}}$	
$pp \to VH+j$	$\mathrm{N^2LO_{QCD}}$	$\mathrm{N^2LO_{QCD} + NLO_{EW}}$
$pp \to HH$	$\mathrm{N^3LO_{HTL} \otimes NLO_{QCD}}$	$\mathrm{NLO_{EW}}$
$pp \to H+t\bar{t}$	$\mathrm{NLO_{QCD} + NLO_{EW}}$, $\mathrm{N^2LO_{QCD}}$ (off-diag.)	$\mathrm{N^2LO_{QCD}}$
$pp \to H+t/\bar{t}$	$\mathrm{NLO_{QCD}}$	$\mathrm{N^2LO_{QCD}}$, $\mathrm{NLO_{QCD} + NLO_{EW}}$
$pp \to V$	$\mathrm{N^3LO_{QCD}}$, $\mathrm{N^{(1,1)}LO_{QCD\otimes EW}}$, $\mathrm{NLO_{EW}}$	$\mathrm{N^3LO_{QCD} + N^{(1,1)}LO_{QCD\otimes EW}}$, $\mathrm{N^2LO_{EW}}$
$pp \to VV'$	$\mathrm{N^2LO_{QCD} + NLO_{EW}}$, $+\,\mathrm{NLO_{QCD}}$ (gg)	$\mathrm{NLO_{QCD}}$ (gg,massive loops)
$pp \to V+j$	$\mathrm{N^2LO_{QCD} + NLO_{EW}}$	hadronic decays
$pp \to V+2j$	$\mathrm{NLO_{QCD} + NLO_{EW}}$, $\mathrm{NLO_{EW}}$	$\mathrm{N^2LO_{QCD}}$
$pp \to V+b\bar{b}$	$\mathrm{NLO_{QCD}}$	$\mathrm{N^2LO_{QCD} + NLO_{EW}}$
$pp \to VV'+1j$	$\mathrm{NLO_{QCD} + NLO_{EW}}$	$\mathrm{N^2LO_{QCD}}$
$pp \to VV'+2j$	$\mathrm{NLO_{QCD}}$ (QCD), $\mathrm{NLO_{QCD} + NLO_{EW}}$ (EW)	Full $\mathrm{NLO_{QCD} + NLO_{EW}}$
$pp \to W^+W^+ + 2j$	Full $\mathrm{NLO_{QCD} + NLO_{EW}}$	
$pp \to W^+W^- + 2j$	$\mathrm{NLO_{QCD} + NLO_{EW}}$ (EW component)	
$pp \to W^+Z + 2j$	$\mathrm{NLO_{QCD} + NLO_{EW}}$ (EW component)	
$pp \to ZZ + 2j$	Full $\mathrm{NLO_{QCD} + NLO_{EW}}$	
$pp \to VV'V''$	$\mathrm{NLO_{QCD}}$, $\mathrm{NLO_{EW}}$ (w/o decays)	$\mathrm{NLO_{QCD} + NLO_{EW}}$
$pp \to W^\pm W^+ W^-$	$\mathrm{NLO_{QCD} + NLO_{EW}}$	
$pp \to \gamma\gamma$	$\mathrm{N^2LO_{QCD} + NLO_{EW}}$	$\mathrm{N^3LO_{QCD}}$
$pp \to \gamma + j$	$\mathrm{N^2LO_{QCD} + NLO_{EW}}$	$\mathrm{N^3LO_{QCD}}$
$pp \to \gamma\gamma + j$	$\mathrm{N^2LO_{QCD} + NLO_{EW}}$, $+\,\mathrm{NLO_{QCD}}$ (gg channel)	
$pp \to \gamma\gamma\gamma$	$\mathrm{N^2LO_{QCD}}$	$\mathrm{N^2LO_{QCD} + NLO_{EW}}$
$pp \to 2\,\mathrm{jets}$	$\mathrm{N^2LO_{QCD}}$, $\mathrm{NLO_{QCD} + NLO_{EW}}$	$\mathrm{N^3LO_{QCD} + NLO_{EW}}$
$pp \to 3\,\mathrm{jets}$	$\mathrm{N^2LO_{QCD} + NLO_{EW}}$	
$pp \to t\bar{t}$	$\mathrm{N^2LO_{QCD}}$ (w/ decays)+ $\mathrm{NLO_{EW}}$ (w/o decays) $\mathrm{NLO_{QCD} + NLO_{EW}}$ (w/ decays, off-shell effects) $\mathrm{N^2LO_{QCD}}$	$\mathrm{N^3LO_{QCD}}$
$pp \to t\bar{t}+j$	$\mathrm{NLO_{QCD}}$ (w/ decays, off-shell effects) $\mathrm{NLO_{EW}}$ (w/o decays)	$\mathrm{N^2LO_{QCD} + NLO_{EW}}$ (w/ decays)
$pp \to t\bar{t}+2j$	$\mathrm{NLO_{QCD}}$ (w/o decays)	$\mathrm{NLO_{QCD} + NLO_{EW}}$ (w/ decays)
$pp \to t\bar{t}+Z$	$\mathrm{NLO_{QCD} + NLO_{EW}}$ (w/o decays) $\mathrm{NLO_{QCD}}$ (w/ decays, off-shell effects)	$\mathrm{N^2LO_{QCD} + NLO_{EW}}$ (w/ decays)
$pp \to t\bar{t}+W$	$\mathrm{NLO_{QCD} + NLO_{EW}}$ (w/ decays, off-shell effects)	$\mathrm{N^2LO_{QCD} + NLO_{EW}}$ (w/ decays)
$pp \to t/\bar{t}$	$\mathrm{N^2LO_{QCD}}$*(w/ decays) $\mathrm{NLO_{EW}}$ (w/o decays)	$\mathrm{N^2LO_{QCD} + NLO_{EW}}$ (w/ decays)
$pp \to tZj$	$\mathrm{NLO_{QCD} + NLO_{EW}}$ (w/ decays)	$\mathrm{N^2LO_{QCD} + NLO_{EW}}$ (w/o decays)

different approaches to achieve the first $2 \to 3$ N^{2}LO calculations of hadron collider process. There have also been significant steps forward in the development of improved infrared subtraction schemes including methods to deal with higher-multiplicity processes at N^{2}LO. The computation of full SM corrections has seen major improvements as well [134]. A summary of the state of the art and targets for future measurements is shown in Tab. 2-11. This Les Houches precision wish-list has served as a summary and repository for the higher-order QCD and EW calculations relevant for high-energy colliders, providing a crucial link between theory and experiment.

2.4.1.2 Strong Coupling

The strong coupling, α_s, is a fundamental parameter of the SM and the least well known of its gauge couplings. The uncertainty on α_s will be one of the limiting factors in many measurements including Higgs couplings at the HL-LHC. BSM physics can also impact extractions of α_s in different ways and introduce tensions between their results. The relative uncertainty in the current world average, assuming no new physics or systematic discrepancies among extractions, is 0.8% and, within the next decade, can be reduced to $\approx 0.4\%$ [81]. This requires completing the necessary pQCD calculations and control of various commensurate factors to the same level. Many lattice QCD (LQCD) methods have been developed to extract α_s, and to provide systematic checks of these LQCD methods [139, 140, 141, 142]. There are proposals to apply similar checks to phenomenological determinations [143, 144, 81].

Table 2-12. *Summary of current and projected future (within the decade ahead or, in parentheses, longer time scales) uncertainties in the $\alpha_s(m_Z)$ extractions used today to derive the world average of α_s.*

	Relative $\alpha_s(m_Z)$ uncertainty	
Method	Current	Near (long-term) future
(1) Lattice	0.7%	$\approx$ 0.3% (0.1%)
(2) τ decays	1.6%	$<$ 1.%
(3) $Q\overline{Q}$ bound states	3.3%	$\approx$ 1.5%
(4) DIS & global PDF fits	1.7%	$\approx$ 1% (0.2%)
(5) e^+e^- jets & evt shapes	2.6%	$\approx$ 1.5% ($<$ 1%)
(6) Electroweak fits	2.3%	($\approx$ 0.1%)
(7) Standalone hadron collider observables	2.4%	$\approx$ 1.5%
World average	0.8%	$\approx$ 0.4% (0.1%)

The FCC-ee, which combines 3×10^{12} Z bosons decaying hadronically at the Z pole, and an $\sqrt{s}$ calibration to tens of keV accuracy [145], would provide measurements with unparalleled precision. The FCC-ee extraction of $\alpha_s(m_Z)$ will enable searches for small deviations from SM predictions that could signal the presence of new physics contributions. Dedicated high-luminosity e^+e^- runs at the Z-pole would also enable further precision tests of QCD through the study of the renormalization group running of the bottom quark mass [146, 147]. Future *ep* collider experiments would also provide many opportunities for precision determinations of α_s. The EIC [148, 129] and EicC [149] will provide new high-luminosity data that could lead to a few percent uncertainty level [129]. The LHeC [131, 132] would provide hadronic final-state observables covering a considerably larger range than was possible at HERA. It could determine α_s from inclusive DIS data alone, something not feasible with HERA data, and an experimental uncertainty possibly reduced to 0.02% [132].

2.4.1.3 Jet Substructure

Quark- and gluon-initiated jets are used in measurements of α_s, the extraction of universal objects within factorized QCD, and for tuning parton-shower Monte Carlo generators. They are statistically distinguishable due to their different fragmentation processes and can be separated using new tools such as jet substructure [150, 151, 152, 153, 120, 154, 121, 155]. Charm- and bottom-quark jets, such as in the $H \to b\bar{b}$ and $H \to c\bar{c}$ final states, can be effectively separated from other jets due to the long lifetime of the heavy quark and the mass of the heavy-flavored hadrons [156, 157, 158, 159, 160, 161, 162]. Identifying these types of jets is a standard benchmark for development of new classical and machine learning-based jet taggers and can help enhance certain BSM signals [163, 164, 136]. Tagging has not realized its full potential due to large uncertainties in the modeling of gluon jets. High purity samples of gluon jets provided by future lepton colliders through the process $\ell^+\ell^- \to H[\to gg]Z[\to \ell\ell]$ would significantly change this situation [124].

Jet substructure techniques are usually applied to identify Lorentz-boosted massive particles such as W, Z, H bosons, top quarks, and BSM particles in complex final states. Many collider scenarios also result in H, W, and Z bosons radiating off of very high energy jets ("Weak-strahlung"). There may also be top quarks produced via gluon splitting to $t\bar{t}$ within a jet that originates from light quarks or gluons. Identification of these signatures will be crucial for future high-energy colliders [116]. Unconventional signatures include cases where jets are composed of leptons and hadrons, only leptons, only photons, hadrons and missing transverse energy etc. In addition to the jet kinematics and substructure, the jet timing information [165] and other information can be used for classification. Examples include jets containing one or more hard leptons [166, 167, 168, 169, 170], displaced vertices [171, 168, 172], hard photons [173, 174], or significant missing transverse momentum [175, 176]. Some of these anomalous signatures are already starting to be explored at the LHC [177, 178, 179, 180, 181].

The jet substructure program has led to the introduction of techniques that systematically remove low-energy soft radiation [150, 151, 152, 153, 182, 183] and can significantly reduce the dependence of observables on nonperturbative QCD effects. For a generic infrared and collinear safe observable, one can measure its "groomed" counterpart, which will be IRC safe. Although these observables are theoretically cumbersome to compute, they can be very useful, for example for measurements of α_s.

Novel detector technologies such as finer calorimeter granularity [184, 185], more hermetic coverage of tracking detectors, and precise timing information are expected to improve substructure measurements in the future. In particular, at future muon colliders, 'beam background' detectors could also in principle be deployed to reduce the impact on jet substructure.

2.4.1.4 New Observables

Measurements of the flow of radiation, traditionally studied using event shapes or energy correlation functions, provide some of the most informative tests of QCD [186]. Energy correlators exhibit simple structures in perturbation theory [187, 188, 189, 190, 191, 192]. Their measurements at future colliders would provide remarkable insights into the dynamics of jets and hadronization [193, 186].

Modern measurements rely strongly on the use of particle flow and tracking information. However, only observables that are completely inclusive over the spectrum of final states can be computed purely from perturbation theory. The non-perturbative input needed for theoretical predictions of track-based observables is universal and can be parametrized by so-called "track functions" [194, 195], which describe the fraction of energy carried by charged particles from a fragmenting quark or gluon. Recently it has been shown how to compute jet substructure observables at high precision by incorporating track functions [196, 197], which gives promise for precision jet substructure measurements at the HL-LHC. Track functions could be measured precisely at the ILC and other future e^+e^- colliders.

Table 2-13. *Top part: PDF-focused topics explored in Snowmass'2013 [198] and '2021 studies [115]. Bottom part: a selection of new critical tasks to develop a new generation of PDFs that meet the targets of the HL-LHC physics program.*

TOPIC	STATUS, Snowmass'2013	STATUS, Snowmass'2021
Achieved accuracy of PDFs	N^2LO for evolution, DIS and vector boson production	N^2LO for all key processes; N^3LO for some processes
PDFs with NLO EW contributions	MSTW'04 QED, NNPDF2.3 QED	LuXQED and other photon PDFs from several groups; PDFs with leptons and massive bosons
PDFs with resummations	Small x (in progress)	Small-x and threshold resummations implemented in several PDF sets
Available LHC processes to determine nucleon PDFs	W/Z, single-incl. jet, high-p_T Z, $t\bar{t}$, $W+c$ production at 7 and 8 TeV	$+\ t\bar{t}$, single-top, dijet, $\gamma/W/Z$+jet, low-Q Drell Yan pairs, ... at 7, 8, 13 TeV
Current, planned & proposed experiments to probe PDFs	LHC Run-2 DIS: LHeC	LHC Run-3, HL-LHC DIS: EIC, LHeC, MuIC, ...
Benchmarking of PDFs for the LHC	PDF4LHC'2015 recommendation in preparation	PDF4LHC'21 recommendation issued
Precision analysis of specialized PDFs		Transverse-momentum dependent PDFs, nuclear, meson PDFs
	NEW TASKS in the HL-LHC ERA	
Obtain complete N^2LO and N^3LO predictions for PDF-sensitive processes	Improve models for correlated systematic errors	Find ways to constrain large-x PDFs without relying on nuclear targets
Develop and benchmark fast N^2LO interfaces	Estimate N^2LO/N^3LO theory uncertainties	New methods to combine PDF ensembles, estimate PDF uncertainties, deliver PDFs for applications

2.4.2 Non-perturbative QCD

2.4.2.1 Parton distribution functions in the nucleon

An overwhelming number of theoretical predictions for hadron colliders require parton distribution functions (PDFs) [199, 200, 201, 202, 203, 204, 205, 206, 207, 208, 209], the non-perturbative functions quantifying probabilities for finding quarks and gluons in hadrons in high-energy scattering processes. PDFs contribute to precise measurements of the QCD coupling constant, heavy-quark masses, weak boson mass, and electroweak flavor-mixing parameters. PDFs often introduce the dominant source of uncertainty in collider experiments, such as in the CDF II high-statistics measurement of W boson mass [71]. Reducing these uncertainties requires continuous benchmarking and improvements of the theoretical framework [210, 211]. Precise and accurate knowledge of PDFs is also critical for searches for BSM interactions.

Table 2-13 illustrates the progress that on the PDF determinations since the previous Snowmass Summer Study in 2013 [198]. Details are presented in the Snowmass PDF whitepaper [115]. The N^2LO QCD accuracy became the standard for the modern nucleon PDFs, with N^3LO being on the horizon within the next decade.

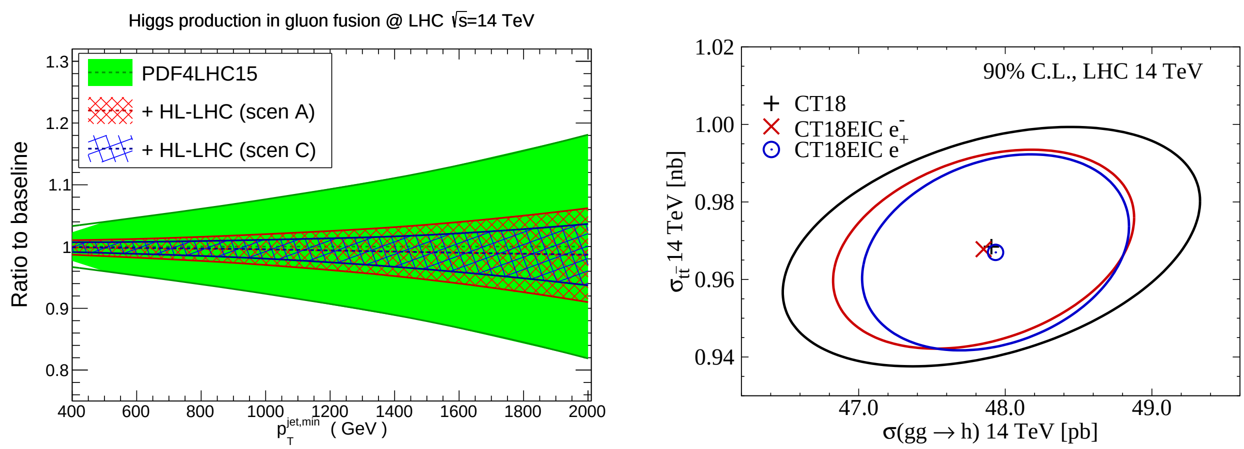

Figure 2-29. *Examples of projections for PDF uncertainties in the HL-LHC era.* **Left:** *Uncertainties for N^2LO Higgs production via gluon fusion at $\sqrt{s} = 14$ TeV obtained with published PDF4LHC15 N^2LO PDFs [214] (green band) and after additional constraints are imposed on these PDFs using simulated HL-LHC data in two scenarios (red and blue bands) [215].* **Right:** *90% C.L. uncertainty ellipses for N^2LO predictions for $gg \to H_{\rm SM}$ and $t\bar{t}$ production at the LHC 14 TeV obtained using CT18 N^2LO PDFs [205] and after imposing simulated constraints from inclusive DIS at the EIC [129].*

In addition, some PDF sets for precision physics include photon PDFs and QCD resummations. Current PDF predictions for parton luminosities agree within uncertainties at invariant masses $30 \lesssim m_X \lesssim 10^3$ GeV, relevant e.g. for Higgs and gauge boson production, but in the gluon sector (gluon-gluon and gluon-quark parton luminosities), differences are seen at large masses [115]. These differences are a consequence of both methodology and data sets included in PDF fits. The available PDF ensembles account for a combination of experimental, theoretical, and methodological uncertainties [212] in different ways, and the provided PDFs can differ as a result. The PDF-dependent cross sections can differ as well by the amounts exceeding the missing N^3LO contributions.

The bottom part of the table lists new tasks for the PDF analysis that emerge in the era of precision QCD. While the most precise N^2LO or even N^3LO theoretical cross sections should be preferably used, the accuracy of the theoretical predictions in the fits also depends on the other factors. For the complex N^2LO/N^3LO calculations, their fast approximate implementations (such as fast N^2LO interfaces) must be developed. Propagation of correlated systematic errors into PDFs is a challenging task that requires collaborations of experimentalists and theorists. Control of uncertainties requires, in particular, to either fit the experiments that are minimally affected by the unknown factors (for example, to include cross sections only on proton, rather than on nuclear targets), or to estimate the associated uncertainties from these factors directly in the fit. The PDF uncertainties must representatively reflect all PDF behaviors compatible with the fitted data [213]. PDFs must be developed to a wide range of users in a format that optimizes for accuracy, versatility, and speed across a broad range of applications — a highly non-trivial task.

Recent studies [215, 129] provide projections using various techniques for the reduction of PDF uncertainties under anticipated near-future theoretical and experimental developments. As an illustration, the left panel of Fig. 2-29 compares the current PDF uncertainty for $gg \to H_{\rm SM}$ production and its reduction when simulated HL-LHC measurements are included in the conservative (scen A) and optimistic (scen C) scenarios, using PDF4LHC15 N^2LO PDFs [214] as the baseline. The right panel shows an analogous projection for the reduction of the PDF uncertainty on the SM Higgs and $t\bar{t}$ cross sections at the LHC upon including the simulated measurements in DIS at the EIC, this time using the CT18 N^2LO framework [205]. The ability of the LHC measurements to reduce the PDF uncertainty critically depends on the control of systematic effects.

Deep inelastic scattering and hadroproduction at the EIC will constrain the PDFs for the LHC high-mass BSM searches most directly and without systematic or new-physics factors relevant at the LHC.

2.4.2.2 Predicting hadron structure in lattice QCD

As lattice QCD techniques advance in computations of PDFs from the first principles, unpolarized phenomenological PDFs in the nucleon serve as important benchmarks for testing the lattice QCD methods [216, 217]. Namely, precisely determined phenomenological PDFs in the nucleon serve as a reference to validate lattice and non-perturbative QCD calculations. The combination of the observation-driven PDF analysis and lattice QCD is thus especially promising and drives related studies of three-dimensional structure of baryons and mesons, including dependence on transverse momentum and spin. Figure 2-30 (left) shows the impact of lattice QCD calculations on a quantity affecting precision measurements at hadron colliders — the difference between the strange quark and antiquark PDFs. Such novel calculations can significantly constrain quantities that are difficult to assess with conventional PDF estimates. Figure 2-30 (right) illustrates that recent lattice QCD calculations are now able to predict quark PDFs. Lattice QCD is most potent in predicting various QCD charges and distributions of partons carrying 10% of the hadron's energy or more.

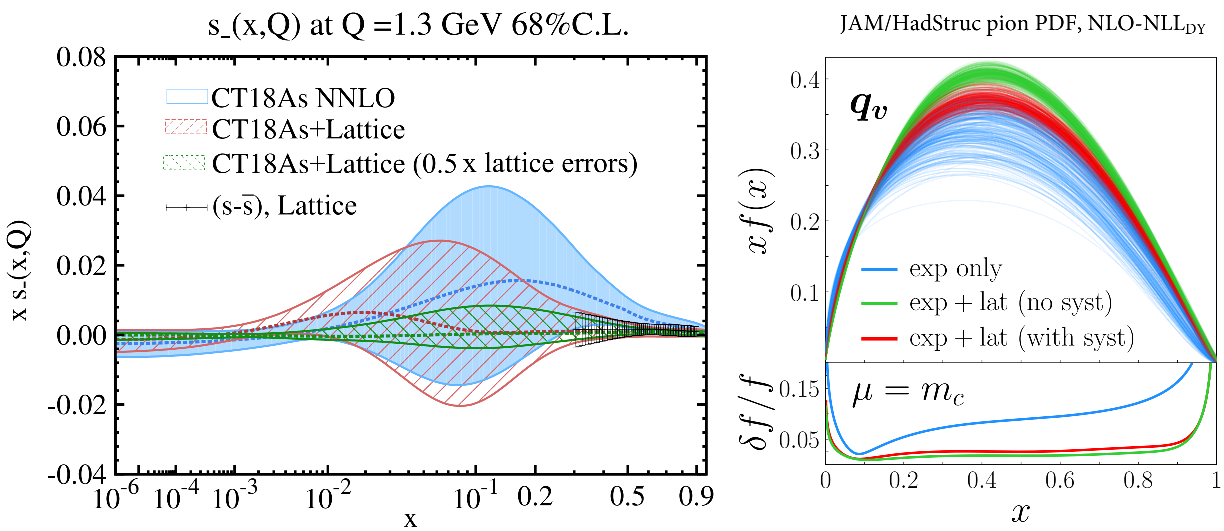

Figure 2-30. *Left: Impact of constraints from lattice QCD (black dashed area) on constraining the difference between strange quark and antiquark PDFs in a recent CT18As N^2LO fit [218]. The red (green) error bands are obtained with the current (reduced by 50%) lattice QCD errors. Right: determination of a quark PDF in a pion using a combination of experimental and lattice QCD data, and including resummation of threshold radiative contributions [219].*

A Snowmass whitepaper [220] details rapid advances in lattice QCD calculations of PDFs and other QCD functions. New experiments and facilities will pursue exploration of the three-dimensional structure described by transverse-momentum–dependent distributions (TMDs) as well as generalized parton distributions (GPDs) – hybrid momentum- and coordinate-space distributions that bridge the conventional form factors and collinear PDFs. These experiments will match the ongoing theoretical advancements that open doors to many previously unattainable predictions, from the x dependence of collinear nucleon PDFs to TMDs [221, 222, 223, 224, 225] and related functions [226, 227, 228, 229, 230], GPDs [231, 232, 233, 234], and higher-twist terms – the progress that was not envisioned as possible during the 2013 Snowmass study.

There remain challenges to be overcome in the lattice calculations, such as reducing the noise-to-signal ratio, extrapolating to the physical pion mass, and increasing hadronic boosts to suppress systematic uncertainties. Computational resources place significant limitations on the achievable precision, as sufficiently large and fine lattices are necessary to suppress finite-size and higher-twist contaminating contributions. New ideas can bypass these limitations. With sufficient support, lattice QCD can fill in the gaps where the experiments are difficult or not yet available, improve the precision of global fits, and provide better SM inputs to aid new-physics searches across several HEP frontiers.

2.4.2.3 Hadronization and Fragmentation Functions

The process of hadronization describes how detected final-state hadrons are formed from partons. Since hadronization is governed by non-perturbative dynamics, it cannot be calculated analytically and, in contrast to the partonic structure of hadrons, is elusive in lattice calculations. Having an accurate description of hadronization is, however, crucial for most measurements in high-energy physics and absolutely indispensable for all measurements at hadron colliders.

Precision measurements of fragmentation functions (FFs) are instrumental for extracting the spin-averaged and spin-dependent nucleon structure [235] in the planned experiments at the EIC and Belle II. The emphasis of the Belle II program will be on investigation of full multidimensional dependency of FFs with complex final states, such as dihadrons or polarized hyperons. These final states are sensitive to spin-orbit correlations in hadronization. Their factorization universality properties and kinematic dependencies are still to be fully mapped out. However, they are important, as tagging on such final-state degrees of freedom allows more targeted access to the hadron structure in semi-inclusive deep inelastic scattering (SIDIS) experiments, e.g., at JLab and the EIC. [See examples in [236, 237, 238, 239].] Transverse-momentum-dependent (TMD) PDFs and FFs will become the primary means to investigate the mechanism of hadronization in a 3D-picture [240]. Historically, they have been accessed through Semi-Inclusive DIS (SIDIS) and e^+e^- annihilation in two almost back-to-back hadrons. However, phenomenological extractions based on such processes are complicated by the fact that, in the cross section, the TMD FF does not appear on its own, but it is always convoluted with another TMD (two TMD FFs in e^+e^- annihilations, one TMD PDF and one TMD FF in SIDIS). Disentangling these functions is usually difficult, but recent proposals [241, 242, 243] offer a clean way of dealing with one single unknown at a time and extract successively the TMD FF, the so-called soft model, and finally the TMD PDF.

Detailed understanding of hadronization is necessary to model background and signal processes for new physics discoveries at B-factories themselves, but also at the LHC. Currently, modeling of backgrounds originating from light-quark fragmentation is mainly performed by Monte-Carlo Event Generators (MCEG). Tuning those generators to a precision needed for discovery science requires a model for correlated production of multiple hadrons that can only be verified with clean semi-inclusive e^+e^- annihilation data. Experimental data for this purpose are mostly available from LEP, but, to confidently extrapolate the model to LHC energies, input measurements are also necessary at CM energies an order of magnitude below LEP. The relatively low center-of-mass energy at Belle II, paired with extremely high luminosity, provides a large lever arm when combining Belle II and LEP/SLD data to probe hadronization effects over a wide energy range.

Where MCEGs describe full events, and the most common single-hadron FFs integrate over the whole event with the exception of the hadron in question, intermediate representations accounting for more correlations in hadronization gain more recognition in the field. The fragmentation functions for production of hadron pairs mentioned above are such an example. Beyond the current factorization theorems, there have been significant recent efforts to define correlation measurements that are sensitive to hadronization dynamics, can be interpreted within hadronization models (e.g., a QCD string model), and, while not yet realized, might be describable in a full QCD calculation with future. These kinds of correlation measurements have already been a focus at the LHC (see *e.g.*, Ref. [244]).

Accurate knowledge of parton (in particular gluon [245]) FFs into hadrons (both inclusively and for individual hadron species) in e^+e^- collisions is also of utmost importance to have an accurate "QCD vacuum" baseline to compare with the same objects measured in proton-nucleus and nucleus-nucleus collisions and thereby quantitatively understand final-state ("QCD medium") modifications of the FFs [246, 247].

Non-perturbative uncertainties from final-state hadronic effects linked to power-suppressed infrared phenomena, such as color reconnection (CR), hadronization, and multiparticle correlations (in spin, color, space, momenta) — which cannot be currently computed from first-principles QCD and often rely on phenomenological Monte Carlo modeling — may limit the ultimate accuracy at hadron-hadron colliders. In contrast, the FCC-ee offers a clean radiation environment that allows for systematic study of such effects [248]. In $e^+e^- \to t\bar{t}$, as the top quarks decay and hadronize closely to one another, their mutual interactions, decays into bottom quarks, and/or gluon radiation affect the rearrangement of the color flow and thereby the kinematic distributions of the final hadronic state. Whereas the perturbative radiation in the process can be in principle theoretically controlled, there is a CR "cross talk" among the produced hadronic strings that can only be modelled phenomenologically [249]. In the pp case, such CR effects can decrease the precision that can be achieved in the extraction of the top mass, and constitute 20–40% of its uncertainty [250]. Color reconnection can also impact limits for CP-violation searches in $H \to W^+W^-$ hadronic decays [251]. Searches for such effects can be optimally studied in the process $e^+e^- \to W^+W^- \to q_1\bar{q}_2q_3\bar{q}_4$ [251], where CR can lead to the formation of alternative "flipped" singlets $q_1\bar{q}_4$ and $q_3\bar{q}_2$, and correspondingly more complicated string topologies [252]. The combination of results from all four LEP collaborations excluded the no-CR null hypothesis at 99.5% CL [253], but the size of the WW data sample was too small for any quantitative studies. At the FCC-ee, if the W mass is determined to better than 1 MeV by a threshold scan, the semileptonic WW measurements (unaffected by CR) can be used to probe the impact of CR in the hadronic WW events [248, 254].

2.4.3 Forward Physics

The LHC experiments opened access to a wide range of forward and diffractive processes, which in turn drive advances in relevant QCD theory, such as charting the gluon at very low x, revealing dynamics at high partonic densities, and testing Monte Carlo models for forward hadron production. Understanding small-x dynamics in pp collisions, already important at the LHC and HL-LHC [255, 112], is crucial for any future higher-energy pp collider such as FCC-hh [256, 257, 258, 259], since even standard electroweak processes such as W and Z production become dominated by low–x dynamics, and an accurate calculation of the Higgs production cross section requires accounting for BFKL resummation [260, 261, 262, 263] or partonic saturation [264] effects.

2.4.3.1 Diffraction

Some configurations of final states with high forward multiplicities, as well as those with the absence of energy in the forward region (so-called rapidity gaps), in elastic, diffractive, and central exclusive processes originate from purely nonperturbative reactions, while others can be explained in terms of multi-parton chains or extensions of perturbative QCD such as the BFKL formalism. These processes are interesting for the exploration of electroweak and BSM physics. Understanding the elastic cross section and diffraction better, and probing models for Odderon [265, 266, 267, 268, 269, 270, 271] and Pomeron production, will be key studies at the HL-LHC, EIC, and any future hadron collider. Further progress in this fundamental area requires the combination of experimental measurements, including at the EIC and FPF, and theoretical work. The FPF also allows exploration of BFKL evolution and gluon saturation.

2.4.3.2 Physics opportunities at the CERN Forward Physics Facility

Given its unique configuration, the FPF [117, 118] would extend the coverage of the LHC measurements (notably, the LHCb) in the low–x region by almost two orders of magnitude at low Q, reaching down to $x \simeq 10^{-7}$ (Fig. 2-31). In its proposed main configuration, the FPF will detect far-forward neutrinos, produced from charm meson decays in one of the main LHC detectors, by DIS on a tungsten target. Therefore, FPF measurements would provide a bridge between the physics program at the HL-LHC and that of a higher-energy pp collider. Successful interpretation of FPF measurements will require a coordinated program including forward production at LHCb [272, 273, 274, 275], large-x CC DIS at EIC [129], and small-x scattering at the HL-LHC and future DIS facilities such as the MuIC [130] and LHeC [132]. In turn, this will provide improved predictions for key astroparticle physics processes, such as ultra-high energy neutrino-nucleus and cosmic ray interaction cross-sections.

Fig. 2-31 also demonstrates that the FPF will be sensitive to very high–x kinematics and in particular the intrinsic charm component of the proton [276]. While charm production in pp collisions is dominated by gluon–gluon scattering, in the presence of a non–perturbative charm PDF in the proton, the charm-gluon initial state may be dominant for forward D-meson production. FPF measurements, as part of a broader physics program including LHCb and the EIC, would provide complementary handles on high-x intrinsic charm. At the small-x end, FPF observations would reduce the currently large uncertainties on the expected flux of prompt neutrinos arising from the decays of charm mesons produced in cosmic-ray collisions in the atmosphere [277, 278, 279, 280]. These represent an important background for astrophysical neutrinos at neutrino telescopes such as IceCube [281] and KM3NET.

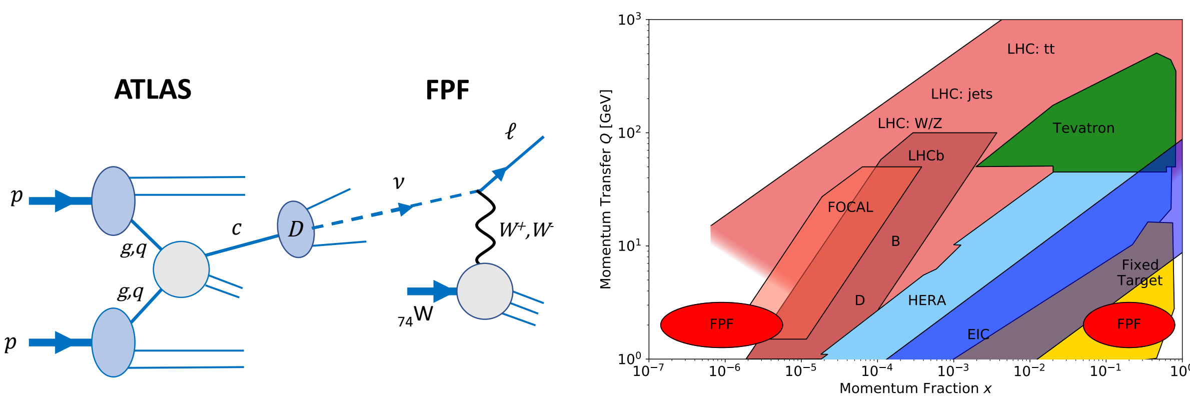

Figure 2-31. *(a) The production and detection processes for forward D-meson production at the HL-LHC followed by their decay into neutrinos falling within the FPF acceptance and (b) the (x, Q) regions (red ovals) that can be accessed at the FPF via this process.*

2.4.3.3 Neutrino-Induced Deep Inelastic Scattering

The ability of the weak current to probe specific quark flavors in neutrino DIS measurements, such as those at the FPF [282], significantly improves global determinations of proton and nuclear PDFs [282]. Neutrino–

induced CC DIS structure functions provide access to different quark flavor combinations compared to charged lepton DIS, and hence FPF data can complement other planned experiments such as the EIC. The coverage for CC nuclear structure functions at the FPF in Fig. 2-31 broadly overlaps with that for NC charged-lepton expected at the EIC [129, 283]. Analogous information from previous neutrino-induced DIS measurements on nuclear targets, such as NuTeV [284], NOMAD [285], CCFR [286], and CHORUS [287], plays a prominent role in many global PDF fits of nucleon and nuclear PDFs (with the two related via nuclear corrections). Inclusive CC DIS and especially semi-inclusive charm production in CC DIS are the primary channels to probe the PDFs for strange quarks and anti-quarks. Strangeness PDFs offer insights about the nonperturbative proton structure [288], while they are also responsible for a large part of the PDF uncertainty in weak boson mass measurements at the LHC [289]. On the experimental side, determination of the (anti-)strangeness PDF has been a hot topic for the PDF community as the fits prefer somewhat different shapes for the strangeness PDFs [290, 291, 205, 292]. The elevated PDF uncertainty from fitting such inconsistent experiments propagates into various pQCD predictions [293, 115, 81].

2.4.4 Heavy Ions

The chief aim of the heavy-ion (HI) program is the identification and characterization of the quark-gluon plasma (QGP), and advances in the understanding of the partonic nuclear structure, collectivity in small collision systems [294, 295, 296, 297, 298], and electromagnetic (EM) interactions [299, 300]. The heavy-ion (HI) program at the LHC has been a successful and important part of the LHC physics program. A detailed plan for the goals and expected measurements at the HL-LHC is presented in Ref. [301]. Detector improvements for ALICE, ATLAS, and CMS will greatly benefit the HI program. In particular, the increased charged particle tracking pseudo-rapidity acceptance will be a boon to bulk particle measurements, the upgraded Zero Degree Calorimeters (ZDC) [302, 303] will improve triggering and identification for ultra-peripheral collisions (UPC), and the addition of time-of-flight particle identification capability enabled by timing detector [304, **?**] will allow differentiating among low momentum pions, kaons, and protons, improving the heavy flavor (HF) measurements. The planned major upgrade of the ALICE detector for HL-LHC Run 5 (ALICE 3 [305]) will enable an extensive program to fully exploit the HL-LHC for the study of the properties of the QGP. At RHIC, the sPHENIX detector [306], will start HI data-taking in 2023 with the aim to provide high precision heavy-flavor meson and quarkonium data in Au-Au collisions.

2.4.4.1 Hard Probes

High momentum-transfer interactions between partons in the nuclei produce hard probes with QGP. One can study the impact of QGP on color charges with fast-moving partons and slow-moving heavy quarks. The effect of QGP on color charges can therefore be observed as the attenuation of the jets [307, 308, 309, 310, 311, 312, 313, 314, 315, 316, 317, 318, 319, 320], and the modification of their substructure [321, 322, 323, 324, 325, 326, 327, 328, 329, 330, 331, 332, 333], often referred to as jet quenching. CMS, ATLAS, and ALICE detectors at LHC will provide significantly reduced statistical and systematic uncertainties for key measurements of medium modification of light (heavy) quark jets using photon/Z (D^0-meson) tagged samples [334, 335]. The sPHENIX detector [336] will enable high precision full jet measurements at RHIC [334]. In addition, the large low-pileup pp data samples at HL-LHC can be a great opportunity for precision measurements of the system-size dependence of the jet quenching phenomena. By comparing the LHC and RHIC data, we aim to constrain the temperature dependence of the transport coefficients of QGP.

Heavy quarks provide a unique opportunity to probe the QGP with slow-moving probes. Charm and beauty quarks are mostly produced during the early stages of the collision in hard scattering processes. As HF quarks propagate through the medium, they quarks are expected to lose less energy than light flavor through radiation due to the dead-cone effect. These interactions in QGP may lead to the thermalization of low-momentum HF quarks, which would then take part in the expansion and hadronization of the medium. In addition, HF mesons, such as quarkonia, can be dissociated in the medium due to Debye color screening or recombined from individual heavy quarks and anti-quarks diffusing through the medium [337, 338, 339]. At the HL-LHC, the ALICE, CMS, and ATLAS experiments will significantly improve over the current HF hadron [340, 341, 342, 343, 344, 345, 346, 347, 348], and quarkonia [349, 350, 351, 352, 353, 354, 355, 356] measurements. The p_{T} dependence of the quarkonium nuclear modification factor (R_{AA}) will be measured with high precision up to about 80 GeV for prompt J/ψ and 50 GeV for $\Upsilon(1S)$ [357], allowing to discern whether quarkonium formation at high p_{T} is determined by the Debye screening mechanism, or by energy loss of the heavy quark or the quarkonium in the medium. The elliptic flow measurements of charm mesons in p-Pb collisions [358] and of HF decay muons [359] and $\Upsilon(1S)$ mesons [357] in Pb-Pb collisions will be significantly improved, providing insights on the collective expansion and degree of thermalization of HF quarks in the medium at low p_{T}, and on the presence of recombination of bottomonia from deconfined beauty quarks in the QGP. The production of strange B mesons and charm baryons in pp and Pb-Pb collisions [357] will also be measured with sufficient precision to further investigate the interplay between the predicted enhancement of strange quark production and the quenching mechanism of beauty quarks, and the contribution of recombination of HF quarks with lighter quarks to the hadronization process in HI collisions. Finally, the precise measurements of beauty mesons in p-Pb collisions [357] will help to elucidate the relative contribution of hadronization and nuclear-matter effects. At RHIC, the sPHENIX detector with enhanced capability for the studies of heavy flavor mesons and baryons could provide high precision data at lower collision energy. Together with data from HL-LHC, the measurements of HF hadron spectra, HF particle ratio, and azimuthal anisotropy will provide strong constraints on the heavy quark diffusion coefficient and its temperature dependence.

2.4.4.2 Hadronic Structure

The abundant production of light nuclei and anti-nuclei measured by ALICE can be greatly improved in HL-LHC. In analogy with the case of light nuclei and of charmonium, the statistical hadronization or coalescence ansatz can be used to gain a unique insight into the structure (e.g. tetraquark or molecular state) of exotic hadrons, such as the $X(3872)$ studied by LHCb in high-multiplicity pp collisions [360] and by CMS in Pb+Pb collisions [361]. Those initial measurements will be followed up with the high statistics data in LHC Runs 3 and 4. In LHC Run 5, the ALICE 3 detector would provide high precision measurement of multi-charm baryons, expanding the studies of hadronization performed in Run 3 and 4. ALICE 3 would also be the perfect tool for the study of the formation of light nuclei, hyper-nuclei, super-nuclei, and the experimental investigation of exotic states such as $X(3872)$ and the newly discovered T_{cc}^{+}.

2.4.4.3 Collective Phenomena

With the large samples of pp, pPb, and PbPb datasets of HL-LHC, it will be possible to reach an unprecedented experimental precision that will help us to understand the collectivity of small and large systems. The pivotal upgrades of trackers in CMS and ATLAS will enable the measurement of charged particles in the wide pseudo-rapidity range ($|\eta| < 4$). In addition, we expect a crucial improvement in our understanding of the system size of collisions by measuring the Hanbury Brown and Twiss (HBT) radii in small systems [359]. With azimuthally sensitive femtoscopy, the spatial ellipticity of the medium at freeze-out can be measured. In particular, the HL-LHC p-Pb data will allow us to unambiguously investigate the normalized second-order Fourier component of the transverse HBT radius as a function of the magnitude of flow. The extended η

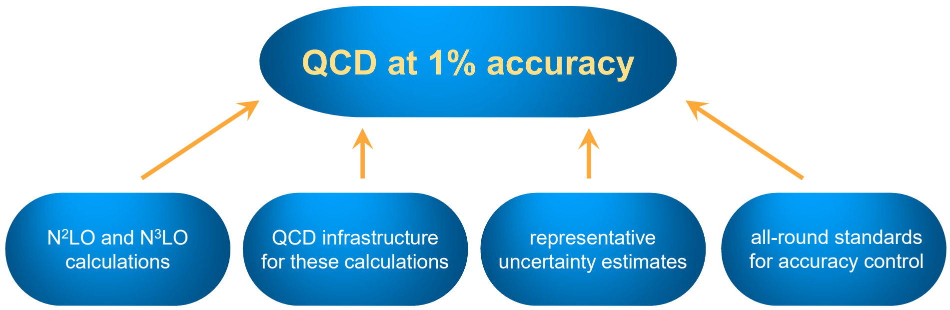

Figure 2-32. *Prerequisites for achieving percent-level accuracy in QCD calculations.*

acceptance in Run 4 will lead to significant improvement in characterizing the rapidity dependence of the factorization breaking. A significant improvement of the forward-backward multiplicity correlation and multi-particle cumulants will bring a better understanding of the fluctuations of the medium in early stages [359].

2.4.4.4 Photon-Nuclear Collisions

The large EM fields generated by ultra-relativistic charged ions, which may be thought of as Weizsäcker-Williams photons, may also interact with the nucleus (photo-nuclear) or with each other (photon-photon). These UPCs, characterized by an impact parameter greater than twice the nuclear radius, have become an important part of the heavy-ion program allowing unique avenues of study for both EM and nuclear interactions. ALICE, CMS, and ATLAS have a suite of planned measurements, and it is worth noting that the ZDCs — key detectors for the identification of UPC — are being upgraded for better triggering capabilities, segmentation, and radiation hardness in both experiments. LHCb is well suited for exclusive production studies in UPC, in particular, for its optimization for flavor physics within its acceptance $2 < \eta < 5$.

Photo-nuclear collisions are an effective tool for the study of the nuclear structure, and several photo-nuclear collision observables may be used to constrain the nPDF. It is expected that the cross-section for coherent photoproduction of vector mesons is proportional to the gluon density, and in particular, the HL-LHC will allow ALICE and CMS to extend these measurements to the $\Upsilon(1S)$ meson [362]. The ATLAS measurement of di-jets from photonuclear Pb-Pb collisions is expected to be statistically significant down to nuclear $x \approx 10^{-4}$ with the full integrated luminosity of the HL-LHC [301]. Finally, the light-by-light scattering process in heavy-ion collisions will provide important experimental data for new physics searches as discussed in previous sections.

2.4.5 Cross-Cutting QCD

QCD interactions play a ubiquitous and multifaceted role in collider phenomenology, and hence successes across many areas depend on future developments at the intersections of QCD and other domains. To take the full advantage of precise perturbative QCD calculations discussed in Sec. 2.4.1.1, commensurate advances must be achieved in determinations of long-distance QCD contributions including PDFs, computations of electroweak radiative contributions, event generation, machine learning, and last but not least, accurate and fast practical implementations. These tasks require collaboration between experimentalists and theorists, model-builders and QCD experts, and, more broadly, support of the *QCD infrastructure* that adapts theoretical tools for experimental analyses and provides protocols to validate these tools and assess uncertainties from experimental or theoretical sides. This subsection presents examples of such cross-cutting issues.

2.4.5.1 Comprehensive uncertainty estimates

Achieving the targeted accuracy on the PDFs and key measurements such as W boson mass at the HL-LHC requires better control of systematic uncertainties at all stages [115], in experimental measurements as well as in numerical computations. This requires a close collaboration between experimentalists and theorists on the consistent usage of QCD predictions and the conversion from parton to particle level (see also Sec. 2.6.2). Making higher-order calculations for complex final states available in a form suitable for experimental analyses remains a significant part of this challenge [363, 364, 365]. In addition, more efforts are necessary to present models of systematic uncertainties in the complete form that can be interpreted by external users [366]. New types of complexity issues emerge in comparisons of models with many parameters to very large data samples expected at the LHC Run-3 and HL-LHC. Such comparisons may be subject to increased risks of undetected biases due to non-representative exploration of contributing systematic factors [367], as has been recently demonstrated on the example of a PDF global fit [213]. In short, elevating the accuracy of QCD calculations to one percent requires both individual precise theoretical calculations as well as accurate supporting theoretical infrastructure that would allow, in particular, to explore exhaustively the relevant systematic factors. Reaching this target also requires agreed-upon standards and practices for accuracy control at all stages of the analyses, as is illustrated in Fig. 2-32.

2.4.5.2 QCD in new physics searches and SM EFT fits

The energy reach of many BSM searches depends on the interplay between precision calculations of matrix elements and global PDF analyses. Examples include searches for new vector bosons, referred to as Z's and W's. Current LHC bounds on mass disfavor extra vector bosons lighter than approximately 4-5 TeV. BSM searches of W'/Z's with even larger masses are progressively more sensitive to PDFs at large x where uncertainties are still large [368] and affected by nuclear corrections, higher-twist contributions, intrinsic heavy-quark components. Either forward particle production at the LHC or, often more cleanly, DIS at the EIC can constrain PDFs in the large-x region and increase sensitivity of BSM searches in the TeV mass range.

Search for deviations from SM examined in the language of Effective Field Theories (EFTs) can set lower bounds on the scales in a number of new physics scenarios [370]. Such analysis is an active research area, for example, in a widely adopted EFT expansion of the Standard Model, or SMEFT [371]. Although the proton structure parametrized by PDFs is intrinsically a low-energy input and should in principle be separable from the imprints of SMEFT operators, the complexity of the LHC environment might well intertwine them [372, 373, 369, 374, 375, 376, 373, 372]. As illustrated in Fig. 2-33, when including high-mass LHC data in a fit of PDFs and in a fit of SMEFT coefficients, and neglecting the interplay between them, the uncertainties on the EFT parameters may be underestimated. The bounds on the respective Wilson coefficients are relaxed once the are fitted together with the PDFs. Constraints on either the PDFs or EFT operators in low-energy experiments, where at least some new physics contributions are absent, can be crucial for disentangling the SM/BSM degeneracies. In this light, the SM and SMEFT studies at the EIC and other low-energy facilities again are synergistic to those at the (HL-)LHC [377, 378], especially for spin-dependent EFT operators.

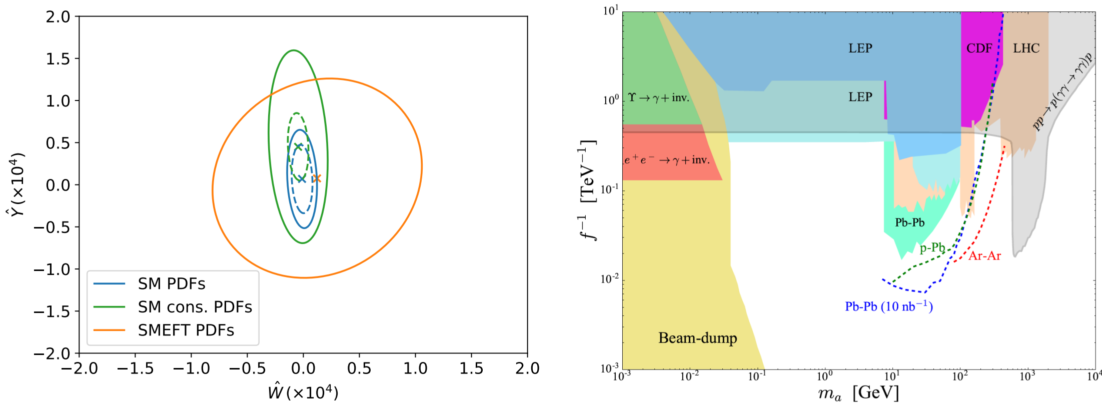

Figure 2-33. *Left: The 95% confidence level bounds on the plane of the Wilson coefficients considered in Ref. [369] obtained using either fixed SM PDFs (blue) or conservative SM PDFs that do not include high-energy data (green). PDF uncertainties are included in the solid lines and not included in the dashed lines. Results are compared to those obtained in a simultaneous fit of SMEFT and PDFs, when the PDFs are allowed to vary when varying the values of the Wilson coefficients (orange). Right: Coupling vs ALP mass sensitivity plot. The reach using the measurement of two intact protons and the two photons for photon-induced processes is shown as a grey area.*

2.4.5.3 Photon–Photon Scattering

Photon-induced reactions can be observed at the LHC in events with either one or both initial-state protons or ions acting as a photon source. The one-photon mode allows for observation of exclusive photon-hadron interaction at highest CM energies, yielding a tool to precisely study highest parton densities in the regime that is complementary to measurements at the EIC. At the LHC such large parton densities are predominately generated due to high-energy evolution, while the EIC can create similar densities in nuclear scattering at a lower CM energy. Quantitative predictions for photon-photon scattering require coordinated computations of QCD and electroweak contributions, serving as an example of cross-cutting connections between various domains of SM theory.

Considering the LHC as a $\gamma\gamma$ collider at high energies leads to unprecedented sensitivities to quartic anomalous couplings such as $\gamma\gamma\gamma\gamma$, $\gamma\gamma WW$, γZZ, $\gamma\gamma\gamma Z$, $\gamma\gamma t\bar{t}$ only to quote a few [379, 380, 381, 382, 383, 384, 385, 386, 387]. The events produced in $\gamma\gamma$ interactions at the LHC are extremely clean (like at LEP) since all particles in the final state including the intact protons can be measured. This leads to sensitivities to quartic anomalous couplings and to the production of axion-like particles at high masses better by two or three orders of magnitude than more usual searches at the LHC without measuring the intact protons. The reach on axion-like particles in shown in Fig. 2-33, right, where the sensitivity to axion-like particles at the LHC in pp and heavy ion interactions is displaced in the coupling versus mass plane [388].

2.4.5.4 Detectors and QCD theory for FCC-hh

Detectors for a possible 100 TeV hadron-hadron collider should be able to provide the necessary precision to measure the SM processes while also precisely reconstructing multi-TeV physics objects. Detector capabilities to reconstruct these objects are fairly challenging (for instance, the average Z boson from ZZ production would shower mostly within a single LHC calorimeter cell). This challenge is accentuated by so-called "hyper-boosted" jets, whose decay products are collimated into areas the size of single calorimeter cells. Holistic detector designs that integrate tracking, timing, and energy measurements are needed to mitigate for these conditions [389, 390, 391, 392, 393, 394].

The extreme levels of radiation present in a 100 TeV collider pose another challenge. A factor-of-five larger pileup than at the HL-LHC is expected posing stringent criteria on the detector design [395]. Hadronic and electromagnetic shower components up to several TeV need to be simulated, where extrapolations to these high energies come with large uncertainties. Differences in the hadronic shower simulation models in Geant4 [396] have been reported for pions in the energy range 2–10 GeV [397]. Detailed studies of hadronic showers will be needed in the next few decades to achieve the best possible precision in QCD measurements at future colliders. Innovations in QCD theory will be also crucial for quantitative FCC-hh predictions. A BFKL-like QCD formalism will be necessary to predict parton scattering at momentum fractions as low as 10^{-7}. Electroweak gauge bosons W and Z, leptons, and top quarks will be copiously produced at the FCC-hh energy and will need to be included into the PDFs together with quarks and gluons [398].

2.5 The physics beyond the Standard Model

There are abundant reasons why physics beyond the Standard Model (BSM) of particle physics is likely and, in some cases, unavoidable. Such reasons are connected to fundamental questions, answering which is among the highest priorities of particle physics. Current and future experiments at the energy frontier offer unique capabilities to explore many of these questions.

A subset of the most relevant questions to energy frontier approaches can be grouped in three broad categories:

1. Phenomena that have been observed but where a fundamental explanation is still lacking. These include
    - What is the fundamental composition of Dark Matter?
    - What is the additional source of CP violation needed to explain the matter-antimatter asymmetry observed in the universe?
    - Possible observations of BSM physics referred to broadly as *Anomalies*.
2. Guiding principles forming the basis of the successful stories behind the current Standard Model (SM) and, more generally, of modern theoretical physics. These may offer us insight on where the theoretical framework is "hinting" for a more complete description of Nature, such as:
    - Naturalness.
    - The flavor structure.
3. As history has shown many times, particle physics should maintain a wide open view for possible new phenomena that might not fit in the simplest theoretical extensions of the SM:
    - Are there new interactions or new particles around or above the electroweak scale?
    - Is lepton universality violated ?
    - Are there long-lived or feebly-interacting particles which have evaded traditional BSM searches?
    - Finally, there is a broad question of how to reduce biases in our searches and conduct them in a more model-independent way ?

Two main theoretical approaches in exploring BSM physics can be commonly identified. The first consists in seeking self-consistent theories that aim to address the questions above and can significantly boost our understanding of the fundamental laws of Nature. These well-motivated models of BSM physics, such as SUSY and Composite models, which are self-consistent to high-energy scales are excellent test cases for exploring possible experimental signatures and their interrelation. Looking beyond these prominent models, the landscape of possible experimental and theoretically-motivated models and signature is very large. In this approach, well-defined but incomplete theories extend specific areas without the expectation of full self-consistency. These *simplified* models or *portal* models are in some cases simplifications of complete theories. It is not practical nor useful to try to be exhaustive in projecting the scientific output of projects targeting all such models. Instead, we focus on a representative set of models and signatures that are deeply connected with the fundamental questions above and represent a wide range of physics that can be explored at the energy frontier. Such an approach has the advantage of providing a manageable framework where different experimental results can be easily compared and, eventually, mapped into the parameter space of complete theories. However, the drawback is that those have intrinsically a larger degree of arbitrariness and should be viewed as simpler guiding frameworks for the more general exploration of BSM physics.

In this section, we summarize and chose a few representative benchmark models and scenarios from the Snowmass EF BSM report [399]. These benchmarks include the dark matter driven considerations, as well as exciting recent development on long-lived particles. We discuss their implications for the current and future collider programs.

2.5.1 Composite Higgs

The question of whether the Higgs boson is an elementary or composite particle remains a fundamental mystery. The idea of a composite Higgs boson is attractive because it avoids the theoretical challenges associated with explaining the relatively small mass of a fundamental scalar particle. A composite Higgs boson requires a new strong gauge interaction whose coupling becomes strong above the TeV scale and binds together new elementary constituents. These constituents inevitably form not only the Higgs boson, but also many other bound states, much like the structure seen with QCD dynamics. In such models, the Higgs boson is the lightest bound state similar to the pion of QCD, protected by an approximate global symmetry, and observing other heavier resonances above the Higgs boson mass at the compositeness scale would be a tell-tale sign of Higgs compositeness. Current searches generically constrain the lowest lying resonances to be heavier than the TeV scale with lower mass limits in the range of 1-3 TeV for resonances with spin 1/2, 1, and 2 TeV. In addition to direct production of new resonances, Higgs compositeness would also cause deviations in the couplings of the Higgs boson to gauge bosons and the (composite) top quark. These deviations are inversely proportional to the scale of compositeness and therefore require precision measurements for detection.

The phenomenology of Composite Higgs models is mainly governed by two parameters: the mass (compositeness) scale m_* and the coupling g_*, which sets the scale of the couplings in the EFT Lagrangian. The strongly interacting model is expected to have $g_* > 1$ couplings, while unitarity requires $g_* < 4\pi$. The Wilson Coefficients, defined in Ref. [?], can be all parameterized in terms of this mass scale and coupling, modulo order 1 factors. Different colliders have complementary sensitivities to the various operators; the operators providing best sensitivity at colliders are [400, ?]

$$\frac{c_\phi}{\Lambda^2}\frac{1}{2}\partial_\mu\left(\phi^\dagger\phi\right)\partial^\mu\left(\phi^\dagger\phi\right) \qquad ; \qquad C_\phi = \frac{c_\phi}{\Lambda^2} \sim \frac{g_*^2}{m_*^2}\,, \tag{2.4}$$

$$\frac{c_W}{\Lambda^2}\frac{ig}{2}\left(\phi^\dagger \overleftrightarrow{D}\phi\right) D_\nu W^{a\,\mu\nu} \qquad ; \qquad C_W = \frac{c_W}{\Lambda^2} \sim \frac{1}{m_*^2}\,, \tag{2.5}$$

$$\frac{c_{2W}}{\Lambda^2}\frac{g^2}{2}\left(D_\mu W^{a\,\mu\nu}\right)\left(D_\rho W^{a\,\rho\nu}\right) \qquad ; \qquad C_{2W} = \frac{c_{2W}}{\Lambda^2} \sim \frac{1}{g_*^2 m_*^2}\,. \tag{2.6}$$

Sensitivity to toy Composite Higgs model from several future colliders is shown in Fig. 2-34. Curves from HL-LHC, FCC-ee/eh/hh, and CLIC are taken from Ref. [401]. Sensitivity to C_ϕ arises primarily through precision measurements of Higgs couplings; sensitivity to C_{2w} arises from measurements of high energy Drell-Yan events; and sensitivity to C_w more broadly comes from electroweak precision fits. Also shown is the direct search sensitivity for a triplet vector ρ resonance at FCC-hh. The sensitivity from the 10 TeV muon collider is taken from studies of the tree level process $\mu^+\mu^- \to hh\nu\nu$ [68], which provides good sensitivity for C_w and C_{2w}, but not C_ϕ. Sensitivity to C_ϕ from Higgs coupling measurements at a muon collider [402] are expected to be competitive, but are not shown here. We can also see the complementarity between direct resonance searches and the precision measurements on the SMEFT operators in this figure. This implies if

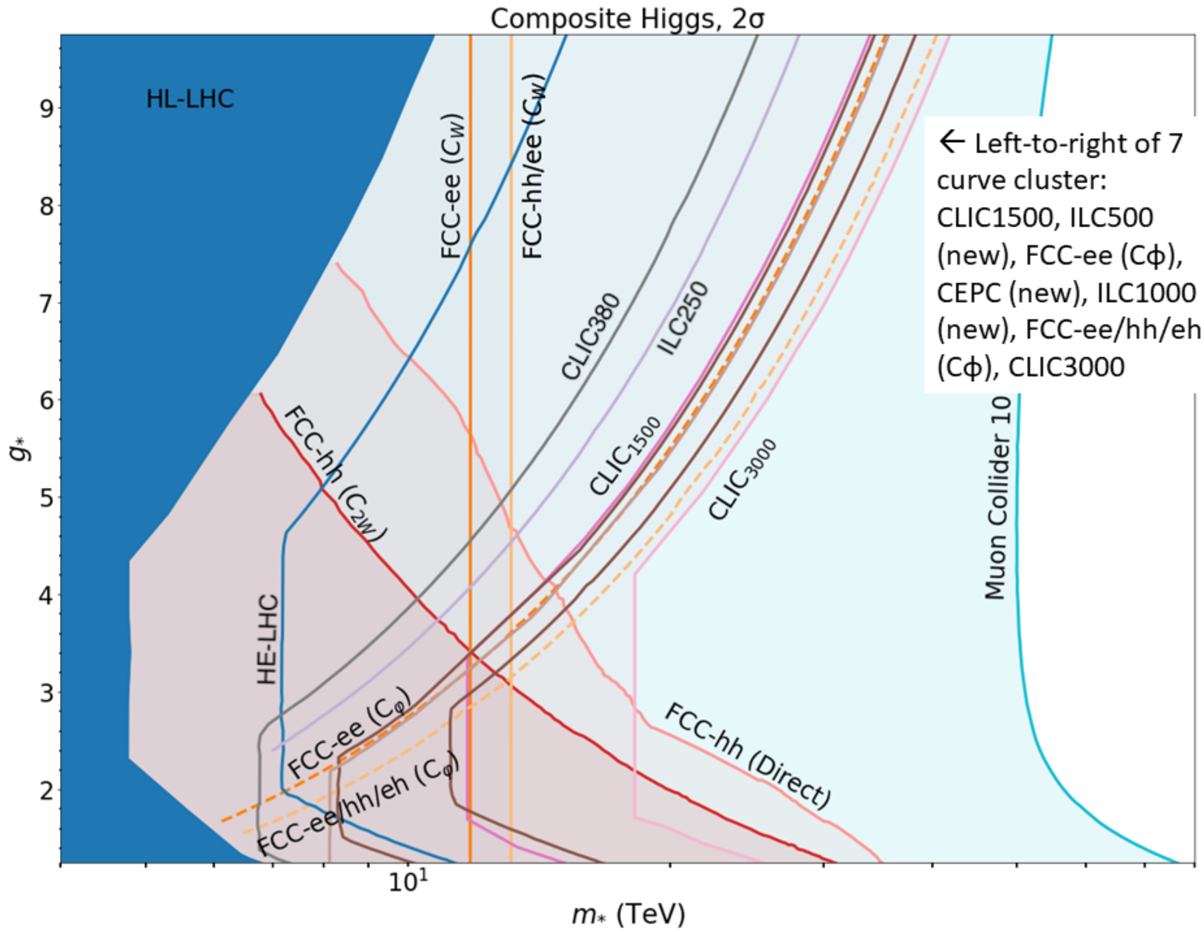

Figure 2-34. *Exclusion (2-σ) sensitivity projections for future colliders as labeled. Plot based on Refs. [400, 68].*

when we make future discoveries on the composite models, we can use a whole class of operators and direct searches to pin down the underlying theory.

2.5.2 SUSY

Supersymmety (SUSY) is a symmetry that extends the Standard Model fields with a set with the same Yukawa couplings and gauge quantum numbers but different spins. An extended Higgs sector is also required for SUSY. The motivations for this symmetry includes that it results in the unification of gauge and Yukawa couplings at high energies, radiative effects directly lead to electroweak symmetry breaking, in some versions it naturally contains a dark matter candidate. Furthermore SUSY appears in low-energy realizations of grand unified theories and superstrings, that allow for a consistent quantization of gravity. SUSY, however, cannot be an unbroken symmetry of nature, because particles with the same mass but different spin are not observed. Instead SUSY is assumed to be broken by a set of soft SUSY-breaking terms. These terms govern the masses of the predicted SUSY partner particles.

There are many specific models within the SUSY framework. The sensitivity studies presented here focus on R-parity conserving decays in the minimal supersymetric standard model (MSSM). In the MSSM, there is a lightest supersymetric particle (LSP) which is protected from decay by R-parity and therefore containes a dark matter candidate. There are many other models including those that violate R-parity in different ways, and the NMSSM which includes an additional singlet.

The Higgs mass in the MSSM is strongly constrained but receives logarithmic corrections due to stop-squark loops. To achieve the observed Higgs mass, these loops need to be above order 1 TeV which is the scale just being reach by the LHC; see Figure 2-35. Conversely, for a small mixing between the two stop squarks and $\tan\beta \gg 1$, the stop-quarks mass can be at most 5-10 TeV [403].

This wide variety of phenomena and the fact that it is widely studied make the MSSM a good context to make comparison plots between different collider scenarios. Figure **??** shows the comparative sensitivity in the MSSM for a representative set of key points in the model space. It includes large mass splittings for stop squarks, which are strongly produced, and two example weakly produced scenarios. The weak production example is a classic Wino-Bino model with large mass splitting, and the second is a Higgsino model with a small mass splitting motivated by naturalness consideration. The relevance of these plots goes beyond the SUSY context. The relative sensitivity to weak and strong, large and small mass-splittings are representative of what sensitivity might be observed in other models with new states. The studies focus on R-parity conserving SUSY where there is a stable lightest-supersymmetric state that is only weakly interacting. This is a challenging scenario, particularly for hadron colliders which have pile-up effects, a range of parton collision energies, and reduced resolution and information about the momentum conservation in the beam direction. The plot show the 95% exclusion limits. For discovery, the sensitivity at a hadron collider would be lower, while at a lepton collider it would be quite similar.

The range of possible SUSY models is vast. Even within the MSSM, there are many parameters and the complex interplay can lead to different signatures. One way to understand this complex space is to construct a Monte Carlo scan over the parameter space. For this purpose, the pMSSM, which reduces the 120-parameter MSSM space to 19 free parameters, specified at the EW scale, based on assumptions related to current experimental constraints (including those from flavor, CP violation, and EW symmetry breaking) rather than details of the SUSY breaking mechanism. Then with the scan points, the masses of particles, the relevant couplings, and impacts on precision measurements, rare processes, and cosmology can be studied.

Figure 2-36 shows the dependence of the Higgs to bb branching fraction on the mass of the psuedo-scalar Higgs m_A and $\tan\beta$, the ratio of the up and down VEVs. The branching fraction is reported as ratio to the SM called κ_b^2. The plot shows the fraction of pMSSM scan points with κ_b within 1% of the SM expectation of unity, where the range of 1% is chosen to approximately reflect the 95% CL corresponding to the 0.48% precision on κ_b expected from a combination of precision measurements at FCC-ee, FCC-eh, and FCC-hh [31]. Expected 95% CL exclusions from direct searches for pseudoscalar Higgs boson (A) at the HL-LHC and FCC-hh are overlaid for reference; points to the left of the lines are excluded. Exclusions at low $\tan\beta$ are obtained from studies of $A \to bb/tt$ [**?**], and those at high $\tan\beta$ come from projections for $A \to \tau^+\tau^-$ [**?**, 21]. As is evident in the plot, direct searches for A at the HL-LHC are expected to provide better sensitivity to the MSSM than the highest precision measurements of κ_b, which shows the strongest MSSM-related deviation of any Higgs coupling parameter.

The $H \to \gamma\gamma$ process is also expected to give some exclusion and a corresponding plot is in preparation.

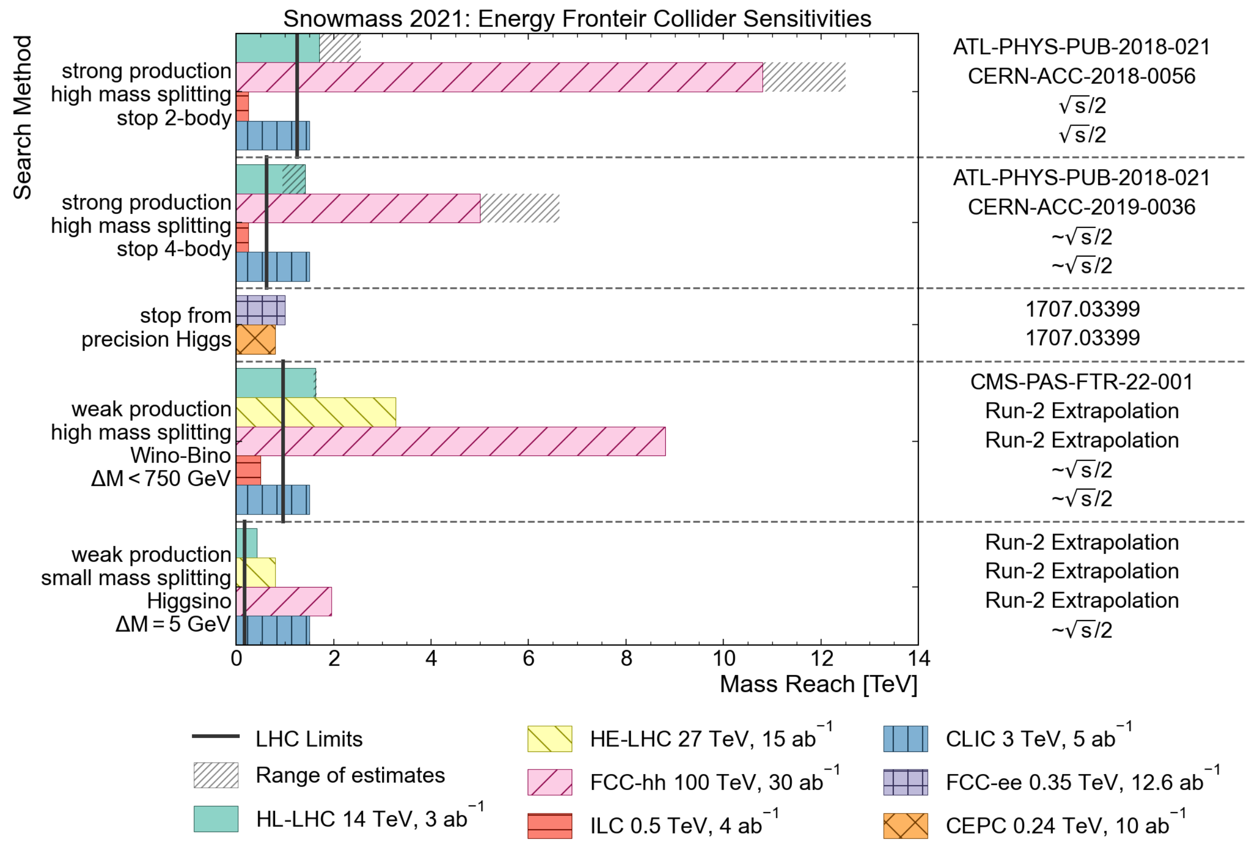

Figure 2-35. *Comparison collider of 95% exclusion SUSY sensitivities for a representative set of scenarios, including small and large mass splittings for stop squarks, which are strongly produced, a large mass splitting Wino-Bino model, and a small mass splitting Higgsino model. The limits come from a combination of dedicated studies and extrapolations based on the collider reach program [?]. For dedicated studies, a hashed grey area gives the difference to the collider reach results as an indication of the consistency of the methods. For the ILC limits (also relevant for other e^+e- colliders, not shown) there are indirect constraints from precision $e^+e- \to f\bar{f}$ measurements [404]*

2.5.3 New Bosons, Heavy Resonances, and New Fermions

Direct searches for new states beyond the standard provides vital information in our explorations for new physics. The new states could appear as heavy resonances, such as new bosons and new fermions, well-motivated from the model-building perspectives. In this section, we chose the new bosons as the example. Various representative examples are studies for the current and future facilities are shown in the EF BSM report [399]. New heavy vector bosons are often regarded as the standard candle for BSM searches. The canonical example is of a Z' boson, which is a neutral vector particle coupling to a SM fermion and antifermion. From the phenomenological perspective, Z' searches are generally characterized by the production coupling, the decay coupling, and the resonance mass, where the decay coupling is typically traded for the branching fraction to the desired final state. A coupling vs. mass framework for Z' searches [406, 407] helps distill the Z' resonance signal from disparate ultraviolet models into the minimal new physics parameter space relevant for resonance searches at colliders. This framework also enables direct

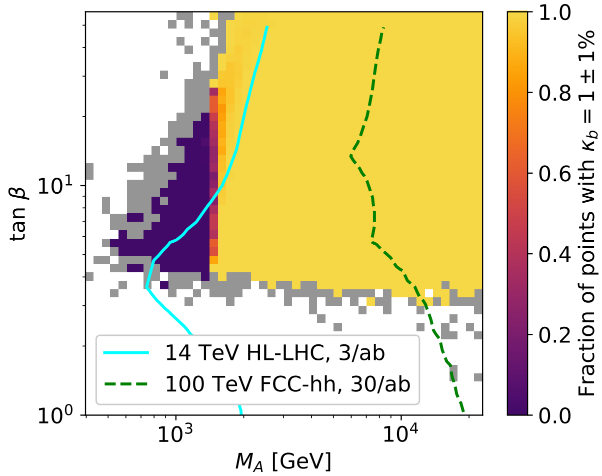

Figure 2-36. *The fraction of pMSSM scan points with κ_b within 1% of the SM expectation of unity as a function of $\tan\beta$ and M_A. The range of 1% is chosen to approximately reflect the 95% CL corresponding to the 0.48% precision on κ_b expected from the FCC-ee/eh/hh combination [31]. Expected 95% CL exclusions from HL-LHC [?, 405] and FCC-hh [?] are overlaid for reference. White bins include no scan points generated by the Markov chain Monte Carlo (McMC) procedure. Gray bins include scan points generated by the McMC, but rejected at a later step because of lack of consistency with current precision measurements and direct searches.*

comparison of experimental reach across different collider proposals, including a comparison of e^+e^-, pp, and $\mu^+\mu^-$ colliders as well as other collider options.

Two specific Z' models studied in the many Snowmass contributions include the universal Z' model and the Sequential Standard Model (SSM). The universal Z' model features a Z' boson with unit charges for all SM fermions, hence its universal designation. The sequential standard model (SSM) Z' boson follows the same coupling pattern of the SM Z boson, and is the benchmark model most commonly used by experimental searches. Figure 2-37 compares the sensitivity to a universal Z' at different colliders [408, 400]. New Snowmass results for the muon collider show that a muon collider at $\sqrt{s} = 3$ TeV is competitive with other colliders, with sensitivity nearly identical to ILC at $\sqrt{s} = 1$ TeV. A muon collider at $\sqrt{s} = 10$ TeV has the highest mass reach for a universal Z' with large couplings $g_{Z'}$, uniquely probing masses $M_{Z'} > 100$ TeV. A muon collider at $\sqrt{s} = 10$ TeV is sensitive to smaller couplings than the other colliders, with the exception of FCC-hh, which has the highest sensitivity from direct searches within the mass region $M_{Z'} < 28$ TeV. Lepton colliders have an edge in sensitivity when the boson is so heavy that only indirect effects can be measured, arising from the fact that in the signal kinematic distributions, the lepton collider experiments benefit from relatively smaller systematic uncertainties. We can also see the complementarity between direct resonance searches and the precision measurements on the SMEFT operators in this figure. The direct resonance searches allows us to go to small couplings within accessible energies at lepton colliders. The series of chiral determination of the BSM interference effects can also enable us to extra the new resonance's interaction structure [409, 22, 410].

All the different Snowmass contributions related to this topic can be organized into a summary table to enable an illustrative comparison between the various Z' models and current and possible collider scenarios. To enable the comparison and focus on the mass reach of the different colliders, we adopted the $g'_Z = 0.2$ coupling parameter for the universal Z' model, since it roughly aligns with the mass reach for the SSM Z'

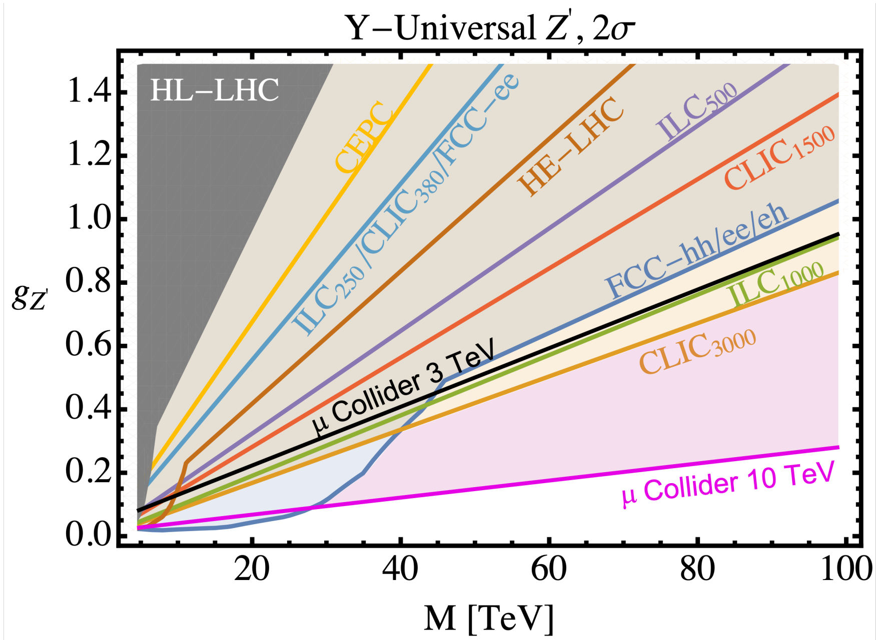

Figure 2-37. *Coupling versus mass reach at 95% CL for electron-positron colliders (CEPC, ILC, CLIC and FCC-ee) and proton-proton colliders (HL-LHC, HE-LHC and FCC-hh) and an electron-proton collider (FCC-eh) from [400] and the muon collider [408].*

model in the resonance channels studied. As we move down the table shown in table 2-14, the Z' mass reach steadily increases.

At first glance, this table shows the obvious correlation that higher center of mass collider energy affords higher reach in Z' mass, where the orders of magnitude spanned in collider energy pay off in orders of magnitude in Z' mass reach. This is justified since the resonance signal is assured when the Z' boson is within the kinematic reach of the collider. Moreover, for a given operating point of a collider, we see that the two Z' model benchmarks have very comparable results, which reflects the fact that the underlying charge assignments of SM fermions to the Z' currents only differ by $\mathcal{O}(1)$ factors, and so these results would be broadly applicable in other models where Z' bosons couple to all SM fermions, such as in gauged $B - L$ models. For more fermion-specific models, such as $L_\mu - L_\tau$ or gauged baryon number, which are equally relevant to the model benchmarks shown in table 2-14, the distinction between the different colliders becomes dramatically more important since the Z' resonance would be produced via a tree-level coupling in some colliders while only produced via a kinetic mixing coupling or a loop-induced coupling in others. As a first estimate, the corresponding reach for a point of comparison to table 2-14 would then adopt a coupling suppressed by a loop factor when the model does not couple to the initial partons at tree-level.

In table 2-14 the relationship between the Z' mass reach at 95% CL and the mass reach at 5σ depends on the collider type and final state. The two sensitivities are roughly equal for dilepton final states at pp colliders, because the Z' peak is beyond the highest masses of the dilepton continuum background from electroweak production via Drell-Yan, a convincing and background-free exclusion or discovery. For dijet final states at pp colliders, the direct searches for a Z' dijet mass bump has a 95% CL mass reach that is roughly 20-30% larger than the 5σ mass reach, because here the continuum background is larger from strong production of dijets via QCD. Finally, lepton colliders search within the kinematic distributions of fermion pairs for the indirect effects of a Z', with huge backgrounds at di-fermion masses significantly lower than the Z' pole mass, resulting in a 95% CL mass reach that is roughly 60-100% larger than the 5σ mass reach. Therefore, table 2-14 illustrates both the power of lepton colliders for indirect discovery of new physics, and the subsequent necessity of a higher energy to directly produce and confirm that new physics.

Machine	**Type**	$\sqrt{\mathbf{s}}$ (TeV)	$\int$ **Ldt** (ab^{-1})	**Source**	**Z′ Model**	$\mathbf{5\sigma}$ (TeV)	**95% CL (TeV)**
HL-LHC	pp	14	3	RH [411]	$Z'_{SSM} \to$ dijet	4.2	**5.2**
				ATLAS [412]	$Z'_{SSM} \to l^+l^-$	6.4	**6.5**
				CMS [413]	$Z'_{SSM} \to l^+l^-$	–	**6.8**
				EPPSU [400]	$Z'_{Univ}(g_{Z'} = 0.2)$	–	**6**
ILC250, CLIC380 or FCC-ee	e^+e^-	0.25	2	ILC [414]	$Z'_{SSM} \to f^+f^-$	4.9	**7.7**
				EPPSU [400]	$Z'_{Univ}(g_{Z'} = 0.2)$	–	**7**
HE-LHC	pp	27	15	EPPSU [400]	$Z'_{Univ}(g_{Z'} = 0.2)$	–	**11**
				ATLAS [412]	$Z'_{SSM} \to e^+e^-$	12.8	**12.8**
ILC	e^+e^-	0.5	4	ILC [414]	$Z'_{SSM} \to f^+f^-$	8.3	**13**
				EPPSU [400]	$Z'_{Univ}(g_{Z'} = 0.2)$	–	**13**
CLIC	e^+e^-	1.5	2.5	EPPSU [400]	$Z'_{Univ}(g_{Z'} = 0.2)$	–	**19**
Muon Collider	$\mu^+\mu^-$	3	1	IMCC [408]	$Z'_{Univ}(g_{Z'} = 0.2)$	10	**20**
ILC	e^+e^-	1	8	ILC [414]	$Z'_{SSM} \to f^+f^-$	14	**22**
				EPPSU [400]	$Z'_{Univ}(g_{Z'} = 0.2)$	–	**21**
CLIC	e^+e^-	3	5	EPPSU [400]	$Z'_{Univ}(g_{Z'} = 0.2)$	–	**24**
FCC-hh	pp	100	30	RH [411]	$Z'_{SSM} \to$ dijet	25	**32**
				EPPSU [400]	$Z'_{Univ}(g_{Z'} = 0.2)$	–	**35**
				EPPSU [415]	$Z'_{SSM} \to l^+l^-$	43	**43**
Muon Collider	$\mu^+\mu^-$	10	10	IMCC [408]	$Z'_{Univ}(g_{Z'} = 0.2)$	42	**70**

Table 2-14. *For each collider we list the operating point and mass reach, for 5σ discovery and 95% CL exclusion, of the SSM Z' model taken from Refs. [411, 415, 412, 413, 414], and the mass reach of the universal Z' model with a coupling $g_{Z'} = 0.2$ from Refs. [408, 400] that we determined from Fig. 2-37.*

Searches for light but very weakly coupled new particles are motivated by a variety of new physics scenarios. One prime example covers axion-like particles (ALPs) which are new pseudoscalar particles whose Lagrangian interactions are generally governed by a discrete shift symmetry. These pseudoscalars arise as pseudo-Nambu Goldstone bosons from a spontaneously broken global $U(1)$ symmetry in the ultraviolet theory. In analogy with the QCD axion arising from the Peccei-Quinn mechanism or the pion from the QCD chiral Lagrangian, ALP interactions are characterized by a decay constant f_a associated with their PNGB nature and, unlike traditional QCD axions, ALP masses are free parameters and provide the leading explicit shift symmetry breaking. While ALP Lagrangians have a rich phenomenology, including prompt and long-lived signatures, the main phenomenological target at experiments is the ALP coupling to two photons, allowing a smooth transition between traditional QCD axion and ALP parameters. Figure 2-38 (left) overlays the result of a new Snowmass study on the sensitivity of the muon collider to an ALP [28, 416] on a plot with other colliders [25, 400]. For ALP decays to diphotons, the muon collider and CLIC are the most sensitive to high ALP masses $m_a > 100$ GeV, and FCC-ee has the best sensitivity in the medium mass range $1 < m_a < 100$ GeV. It worthies noting that the ALP is typically expected to have non-suppressed coupling to gluons, in particular in its connection to the Strong CP puzzle of QCD [417, 418]. Having gluonic couplings changes the considerations for the search channels and the performance at different facilities appreciably (see recent phenomenological studies [419, 420, 118]).

The sensitivity to dijet resonances at pp colliders was explored during Snowmass 2021 as discussed in Refs. [411, 25, 421]. The process, $pp \to X \to 2$ jets, is an essential benchmark of discovery capability of pp colliders and is sensitive to a variety of models of new physics at the highest mass scales. The sensitivity to a dijet resonance is mainly determined by its cross section. The study considered strongly produced models, those with large production cross sections, that include scalar diquarks, colorons and excited quarks. At the highest resonance masses these strongly produced models can only be observed at a pp collider, as lepton colliders can only produce diquarks and excited quarks in pairs at significantly lower masses. Also considered are weakly produced models, with production cross sections that are roughly two orders of magnitude smaller, that include W's, Z's and Randall-Sundrum gravitons, which can also be observed at lepton colliders as previously discussed. The 5σ discovery mass is shown as a function of integrated luminosity in Fig. 2-38

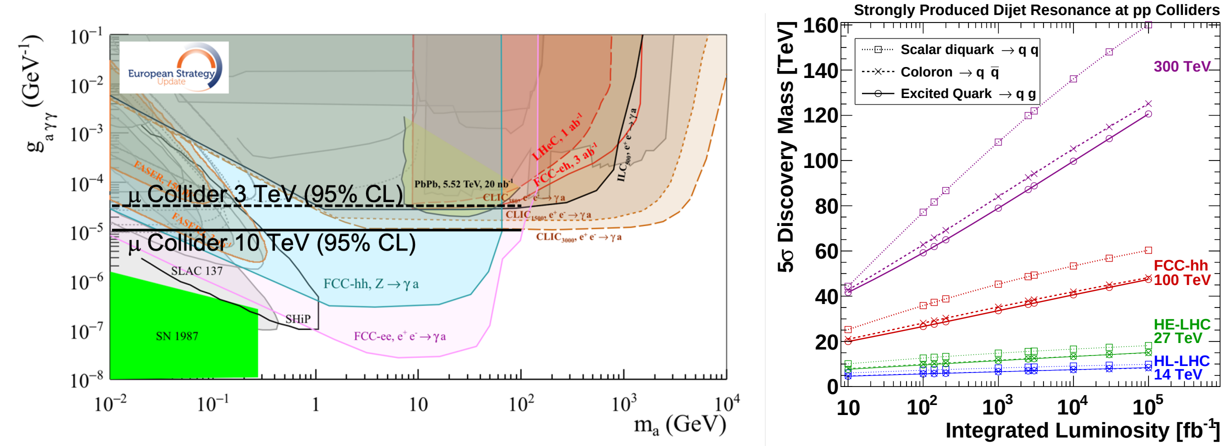

Figure 2-38. *(left) The axion-like particle (ALP) coupling in the diphoton channel $g_{a\gamma\gamma}$ versus 95% CL mass reach is shown at multiple colliders [25, 400] and superimposed is the same at the muon collider (black) for $m_a < 100$ GeV [28]. Note: figure is being updated/re-done and simplified. (right) Sensitivity to strongly produced dijet resonance models. The 5σ discovery mass for four values of pp collider $\sqrt{s}$ (colors) as a function of integrated luminosity for dijet resonances from (left) the large cross section models of diquarks (boxes), colorons (Xs), and excited quarks (circles). From Ref. [411].*

2.5.4 Long Lived Particles

Particles with long lifetime arise in many generic BSM models. The space of signatures for these long-lived particles (LLP) signatures is very rich and complicated, ranging from exotic-looking tracks to heavy stable charged particles to various types of displaced objects (e.g. vertices, jets, leptons). Here we highlight two examples. More benchmark cases, results and discussions can be found in the Snowmass EF BSM report [399].

The first example is that of LLPs that are electrically charged and can be produced by many different models. In the case of one particular signature, if the charged LLP decays within the detector, the LLP could produce a disappearing track signature if it decays to neutral and/or very soft particles that cannot be reconstructed. Disappearing tracks are particularly motivated in models of SUSY and dark matter.

Figure 2-39 shows the projected reach of disappearing track signatures at the HL-LHC [18], HE-LHC [422], LE-FCC [400], FCC-ee [400], CEPC [400], CLIC [423], ILC [424], FCC-eh [133], FCC-hh [425], and several high energy muon colliders [426], assuming a pure Higgsino with its natural mass splitting. Further discussion on these constraints and their implications for dark-matter can be found in the section on dark matter. The sensitivities are driven by many factors, and in particular, the proximity of the tracking system to the interaction points and low pile-up environment could help enhance them.

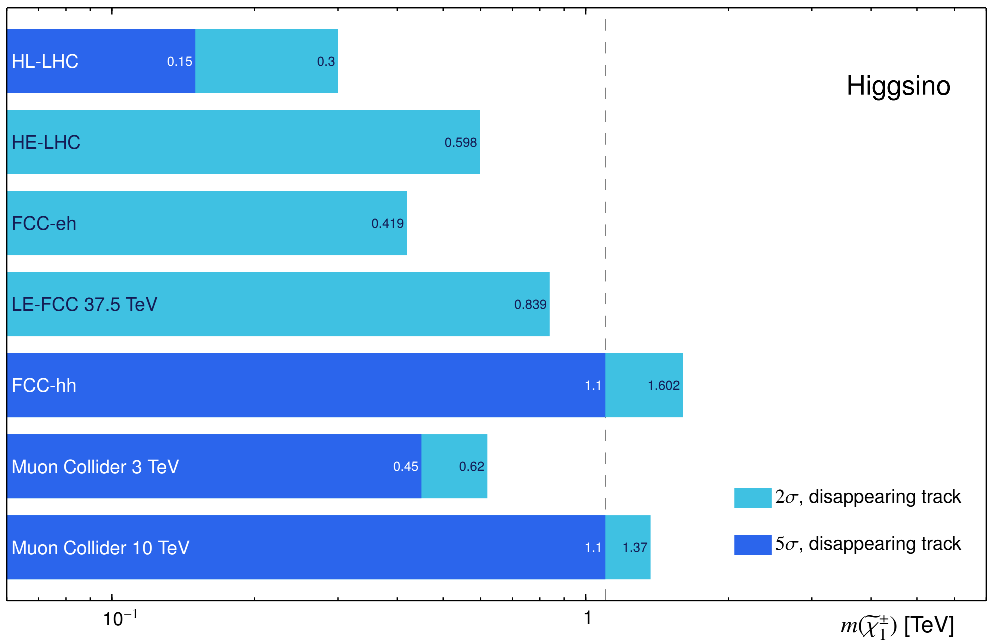

Figure 2-39. *Overview plot for the sensitivity to the pure Higgsino, assuming its natural mass splitting, for various future colliders. Figure adapted from [426].*

Many hidden sector new physics models could lead to long-lived signatures and displaced vertices. Here we use a simplified heavy neutral lepton model, motivated by the neutrino mass model building and the seesaw mechanism, as an example to show the different coverage of displaced signatures in the current and future experiments. For more detailed discussion and information on different models and search coverage, see the discussion in the Snowmass EF BSM report [399]. Extensions to the SM that account for neutrinos masses typically incorporate heavy neutrinos that are "sterile" with very small mixings to SM neutrinos, and they have masses much larger than the eV scale. Neutral leptons with masses on the MeV scale or higher are referred to as *heavy* neutral leptons (HNLs).

In the timescale of HL-LHC and beyond, many proposed experiments could offer discovery potential for Type-1 Seesaw HNLs, particularly in the low-mass / small-coupling region where long-lived searches will be required. Figure 2-40, adapted from [448, 465], shows the expected reach of experiments such as FASER2, MATHUSLA, CODEXb, and the FCC. Many of these experiments are proposed to be realized within the HL-LHC timescale. In a longer timescale, the FCC-ee could probe the deepest into small couplings for GeV-scale HNLs. To guide the eye, the "type-I seesaw" line indicates the approximate parametric scaling BSM report. associated with a simplified model with just a single neutrino flavor. Realistic three-generation models can populate the experimentally accessible regions in Fig 2.35. (see Ref. [464] for details). The region probed by the LHC, FCC-ee, and other future colliders is also motivated by low-scale leptogenesis models [459].

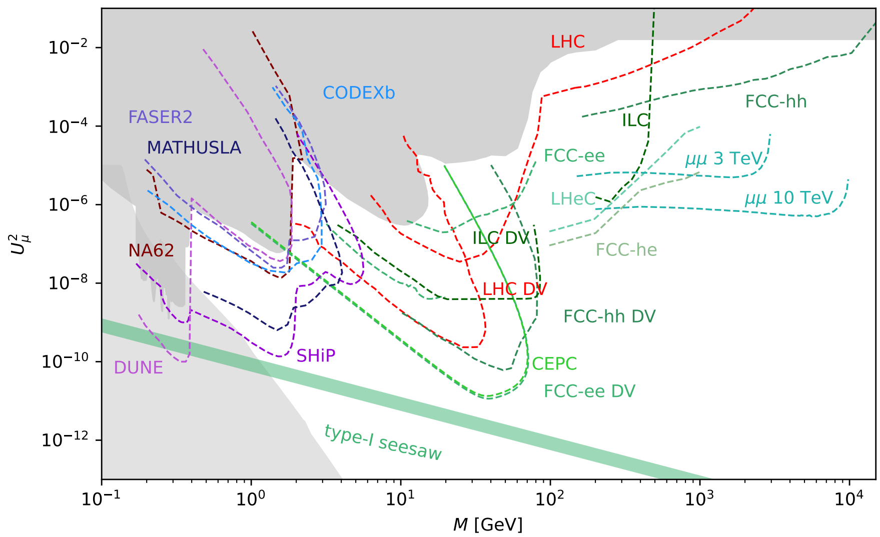

Figure 2-40. *Constraints and future sensitivities for HNLs with mass M and mixing U_μ^2 with muon neutrinos (summed over three HNL flavours).* Medium gray: *Constraints on the mixing of HNLs from past experiments [427, 428, 429, 430, 431, 432, 433, 434, 435, 436, 437].* Colourful lines: *Estimated sensitivities of the main HL-LHC detectors (adapted from [438, 439, 440]) and NA62 [441], with the sensitivities of selected planned or proposed experiments (DUNE [442], FASER2 [443], SHiP [444, 445], MATHUSLA [446], CODEX-b [447], cf. [420] for a more complete list) as well as selected proposed future colliders (FCC-ee or CEPC [448, 449, 450], FCC-hh [451, 440], ILC [452, 453] LHeC and FCC-he [454], and muon colliders [455], with DV indicating displaced vertex searches).* Green band: *Indicative lower bound on the total HNL mixing $U_e^2 + U_\mu^2 + U_\tau^2$ from the requirement to explain the light neutrino oscillation data [456] when varying the lightest neutrino mass and marginalising over light neutrino mass orderings. The matter-antimatter asymmetry of the universe [457] can be explained via low scale leptogenesis [458, 459, 460] along with the light neutrino masses in most of the white region above this band [461].* Light gray: *Lower bound on U_μ^2 from BBN [462, 463]. Plot adapted from [464].*

2.5.5 Dark Matter

The existence of dark matter (DM) in our universe is one of the most concrete pieces of evidence for physics beyond the Standard Model. However, very little has been observed so far about dark matter beyond its gravitational effects. Any signal pointing to dark matter interactions beyond gravity would bring us closer to answering one of the central questions of particle and astroparticle physics: *What is the nature of dark matter and how does it interact with ordinary matter?*.

When searching for particle DM, many experiments target theoretical hypotheses that foresee some kind of interaction between the DM and the SM. The presence of these interactions can be motivated by the processes that led to obtain the measured relic dark matter density in the universe. Such DM-SM interactions are the key to directly produce massive dark matter particles at the highest possible energies, via SM particle collisions in a terrestrial lab. Since DM-SM interactions are generally feeble (as a direct consequence to the dark matter's *darkness*), DM particles escape detection at collider experiments. These invisible particles can be discovered in the products of collisions where some of the total transverse momentum required by conservation laws is missing, leading to missing transverse momentum in a hermetic detector.

While a discovery of an invisible particle at colliders must be complemented by an observation of DM in astrophysics experiments[4], to verify the new particle's cosmological connection, collider experiments have the unique ability to probe the dark interaction and study the properties of DM in detail. In particular, colliders are crucial in establishing the interaction between the DM particle and SM particles, enabling discrimination between different DM models and eventually discovering new high energy particles as mediators of this interaction.

An intriguing historical parallel is another SM invisible particle – the neutrino. The neutrino was discovered in observations of the neutron decay at low energies, but only collider experiments at much higher energies could fully establish that neutrinos interacted via the weak force. It is with high energy colliders that we discovered the weak force mediators, the W and Z bosons, and measured their properties and couplings.

Following this example, in this report we focus on DM search targets where the SM-DM interaction is mediated by either an existing or a new particle, which in turn decays into invisible (DM) particles and can also decay back into SM particles allowing for a discovery in visible final states. With collider experiments, we are also able to investigate the wealth of particles that are created in the presence of complex dark sectors, which play an important role in the physics of DM.

2.5.5.1 Testing the traditional WIMP paradigm

Among the possible theories of particle DM, testing whether DM is a Weakly Interacting Massive Particle (WIMP) is one scenario to which colliders are well-suited. In the traditional WIMP scenario, DM consists of a single particle of mass between roughly 1 GeV and 100 TeV. The DM particle has sizable couplings with the SM to allow it to reach a common thermal equilibrium in the early universe. As it is a thermal relic, the present abundance of dark matter is determined by particle physics parameters, such as mass and coupling, that controlled reactions between DM and the SM in the early universe, and is largely independent of the universe's initial conditions and evolutionary history. WIMP candidates feature in a number of theories with connections with other electroweak-scale new physics, including supersymmetry, the archetype for the WIMP idea [466].

Since the 2013 Snowmass report, there has been significant progress made in the search for WIMPs with experiments at LHC Run 2 as well as at underground facilities, and with astrophysical observations. The null results obtained by these experiments do not yet cover the parameter space of such benchmarks, and so WIMPs remain a compelling target for DM searches at colliders and beyond.

Broadly speaking, WIMP scenarios can be classified according to the way in which the DM particle coupled with the Standard Model. Here we discuss some of the most widely-studied model categories.

Minimal WIMPs Among the WIMP scenarios, one particularly simple case is the dark matter particle being the lightest member of an electroweak (EW) multiplet. Most familiar examples are the Higgsino (a Dirac fermion doublet) and the wino (a Majorana Fermion triplet) in the context of supersymmetry. At the same time, more general cases have also been considered [467, 468]. This is a very predictive scenario. In the simplest case, the interaction strengths are the SM gauging couplings. The only free parameter, the mass of the dark matter particle, m_χ, is fixed by the by requiring thermal relic abundance matches the observation [469]. These so called thermal targets are typically in the TeV range [470, 471, 472, 473, 474, 475].

[4]The search for dark matter must be conducted in synergy between different Frontiers, using multiple probes and assumptions. This will be discussed in an upcoming cross-Frontier report

Covering these cases is among the main physics drivers for future high energy colliders. A summary of the 2σ reaches of the Higgsino and wino at future colliders is shown in Figure 2-41. An earlier summary can be found in the Physics Briefing Book for the European Strategy for Particle Physics Update 2020 [401]. In the last couple of years, there have been new studies on the reach of a high energy muon collider [476, 477, 426, 478, 479, 480, 481]. These results were also contributed to the EF10 topical group.

A main signal at high energy colliders is large missing energy-momenta recoiling against energetic SM particles. At hadron colliders, the dominant channel is often (but not always) jets+MET [482, 422]. At high energy lepton colliders, there are a number of channels [476, 479, 477, 480, 481] with SM EW gauge bosons and leptons in the final state. It is worth emphasizing that this class of signals is relatively insensitive to the mass splitting between the members of the EW multiplet. Hence, they are more robust against variations beyond the minimal scenario. The loop-induced mass splitting among the component states of the EW multiplet also results in a disappearing track signature which can be used to enhance the reach. This set of signal is more sensitive to additional model dependent mass splittings, and detector background. Preliminary estimates of the reach have been made for high energy hadron colliders [425, 483] and muon colliders [476, 426, 477].

The basic lesson from Figure 2-41 is that high energy colliders, such as a hadron collider with $E_{\mathrm{CM}} \simeq 100$ TeV or a muon collider with $E_{=10}$ TeV, can definitively these scenarios. High energy e^+e^- colliders, with energies up to 3 TeV, are useful in covering lower mass regions. At the same time, they can not completely cover all cases.

See Sec. X of the BSM report [399] for further discussion.

Higgs mediation DM could also couple to the SM via so-called *portals*, which include a direct coupling via gauge-invariant operators. The Higgs boson provides a prime example of such a portal: as a spin-0 particle, this 'Higgs portal' gives us the possibility to write down a renormalizable coupling with the DM, that can have a sizable effect on SM Higgs decay and properties. At high energy colliders, such a coupling gives rise to dark matter production, mediated by the Higgs boson. If the DM has a mass that is less than half the Higgs mass, then experiments at colliders can directly detect decays of the Higgs to invisible particles, and interpret excesses in terms of the Higgs portal. Precision measurements of the Higgs couplings, which are one of the objectives of a future collider, can also contribute to discovery or constraints on the Higgs portal scenario. Thus, searches at colliders are powerful probes of the Higgs portal – in particular, the FCC complex would allow us to close up on BSM Higgs to invisible decays by being sensitive to the very small SM branching ratio of the Higgs into four neutrinos, via ZZ decays. Future prospects for the Higgs portal were studied in detail in the European Strategy physics Briefing Book [401]. and are discussed in Sec. X of the EF10 report.

Models involving a larger extension of the scalar sector can also be probed with Higgs measurements and BSM Higgs searches as discussed in Section XX. Example of such models are the Inert Doublet Model, where an extra scalar doublet provides a DM candidate, and an extension of the two-Higgs Doublet Model (2HDM) where a new pseudoscalar has direct couplings to DM. The HL-LHC and lepton colliders are expected to be sensitive to large parts of the parameter space for these models, as it can be seen in the following studies targeting specific signatures [18, 484, 485].

BSM mediation Instead of coupling through SM gauge interactions or one of the portals, another category of model involves DM interacting with the SM only via one or more new bosons. Though this category encompasses a huge set of possible models, it is reasonable to assume that only a few new particles will be

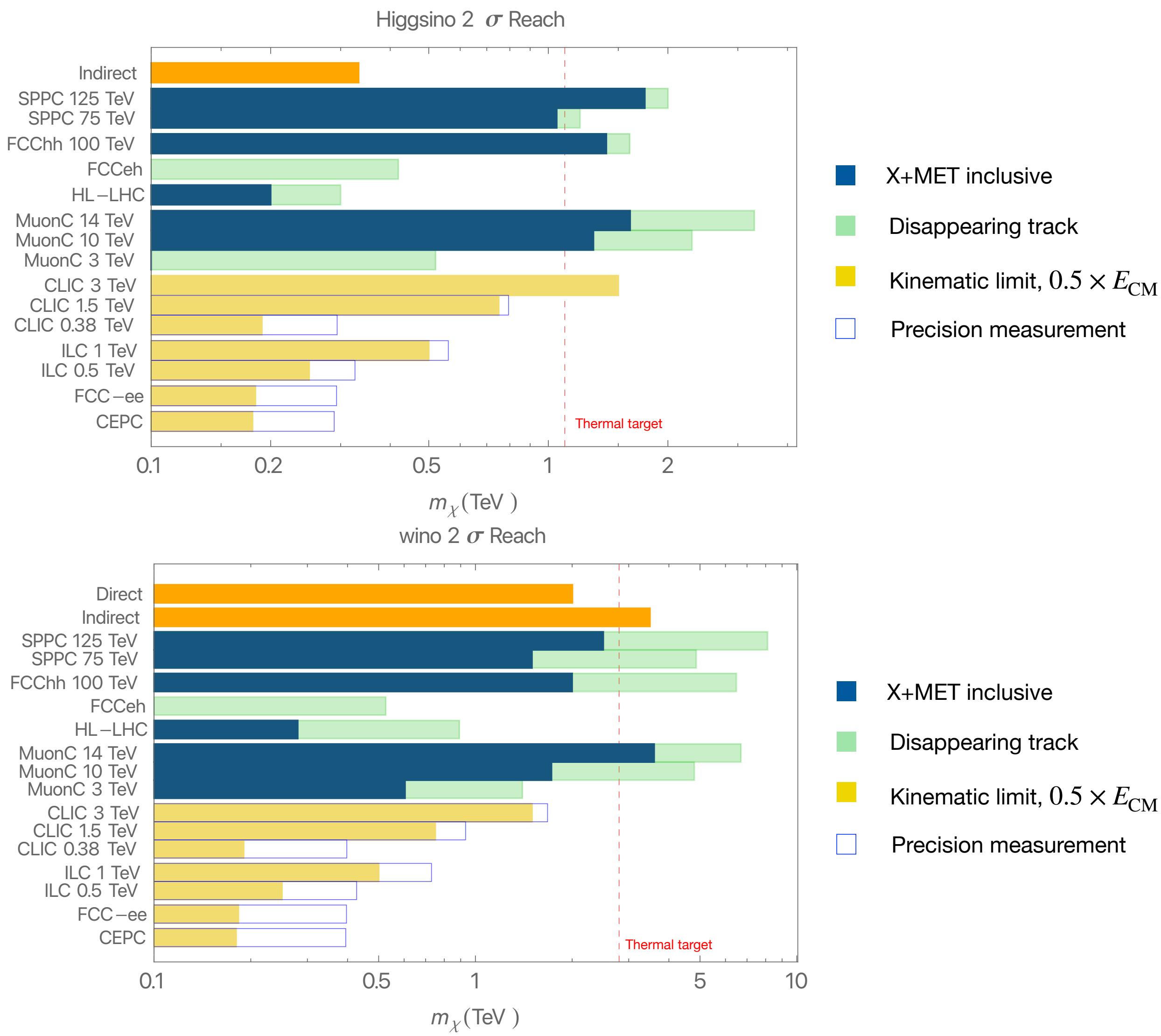

Projections in the figure will be updated if new inputs are received.

Figure 2-41. *A summary of the reach of future colliders for simple WIMPs. For comparison, the reaches of the direct and indirect detections are also included. For lepton colliders where a detailed study is not available, the kinematical limit $m_\chi = 0.5 \times E_{\rm CM}$ is used to indicate its potential reach. However, as demonstrated in the studies for the muon collider, this is likely to be an overestimate.*

relevant in the early phase of a discovery, and therefore simplified models of collider DM production can be sufficient to capture a broader phenomenology.

The set of such models currently used to design collider searches, described in Ref. [486], are inspired by the vector and scalar bosons of the SM. They involve a single species of fermionic DM particle and a mediator particle, either a vector (Z') with pure vector or axial-vector couplings to SM and DM fermions, or a scalar boson with Yukawa couplings to the SM and DM fermions of either scalar or pseudoscalar Lorentz structure.

There are 4 to 6 free parameters such as the masses of the DM and the mediator, and their couplings to the SM and DM.

Contributions to Snowmass that studied these models have significantly extended the projections made for the recent European Strategy update [401]. Both earlier and new projections use the LHC Dark Matter Working Group benchmarks for models involving Dirac fermion DM, discussed in Ref. [486]. Prior results, originally focusing on a limited set of scenarios in terms of couplings between the BSM particle and SM particles [487, 488], can now be extended to arbitrary coupling values between SM and DM [489]. This allows us to understand how future collider experiments would improve upon current LHC searches and how collider searches would complement direct-detection and indirect-detection experiments, especially when the dark matter mass is less than a few GeV. The new studies of coupling dependence are especially useful in understanding how this comparison is affected by different coupling values assumed for the signal at colliders [490], while direct detection only depends on a specific combination of the couplings and the mass of the mediator.

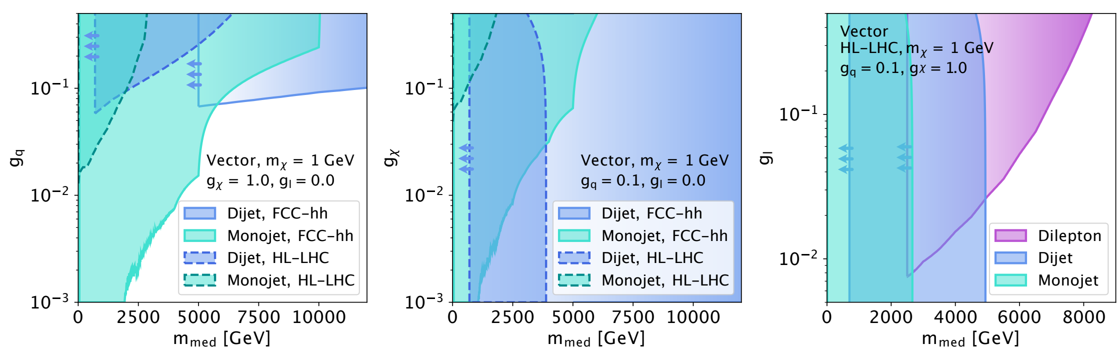

(a) (b) (c)

Figure 2-42. *Projected exclusion limits on the couplings g_q ((a)), g_χ ((b)), and g_l ((c)) for a vector mediator at the HL-LHC and FCC-hh (for quark and DM couplings only). The result is shown as a function of the mediator mass m_{med}; the mass of the DM candidate is fixed to 1 GeV in all cases. The coupling on the y axis is varied while the other two couplings are fixed: in ((a)), g_χ=1.0 and g_l=0.0; in ((b)), g_q=0.1 and g_l=0.0; and in (c), g_q=0.25 and g_χ=1.0. The arrows in the lower edge of the contours indicate that other searches for lower mass mediators that are normally performed at colliders could be sensitive to these models, but are not shown because the inputs received focused on the highest mediator masses only. It is worth noting that the lower bounds for both HL-LHC and FCC-hh for mediator (resonance) searches shown in the figure can be significantly improved by using non-standard data taking techniques such as data scouting / trigger-level analysis described in Section 2.6.3 and in Refs. [491, 492] specifically for dijet resonances.*

Fig. 2-42 shows the limits at future hadron colliders on couplings to the SM fermions and DM fermion. These are derived from the projections of searches for invisible decays of the mediator via missing-momentum signatures (e.g. jet plus missing transverse momentum, or *mono-jet*) as well as searches for the visible decays of the mediator (e.g. dijet and dilepton resonances).

Searches for visible and invisible (DM) mediator decays are complementary, as they allow us to further shed light on the DM-SM interactions in case of a discovery in both kinds of final state. As expected and already discussed in terms of Z' models with quark couplings in this section, hadron colliders with a higher center-of-mass energy can reach higher mediator and dark matter masses. Future collider searches for invisible particles are able to constrain models with much smaller couplings than current searches, especially at mediator masses below the TeV. These results can also be recasted in terms of dark photon benchmark models used by the Rare Process and Precision Frontier, as discussed in the next Section.

The exact reach of future colliders for these simplified models is dependent on the interaction strength between the mediator and the SM, especially the quark coupling of the mediator, which governs its production. It is expected that lepton colliders will also strongly constrain models with lepton couplings, especially in the case of polarized beams [**?**].

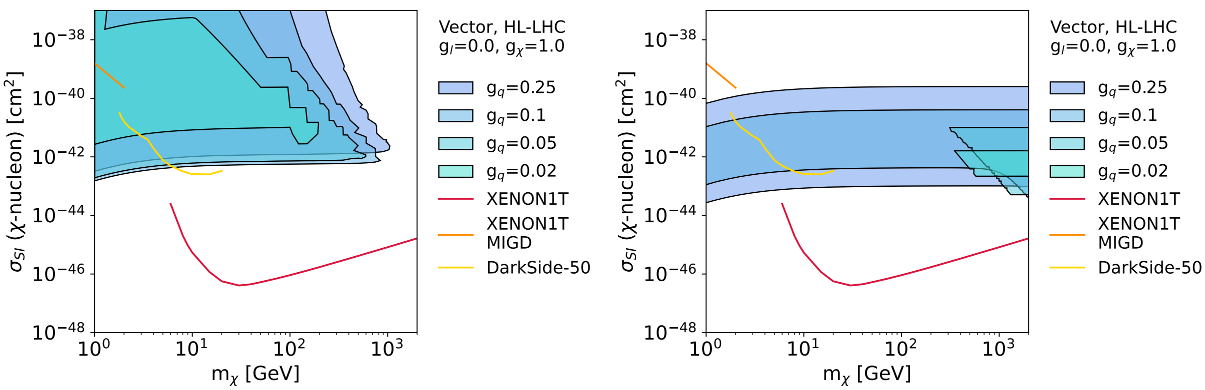

(a) Monojet searches

(b) Dijet searches

Figure 2-43. *Effects on the HL-LHC exclusion limits in $\sigma_{\rm SI}$ for the monojet ((a)) and dijet ((b)) signatures when varying the g_q coupling. The dark matter coupling is held fixed to $g_{\rm DM} = 1$; there is no coupling to leptons. Limits from existing direct detection experiments are shown for context.*

The next version of these plots will include the new LZ limits and FCC overlaid.

A discovery of invisible mediator decays at a collider experiments requires direct and indirect detection experiments to confirm that the invisible particles are connected to dark matter found in the galaxy. In order to understand the situations in which this complementarity is possible, the European Strategy Briefing Book included plots comparing both collider and direct/indirect detection experiments, highlighting the region where a simultaneous discovery was possible.

Following these studies, the projections in Fig. 2-42 can be translated into to limits in the DM-nucleon cross-section plane used to display direct detection searches, as shown in Figure 2-43. As expected from the conversion of collider results on this plane in [487, 488], as future collider searches reach smaller SM-DM and SM-SM couplings, their coverage in the DM-nucleon cross-section plane improves. When the coupling sensitivity limit approaches, collider projections gradually disappear.

The sensitivity of collider searches also depends on the ratio of the DM to mediator mass. Searches at high energy colliders are most sensitive in the region where the mediator can be produced directly from SM particle collision, and when the mediator is much heavier than the DM particle. This is a strength of collider experiments: constraints on the dark interactions for these models can also be obtained when the DM is too heavy to be produced directly. Since, in BSM mediation (as well as EFT) models, different mass hierarchy hypotheses are plausible, different mass ratios as well different as couplings should be tested by DM experiments. We refer to the following section for a specific choice of a benchmark model scenario for a vector mediator, motivated by thermal relic DM.

The main message from these plots remains the same as in the European Strategy Briefing Book [401]. In a scenario where particle dark matter is discovered at a direct- or indirect-detection search, Figures 2-43 illustrate—in a necessarily model-dependent fashion for the specific simplified model considered—the parameter space of the model in which collider searches for invisible particles would also be sensitive to production of the mediator. In roughly these regions, both types of searches would have complementary discovery potential, as discovery at a direct-detection experiment would be combined with further study of the type and properties of the interaction between the DM and the Standard Model at a hadron collider.

These figures also indicate where collider searches for invisible particles would supplement the search coverage of the other DM experiments with unique sensitivity. Nevertheless, even in these regions, it would be essential to confirm that the collider discovery is indeed associated with galactic dark matter when considering models where the DM particle is stable.

2.5.5.2 Beyond WIMP dark matter

Since the evidence we have for dark matter so far does not point to a particular mass scale for DM particles, there are many other DM hypotheses that can be discovered at colliders and neighboring facilities, and go beyond the canonical WIMP scenarios. The paradigm of the WIMP as a thermal relic can be extended to lighter DM (below the GeV), provided it has feeble couplings to SM. Dark matter particles can also be part of a more complex dark sector, with signatures that can also include long-lived particles as discussed earlier in this section. In this Section, we will highlight some representative beyond-WIMP DM models and the perspectives for their discovery at future colliders and complementary facilities.

Portal models for DM: dark photon and dark Higgs A broad class of models including feebly-coupled, low-mass thermal relic dark matter particles can be represented by a small set of relevant interactions. These interactions are mediated by new *portal* particles, akin to the simplified models mediators mentioned above.

An example of such a portal particle is a new, low-mass vector boson, commonly called *dark photon*. It couples to the SM particles via a new electromagnetic-like interaction (kinetic mixing), as well as to DM particles. This benchmark model has been adopted by the Rare and Precision Frontier (RPF) [cite] to compare the sensitivity of accelerator experiments to thermal dark matter below the GeV. Colliders can also discover visible and invisible decays of such a dark photon, in a way that is complementary to accelerator experiments in the RPF.

It is possible to reinterpret present and future collider searches for invisible particles in terms of dark photon parameters extending the DM mass coverage used by the RPF, owing to the similarities between the previously mentioned vector-mediated and the dark photon-mediated model. The results of this reinterpretation can be seen in Fig. 2-44, including the thermal relic milestone also targeted by the RPF, for a pseudo-Dirac DM particle with a mass below the TeV. From this figure, we see that the HL-LHC dataset is needed to be sensitive to the thermal relic milestone (where this model provides all the DM relic density[5]) for DM masses above roughly 100 GeV, while FCC-hh is needed to cover the remaining parameter space. This region is only partially covered by accelerator and B-factory experiments, and requires high energy collider experiments to be fully explored.

Even though it is not immediately obvious from the formulation of minimal benchmarks [493, 494, 495], almost all portal models require the presence of both low and high mass particles to be self-consistent. New particles at the TeV scale at loop-level are needed to generate the kinetic mixing interaction that characterizes dark photon models, particles that can be produced and discovered at high energy collider such as HL-LHC or the FCC complex, or inferred from precision measurements at lepton colliders [495]. As a concrete example with future collider projections, if a light scalar singlet (a dark Higgs) decaying to light dark matter couples predominantly to one SM fermion family, then new heavy states are required to keep

[5] It's worth keeping in mind that this is not a strict requirement if other processes enhancing or depleting the DM abundance are present in addition to the minimal model.

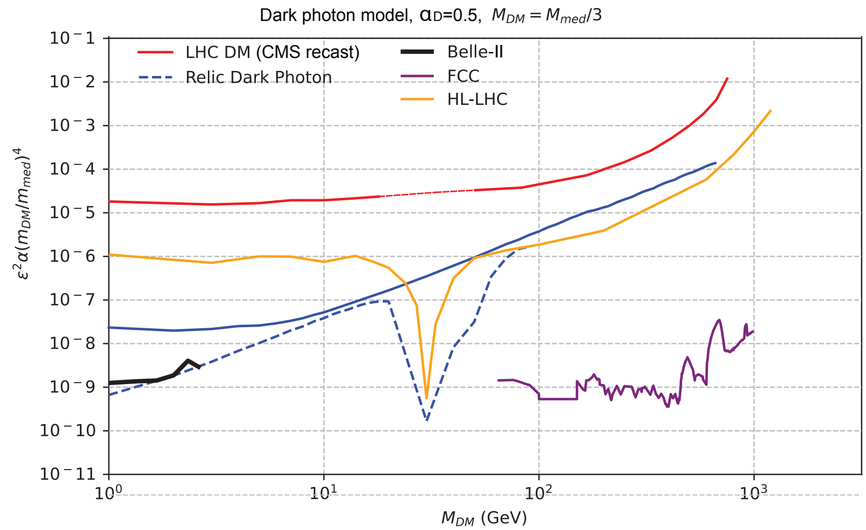

Figure 2-44. *Comparison of the expected constraints frfor the dark photon model, starting from the reinterpre the reinterpretation of the results in [**?**] in terms of the simplified vector mediator model (LHC DM), and for HL-LHC, FCC-hh and Belle-II 20/fb [**?**, **?**] in terms of the dark photon model. The dashed "relic" lines represent the minimum parameter combinations that would reproduce the observed thermal relic density for the dark photon model.*

The relic density line will be extended, and the Belle-II results with 50/ab will be also shown in the next version.

the model self-consistent at higher energy scales [493, 494, 496, 39]. In this example, the Higgs boson mass and the dark matter mass are both of the order of a GeV, while the new particles needed to complete this model have masses of the order of a TeV. The sensitivity of current and future collider searches to these new particles is shown in Fig. 2-45.

These considerations are generically applicable to different types of portal models, and encourage the use of complementary probes for the lower-energy phenomenology of this model and higher-energy particles required for the completion. Light portal particles (e.g. light dark Higgs, dark photon) with feeble couplings can be discovered at Rare and Precision Frontier experiment, while the higher-energy particles can be produced and discovered at higher energy colliders such as the Future Hadron Collider or the Muon Collider. A corresponding discovery in low-threshold Cosmic Frontier experiments will determine the cosmological nature of the dark matter particle.

More complex dark sectors: dark showers and dynamical DM The constituents of the dark sectors could be as numerous and diverse as those of standard matter. Models where a portal particle with feeble couplings connect ordinary matter to a more complex dark spectrum are part of a larger class of *Hidden Valley* models [497]. There are also models which predict a huge number of states with different masses and lifetimes[498], leading to qualitatively different signals. It is possible to engineer a viable DM candidate among the non-charged states of this dark sector [499, 500, 501, 498].

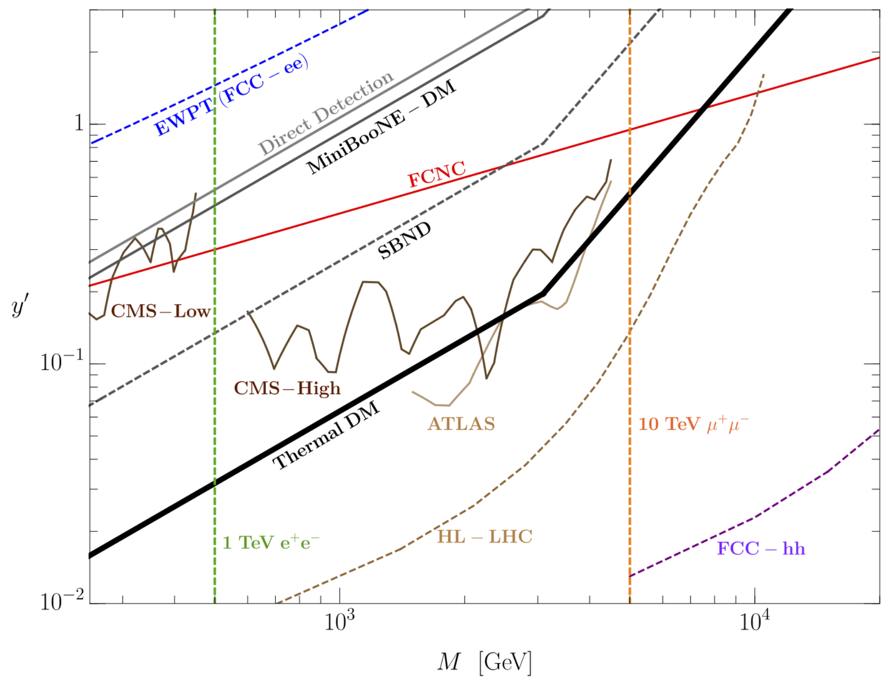

Figure 2-45. *Existing constraints and future prospects for the up-specific scalar mediator S in the renormalizable completion described in [493, 494]. together with parameter choices leading to the correct thermal dark matter abundance.*

New mechanisms for the relic density relying on interesting dark sector dynamics can point to new dark matter candidates and parameter regions. In particular, when focusing on new confining forces within the dark sector, one can make an analogy between QCD and the new force, also called 'dark QCD' [502]. Similarly to how QCD leads to stable massive particles (e.g. the proton), a QCD-like dark interaction gives rise to stable dark hadrons that can be viable DM candidates. These dark hadrons can be embedded in the *dark shower* predicted by the dark QCD, with a potential to be discovered at present and future colliders [503]. As for other collider searches, establishing a cosmological connection after a discovery requires complementary experiments[6]. A dark sector confining phase transition can also lead to new viable masses for dark matter [505].

Even though the connection between colliders and cosmology depends on the model and parameters of the chosen dark sector, future efforts to establish such a connection are encouraged. This information can be used (in the same way as in other Frontiers, e.g. BRN targets) to motivate parameter scans where the cosmological constraints are satisfied, and to help contextualise future discoveries in multiple Frontiers.

Dark sector discoveries at facilities co-located with high energy colliders: the example of the Forward Physics Facility The signatures generated by feebly coupled models often include particles with long lifetimes, also described in this chapter. Optimal coverage for this kind of signatures requires a dedicated experimental toolkit for experiments at high energy collider, as well as dedicated experiments. In particular, portal models and beyond-WIMP models are a dedicated search target for facilities or experiments that are designed to profit from the presence of a high energy beam, or from complementary information recorded

[6] Additional information on the dark sector spectrum can come from interactions with the lattice community, see e.g. [504]

at collider experiments. Collisions of high energy beams produce a large flux of secondary particles in the forward region that cannot be fully detected by general-purpose experiments. Light dark matter or dark sector particles can be produced preferrably in the forward direction, which can be investigated by dedicated experiments placed in facilities downstream from the standard collider detectors.

An example of such a facility is the Forward Physics Facility (FPF), proposed to be installed in the long shutdown between the LHC Run-3 and the start of the HL-LHC [117, 118]. In particular, the proposed FLArE [506] experiment would be sensitive to thermal relic DM mediated by a dark photon, and experiments such as FASER2 [443] and FORMOSA [507] would target a number of dark matter and dark sector scenarios. The opportunities for dark matter discoveries (as well as of neutrino measurements relevant to cosmic DM experiments) offered by the FPF would further enhance the HL-LHC dark matter and dark sector search program, especially since development and building can be performed in parallel to current experiments.

The DM physics opportunities of forward facilities and related experiments are expected to remain relevant at future colliders. Smaller-scale experiments can be optimized to cover a number of beyond-WIMP scenarios that complement and enhance what can be discovered at the larger, general-purpose experiments, while exploiting the same colliding beams, at a reasonable additional cost.

2.6 Detectors, reconstruction, simulation and data analysis

Enabling particle detection techniques, data computation and analysis methods, as well as precision calculations and simulations are critical for any future project at the energy frontier. Different collider projects have different requirements on detector layout and performance. For example e^+e^- collider require detectors with high granularity and low material budget, while hadron colliders as well as muon colliders have additional requirements on radiation tolerance for detectors to be placed close to the beam pipe. The detector design directly impacts the computational resources and affects the data analysis methodology.

Computational resource requirements are set by detector design parameters such as number of readout channels, luminosity, trigger system, data compression as well as the experimental computing model and the analysis methods.

The sophistication of artificial intelligence and machine learning (AI/ML) techniques is growing ever more, and collider physics should continue to play a pioneering role in this expanding field of research by capturing and leading such developments. As we experienced at the LHC experiments, AI/ML techniques have become necessary tools to perform precision measurements and expand the reach of searches for new physics. We expect AI/ML techniques will play even greater roles at the HL-LHC. The direction of current research also suggests that such techniques will be employed in future experiments not only in offline data analyses but also in online data selection and reconstruction, making their accuracy and reliability even more critical.

Most measurements at high-energy colliders require the understanding of radiative corrections on observables. A close interplay between theory and experiment is mandatory to design observables that have a reduced exposure to high-order effects and exploit detector capabilities as well as the latest developments in precision calculations and Monte-Carlo simulations. Essential tools in all experimental analyses are also the Monte Carlo simulations of final state particles in a detector. The computational need for such simulations strongly depends on experiment computing model and the chosen analysis format in addition to the detector layout.

Some of the most relevant aspects of needs for detector, method and tool development and research for the coming decade will be discussed in this subsection.

2.6.1 Detectors

Today, particle detectors are key to address future science challenges and their development is based on our understanding of fundamental laws of physics. Thus we have a "virtuous cycle" which must remain strong and unbroken – laws of nature enable novel detector concepts and techniques, which in turn lead to a greater physics discoveries, such as the Higgs Boson and Gravitational Waves, and better understanding of our Universe. In this context, detectors in high-energy physics face a huge variety of operating conditions and employ technologies that are often deeply intertwined with developments in industry. The environmental credentials of detectors are also increasingly in the spotlight.

At the Energy Frontier, one can distinguish two major drivers for detector R&D: detector upgrades towards future hadron colliders and development of advanced technologies for the future e^+e^- machines. The detectors for the next Higgs Factory must provide excellent precision and efficiency for all basic signatures, i.e. electrons, photons, muon and tau leptons, hadronic jets, and missing energy over an extensive range of momenta. The tracking resolutions should enable high-precision reconstruction of the recoil mass in the $e^+e^- \to Zh$ process for instance. These inherently very accurate physics probes requiring integrated concepts with ultimate precision, minimal power consumption and ultra-light structures; these concepts are in most cases orthogonal to the main requirements for HL-LHC experiments. Rather than emphasizing radiation hardness and rate capability, the demands for resolution (granularity) and material budget on one hand, and acceptable power consumption on the other hand, exceed significantly what is the state-of-the-art today. Such leaps in performance cannot be achieved by simple extrapolation of the known, but only by entering new technological territory in detector R&D. Several new concepts for silicon sensor integration, such as monolithic devices, are being pursued for pixel vertex detectors, new micro-pattern gas amplification detectors (MPGD) are explored for tracking and muon systems, and the particle-flow approach to calorimetry promises to deliver unprecedented jet energy resolution, to quote just some examples. The proposed collision energies and data rates of the next generation of energy frontier colliders and the ambitious target precision on various Higgs measurements impose unprecedented requirements on detector technology. The Basic Research Needs for High Energy Physics Detector Research & Development document [508] compiles a list of requirements for transformative and innovative technologies at the next generation of energy frontier experiments focused on precision Higgs and SM physics and searches for BSM phenomena, such as (1) low-mass, highly-granular tracking detectors and (2) highly-granular calorimeters, both with high-precision timing capabilities. The "particle flow" (PFlow) concept, originally developed for the electron-positron Linear Collider (LC), aims at measuring the energy of all the particles in a jet, exploiting track information for the charged particles, ECAL for prompt photons, and HCAL to capture the neutral hadrons. Due to this, PFlow has led to calorimeter designs, as part of a complex system of inter-connected detectors rather than as a stand-alone device. Particle flow methods benefit from high calorimeter granularity. Future collider detectors will also face a large number of diverse engineering challenges, in the areas of system integration, power distribution, cooling, mechanical support structures, and production techniques. Within the field of particle physics, technologies developed under generic R&D studies or with the aim to address experiment-oriented challenges at future colliders provide a boost in innovation and novel designs that often suit the needs of the Intensity or Cosmic Frontiers, i.e. neutrino or astroparticle physics.

Emerging novel vertex and tracking detector technologies are the vital backbone for the success at a future electron-positron machines. These will operate in an environment with high (continuous or bunched) beam currents, a minimum distance from beam axis of about 20 mm, a requirement of $< 5\ \mu m$ single point resolution, high granularity ($< 30 \times 30\ \mu m^2$), power dissipation ($< 50\ mW/cm^2$), low mass (~ 0.1 % of X_0, or 100 μm Si-equivalent per layer).

Table 2-15. *Physics goals and detector requirements [508, 509].*

Initial state	Physics goal	Detector	Requirement
e^+e^-	hZZ sub-%	Tracker	σ_{p_T}/p_T=0.2% for $p_T < 100$ GeV
			$\sigma_{p_T}/p_T^2 = 2 \cdot 10^{-5}$/ GeV for $p_T > 100$ GeV
		Calorimeter	4% particle flow jet resolution
			EM cells 0.5×0.5 cm^2, HAD cells 1×1 cm^2
			EM $\sigma_E/E = 10\%/\sqrt{E} \oplus 1\%$
			shower timing resolution 10 ps
	$hb\bar{b}/hc\bar{c}$	Tracker	$\sigma_{r\phi} = 5 \oplus 15(p \sin\theta^{\frac{3}{2}})^{-1}\mu$m
			5μm single hit resolution
pp-100 TeV	Higgs	Tracker	σ_{p_T}/p_T=0.5% for $p_T < 100$ GeV
			$\sigma_{p_T}/p_T^2 = 2 \cdot 10^{-5}$/ GeV for $p_T > 100$ GeV
			300 MGy and $\approx 10^18$ n$_{eq}$/cm^2
		Calorimeter	4% particle flow jet resolution
			EM cells 0.5×0.5 cm^2, HAD cells 1×1 cm^2
			EM $\sigma_E/E = 10\%/\sqrt{E} \oplus 1\%$
			shower timing resolution 5 ps
			4 MGy / 5 GGy and $\approx 10^16/10^18$ n$_{eq}$/cm^2 central/forward
μ	Higgs & LLP	Tracker	30 ps timing resolution and 0.01 rad angular resolution
			5μm single hit resolution

The tracking resolutions should enable high-precision reconstruction of the recoil mass in the $e^+e^- \to Zh$ process, as shown in Table 2-15, and allow very efficient b and c tagging and tau-lepton identification through the reconstruction of secondary vertices.

Gaseous and semiconductor detectors are the two main types of tracking detectors; other, more exotic ones are fiber-based or transition radiation tracking devices. While gaseous detectors offer sizeable low-mass volumes and many measurement points for an excellent pattern recognition and ultimate dE/dx measurement (e.g. cluster counting technique can be exploited instead of the charge-analog information), the silicon-based approach offers the most accurate single point resolution. The breakthrough technology is expected to come from monolithic devices incorporating complex readout architectures in CMOS foundries. To minimize material budget, new technologies, like stitching, will allow developing a new generation of large-size CMOS MAPS with an area up to the full wafer size [510, 511]. In this technology, the reticles which fit into the field of view of the lithographic equipment are placed on the wafer with high precision, achieving a tiny but well defined overlap. In addition to large-size sensors, it may also be useful to bend thin (50 μm) sensors to make cylindrical assemblies. Fast picosecond-time sensors based on Low-Gain Avalanche Detectors (LGAD) [512] and 3D-devices can be also exploited. Aiming for an excellent position and timing resolution ($\sim$ 10 ps and $\sim$ 10 μm) with GHz counting capabilities to perform 4D tracking, LGADs represent a very attractive option for PID and TOF applications. For future applications at the Energy Frontier, alternative technologies, by employing beyond state-of-the-art interconnection technologies, such as 3D vertical integration, through-silicon-vias (TSV), or micro bump-bonding, which, while retaining the advantages of separate and optimized fabrication processes for sensor and electronics, would allow fine pitch interconnect of multiple chips. At future muon collider to reject a good fraction of beam induced background, accurate timing information with a resolution of 30 ps is assumed to be available in the vertex detectors [509].

Present and future challenges in calorimeters are closely linked to all aspects of ultimate exploitation of the "particle flow" technique and the dual-readout calorimetry [513] approach, developed by the RD52, DREAM, IDEA and CalVision collaborations. Silicon photomultipliers have seen a rapid progress in the last decade, becoming the standard solution for scintillator-based devices, but also enabling substantial improvement in dual-readout calorimetry, based on scintillating and clear plastic fibers embedded in absorber structures. Ultra-fast timing in calorimetry can be also used to resolve the development of hadron showers, by separating their electromagnetic and hadronic components, and therefore simplifying the implementation of the particle flow algorithm. In general, space–time tracking could be used in many physics analysis at LHC – Higgs, BSM searches for long-lived particles, by measuring precisely the time-of-flight between their production and decay, and/or in assigning beauty and charm hadrons to their correct primary vertex. An ultimate concept is to develop 4D real-time tracking system for a fast trigger decision and to exploit 5D imaging reconstruction approach, if space-point, picosecond-time and energy information are available at each point along the track.

An emerging effort during Snowmass has focused on strange tagging [41]. Particle identification at high momenta could further boost strange tagging capabilities at future e^+e^- machines as well as the analysis sensitivity in constraining the available phase space for new physics. Gaseous Ring Imaging Cerenkov system (RICH) detector can be capable of π/K separation up to 25 GeV. A preliminary study based on ILD geometry at ILC, shows that in a compact RICH with a radial extension of 25 cm, the Cherenkov angle resolution can be maintained at the level of $\sim$5 mrad in magnetic fields up to 5 T. This leads to a discrimination power of 3σ between kaons and pions up to momenta of approximately 25 GeV. Further simulation studies and system optimization are needed to evaluate globally the impact of a RICH system on object reconstruction, such as particle flow jets, and on other physics benchmarks, when used in conjunction with silicon tracking detectors.

The detector requirements for the completion of the Tera-Z physics program at circular machines are very similar to those set by Higgs physics measurements. Except the detector solenoid magnetic field must be limited to 2 T when operating at the Z pole, to avoid a blow up of the vertical beam emittance and a resulting loss of luminosity [?]. The 2T magnetic field limit is not a significant handicap since the momentum scale of the produced partons is typically distributed around 50 GeV and does not exceed 182.5 GeV.

While research has always required state-of-the-art instrumentation in trigger and data acquisition systems, the demands for the next generation of hadron colliders are the increasingly large local intelligence, integration of advanced electronics and data transmission functionalities (e.g. using FPGA). Another important trend is the progressive replacement of the complex multi-stage trigger systems by a new architecture with a single-level hardware trigger and a large farm of Linux computers to make the final online selection and to reduce Level-1 trigger rate to O(kHz) for permanent storage. This clearly illustrates the trend towards moving more complex algorithmic processing into the online systems. Modern technologies allow the integration of significant intelligence at the sensor level and many different R&D lines are being explored, like local hit clustering for strip and pixel detectors, local energy summing for calorimeters, local track-segment finders. The use of advanced machine learning algorithms, such as neural networks (NN), boosted decision trees (BDT) and many others, is a long-standing tradition in particle physics since 1990's and has been already key enabler for discoveries (e.g. single-top production at Tevatron). Bringing the modern algorithmic advances from the field of machine learning from offline applications to online operations and trigger systems is another major challenge.

As the high-energy particle physics community and particularly the Snowmass community begins to design future detectors, it is important to keep the many, varied LLP signatures in mind, lest we design new detectors that are biased against them. For example, overly-aggressive filtering can introduce biases that limit the acceptance for displaced tracks [514]. At the same time, we can develop technologies, such as dedicated trigger algorithms [515], displaced tracking algorithms [516], and timing detectors [304, 517], to explicitly reconstruct and identify LLPs. Careful studies of beam-induced backgrounds will be necessary to reduce and/or quantify these background contributions without removing possible LLP signals. Other important factors to consider for LLPs include the time between collisions and how that interplays with the detector readout, as well as the size of the beamspot, the amount of pileup and the material budget of the detector areas closest to the interaction point.

Different geometry choices that provide similar hermeticity for prompt particles can differ drastically in their ability to reconstruct particles that do not originate from the interaction point. In particular, high granularity at large radii enables better reconstruction efficiency of displaced tracks and vertices, and helps to distinguish them from beam-induced and non-collision backgrounds.

A high volume, (partially) shielded subdetector system like the current muon systems at LHC experiments would therefore play an important role in searches for LLPs at future hadron colliders. For a future e^+e^- collider, on the other hand, the background yields are expected to be much lower and it could be beneficial to invest the equivalent amount of space into a larger inner detector, and restrict the muon system to the minimum required for muon identification. Finally, muon colliders [28] come with a new set of challenges for LLP searches, as their detectors are bombarded from both sides with ultrahigh energy electrons/positrons from the in-flight decay of the muon beam [514, 518]. It is difficult to shield the detectors from this qualitatively new beam background, but over 99% background rejection can be achieved by making use of timing and angular measurements from paired layers [518]. Whether simultaneously a good signal efficiency for LLPs can be maintained needs to be studied further.

2.6.2 Monte Carlo Event Generators

Nearly all high-energy experiments rely on the detailed modeling of multi-particle final states through Monte-Carlo simulations [519]. A particular strength of general-purpose simulation tools derives from the factorization of physics effects at different energy scales, making their underlying physics models universal. Uncertainties on experimental measurements are often dominated by effects associated with event simulation. These uncertainties arise from the underlying physics models and theory, the truncation of perturbative expansions, the parametrization or modeling of nonperturbative QCD effects, the tuning of model parameters, and the fundamental parameters of the theory. Addressing and reducing the uncertainties is crucial to meet the precision targets in current and future measurements.

The experimental facilities discussed in this report span a wide range of energies, beam particles, targets (collider vs. fixed target), and detected final states. Each experiment may require some dedicated theory input to the simulation, such as high-precision QED calculations for TeraZ or an electroweak parton shower for a muon collider. Other aspects, such as parton-to-hadron fragmentation or hadronic transport models can be similar for many facilities, enabling the modular assembly of (parts of) a generator from existing codes when targeting a new facility. In this manner, previously gained knowledge and experience can be transferred, and a more comprehensive understanding of the physics models is made possible by allowing them to be tested against a wealth of data. These cross-cutting topics in event generation have been identified as a particular opportunity for theoretical developments in a broad HEP program [519].

The extraction of SM parameters at the HL-LHC will depend on the precision of perturbative QCD and EW calculations, both fixed order and resummed, and on their faithful implementation in particle-level MC simulations. The results of some analyses will however also be limited by the number of Monte Carlo events that can be generated, and computing efficiency will play a crucial role, cf. Sec. 2.6.3. Future highest-energy colliders, including a potential muon collider, will likely require electroweak effects to be treated on the same footing as QCD and QED effects.

The Forward Physics Facility at the LHC will leverage the intense beam of neutrinos, and possibly undiscovered particles, in the far-forward direction. These measurements will require an improved description of forward heavy flavor – particularly charm – production, neutrino scattering in the TeV range, and hadronization inside nuclear matter, including uncertainty quantification [118].

Future lepton colliders would provide permille level measurements of Higgs boson couplings and W and top-quark masses. The unprecedented experimental precision will require event generators to cover a much wider range of processes than at previous facilities, both in the Standard Model and beyond. In addition, predictions for the signal processes must be made with extreme precision, involving QED up to fourth and EW corrections up to second order. Some of the related methodology is available from the LEP era, while other components will need to be developed from scratch.

With the next generation neutrino experiments not being limited by statistical uncertainties, and all running and planned experiments using nuclear targets, one of the leading systematic uncertainties to their measurements arises from the modeling of neutrino-nucleus interactions. This requires the use of state-of-the-art nuclear-structure and -reaction theory calculations. While not a traditional topic for general-purpose high-energy event generators, there is strong overlap with topics relevant to simulating high-energy neutrino DIS in the FPF detectors and at IceCube. This is expected to become an area of active development and cross-collaboration between frontiers.

The EIC will use highly polarized beams and high luminosity to probe the spatial and spin structure of nucleons and nuclei. Simulating spin-dependent interactions of this type at high precision is currently not possible with standard event generators and requires the development of new tools at the interface between particle and nuclear physics. It is expected that measurements at the LHC can greatly benefit from these developments [520, 240].

Various experiments also require the understanding of heavy-ion collisions and nuclear dynamics at high energies as well as intricate heavy-flavor effects. In addition to the physics aspects, there are similar computational aspects, such as interfaces to external tools, handling of tuning and systematics, data preservation, the need for improved computing efficiency (cf. Sec. 2.6.3), and connections to artificial intelligence and machine learning [521].

2.6.3 Computational resources

Experiments require computational resources during their design, operation, and data analysis phases. Experiments must generate and simulate collision events and other backgrounds, reconstruct events, optimize their design, trigger on collisions, reconstruct events, calibrate the experiment, and analyze the reconstructed data to extract physics.

Software trigger systems are ubiquitous for hadron collider detectors, which face significant data reduction challenges even before recording events to long-term storage. Such triggers are large computing farms that must execute a pared-down reconstruction of high multiples of the eventual recorded event rate in real time, and hence typically constitute very powerful computing sites on their own which can be repurposed when collisions are not being recorded. The challenges of offline reconstruction and software triggering go hand-in-hand.

There are many physical resources that are needed — long-term storage, both “hot” and “cold” (today represented by disk and tape); compute, both traditional CPU and accelerators like GPUs; and network bandwidth. Given the speedy evolution of computing, it is hard to predict what mixtures of available technologies will be optimal on the timescale of new energy frontier experiments. Nevertheless the scale of the computing problems posed by proposed facilities is roughly indicated by the data volume of the experiments. Estimates are summarized in Table 2-16. FCC-hh is the only facility with offline data sizes exceeding those of HL-LHC by more than an order of magnitude.

Table 2-16. *Computational resources expected at future Energy Frontier colliders.*

Collider Scenario	Event size	Event rate	Data/year
HL-LHC general purpose expt	4.4 MB	10 kHz	0.6 EB
FCC-ee Z-pole, one expt	1 MB	100 kHz	2 EB
CEPC 240 GeV, one expt	20 MB	2 Hz	260 PB
ILD 500 GeV	178 MB	5 Hz	14 PB
CLIC 3 TeV, 1 expt	88 MB	50 Hz	110 PB
Muon Collider, 1 expt	50 MB	2 kHz	2 EB
FCC-hh, 1 expt	50 MB	10 kHz	10 EB

Monte Carlo simulations generally constitute the majority of offline compute and hot storage use by experiments. For example, ATLAS projections for HL-LHC anticipate $\approx 70\%$ of CPU and $\approx 60\%$ of disk use to arise from MC simulation [522, 523]. In general the proportion is expected to be even higher for lepton colliders, due to the more democratic cross sections of relevant processes. Therefore efforts to optimize MC event generation and detector simulation through aggressive optimization, use of computing accelerators, and machine learning approximations may have significant payoff in the ability to extract physics from future facilities.

The optimal way to provision the required resources will likely evolve over time. Trigger farms will still need to be located in physical proximity to experiments due to latency requirements, but offline processing may take additional advantage of resources that are shared with other sciences (such as supercomputing centers) or which are provided by industry (cloud resources). The design of experiment computing architectures will be influenced by the cost structure and technology availability imposed by such use.

The high energy physics community is already active in cross-collaboration forums such as the HEP Software Foundation [524, 525].

Cite CompF where various US efforts are mentioned

to find solutions that can meet the challenges brought forward by the amount of data delivered by HL-LHC and future colliders.

LHC experiments are also putting in place non-traditional analysis workflows and computing architectures [cite]

Cite TDAQ report in IF

in order to exploit the physics potential of the data discarded by their triggers. For example, real-time analysis (Data Scouting in CMS, Turbo Stream in LHCb, and Trigger-level analysis in ATLAS) [cite] move part of the data reduction (reconstruction and calibration) into the trigger system, allowing data to be recorded with significantly lower trigger thresholds with negligible increase in bandwidth. These workflows can also exploit upgrades to the processing capabilities of trigger systems designed to tackle more challenging data taking conditions; for example, LHCb and CMS have begun to employ GPUs in their software trigger in Run-2 to parallelize problems such as particle tracking.

2.6.4 Artificial Intelligence and Machine Learning

Artificial intelligence and machine learning have come to pervade particle physics. Particle identification and event classification in data analysis and software triggering routinely use ML models. There are many proposals to extend the use of AI/ML in other realms which are just beginning to be explored, and we mention a few examples below.

The ability to find unexpected deviations from the Standard Model — and not just classify signals from specifically-targeted processes — has been a goal in the field for a long time and is important for fully exploiting the datasets collected by new facilities. Efforts are underway using a number of techniques to try to find such events, using semi-supervised and unsupervised learning methods. Such methods could be implemented at the data analysis level or even earlier in the trigger system. Similar anomaly detection techniques can also improve effective operation of experiments by rapidly identifying periods of bad data. Algorithms that can be used for identifying outliers can also learn the optimal way to compress data with tolerable losses in fidelity [cite], and studies are in progress to assess how these can be employed for HL-LHC and future colliders.

Work is in progress in the US and internationally to provide tools to transform ML models into FPGA code. This opens the door to deploying ML in hardware triggers, improving signal discrimination for experiments (especially at hadron colliders) with strong bottlenecks at this level.

Generative ML techniques hold the potential to accelerate event generation and simulation. By learning accurate approximations to a full physics model that can be executed much faster, generative ML can increase the amount of Monte Carlo that can be produced with limited computing resources, improving the optimization of analyses and final statistical uncertainties [521].

The core technology of model training (optimizing a function of many parameters relative to some objective) motivates the idea of "differentiable programming," in which more generic user code, written in an appropriate framework, can be rapidly optimized in a similar fashion if analytic derivatives are available. If deployed at scale, this opens the possibility of end-to-end optimization of data analysis and other computations, as well as more sophisticated methods of handling systematic errors.

Detector design is also an optimization problem. By linking together appropriate methods, it may be possible to do a practical end-to-end optimization of a detector from scratch using target physics measurements as the benchmark, rather than intermediate figures of merit for each subdetector (such as momentum or energy resolution). The simultaneous global optimization of detector designs could allow improved physics performance for reduced cost.

From a theoretical perspective, there are cases where it is possible to implement machine learning models that respect important symmetries by construction and are potentially capable of being mapped onto first-principles theory; such approaches may provide acceleration for otherwise computationally-difficult problems, or rigorous interpretability. The use of neural networks for tackling inverse problems (determining regions of theory space that are compatible with observation) is another promising direction at this interface [521].

As it is the case with other data selection and data processing tools used in high energy physics, cross-collaboration and cross-field activities should be encouraged. Challenges such as having the shortest possible time-to-insight on large amounts of data, and extracting small signals from large backgrounds, are not unique to high energy physics. Developing and discussing solutions for similar problems in different fields can be mutually beneficial. Computer science and industry are routinely developing ML algorithms, tools and hardware beyond the state-of-the-art, and their involvement in high energy physics projects can accelerate the field's development.

2.6.5 Analysis reinterpretation, preservation and Open Data

This section will be completed after discussion with the CF7 conveners

.

Reference CompF7 (preservation) report and summarize briefly:

- importance of re-usable data and interoperable software
- Likelihood-sharing for combinations
- Reinterpretation of BSM searches using different models
- Data sharing for common summary plots (HEPData)

2.7 Enabling the Energy Frontier research

2.7.1 Goals

What enabling tools, technologies, or facilities studied by each frontier are needed to address the pressing scientific questions in particle physics during this period?

Addressing the Big Questions outlined in Sec. 2.1 is the main scientific goal of the Energy Frontier. To accomplish such a goal, it is essential that the two complementary directions are pursued: 1) Study known phenomena, and 2) Search for direct evidence of BSM physics. It is well established that discoveries at the Energy Frontier are intricately linked to new accelerators, detector instrumentation, advances in theory (including calculation tools), and innovative analysis technologies and frameworks.

The studies of known phenomena include extensive studies of Higgs bosons, Electroweak (EW) physics, and QCD strong interactions, at the various operational scenarios of Higgs Factories. Indirect evidence of BSM physics may emerge from precision measurements of such known phenomena and fundamental parameters of the SM. Among these indirect probes precision measurements and studies of rare phenomena, including flavor and neutrino-related observables among others, contribute with complementary information. The search for direct and indirect evidence of BSM physics requires the next high energy frontier collider. Both approaches require substantial research and development in several scientific sectors that are necessary conditions for the accomplishment of those goals, such as collider physics, detector, trigger, DAQ and computing technologies as well as theoretical calculations and modeling.

2.7.2 Context

What can be expected from ongoing, approved, planned, or proposed scientific, technical, or community programs in addressing the issues identified by each frontier

The Energy Frontier is at a turning point, in which experimental guidance is needed to shed light on new physics beyond the SM. Several projects have been proposed to provide such guidance. The HL-LHC is the most awaited and the approved short-term project with a potential to shed light on BSM physics directly through searches and indirectly via precision measurements of the Higgs boson and all SM parameters. Several other projects have been identified for their capability to extend the reach of the HL-LHC in terms of precision measurements and direct searches, these include Higgs factories and multi-TeV colliders. The programs proposed by those projects are often complementary in their approaches to the common goals. A clear path towards the identification of the next collider project is very much needed. Such a path has to be well supported by the US and international community as a whole. Preparations for the next collider experiments beyond the HL-LHC have to start now, such that they can be positioned to start operations during or soon after the end of the HL-LHC data-taking. Such a time scale calls for no further delays in pursuing the scientific goals of the Energy Frontier, and in addition, to maintain and to strengthen the vitality and motivation of the community.

2.7.3 Collaboration

What opportunities exist for cross-frontier, cross-disciplinary, or international collaboration and cooperation in the coming decade to enhance our ability to address the issues identified (including training or mentorship)? How do these collaborations affect the timescales or resources needed for these activities?

The Energy Frontier community in the US is fully integrated in and interdependent with the broad international community of particle physicists, which includes experimentalists, theorists, accelerator and detector physicists in the various domains that pertain to HEP as well as nuclear physics. The cross-fertilisation between different domains of particle physics is a strength of the Energy Frontier and will continue to offer opportunities in the future, thus has to be nurtured and supported.

2.7.3.1 Interdependence between Frontiers

Given the strong dependence of the Energy Frontier on collider technology, there is a unique opportunity for collaborations. We have seen growing interest in the Energy Frontier community for the development of collider technologies that enable the targeted physics research.

There is a clear interdependence between the communities of experimentalists and theorists. Such interdependence offers an opportunity for the Energy Frontier and Theory Frontier to work hand-in-hand on physics studies for the next generation of collider physics experiments.

At the LHC we already experience a strong cross-fertilization between the Energy Frontier and the Rare Processes and Precision Measurements Frontier. Such cooperation will be even more useful and necessary in the HL-LHC and at future colliders to tackle experimental and theoretical challenges, for example on detector solutions as well as analysis and computational methods and techniques. On the latter, the cooperation with the Instrumentation Frontier is instrumental for the development and eventual use of transformative technologies that will enable the realization of novel detectors for future collider experiments.

The Energy Frontier must keep working in concert with the Theory, Rare Processes and Precision Measurements, Cosmic, and Neutrino Frontiers to discover particle dark matter and probe its interactions with the SM at future collider experiments. Section 2.3.1.2 provides examples of how searches for invisible particles with future experiments at the energy frontier are a vital complement to the efforts in the other frontiers. Collider experiments offer both unique possibilities for discovery as well as the ability to connect signals of astrophysical dark matter observed at the other frontiers with measurements of the interaction(s) responsible. To highlight this complementarity that is central to understanding the nature of dark matter, representatives from the different frontiers are compiling separate cross-frontier contributions that will be cross-referenced here.

2.7.3.2 Interdependence between US and international communities

The US community in the energy frontier is fully embedded in the international community. Mutual support and exchanges of ideas, expertise and future plans is advisable and inevitable. The growth of one member of the community is the growth of the whole community. Constructive and multi-directional communication within the broad international community is vital to keep the field vibrant and make concrete scientific progress.

2.7.3.3 Cross-fertilization between Energy Frontier and other domains of physics

The planned construction of EIC in the USA within the next decade offers a unique opportunity for strengthening the central role of the US scientific community in the field of particle physics, seen as a whole. The consideration of EIC, within the Energy Frontier topical groups for this Snowmass study, has been instrumental in fostering opportunities for cross-fertilization between the two fields of HEP and Nuclear Physics in terms of physics, experimental technologies, data analysis techniques and methods, as well as theoretical and phenomenological tools. The two (international) communities are well integrated, beyond the artificial and too-often restricting boundaries set by funding agencies.

Emerging technologies and detection techniques in other realms of physics, e.g. quantum computing and detectors, novel materials, new detection techniques and methods, including AI/ML etc. will offer new opportunities for enhancing our experimental capabilities in ways that can be difficult to predict with our current knowledge.

2.7.4 Building a diverse Energy Frontier community

How can we ensure that the US particle physics community is vibrant, inclusive, diverse, and capable of addressing the scientific questions identified, and of fulfilling our obligations to society during this period?

A vibrant, inclusive, diverse and capable scientific community are necessary for any success of the US scientific community in the Energy Frontier. These can be achieved by innovation as well as empowerment and training of the next generation of leaders in the Energy Frontier.

2.7.4.1 Continue to innovate and empower

A vibrant Energy Frontier community requires a large base of well motivated early career scientists with a vision for the future of the field. Such motivations and vision are acquired by training, mentorship, and empowerment. The complexity of modern experiments and the dispersion of large collaborations too often prevent young scientists from developing a vision and solid foundation in different sectors, as they are often confined in specific niches of their research. It is important to introduce young scientists to participate in different and diverse collaborations, similar to the variety of scientific methods and techniques they engage in.

In large collaboration such as those at the LHC, the contribution to specific research is often hidden by the large author list in papers or conference presentations given by people who did not directly participated to the presented studies. In addition, too often the students do not have an opportunity to present their analyses at a conference during the course of their studies due to the complex decision making process of the speaker committees. The main vehicle for an early career physicist to get visibility inside and outside the collaboration is by appointments in managerial roles such as subgroup or group convenorship, which has become a coveted (instead of longed-for) role by young physicists and used as a trampoline for a permanent job. Such strict hierarchy and opaqueness of large collaboration often causes lack of ownership of projects and physics studies by early career physicists. A more transparent and merit-based empowerment of early career scientists will help the community grow in the long term.

Inclusiveness and diversity are at the core of the scientific endeavor, which is motivated solely by the goal of advancing fundamental scientific knowledge with a potential societal impact. Scientists are trained to question assumptions and to overcome barriers between members of the scientific community to pursue scientific progress.

In addition, the Energy Frontier crucially relies on synergy between theorists and experimentalists that needs to be maintained for the success of the field.

By pursuing our goals of fundamental knowledge at the energy frontier we will inevitably continue to push the boundaries of innovation in several areas of research and we will fulfill our obligations towards society, not only with augmented knowledge but also with concrete technological advances.

2.7.4.2 Training the next generation of scientists

The Energy Frontier experiments are the largest scientific experiments in the world and offer young researchers unique exposure to open research within diverse international collaborations. Junior scientists engaged in particle physics research receive hands-on training in quantitative, computational, engineering domains as a part of their work on big collider data.

The Energy Frontier community has been pioneering new technologies and methods (both theoretical and experimental) that have found applications in a variety of scientific fields that greatly benefited society as a whole. The Energy Frontier has a long-standing record of training young scientists. Keeping this tradition is of paramount importance as it is necessary to keep the field thriving. There is a unique opportunity to engage early career scientists with challenging new problems on physics prospects for future colliders, detector design, software development, analysis and computational techniques. The vast range of challenges that we face at future colliders are the perfect training ground for future scientists.

2.7.5 Investments essential to the progress of the Energy Frontier

What investments need to be made during 2025-2035 for the continuing scientific, technical, or community progress identified by your frontier in the decades beyond, on what timescales can these be implemented, and what resources would be required?

The realization of the Energy Frontier scientific program depends on transformative advances in several critical areas of research, such as innovation in collider and detector technologies, use and development of cutting-edge computational and data acquisition techniques as well as novel theoretical ideas and accurate calculations. These areas of research need significant and immediate support and investment in order to accomplish the energy frontier programmatic goals and have a competitive scientific community in the next decade. The resources to be allocated will have to be commensurate to the vast range and amount of scientific output that is expected by those experiments. Such a scientific output is not only measured in terms of scientific articles and size of the community, but also in terms of the societal impact that can be considered as a return of investment, such as training of young professionals, dissemination of scientific knowledge, development of new technologies and methods, etc. History has demonstrated that the activities of the Energy Frontier community have always had large societal return of investment, therefore the resources allocated to such enterprises should be commensurate to their expected return.

- **Collider R&D:** progress in the energy frontier is dependent on progress in collider technologies. It is vital for future energy frontier experiments to secure support for collider R&D that enables transformative changes in accelerator and magnet technologies in the next decade, for electron, hadron, and muon colliders.

- **Detector Technology R&D:** as the 2020 BRN [508] report identified, there is an opportunity to capture advances in detector technologies, e.g. for low-mass and high granularity detectors, to use at future electron colliders. In parallel there is the need at future hadron and muon colliders for innovative technologies that can withstand an unprecedented level of harsh environmental conditions.
- **Computing Resources:** computing is a fast-evolving field, mostly driven by industry. However, HEP has historically pioneered techniques, e.g., ML, and has developed its specific solutions to its specific computational and data acquisition requirements. While it is difficult to predict advances in such a dynamic field in the next decade, we surely know that we have an opportunity to capture and lead the progress in computing for the next generation of accelerator-based experiments. For example, while lepton colliders do not provide the same computing challenges as hadron colliders, the sheer amount of channels and information to be analyzed requires the use of cutting-edge computational resources for all proposed collider experiments. Not to be forgotten is the ever growing computational need in theoretical calculations and simulations.
- **Theoretical Physics:** Advances in theoretical calculation and modeling for new physics are expected to maintain an important role in the unveiling of new opportunities for experimental measurements and searches for new physics beyond the Standard Model. As the experimental measurements become more precise, theoretical calculations need to become more accurate. In the past decade we have seen transformative advances, often called 'revolutions', in theoretical calculations and Monte Carlo simulations that allowed to achieve unprecedented levels of precision in measurements that are dominated by theoretical or modeling uncertainties, and extended the reach of searches at the HL-LHC. Similarly, we have a unique opportunity to capitalize on the expected progress in the next decade. For example, at e^+e^- colliders, where extremely high precision is expected to be reached in a broad range of experimental measurements, high-order calculations as well as fast and accurate Monte Carlo simulations are needed to match that precision. In another direction, as shown in a number of examples in this report as well as in the report of the Theory Frontier, theorists have discovered new ideas in QFT and model building which have led to new observables and clarified the meaning of others in the quest for new physics. For example in Higgs-boson physics, contributions from theory have been crucial to build a precision physics program and have led to qualitative changes in studying the possibility of an EW phase transition, new ideas for investigating the relation between the Higgs boson and the flavor dynamics of fermions, and EFT techniques that have all broadened the experimental program. Therefore, continued investment in theory is crucial to the success of the Energy Frontier.

2.8 The Energy Frontier vision

What opportunities identified by each frontier are there for new scientific, technical, or community activities to create transformative change in particle physics, on what timescales could these occur, and what resources are required to realize these activities?

The Energy Frontier community has proposed several opportunities for pursuing its scientific goals, among them the most prominent ones are Higgs-boson factories and multi-TeV colliders at the Energy Frontier. These projects have the potential to be truly transformative as they will push the boundaries of our knowledge by testing the limits of the SM and by directly discovering new physics beyond the SM.

2.8.1 Community input

The Energy Frontier vision, as outlined in the following, has been formulated from the input received from the Energy Frontier community during the Snowmass process, including the energy-frontier-wide meetings and workshops, the regular topical group meetings, the Agorá events on future colliders, and the direct input from the community. The vision shared by members of the Energy Frontier community after the Energy Frontier Workshop in March/April 2022 is included verbatim in Ref. [526].

2.8.2 Vision overview

The Energy Frontier aims to facilitate US leadership in an innovative, comprehensive, and international program of collider physics. The timescales to fully realize the Energy Frontier vision extend to the end of this century, and the ultimate goals can only be realized if our actions foster a vibrant, diverse, and intellectually rich US Energy Frontier community. Building such a community is only possible if our plans reflect the aspirations of and provide a rich and continuous string of opportunities for Early Career physicists.

During the coming decade it is essential to complete the highest priority recommendation of the last community planning exercise (P5) and to fully realize the scientific potential of the HL-LHC by collecting and analyzing at least 3 ab^{-1} of integrated luminosity.

As documented in this report, the precision electroweak measurements possible at an e^+e^- collider (Higgs factory) would greatly extend and complement the scientific results provided by HL-LHC. The Energy Frontier endorses making the investments now to enable US leadership in a Higgs factory and start the construction for a Higgs factory in parallel with HL-LHC operations. To realize this goal, the US Energy Frontier community needs to expand the R&D in collaboration with the international community on the detector and accelerator technologies which will be required for a Higgs factory. In addition, the global HEP community should consider opening a dialogue for a US-based site for a future e^+e^- collider.

The next step in our exploration of the fundamental properties of matter requires the exploration of the multi-TeV energy scale. Any deviations observed at HL-LHC or an e^+e^- Higgs factory would strongly motivate such a program. Two possible and potentially complementary paths forward appear most promising to develop the capability to explore the energy-scale frontier: 1) a 100 TeV (or higher) hadron collider, and 2) a high-energy muon collider The community proposes the US (in collaboration with international partners) embark on a R&D program addressing high priority, critical aspects of accelerators to reach these high energies, and to develop the detector technologies needed to withstand the complex backgrounds and high radiation environments envisioned for these two types of future colliders.

Thus, the energy frontier believes that it is essential to complete the HL-LHC program, to support construction of a Higgs factory and to ensure the long-term viability of the field by developing a multi-TeV energy frontier facility such as a muon collider or a hadron collider.

A key role in the success of the US Energy Frontier at the HL-LHC, at future e^+e^- colliders (Higgs factories) as well as at future multi-TeV colliders is played by the Theory Frontier. Model building, precision calculations and simulations are necessary for precision measurements and searches of new physics. The theory community must be adequately funded to support the success of the Energy Frontier community as a whole. In addition, the Energy Frontier community thrives on collaborating with other frontiers within HEP, and has relied on cross-fertilization opportunities available via the interdependence with various fields and opportunities, see Sec. 2.7.3.

It is essential for the US and global HEP community to develop an integrated plan for future colliders to pursue to reach our ultimate goal of uncovering new particles, forces and unveiling more fundamental laws of nature.

2.8.3 The immediate-future Energy Frontier collider

The immediate future is the HL-LHC. The physics case for this program rests on its ability (1) to extend the direct search for new elementary particles, (2) to measure the couplings of the Higgs boson at a level that is sensitive to corrections from beyond the Standard Model, (3) to demonstrate the presence of a quartic self-coupling of the Higgs boson, (4) to measure the couplings of the top quark at a level that is sensitive to corrections from beyond the Standard Model, and (5) to extend our understanding of QCD and strong interactions by improving the precision of the measurements.

The Energy Frontier currently has a vigorous top-notch program with the LHC at CERN. We are looking forward to Run 3 of the LHC. It will significantly increase the integrated luminosity collected at more than 13 TeV by the LHC experiments. The HL-LHC is scheduled to start operation in 2029 and to increase the integrated luminosity by another factor of 5 over the following decade. It will set the basis for any vision of the future of the Energy Frontier program. While so far the LHC experiments (ATLAS, CMS, LHCb, and ALICE) see no evidence for physics beyond the SM, they have been exposed to barely 5% of the total data set envisaged to be delivered in the lifetime of the LHC; the HL-LHC will provide the experiments with 20 times the data set they currently have available. These unprecedented data sets will allow particle physicists to observe and study SM phenomena that remain elusive so far because of their small rates, as well as to extend the reach of searches for new processes beyond the SM. At the same time, these new data will boost the potential of the experiments to make direct discoveries that could revolutionize the human understanding of nature. It must be emphasized that the HL-LHC program goals will rely upon a major theoretical effort to reduce the expected theoretical systematics.

The HL-LHC program spans a very wide range of physics topics, where the sensitivities of measurements or searches are expected to reach unprecedented levels. Among the final HL-LHC legacy results, some are expected to remain the most sensitive for a long period of time after the end of the HL-LHC data-taking. The study of the Higgs boson self-interaction is one of the primary goals of the HL-LHC due to its role in cosmological theories, involving, for example, the vacuum stability. Higgs boson pair production is a flagship measurement, with a projected evidence of a di-Higgs signature at the 4σ level, by the end of HL-LHC running. Among all the Higgs boson self-interaction terms, the trilinear self-interaction is the only one in the reach of the HL-LHC and it is parametrized by the coupling strength, which can be measured with a sensitivity of 50%.

Studying the properties of the Higgs boson is a key mission of the HL-LHC. Uncertainties in the signal strength modifier and coupling measurements in the main production and decay channels will reduce from their current levels of 10-50% to less than 5%, moving Higgs-boson measurements into the regime of precision physics, and allowing for spotting deviations from the SM. Rare processes such as Higgs decays to $c\bar{c}$, which are challenging, and currently at the level of about 7.6 times the SM cross section, will become accessible at the HL-LHC. The sensitivity to the H $\rightarrow$ invisible branching ratio would reduce from the current $\sim$20% to a few percent, approaching the SM prediction of 0.1%. For the heavy Higgs bosons predicted by BSM theories with extended scalar sectors, the reach would increase to masses up to 1 TeV.

HL-LHC will also extend the sensitivity in direct searches for BSM particles. For example, in supersymmetry, reach for gluinos and squarks will increase by up to 1-2 TeV, while chargino, neutralino and slepton reach will increase by up to 0.5-1 TeV. This will allow making a more conclusive statement on the naturalness hypothesis. The reach for new resonances decaying to SM particles will extend on average by 2-3 TeV. Moreoever, HL-LHC will provide the ability of studying resonance decays to lighter BSM particles, such as in the case of Z' decays to charginos, which are barely accessible at the LHC, due to typically small branching ratios. Another set of dedicated searches will look for dark matter, typically in final states with invisible dark matter and visible mono-X and increase the current sensitivity. Sensitivity to long-lived particles will be especially enhanced at the HL-LHC due to improved and innovative detectors. The reach for Higgsinos via a disappearing track search will increase to masses up to 350 GeV. Sensitivity to long lived neutralinos decaying to photon and graviton is expected to increase to masses of 700 GeV, improving reach in short $c\tau$ and high masses. Additionaly, dedicated displaced muon reconstruction will improve cross section reach for smuons or dark photons by 1-2 orders of magnitude for different values of lifetime with respect to Run 3 at 300 fb^{-1}.

With the expected measurements of QCD interactions, e.g. in jet, photon as well as in W and Z boson productions, we expect to considerably improve the understanding of the Parton Density Functions at low and high momentum fraction x, which are critical for carrying out the vast and complex physics program of precision Higgs-boson measurements as well as BSM searches. Heavy Ion studies at the HL-LHC will include measurements of parton densities in broad kinematic range and search for saturation, measurement of macroscopic long wavelength Quark Gluon Plasma (QGP) properties with unprecedented precision, developing a unified picture of collectivity across colliding systems, assessing microscopic parton dynamics underlying QGP properties, and performing precision QED and BSM physics, for example in ultra-peripheral collisions.

The international collaborations at the LHC recognize the importance of the Snowmass process to the HEP community in the US and beyond. Continued strong US participation is in particular critical to the success of the HL-LHC physics program, as the Phase-2 detector upgrades, the HL-LHC data-taking operations and the physics analyses based on the HL-LHC dataset. These activities will not be able to proceed without the support of the US community.

Additionally, auxiliary experiments and facilities are proposed to take advantage of the wealth of collision events being produced at the HL-LHC in kinematic regions that escape those covered by the central detectors. Forward physics facilities allow to further extend the breadth of the HL-LHC physics: they can study regions of parameter phase space for BSM, for example in LLPs and DM searches, that would otherwise remain uncovered, and can perform novel QCD and neutrino measurements in the very forward region. As an example of collaboration across different fields, we note that the the synergies and complementarities with the Electron Ion Collider (EIC) measurements, which is a near term priority of DOE NP, were identified in many physics studies, experimental technologies, data analysis techniques, as well as theoretical and phenomenological tools during this Snowmass discussion.

The US HEP community is heavily involved in ATLAS, CMS, LHCb, and ALICE, and it contributes to aspects of the LHC accelerator infrastructure. More than half of the US HEP community is involved in LHC. Over the last years, US institutions have graduated about 100 PhDs/year based on research carried out with LHC data. During the last decade, both LHC experiments have together published more than 2000 scientific papers in peer reviewed journals. This has had a significant impact on the advancement of the field, and is an unprecedented achievement for the LHC Collaborations. In addition, the PhDs apply the valuable skills they learn during their research to many domains of science and industry, which is an essential positive economic return on the LHC program. The vibrant scientific program of the HL-LHC will continue this tradition and provide excellent training environment to the next generation of students and postdoctoral researchers. Given the broad portfolio of HL-LHC, similar number of student cohorts, i.e. about 100 PhDs/year from the US are expected to benefit from the HL-LHC program.

Our highest immediate priority accelerator and project is the HL-LHC, the successful completion of the detector upgrades, operations of the detectors at the HL-LHC, data taking and analysis, including the construction of auxiliary experiments that extend the reach of HL-LHC in kinematic regions uncovered by the detector upgrades.

In addition, the time scales for realizing what comes next requires also an effort to advance preparations for the next collider of the intermediate future during this time frame. This is reflected in the sub-section on resource needs and timelines, Sec. 2.8.7.

2.8.4 The intermediate-future Energy Frontier collider

The intermediate future is the an e^+e^- Higgs factory, either based on a linear or a circular collider. The physics case for this program rest on its ability to (1) measure the couplings of the Higgs boson to the sub-percent level and discern the pattern of modifications from beyond the Standard Model, (2) search for exotic Higgs decays due to a "Higgs portal" to a hidden sector of forces, (3) measure the parameters of the Standard Model, including the Z, W, top, and Higgs-boson masses to very high precision, and to provide stringent tests of couplings in the electroweak sector, (4) measure the electroweak couplings of the top quark at a level that can clearly reveal corrections from beyond the Standard Model, and (5) perform precision measurements of QCD phenomena which are testing-grounds of QFT in both perturbative and non-perturbative regimes, and provide complementary information relevant to cosmology and BSM physics.

The e^+e^- colliders are the vehicle that will enable a program in the electroweak sector and will increase the precision of the measurements. The physics case for an e^+e^- Higgs factory is compelling and the program is possible essentially with current technology.

Several options for its realization — linear and circular — are under consideration. The various proposed facilities have a strong core of common physics goals that underscores the importance of realizing at least one such collider somewhere in the world. A timely implementation of a Higgs factory is important, as there is considerable US support for initiatives that can be achieved on a time scale relevant for early career physicists now engaged in experimental particle physics. Planning the center-of-mass energy of the future e^+e^- collider is important, and planned upgrades of the center-of-mass energy will provide access to a broader spectrum of Standard Model physics, including top physics, which is an important component of the energy frontier physics program.

Circular e^+e^- colliders will be implemented in stages as electroweak, flavor, QCD, Higgs, and top factories by spanning the energy range from the Z pole (and below) up to the top-pair threshold and beyond. The highlights of such colliders are the highest luminosities at the Z pole, WW threshold, and ZH energies (the "intensity frontier"); the exquisite beam energy calibration at the Z pole and WW threshold; the possibility of center-of-mass energy monochromatization at $\sqrt{s} = m_H$; the compatibility with four interaction points; and the cleanest experimental environment. Circular e^+e^- colliders are therefore excellent Higgs factories: they produce over a million Higgs bosons in three years at 240 GeV center-of-mass energy. They provide the most precise determination of the Higgs-boson coupling to the Z boson, and of the Higgs-boson width (and mass), and they could provide the opportunity for the discovery of the Higgs-boson self-coupling and for a first measurement of the electron Yukawa coupling. These colliders are also much more than Higgs factories. At the Z pole, the TeraZ factory, with several trillions Z produced, offers opportunities for a comprehensive set of electroweak measurements with the best prospects for precision, such as Z-boson mass and width (10's of keV), effective weak mixing angle (few 10^{-6}), a direct determination of the electromagnetic coupling constant, which allow sensitivity to mass scales up to 70 TeV to be reached. In addition, a TeraZ factory has comprehensive programs for QCD physics, e.g. the most precise measurement of the strong coupling constant, flavor and rare decay physics, e.g. the search for lepton-flavor violation, as well as direct searches for heavy neutral leptons, axion-like particles, and other feebly coupled dark matter particle candidates. Collisions at the WW threshold will allow the most precise determination of the W mass (300 keV) and width (1 MeV), while running at the top-pair threshold, will provide the best prospect for the top mass measurement.

The linear e^+e^- collider is primarily aimed at precision measurement of the Higgs boson properties with the aim to potentially flag violations of the SM. The linear e^+e^- colliders will also run at center-of-mass energies covering the production thresholds of Z bosons, WW pairs, ZH pairs, $t\bar{t}$ pairs, and tH and Higgs pair production. The center-of-mass energy can be chosen flexibly depending on new discoveries at the LHC, or elsewhere. The e^+e^- linear collider will use polarized electron and positron beams to enhance signal reactions and allow the measurement of helicity-dependent observables, multiplying the physics output per unit of luminosity. Beam polarization also enables the suppression of backgrounds and provides cross-checks for the control of systematic errors. In electroweak measurements, beam polarization gives direct access to Z left-right asymmetries, which are very sensitive precision probes. For example, in a dedicated run at the Z pole, it allows a measurement of $\sin^2\theta_w$ at the level of 10^{-5}, comparable to the TeraZ capability. The nominal e^+e^- collider physics program begins with running at a center of mass energy of 250 GeV. At this energy the total cross section and the branching ratios for all Higgs decays can be determined, including decays to invisible final states. It provides the potential to search for exotic Higgs decays. These measurements will improve our knowledge of Higgs-boson couplings by a large margin over HL-LHC results. A global fit using an EFT framework allows for a determination of the Hbb couplings to 1%, the HWW and HZZ to 0.7%, and all other important Higgs boson couplings to close to 1%. These levels of precision are sufficient to be sensitive to new physics beyond the reach of direct searches at the LHC. The second step in the linear e^+e^- collider program would be and energy upgrade to $\sim$600 GeV. This would improve the precision of all measurements from the 250 GeV running by a factor two. Beyond the improved precision of the Higgs couplings the couplings of the top quark can be explored and it is possible to search for pair production of new particles produced in electroweak interactions that are difficult to discover at LHC. At $\sqrt{s}$ of 500 GeV, the Higgs pair production can be observed and the Higgs-boson trilinear coupling can be measured with a precision of 22%.

The physics case for a Higgs factory is strong. Therefore, the US should participate in global efforts to construct at least one Higgs factory somewhere in the world. The accelerator R&D should aim at developing sustainable facilities for Higgs research at a reasonable cost. To enable the realization of a Higgs factory in the shortest possible timescale, a targeted program on detector R&D for Higgs factories should be supported. In order for the US to build a strong community of young physicists engaged in Higgs factory research, the EF community supports the case for establishing a program for detector R&D that covers the range of proposed accelerator facilities, with initial emphasis on areas that are applicable across facilities. The critical detector R&D areas have been identified as 4D tracking and vertexing, i.e. providing precision time and spatial measurements in a single detector unit, low-mass detectors, e.g. monolithic detectors that embed the electronics in the sensing elements, wireless data transmission technologies, implementation of advanced AI/ML algorithms in on-detector electronics, radiation-hard technologies, dual calorimetry among others.

The Energy Frontier also supports the possibility of a Higgs factory in the US. Given global uncertainties, consideration should also be given to the timely realization of a possible domestic Higgs factory, in case none of the currently proposed global options are realized. To enable the realization of a Higgs factory in the shortest possible timescale, a targeted program on detector R&D for Higgs factories should be supported. In order for the US to build a strong community of young physicists engaged in Higgs factory research, the EF community supports the case for the establishing a program for detector R&D that covers the range of proposed accelerator facilities, with initial emphasis on areas that are applicable across facilities.

2.8.5 The long-term-future Energy Frontier collider

In the long-term future we envision a collider that probes the multi-TeV energy scales, i.e. up to about hundred TeV center-of-mass energies. Its physics case rests on its ability to (1) produce the fundamental particles that generate the mechanism of electroweak symmetry breaking, (2) to produce particles with flavor-dependent couplings to quarks and leptons, (3) to search for thermal dark matter particles into the region of strong coupling in the dark sector, and (4) in general to explore the unknown at the highest possible energy scale.

A 100 TeV proton-proton collider (e.g. FCC-hh, SppC) provides an effective energy reach similar to that of a 10-TeV scale muon collider with sufficient integrated luminosity. The similarity between high energy lepton colliders (effectively W-W colliders) and hadron circular colliders (effectively gluon-gluon colliders) is outstanding. Studies indicate that both the muon and hadron colliders have similar reach and can significantly constrain scenarios motivated by the naturalness principle. The 100 TeV hadron collider will have an advantage when it comes to searching for colored states, while the muon collider naturally is stronger for EW states. Multi-TeV muon colliders will have the benefit of excellent signal to background, taking advantage of the vector boson fusion production processes. As the multi-TeV colliders are planned for after the Higgs Factory, they will benefit from the precision studies of the Higgs-boson properties in understanding the possible scale of new physics. One of the key measurements from the multi-TeV colliders is the measurement of the Higgs self-coupling measurement to a precision of a few percent, and the possibility of scanning (establishing?) the Higgs potential.

This program to enable new physics insight into higher scales is currently limited by technological readiness. Among the most prominent projects that have been proposed to probe the energy frontier are hadron and muon colliders. Other auxiliary proposals include high-energy e^+e^- colliders using plasma wakefield or structure advanced acceleration. All of these proposals require substantial accelerator R&D.

A vigorous R&D program into accelerator and detector technologies will be critical to position the US and international community at the forefront of this research on a long term. This R&D program must specifically enable instrumentation research that goes beyond current projects, so that the detector technology will be available to make use of these high-energy colliders once they can be built. The critical detector R&D areas have been identified as 4-dimensional tracking with precision timing detectors, small area silicon pixels. Besides that, Particle Flow calorimeters with hybrid segmented crystal, and fiber readout may offer a better alternative to silicon.

During the last two years, with the start of the Snowmass 2021 studies, there has been a surge in the interest of the US and the international community, for the Muon Collider option because of advances in technology and analysis methodologies. There has also been a corresponding surge of interest abroad with the formation of the International Muon Collider Collaboration hosted at CERN. About a third of the contributed papers in the EF are on Muon Colliders. Since the last Snowmass study in 2013, there has been substantial progress in understanding the physics case, the detector requirements, and novel techniques to address the major beam induced backgrounds.

The investment in R&D for hadron and muon colliders, and planning for discussion of siting options for muon colliders have to start now, and to run in parallel with the HL-LHC and any e^+e^- precision electroweak program. Enabling this future, also requires strong input from every area of the theoretical community to understand the discovery potential of such colliders. Investment in a long term robust program of detector and collider R&D focused on multi-TeV colliders (hadron collider, muon colliders) is necessary for solving the many outstanding challenges, and the long term viability of collider physics.

2.8.6 Opportunity for US as a site for a future Energy Frontier Collider

CERN as host of the LHC has been the focus of EF activities for the past couple of decades. Our vision for the EF can only be realized as a worldwide program. In order for scientists from all over the world to buy into the program, it has to be sited all over the world. The US community has to continue to work with the international community on detector designs and develop extensive R&D programs. To realize this, the funding agencies (DOE and NSF) should fund a R&D program focused on participation of the US community in future collider efforts as partners (as currently US is severely lagging behind).

The US community has expressed a renewed ambition to bring back energy frontier collider physics to the US soil, while maintaining its international collaborative partnerships and obligations, for example with CERN. The international community also realizes that a vibrant and concurrent program in the US in energy frontier collider physics is beneficial for the whole field, as it was when Tevatron was operated simultaneously as LEP.

The US Energy Frontier community proposes to develop plans to site a e^+e^- collider in the US. A muon collider remains a highly appealing option for the US, and is complementary to a Higgs Factory. For example, some options which are considered as attractive opportunities for building a domestic EF collider program are listed below:

- **A US-sited linear e^+e^- (ILC/CCC) Collider**
- **Hosting a 10 TeV range muon collider**
- **Exploring other e^+e^- collider options to fully utilize the Fermilab site**

Planning to proceed in multiple parallel prongs may allow us to better adapt to international contingencies and eventually build the next collider sooner. Such a strategy will also help develop a robust long term plan for the global HEP community. Therefore, there are requests to assess the cost of siting a linear e^+e^- Higgs Factory collider option, and a multi-TeV muon collider in the US. In addition, to realize a successful US e^+e^- linear collider program, cost reduction options, and targeted accelerator R&D e.g. CCC, is very important in the near term.

Some of the options listed above capitalize on the existing facilities, and on expertise in key areas of accelerator and detector R&D at Fermilab. Among other sites, Fermilab is proposed as an ideal one for a Muon Collider with a center-of-mass energy reach at the desirable 10-TeV scale. The synergy with the existing/planned accelerator complex and the neutrino physics program at Fermilab is an additional stimulus for such investment of effort. A roadmap of the accelerator R&D timeline [?], indicates that a 3 TeV Muon Collider is possible by 2045, though the timeline is technically limited. A set of Muon Collider design options, with one of the siting options being at Fermilab, should be considered as an integral part of a global discussion for siting and selecting an international Muon Collider. A goal should be preparing a pre-CDR document summarizing design for the Fermilab-sited Muon Collider in time for the next Snowmass. The preparation of such a document will require substantial, yet affordable, investment. Such an investment will reinvigorate the US high-energy collider community and enable much needed global progress towards possible discoveries at the next energy frontier.

2.8.7 Resource needs and timelines

The energy frontier community proposes several parallel investigations over the 2025-2035 period for pursuing its scientific goals, among them the most prominent ones are completing the HL-LHC physics program, proceeding with Higgs boson factories and planning for multi-TeV colliders at the Energy Frontier. These projects have the potential to be transformative as they will push the boundaries of our knowledge by testing the limits of the SM or indirectly or by directly discovering new physics beyond the SM.

Resource needs and plan for the five year period starting 2025:

1. Prioritize HL-LHC physics program, including far-forward experiments,
2. Establish a targeted e^+e^- Higgs Factory detector R&D program for US participation in a global collider,
3. Develop an initial design for a first stage Tev-scale Muon Collider in the US, with pre-CDR document at the end of this period,
4. Support critical detector R&D towards EF multi-TeV Colliders.

Resource needs and plan for the five year period starting 2030:

1. Continue strong support for the HL-LHC physics program,
2. Support construction of a e^+e^- Higgs Factory,
3. Demonstrate principal risk mitigation and deliver CDR for a first stage TeV-scale muon collider.

Resource needs and plan after 2035:

1. Evaluate continuing HL-LHC physics program to the conclusion of archival measurements,
2. Begin and support the physics program of the Higgs Factories,
3. Demonstrate readiness to construct and deliver TDR for a first-stage TeV-scale muon collider,
4. Ramp up funding support for detector R&D for EF multi-TeV Colliders.

The energy frontier community recognizes that our success critically depends on the vision and the resources obtained by the Accelerator Frontier. There is a demonstrated intricate linkage between the EF vision and advances in accelerator R&D. The EF community strongly supports the Accelerator Frontier in its resource needs and request to

1. Establish an e^+e^- Higgs Factory program,
2. Start R&D for EF multi-TeV Colliders and ramp up funding support for these endeavors e.g. muon colliders, hadron colliders etc.

The visibly strong interdependence between Energy Frontier and the Theory Frontier is key to the success of both frontiers. The opportunity for continued collaboration has been at the core of the progress at the Energy Frontier until now, and will continue to be so. The opportunities to work together to interpret the data, to brainstorm to solve challenges, and to forge new directions enhances the returns from the both Frontiers. The Energy Frontier community supports a strong and well funded theory program.

2.8.8 Vision Summary

The Energy Frontier aims to facilitate a comprehensive international program for US participation in the exploration of the ”known unknown” physics beyond current reach, requiring future colliders.

The most viable path forward for the energy frontier that has been identified during the Snowmass process is proceeding forward with the construction of a Higgs factory as soon as possible, to complement the experiments of the HL-LHC, enabling operation during or just after the operation of the HL-LHC. This step should be followed by a multi-TeV energy frontier collider, going beyond the reach of the HL-LHC.

The proposals and R&D efforts to address the innovative detector developments for Higgs factories are well underway globally and many challenges are resolved. Bold “new” projects such as a linear e^+e^- Cool Copper Collider, and a muon collider will offer the next generation some challenges to rise to. It will inspire more young people from the US to join HEP and in the long term help with strengthening the vibrancy of the field.

Realizing our ultimate goal will require significant funding and government support. The community feels that there is potential to raise funds and obtain government buy-in for a future collider project located in the US. However, funding is not all that is needed. We also need a future program that continues to inspire the next generation of high energy physicists, and one that entices the next generation of graduate students to choose high energy physics as their field.

... add a few closing sentences

Bibliography

[1] **CMS** Collaboration, A. M. Sirunyan *et al.*, “A measurement of the Higgs boson mass in the diphoton decay channel,” *Phys. Lett. B* **805** (2020) 135425, arXiv:2002.06398 [hep-ex].

[2] **ATLAS** Collaboration, “Measurement of the Higgs boson mass in the $H \to ZZ^* \to 4\ell$ decay channel with $\sqrt{s} = 13$ TeV pp collisions using the ATLAS detector at the LHC,”.

[3] **ATLAS** Collaboration, “A detailed map of Higgs boson interactions by the ATLAS experiment ten years after the discovery,” arXiv:2207.00092 [hep-ex].

[4] **CMS** Collaboration, “A portrait of the Higgs boson by the CMS experiment ten years after the discovery,” *Nature 607 (2022) 60* (6, 2022) , arXiv:2207.00043 [hep-ex].

[5] **CMS** Collaboration, “Direct search for the standard model Higgs boson decaying to a charm quark-antiquark pair,” tech. rep., 2022.

[6] C. Delaunay, T. Golling, G. Perez, and Y. Soreq, “Enhanced Higgs boson coupling to charm pairs,” *Phys. Rev. D* **89** no. 3, (2014) 033014, arXiv:1310.7029 [hep-ph].

[7] N. M. Coyle, C. E. M. Wagner, and V. Wei, “Bounding the charm Yukawa coupling,” *Phys. Rev. D* **100** no. 7, (2019) 073013, arXiv:1905.09360 [hep-ph].

[8] **CMS** Collaboration, A. M. Sirunyan *et al.*, “Evidence for Higgs boson decay to a pair of muons,” *JHEP* **01** (2021) 148, arXiv:2009.04363 [hep-ex].

[9] **CMS** Collaboration, A. Tumasyan *et al.*, “Search for invisible decays of the Higgs boson produced via vector boson fusion in proton-proton collisions at $\sqrt{s} = 13$ TeV,” *Phys. Rev. D* **105** (2022) 092007, arXiv:2201.11585 [hep-ex].

[10] **ATLAS** Collaboration, “A combination of measurements of Higgs boson production and decay using up to 139 fb^{-1} of proton–proton collision data at $\sqrt{s} = 13$ TeV collected with the ATLAS experiment,”.

[11] **CMS** Collaboration, A. M. Sirunyan *et al.*, “Search for nonresonant Higgs boson pair production in final states with two bottom quarks and two photons in proton-proton collisions at $\sqrt{s} = 13$ TeV,” *JHEP* **03** (2021) 257, arXiv:2011.12373 [hep-ex].

[12] **CMS** Collaboration, “Search for Higgs boson pairs decaying to WWWW, WW$\tau\tau$, and $\tau\tau\tau\tau$ in proton-proton collisions at $\sqrt{s} = 13$ TeV,”.

[13] **CMS** Collaboration, A. Tumasyan *et al.*, “Search for Higgs boson pair production in the four b quark final state in proton-proton collisions at $\sqrt{s} = 13$ TeV,” arXiv:2202.09617 [hep-ex].

[14] **ATLAS** Collaboration, “Combination of searches for non-resonant and resonant Higgs boson pair production in the $b\bar{b}\gamma\gamma$, $b\bar{b}\tau^+\tau^-$ and $b\bar{b}b\bar{b}$ decay channels using pp collisions at $\sqrt{s} = 13$ TeV with the ATLAS detector,”.

[15] **ATLAS** Collaboration, “Search for non-resonant pair production of Higgs bosons in the $b\bar{b}b\bar{b}$ final state in pp collisions at $\sqrt{s} = 13$ TeV with the ATLAS detector,”.

[16] **ATLAS** Collaboration, “Constraining the Higgs boson self-coupling from single- and double-Higgs production with the ATLAS detector using pp collisions at $\sqrt{s} = 13$ TeV,”. https://cds.cern.ch/record/2814153.

[17] "Lhc schedule." `https://lhc-commissioning.web.cern.ch/schedule/LHC-long-term.htm#:~:text=Longer%20term%20LHC%20schedule,to%20last%20for%203%20years.`

[18] **ATLAS** Collaboration, "Snowmass White Paper Contribution: Physics with the Phase-2 ATLAS and CMS Detectors,".

[19] S. Dasu *et al.*, "Strategy for Understanding the Higgs Physics: The Cool Copper Collider," in *2022 Snowmass Summer Study*. 3, 2022. `arXiv:2203.07646 [hep-ex]`.

[20] M. Forslund and P. Meade, "High Precision Higgs from High Energy Muon Colliders," `arXiv:2203.09425 [hep-ph]`.

[21] **CMS** Collaboration, "Snowmass White Paper Contribution: Physics with the Phase-2 ATLAS and CMS Detectors,".

[22] **ILC International Development Team** Collaboration, A. Aryshev *et al.*, "The International Linear Collider: Report to Snowmass 2021," `arXiv:2203.07622 [physics.acc-ph]`.

[23] **CEPC Physics Study Group** Collaboration, H. Cheng *et al.*, "The Physics potential of the CEPC. Prepared for the US Snowmass Community Planning Exercise (Snowmass 2021)," in *2022 Snowmass Summer Study*. 5, 2022. `arXiv:2205.08553 [hep-ph]`.

[24] A. Robson and P. Roloff, "Updated CLIC luminosity staging baseline and Higgs coupling prospects," `arXiv:1812.01644 [hep-ex]`.

[25] G. Bernardi *et al.*, "The Future Circular Collider: a Summary for the US 2021 Snowmass Process," `arXiv:2203.06520 [hep-ex]`.

[26] K. Fujii *et al.*, "The role of positron polarization for the inital 250 GeV stage of the International Linear Collider," `arXiv:1801.02840 [hep-ph]`.

[27] T. Barklow, K. Fujii, S. Jung, R. Karl, J. List, T. Ogawa, M. E. Peskin, and J. Tian, "Improved Formalism for Precision Higgs Coupling Fits," *Phys. Rev. D* **97** no. 5, (2018) 053003, `arXiv:1708.08912 [hep-ph]`.

[28] **Muon Collider** Collaboration, J. de Blas *et al.*, "The physics case of a 3 TeV muon collider stage," `arXiv:2203.07261 [hep-ph]`.

[29] **ATLAS** Collaboration, "Projected sensitivity of Higgs boson pair production combining the $b\bar{b}\gamma\gamma$ and $b\bar{b}\tau^+\tau^-$ final states with the ATLAS detector at the HL-LHC,".

[30] M. L. Mangano, G. Ortona, and M. Selvaggi, "Measuring the Higgs self-coupling via Higgs-pair production at a 100 TeV p-p collider," *Eur. Phys. J. C* **80** no. 11, (2020) 1030, `arXiv:2004.03505 [hep-ph]`.

[31] J. de Blas *et al.*, "Higgs Boson Studies at Future Particle Colliders," *JHEP* **01** (2020) 139, `arXiv:1905.03764 [hep-ph]`.

[32] M. McCullough, "An Indirect Model-Dependent Probe of the Higgs Self-Coupling," *Phys. Rev. D* **90** no. 1, (2014) 015001, `arXiv:1312.3322 [hep-ph]`. [Erratum: Phys.Rev.D 92, 039903 (2015)].

[33] P. Meade and H. Ramani, "Unrestored Electroweak Symmetry," *Phys. Rev. Lett.* **122** no. 4, (2019) 041802, `arXiv:1807.07578 [hep-ph]`.

[34] I. Baldes and G. Servant, "High scale electroweak phase transition: baryogenesis \& symmetry non-restoration," *JHEP* **10** (2018) 053, `arXiv:1807.08770 [hep-ph]`.

[35] A. Glioti, R. Rattazzi, and L. Vecchi, "Electroweak Baryogenesis above the Electroweak Scale," *JHEP* **04** (2019) 027, arXiv:1811.11740 [hep-ph].

[36] M. Carena, J. Kozaczuk, Z. Liu, T. Ou, M. J. Ramsey-Musolf, J. Shelton, Y. Wang, and K.-P. Xie, "Probing the Electroweak Phase Transition with Exotic Higgs Decays," in *2022 Snowmass Summer Study*. 3, 2022. arXiv:2203.08206 [hep-ph].

[37] W. Altmannshofer, J. Eby, S. Gori, M. Lotito, M. Martone, and D. Tuckler, "Collider Signatures of Flavorful Higgs Bosons," *Phys. Rev. D* **94** no. 11, (2016) 115032, arXiv:1610.02398 [hep-ph].

[38] W. Altmannshofer, S. Gori, D. J. Robinson, and D. Tuckler, "The Flavor-locked Flavorful Two Higgs Doublet Model," *JHEP* **03** (2018) 129, arXiv:1712.01847 [hep-ph].

[39] D. Egana-Ugrinovic, S. Homiller, and P. R. Meade, "Higgs bosons with large couplings to light quarks," *Phys. Rev. D* **100** no. 11, (2019) 115041, arXiv:1908.11376 [hep-ph].

[40] D. Egana-Ugrinovic, S. Homiller, and P. Meade, "Multi-Higgs Production Probes Higgs Flavor," *Phys. Rev. D* **103** (2021) 115005, arXiv:2101.04119 [hep-ph].

[41] A. Albert *et al.*, "Strange quark as a probe for new physics in the Higgs sector," in *2022 Snowmass Summer Study*. 3, 2022. arXiv:2203.07535 [hep-ex].

[42] S. Adhikari, S. D. Lane, I. M. Lewis, and M. Sullivan, "Complex Scalar Singlet Model Benchmarks for Snowmass," in *2022 Snowmass Summer Study*. 3, 2022. arXiv:2203.07455 [hep-ph].

[43] T. Robens, "TRSM Benchmark Planes - Snowmass White Paper," in *2022 Snowmass Summer Study*. 5, 2022. arXiv:2205.14486 [hep-ph].

[44] T. Robens, "A short overview on low mass scalars at future lepton colliders - Snowmass White Paper," in *2022 Snowmass Summer Study*. 3, 2022. arXiv:2203.08210 [hep-ph].

[45] I. Low, N. R. Shah, and X.-P. Wang, "Higgs alignment and novel CP-violating observables in two-Higgs-doublet models," *Phys. Rev. D* **105** no. 3, (2022) 035009, arXiv:2012.00773 [hep-ph].

[46] T.-K. Chen, C.-W. Chiang, and I. Low, "Simple model of dark matter and CP violation," *Phys. Rev. D* **105** no. 7, (2022) 075025, arXiv:2202.02954 [hep-ph].

[47] A. Beniwal, F. Rajec, M. T. Prim, P. Scott, W. Su, M. White, A. G. Williams, and A. Woodcock, "Global fit of 2HDM with future collider results," in *2022 Snowmass Summer Study*. 3, 2022. arXiv:2203.07883 [hep-ph].

[48] G. Degrassi, S. Di Vita, J. Elias-Miro, J. R. Espinosa, G. F. Giudice, G. Isidori, and A. Strumia, "Higgs mass and vacuum stability in the Standard Model at NNLO," *JHEP* **08** (2012) 098, arXiv:1205.6497 [hep-ph].

[49] M. Awramik, M. Czakon, A. Freitas, and G. Weiglein, "Precise prediction for the W boson mass in the standard model," *Phys. Rev. D* **69** (2004) 053006, arXiv:hep-ph/0311148.

[50] J. de Blas, M. Ciuchini, E. Franco, A. Goncalves, S. Mishima, M. Pierini, L. Reina, and L. Silvestrini, "Global analysis of electroweak data in the Standard Model," arXiv:2112.07274 [hep-ph].

[51] J. Haller, A. Hoecker, R. Kogler, K. Mönig, T. Peiffer, and J. Stelzer, "Update of the global electroweak fit and constraints on two-Higgs-doublet models," *Eur. Phys. J. C* **78** no. 8, (2018) 675, arXiv:1803.01853 [hep-ph].

[52] P. Nason, *The Top Mass in Hadronic Collisions*, pp. 123–151. World Scientific, 2019. arXiv:1712.02796 [hep-ph].

[53] A. H. Hoang, "What is the Top Quark Mass?," *Ann. Rev. Nucl. Part. Sci.* **70** (2020) 225–255, arXiv:2004.12915 [hep-ph].

[54] R. Schwienhorst, D. Wackeroth, *et al.*, "Top Quark Physics and Heavy Flavor Production,". Snowmass 2021 Community Study.

[55] **D0** Collaboration, M. Czakon, P. Fiedler, D. Heymes, and A. Mitov, "Measurement of the Pole Mass of the Top Quark using Differential $t\bar{t}$ Cross Sections in $p\bar{p}$ Collisions at $\sqrt{s} = 1.96$ TeV," 9, 2016.

[56] **ATLAS** Collaboration, G. Aad *et al.*, "Measurement of the top-quark mass in $t\bar{t}$+1-jet events collected with the ATLAS detector in pp collisions at $\sqrt{s} = 8$ TeV," *JHEP* **11** (2019) 150, arXiv:1905.02302 [hep-ex].

[57] **CMS** Collaboration, A. M. Sirunyan *et al.*, "Measurement of $\mathrm{t\bar{t}}$ normalised multi-differential cross sections in pp collisions at $\sqrt{s} = 13$ TeV, and simultaneous determination of the strong coupling strength, top quark pole mass, and parton distribution functions," *Eur. Phys. J. C* **80** no. 7, (2020) 658, arXiv:1904.05237 [hep-ex].

[58] G. Bernardi, E. Brost, D. Denisov, G. Landsberg, M. Aleksa, D. d'Enterria, P. Janot, M. Mangano, and et al., "The future circular collider: a summary for the us 2021 snowmass process," arXiv:2203.06520. Submitted to EF General, also under IF0.

[59] N. Kidonakis., "Higher-order corrections for t tbar production at high energies," arXiv:2203.03698. Submitted to EF03.

[60] **CMS** Collaboration, "Projections of sensitivities for tttt production at HL-LHC and HE-LHC,".

[61] **ATLAS** Collaboration, "Extrapolation of ATLAS sensitivity to the measurement of the Standard Model four top quark cross section at the HL-LHC,".

[62] M. Czakon and A. Mitov, "Top++: A Program for the Calculation of the Top-Pair Cross-Section at Hadron Colliders," *Comput. Phys. Commun.* **185** (2014) 2930, arXiv:1112.5675 [hep-ph].

[63] I. Brivio, S. Bruggisser, F. Maltoni, R. Moutafis, T. Plehn, E. Vryonidou, S. Westhoff, and C. Zhang, "O new physics, where art thou? A global search in the top sector," *JHEP* **02** (2020) 131, arXiv:1910.03606 [hep-ph].

[64] G. Durieux, M. Perelló, M. Vos, and C. Zhang, "Global and optimal probes for the top-quark effective field theory at future lepton colliders," *JHEP* **10** (2018) 168, arXiv:1807.02121 [hep-ph].

[65] CMS Collaboration, "Projection of the top quark spin correlation measurement and search for top squark pair production at the HL-LHC,". https://cds.cern.ch/record/2813262.

[66] A. Aryshev, T. Behnke, M. Berggren, J. Brau, N. Craig, and et al., "The international linear collider," arXiv:2203.07622. Submitted to EF General.

[67] **CLIC** Collaboration, J. de Blas *et al.*, "The CLIC Potential for New Physics," arXiv:1812.02093 [hep-ph].

[68] S. Chen, A. Glioti, R. Rattazzi, L. Ricci, and A. Wulzer, "Learning from radiation at a very high energy lepton collider," *JHEP* **05** (2022) 180, arXiv:2202.10509 [hep-ph].

[69] G. Banelli, E. Salvioni, J. Serra, T. Theil, and A. Weiler, "The Present and Future of Four Top Operators," *JHEP* **02** (2021) 043, arXiv:2010.05915 [hep-ph].

[70] A. Huss, J. Huston, S. Jones, and M. Pellen, "Les Houches 2021: Physics at TeV Colliders: Report on the Standard Model Precision Wishlist," arXiv:2207.02122 [hep-ph].

[71] **CDF** Collaboration, T. Aaltonen *et al.*, "High-precision measurement of the W boson mass with the CDF II detector," *Science* **376** no. 6589, (2022) 170–176.

[72] **Particle Data Group** Collaboration, P. A. Zyla *et al.*, "Review of Particle Physics," *PTEP* **2020** no. 8, (2020) 083C01.

[73] "The International Linear Collider Technical Design Report - Volume 2: Physics," arXiv:1306.6352 [hep-ph].

[74] P. Bambade *et al.*, "The International Linear Collider: A Global Project," arXiv:1903.01629 [hep-ex].

[75] "Physics and Detectors at CLIC: CLIC Conceptual Design Report," arXiv:1202.5940 [physics.ins-det].

[76] **CLICdp, CLIC** Collaboration, T. K. Charles *et al.*, "The Compact Linear Collider (CLIC) - 2018 Summary Report," arXiv:1812.06018 [physics.acc-ph].

[77] **FCC** Collaboration, A. Abada *et al.*, "FCC-ee: The Lepton Collider: Future Circular Collider Conceptual Design Report Volume 2," *Eur. Phys. J. ST* **228** no. 2, (2019) 261–623.

[78] **CEPC Study Group** Collaboration, M. Dong *et al.*, "CEPC Conceptual Design Report: Volume 2 - Physics & Detector," arXiv:1811.10545 [hep-ex].

[79] **CEPC Physics Study Group** Collaboration, H. Cheng *et al.*, "The Physics potential of the CEPC. Prepared for the US Snowmass Community Planning Exercise (Snowmass 2021)," in *2022 Snowmass Summer Study*. 5, 2022. arXiv:2205.08553 [hep-ph].

[80] A. Freitas *et al.*, "Theoretical uncertainties for electroweak and Higgs-boson precision measurements at FCC-ee," arXiv:1906.05379 [hep-ph].

[81] D. d'Enterria *et al.*, "The strong coupling constant: State of the art and the decade ahead," arXiv:2203.08271 [hep-ph].

[82] A. Blondel, "A muon collider as Z factory," *AIP Conf. Proc.* **435** no. 1, (1998) 597–610.

[83] J. De Blas, G. Durieux, C. Grojean, J. Gu, and A. Paul, "On the future of Higgs, electroweak and diboson measurements at lepton colliders," *JHEP* **12** (2019) 117, arXiv:1907.04311 [hep-ph].

[84] **LCC Physics Working Group** Collaboration, K. Fujii *et al.*, "Tests of the Standard Model at the International Linear Collider," arXiv:1908.11299 [hep-ex].

[85] A. Blondel and P. Janot, "FCC-ee overview: new opportunities create new challenges," *Eur. Phys. J. Plus* **137** no. 1, (2022) 92, arXiv:2106.13885 [hep-ex].

[86] **ATLAS** Collaboration, M. Aaboud *et al.*, "Measurement of ZZ production in the $\ell\ell\nu\nu$ final state with the ATLAS detector in pp collisions at $\sqrt{s} = 13$ TeV," *JHEP* **10** (2019) 127, arXiv:1905.07163 [hep-ex].

[87] **ATLAS** Collaboration, M. Aaboud *et al.*, "Measurement of fiducial and differential W^+W^- production cross-sections at $\sqrt{s} = 13$ TeV with the ATLAS detector," *Eur. Phys. J. C* **79** no. 10, (2019) 884, arXiv:1905.04242 [hep-ex].

[88] **ATLAS** Collaboration, M. Aaboud *et al.*, "Measurement of $W^{\pm}Z$ production cross sections and gauge boson polarisation in *pp* collisions at $\sqrt{s} = 13$ TeV with the ATLAS detector," *Eur. Phys. J. C* **79** no. 6, (2019) 535, arXiv:1902.05759 [hep-ex].

[89] **ATLAS** Collaboration, M. Aaboud *et al.*, "Measurement of the $Z\gamma \to \nu\bar{\nu}\gamma$ production cross section in pp collisions at $\sqrt{s} = 13$ TeV with the ATLAS detector and limits on anomalous triple gauge-boson couplings," *JHEP* **12** (2018) 010, arXiv:1810.04995 [hep-ex].

[90] **ATLAS** Collaboration, M. Aaboud *et al.*, "$ZZ \to \ell^+\ell^-\ell'^+\ell'^-$ cross-section measurements and search for anomalous triple gauge couplings in 13 TeV *pp* collisions with the ATLAS detector," *Phys. Rev. D* **97** no. 3, (2018) 032005, arXiv:1709.07703 [hep-ex].

[91] **CMS** Collaboration, A. M. Sirunyan *et al.*, "Search for anomalous triple gauge couplings in WW and WZ production in lepton + jet events in proton-proton collisions at $\sqrt{s} = 13$ TeV," *JHEP* **12** (2019) 062, arXiv:1907.08354 [hep-ex].

[92] **CMS** Collaboration, A. M. Sirunyan *et al.*, "Measurement of electroweak WZ boson production and search for new physics in WZ + two jets events in pp collisions at $\sqrt{s} = 13$TeV," *Phys. Lett. B* **795** (2019) 281–307, arXiv:1901.04060 [hep-ex].

[93] **CMS** Collaboration, A. M. Sirunyan *et al.*, "Measurements of the pp $\to$ WZ inclusive and differential production cross section and constraints on charged anomalous triple gauge couplings at $\sqrt{s} = 13$ TeV," *JHEP* **04** (2019) 122, arXiv:1901.03428 [hep-ex].

[94] **CMS** Collaboration, A. M. Sirunyan *et al.*, "Measurements of the pp $\to$ ZZ production cross section and the Z $\to 4\ell$ branching fraction, and constraints on anomalous triple gauge couplings at $\sqrt{s} = 13$ TeV," *Eur. Phys. J. C* **78** (2018) 165, arXiv:1709.08601 [hep-ex]. [Erratum: Eur.Phys.J.C 78, 515 (2018)].

[95] **ATLAS** Collaboration, G. Aad *et al.*, "Evidence for the production of three massive vector bosons with the ATLAS detector," *Phys. Lett. B* **798** (2019) 134913, arXiv:1903.10415 [hep-ex].

[96] **ATLAS** Collaboration, M. Aaboud *et al.*, "Study of $WW\gamma$ and $WZ\gamma$ production in *pp* collisions at $\sqrt{s} = 8$ TeV and search for anomalous quartic gauge couplings with the ATLAS experiment," *Eur. Phys. J. C* **77** no. 9, (2017) 646, arXiv:1707.05597 [hep-ex].

[97] **CMS** Collaboration, A. M. Sirunyan *et al.*, "Observation of the Production of Three Massive Gauge Bosons at $\sqrt{s}$ =13 TeV," *Phys. Rev. Lett.* **125** no. 15, (2020) 151802, arXiv:2006.11191 [hep-ex].

[98] **CMS** Collaboration, A. M. Sirunyan *et al.*, "Measurements of the pp $\to W\gamma\gamma$ and pp $\to Z\gamma\gamma$ cross sections and limits on anomalous quartic gauge couplings at $\sqrt{s} = 8$ TeV," *JHEP* **10** (2017) 072, arXiv:1704.00366 [hep-ex].

[99] **ATLAS** Collaboration, G. Aad *et al.*, "Observation of electroweak production of two jets and a *Z*-boson pair with the ATLAS detector at the LHC," arXiv:2004.10612 [hep-ex].

[100] **ATLAS** Collaboration, G. Aad *et al.*, "Evidence for electroweak production of two jets in association with a $Z\gamma$ pair in *pp* collisions at $\sqrt{s} = 13$ TeV with the ATLAS detector," *Phys. Lett. B* **803** (2020) 135341, arXiv:1910.09503 [hep-ex].

[101] **ATLAS** Collaboration, G. Aad *et al.*, "Search for the electroweak diboson production in association with a high-mass dijet system in semileptonic final states in *pp* collisions at $\sqrt{s} = 13$ TeV with the ATLAS detector," *Phys. Rev. D* **100** no. 3, (2019) 032007, arXiv:1905.07714 [hep-ex].

[102] **ATLAS** Collaboration, M. Aaboud *et al.*, "Observation of electroweak production of a same-sign W boson pair in association with two jets in *pp* collisions at $\sqrt{s} = 13$ TeV with the ATLAS detector," *Phys. Rev. Lett.* **123** no. 16, (2019) 161801, arXiv:1906.03203 [hep-ex].

[103] **ATLAS** Collaboration, M. Aaboud *et al.*, "Observation of electroweak $W^{\pm}Z$ boson pair production in association with two jets in *pp* collisions at $\sqrt{s} = 13$ TeV with the ATLAS detector," *Phys. Lett. B* **793** (2019) 469–492, arXiv:1812.09740 [hep-ex].

[104] **CMS** Collaboration, "Evidence for vector boson scattering in events with four leptons and two jets in proton-proton collisions at $\sqrt{s} = 13$ TeV,".

[105] **CMS** Collaboration, A. M. Sirunyan *et al.*, "Measurements of production cross sections of WZ and same-sign WW boson pairs in association with two jets in proton-proton collisions at $\sqrt{s} = 13$ TeV," *Phys. Lett. B* **809** (2020) 135710, arXiv:2005.01173 [hep-ex].

[106] **CMS** Collaboration, A. M. Sirunyan *et al.*, "Measurement of the cross section for electroweak production of a Z boson, a photon and two jets in proton-proton collisions at $\sqrt{s} = 13$ TeV and constraints on anomalous quartic couplings," *JHEP* **06** (2020) 076, arXiv:2002.09902 [hep-ex].

[107] **CMS** Collaboration, A. M. Sirunyan *et al.*, "Search for anomalous electroweak production of vector boson pairs in association with two jets in proton-proton collisions at 13 TeV," *Phys. Lett. B* **798** (2019) 134985, arXiv:1905.07445 [hep-ex].

[108] **CMS** Collaboration, A. M. Sirunyan *et al.*, "Measurement of vector boson scattering and constraints on anomalous quartic couplings from events with four leptons and two jets in proton–proton collisions at $\sqrt{s} = 13$ TeV," *Phys. Lett. B* **774** (2017) 682–705, arXiv:1708.02812 [hep-ex].

[109] **CMS** Collaboration, A. M. Sirunyan *et al.*, "Measurement of differential cross sections for Z boson pair production in association with jets at $\sqrt{s} = 8$ and 13 TeV," *Phys. Lett. B* **789** (2019) 19–44, arXiv:1806.11073 [hep-ex].

[110] "CMS summary of limits on anomalous triple and quartic gauge couplings." https://twiki.cern.ch/twiki/bin/view/CMSPublic/PhysicsResultsSMPaTGC. Last revision: 2020-09-22.

[111] "ATLAS experiment public results - standard model physics." https://twiki.cern.ch/twiki/bin/view/AtlasPublic/StandardModelPublicResults. Last revision: 2021-10-13.

[112] P. Azzi *et al.*, "Report from Working Group 1: Standard Model Physics at the HL-LHC and HE-LHC," *CERN Yellow Rep. Monogr.* **7** (2019) 1–220, arXiv:1902.04070 [hep-ph].

[113] J. de Blas, Y. Du, C. Grojean, J. Gu, V. Miralles, M. E. Peskin, J. Tian, M. Vos, and E. Vryonidou, "Global SMEFT Fits at Future Colliders," in *2022 Snowmass Summer Study*. 6, 2022. arXiv:2206.08326 [hep-ph].

[114] R. K. Ellis *et al.*, "Physics Briefing Book: Input for the European Strategy for Particle Physics Update 2020," arXiv:1910.11775 [hep-ex].

[115] S. Amoroso *et al.*, "Snowmass 2021 whitepaper: Proton structure at the precision frontier," arXiv:2203.13923 [hep-ph].

[116] B. Nachman *et al.*, "Jets and Jet Substructure at Future Colliders," arXiv:2203.07462 [hep-ph].

[117] L. A. Anchordoqui *et al.*, "The Forward Physics Facility: Sites, experiments, and physics potential," *Phys. Rept.* **968** (2022) 1–50, arXiv:2109.10905 [hep-ph].

[118] J. L. Feng *et al.*, "The Forward Physics Facility at the High-Luminosity LHC," arXiv:2203.05090 [hep-ex].

[119] A. Accardi *et al.*, "Opportunities for precision QCD physics in hadronization at Belle II – a snowmass whitepaper," in *2022 Snowmass Summer Study*. 4, 2022. arXiv:2204.02280 [hep-ex].

[120] A. J. Larkoski, I. Moult, and B. Nachman, "Jet Substructure at the Large Hadron Collider: A Review of Recent Advances in Theory and Machine Learning," *Phys. Rept.* **841** (2020) 1–63, arXiv:1709.04464 [hep-ph].

[121] S. Marzani, G. Soyez, and M. Spannowsky, *Looking inside jets: an introduction to jet substructure and boosted-object phenomenology*, vol. 958. Springer, 2019. arXiv:1901.10342 [hep-ph].

[122] R. Abbate, M. Fickinger, A. H. Hoang, V. Mateu, and I. W. Stewart, "Thrust at N^3LL with Power Corrections and a Precision Global Fit for $\alpha_s(mZ)$," *Phys. Rev. D* **83** (2011) 074021, arXiv:1006.3080 [hep-ph].

[123] A. H. Hoang, D. W. Kolodrubetz, V. Mateu, and I. W. Stewart, "Precise determination of α_s from the C-parameter distribution," *Phys. Rev. D* **91** no. 9, (2015) 094018, arXiv:1501.04111 [hep-ph].

[124] J. Gao, Y. Gong, W.-L. Ju, and L. L. Yang, "Thrust distribution in Higgs decays at the next-to-leading order and beyond," *JHEP* **03** (2019) 030, arXiv:1901.02253 [hep-ph].

[125] D. Bertolini, P. Harris, M. Low, and N. Tran, "Pileup Per Particle Identification," *JHEP* **10** (2014) 059, arXiv:1407.6013 [hep-ph].

[126] M. Cacciari, G. P. Salam, and G. Soyez, "SoftKiller, a particle-level pileup removal method," *Eur. Phys. J. C* **75** no. 2, (2015) 59, arXiv:1407.0408 [hep-ph].

[127] P. Berta, M. Spousta, D. W. Miller, and R. Leitner, "Particle-level pileup subtraction for jets and jet shapes," *JHEP* **06** (2014) 092, arXiv:1403.3108 [hep-ex].

[128] P. T. Komiske, E. M. Metodiev, B. Nachman, and M. D. Schwartz, "Pileup Mitigation with Machine Learning (PUMML)," *JHEP* **12** (2017) 051, arXiv:1707.08600 [hep-ph].

[129] R. Abdul Khalek *et al.*, "Science Requirements and Detector Concepts for the Electron-Ion Collider: EIC Yellow Report," arXiv:2103.05419 [physics.ins-det].

[130] D. Acosta, E. Barberis, N. Hurley, W. Li, O. M. Colin, D. Wood, and X. Zuo, "The Potential of a TeV-Scale Muon-Ion Collider," in *2022 Snowmass Summer Study*. 3, 2022. arXiv:2203.06258 [hep-ex].

[131] **LHeC Study Group** Collaboration, J. L. Abelleira Fernandez *et al.*, "A Large Hadron Electron Collider at CERN: Report on the Physics and Design Concepts for Machine and Detector," *J. Phys. G* **39** (2012) 075001, arXiv:1206.2913 [physics.acc-ph].

[132] **LHeC, FCC-he Study Group** Collaboration, P. Agostini *et al.*, "The Large Hadron-Electron Collider at the HL-LHC," *J. Phys. G* **48** no. 11, (2021) 110501, arXiv:2007.14491 [hep-ex].

[133] D. Curtin, K. Deshpande, O. Fischer, and J. Zurita, "New Physics Opportunities for Long-Lived Particles at Electron-Proton Colliders," *JHEP* **07** (2018) 024, arXiv:1712.07135 [hep-ph].

[134] A. Huss, J. Huston, S. Jones, and M. Pellen, "Report on the standard model precision wishlist,". To appear in Les Houches 2021: Physics at TeV Colliders.

[135] N. Craig, C. Csaki, and A. El-Khadra, "Theory Frontier Summary Report,". Snowmass 2021 Community Study.

[136] S. Amoroso *et al.*, "Les Houches 2019: Physics at TeV Colliders: Standard Model Working Group Report," in *11th Les Houches Workshop on Physics at TeV Colliders: PhysTeV Les Houches*. 3, 2020. arXiv:2003.01700 [hep-ph].

[137] G. Heinrich, "Collider Physics at the Precision Frontier," *Phys. Rept.* **922** (2021) 1–69, arXiv:2009.00516 [hep-ph].

[138] F. Febres Cordero, A. von Manteuffel, and T. Neumann, "Computational challenges for multi-loop collider phenomenology," in *2022 Snowmass Summer Study*. 4, 2022. arXiv:2204.04200 [hep-ph].

[139] S. Aoki *et al.*, "Review of Lattice Results Concerning Low-Energy Particle Physics," *Eur. Phys. J. C* **74** (2014) 2890, arXiv:1310.8555 [hep-lat].

[140] S. Aoki *et al.*, "Review of lattice results concerning low-energy particle physics," *Eur. Phys. J. C* **77** no. 2, (2017) 112, arXiv:1607.00299 [hep-lat].

[141] **Flavour Lattice Averaging Group** Collaboration, S. Aoki *et al.*, "FLAG Review 2019: Flavour Lattice Averaging Group (FLAG)," *Eur. Phys. J. C* **80** no. 2, (2020) 113, arXiv:1902.08191 [hep-lat].

[142] Y. Aoki *et al.*, "FLAG Review 2021," arXiv:2111.09849 [hep-lat].

[143] M. Dalla Brida, "Past, present, and future of precision determinations of the QCD parameters from lattice QCD," *Eur. Phys. J. A* **57** no. 2, (2021) 66, arXiv:2012.01232 [hep-lat].

[144] J. Komijani, P. Petreczky, and J. H. Weber, "Strong coupling constant and quark masses from lattice QCD," *Prog. Part. Nucl. Phys.* **113** (2020) 103788, arXiv:2003.11703 [hep-lat].

[145] A. Blondel and E. Gianfelice, "The challenges of beam polarization and keV-scale centre-of-mass energy calibration at the FCC-ee," *Eur. Phys. J. Plus* **136** no. 11, (2021) 1103.

[146] J. Aparisi *et al.*, "Snowmass White Paper: prospects for measurements of the bottom quark mass," arXiv:2203.16994 [hep-ex].

[147] J. Fuster, A. Irles, S. Tairafune, G. Rodrigo, M. Vos, H. Yamamoto, and R. Yonamine, "Prospects for the measurement of the bottom quark mass at the ILC," *ILD note* (2021) , ILD-PHYS-PUB--2021-001.

[148] A. Accardi *et al.*, "Electron Ion Collider: The Next QCD Frontier: Understanding the glue that binds us all," *Eur. Phys. J. A* **52** no. 9, (2016) 268, arXiv:1212.1701 [nucl-ex].

[149] D. P. Anderle *et al.*, "Electron-ion collider in China," *Front. Phys. (Beijing)* **16** no. 6, (2021) 64701, arXiv:2102.09222 [nucl-ex].

[150] A. Abdesselam *et al.*, "Boosted Objects: A Probe of Beyond the Standard Model Physics," *Eur. Phys. J. C* **71** (2011) 1661, arXiv:1012.5412 [hep-ph].

[151] A. Altheimer *et al.*, "Jet Substructure at the Tevatron and LHC: New results, new tools, new benchmarks," *J. Phys. G* **39** (2012) 063001, arXiv:1201.0008 [hep-ph].

[152] A. Altheimer *et al.*, "Boosted Objects and Jet Substructure at the LHC. Report of BOOST2012, held at IFIC Valencia, 23rd-27th of July 2012," *Eur. Phys. J. C* **74** no. 3, (2014) 2792, arXiv:1311.2708 [hep-ex].

[153] D. Adams *et al.*, "Towards an Understanding of the Correlations in Jet Substructure," *Eur. Phys. J. C* **75** no. 9, (2015) 409, arXiv:1504.00679 [hep-ph].

[154] R. Kogler *et al.*, "Jet Substructure at the Large Hadron Collider: Experimental Review," *Rev. Mod. Phys.* **91** no. 4, (2019) 045003, arXiv:1803.06991 [hep-ex].

[155] R. Kogler, *Advances in Jet Substructure at the LHC: Algorithms, Measurements and Searches for New Physical Phenomena*, vol. 284. Springer, 5, 2021.

[156] **CMS** Collaboration, A. M. Sirunyan *et al.*, "Identification of heavy-flavour jets with the CMS detector in pp collisions at 13 TeV," *JINST* **13** no. 05, (2018) P05011, arXiv:1712.07158 [physics.ins-det].

[157] **ATLAS** Collaboration, G. Aad *et al.*, "ATLAS b-jet identification performance and efficiency measurement with $t\bar{t}$ events in pp collisions at $\sqrt{s} = 13$ TeV," *Eur. Phys. J. C* **79** no. 11, (2019) 970, arXiv:1907.05120 [hep-ex].

[158] **CMS** Collaboration, A. Tumasyan *et al.*, "A new calibration method for charm jet identification validated with proton-proton collision events at $\sqrt{s}$ =13 TeV," *JINST* **17** no. 03, (2022) P03014, arXiv:2111.03027 [hep-ex].

[159] **ATLAS** Collaboration, G. Aad *et al.*, "Measurement of the c-jet mistagging efficiency in $t\bar{t}$ events using pp collision data at $\sqrt{s} = 13$ TeV collected with the ATLAS detector," *Eur. Phys. J. C* **82** no. 1, (2022) 95, arXiv:2109.10627 [hep-ex].

[160] J. Erdmann, O. Nackenhorst, and S. V. Zeißner, "Maximum performance of strange-jet tagging at hadron colliders," *JINST* **16** no. 08, (2021) P08039, arXiv:2011.10736 [hep-ex].

[161] Y. Nakai, D. Shih, and S. Thomas, "Strange Jet Tagging," arXiv:2003.09517 [hep-ph].

[162] J. Erdmann, "A tagger for strange jets based on tracking information using long short-term memory," *JINST* **15** no. 01, (2020) P01021, arXiv:1907.07505 [physics.ins-det].

[163] P. Gras, S. Höche, D. Kar, A. Larkoski, L. Lönnblad, S. Plätzer, A. Siódmok, P. Skands, G. Soyez, and J. Thaler, "Systematics of quark/gluon tagging," *JHEP* **07** (2017) 091, arXiv:1704.03878 [hep-ph].

[164] *Les Houches 2017: Physics at TeV Colliders Standard Model Working Group Report.* 3, 2018. arXiv:1803.07977 [hep-ph].

[165] W. H. Chiu, Z. Liu, M. Low, and L.-T. Wang, "Jet timing," *JHEP* **01** (2022) 014, arXiv:2109.01682 [hep-ph].

[166] S. Chatterjee, R. Godbole, and T. S. Roy, "Jets with electrons from boosted top quarks," *JHEP* **01** (2020) 170, arXiv:1909.11041 [hep-ph].

[167] M. Mitra, R. Ruiz, D. J. Scott, and M. Spannowsky, "Neutrino Jets from High-Mass W_R Gauge Bosons in TeV-Scale Left-Right Symmetric Models," *Phys. Rev. D* **94** no. 9, (2016) 095016, arXiv:1607.03504 [hep-ph].

[168] M. Nemevšek, F. Nesti, and G. Popara, "Keung-Senjanović process at the LHC: From lepton number violation to displaced vertices to invisible decays," *Phys. Rev. D* **97** no. 11, (2018) 115018, arXiv:1801.05813 [hep-ph].

[169] K. du Plessis, M. M. Flores, D. Kar, S. Sinha, and H. van der Schyf, "Hitting two BSM particles with one lepton-jet: search for a top partner decaying to a dark photon, resulting in a lepton-jet," arXiv:2112.08425 [hep-ph].

[170] S. Dube, D. Gadkari, and A. M. Thalapillil, "Lepton-Jets and Low-Mass Sterile Neutrinos at Hadron Colliders," *Phys. Rev. D* **96** no. 5, (2017) 055031, arXiv:1707.00008 [hep-ph].

[171] J. Liu, Z. Liu, and L.-T. Wang, "Enhancing Long-Lived Particles Searches at the LHC with Precision Timing Information," *Phys. Rev. Lett.* **122** no. 13, (2019) 131801, arXiv:1805.05957 [hep-ph].

[172] J. Liu, Z. Liu, L.-T. Wang, and X.-P. Wang, "Enhancing Sensitivities to Long-lived Particles with High Granularity Calorimeters at the LHC," *JHEP* **11** (2020) 066, arXiv:2005.10836 [hep-ph].

[173] D. Wang, L. Wu, J. M. Yang, and M. Zhang, "Photon-jet events as a probe of axionlike particles at the LHC," *Phys. Rev. D* **104** no. 9, (2021) 095016, arXiv:2102.01532 [hep-ph].

[174] B. Sheff, N. Steinberg, and J. D. Wells, "Higgs boson decays into narrow diphoton jets and their search strategies at the Large Hadron Collider," *Phys. Rev. D* **104** no. 3, (2021) 036009, arXiv:2008.10568 [hep-ph].

[175] D. Kar and S. Sinha, "Exploring jet substructure in semi-visible jets," *SciPost Phys.* **10** no. 4, (2021) 084, arXiv:2007.11597 [hep-ph].

[176] F. Canelli, A. de Cosa, L. L. Pottier, J. Niedziela, K. Pedro, and M. Pierini, "Autoencoders for semivisible jet detection," *JHEP* **02** (2022) 074, arXiv:2112.02864 [hep-ph].

[177] **CMS** Collaboration, A. Tumasyan *et al.*, "Search for a right-handed W boson and a heavy neutrino in proton-proton collisions at $\sqrt{s} = 13$ TeV," *JHEP* **04** (2022) 047, arXiv:2112.03949 [hep-ex].

[178] **ATLAS** Collaboration, M. Aaboud *et al.*, "Search for a right-handed gauge boson decaying into a high-momentum heavy neutrino and a charged lepton in *pp* collisions with the ATLAS detector at $\sqrt{s} = 13$ TeV," *Phys. Lett. B* **798** (2019) 134942, arXiv:1904.12679 [hep-ex].

[179] **CMS** Collaboration, A. Tumasyan *et al.*, "Search for resonant production of strongly coupled dark matter in proton-proton collisions at 13 TeV," arXiv:2112.11125 [hep-ex].

[180] **ATLAS** Collaboration, G. Aad *et al.*, "Search for light long-lived neutral particles produced in *pp* collisions at $\sqrt{s} = 13$ TeV and decaying into collimated leptons or light hadrons with the ATLAS detector," *Eur. Phys. J. C* **80** no. 5, (2020) 450, arXiv:1909.01246 [hep-ex].

[181] **CMS** Collaboration, A. M. Sirunyan *et al.*, "Search for long-lived particles using nonprompt jets and missing transverse momentum with proton-proton collisions at $\sqrt{s} = 13$ TeV," *Phys. Lett. B* **797** (2019) 134876, arXiv:1906.06441 [hep-ex].

[182] M. Dasgupta, A. Fregoso, S. Marzani, and G. P. Salam, "Towards an understanding of jet substructure," *JHEP* **09** (2013) 029, arXiv:1307.0007 [hep-ph].

[183] A. J. Larkoski, S. Marzani, G. Soyez, and J. Thaler, "Soft Drop," *JHEP* **05** (2014) 146, arXiv:1402.2657 [hep-ph].

[184] C. H. Yeh, S. V. Chekanov, A. V. Kotwal, J. Proudfoot, S. Sen, N. V. Tran, and S. S. Yu, "Studies of granularity of a hadronic calorimeter for tens-of-TeV jets at a 100 TeV *pp* collider," *JINST* **14** no. 05, (2019) P05008, arXiv:1901.11146 [physics.ins-det].

[185] E. Coleman, M. Freytsis, A. Hinzmann, M. Narain, J. Thaler, N. Tran, and C. Vernieri, "The importance of calorimetry for highly-boosted jet substructure," *JINST* **13** no. 01, (2018) T01003, arXiv:1709.08705 [hep-ph].

[186] D. Neill, G. Vita, I. Vitev, and H. X. Zhu, "Energy-Energy Correlators for Precision QCD," in *2022 Snowmass Summer Study*. 3, 2022. arXiv:2203.07113 [hep-ph].

[187] H. Chen, I. Moult, J. Sandor, and H. X. Zhu, "Celestial Blocks and Transverse Spin in the Three-Point Energy Correlator," arXiv:2202.04085 [hep-ph].

[188] H. Chen, I. Moult, and H. X. Zhu, "Spinning Gluons from the QCD Light-Ray OPE," arXiv:2104.00009 [hep-ph].

[189] H. Chen, I. Moult, and H. X. Zhu, "Quantum Interference in Jet Substructure from Spinning Gluons," *Phys. Rev. Lett.* **126** no. 11, (2021) 112003, arXiv:2011.02492 [hep-ph].

[190] H. Chen, M.-X. Luo, I. Moult, T.-Z. Yang, X. Zhang, and H. X. Zhu, "Three point energy correlators in the collinear limit: symmetries, dualities and analytic results," *JHEP* **08** no. 08, (2020) 028, arXiv:1912.11050 [hep-ph].

[191] H. Chen, I. Moult, X. Zhang, and H. X. Zhu, "Rethinking jets with energy correlators: Tracks, resummation, and analytic continuation," *Phys. Rev. D* **102** no. 5, (2020) 054012, arXiv:2004.11381 [hep-ph].

[192] J. Holguin, I. Moult, A. Pathak, and M. Procura, "A New Paradigm for Precision Top Physics: Weighing the Top with Energy Correlators," arXiv:2201.08393 [hep-ph].

[193] M. Kologlu, P. Kravchuk, D. Simmons-Duffin, and A. Zhiboedov, "The light-ray OPE and conformal colliders," *JHEP* **01** (2021) 128, arXiv:1905.01311 [hep-th].

[194] H.-M. Chang, M. Procura, J. Thaler, and W. J. Waalewijn, "Calculating Track-Based Observables for the LHC," *Phys. Rev. Lett.* **111** (2013) 102002, arXiv:1303.6637 [hep-ph].

[195] H.-M. Chang, M. Procura, J. Thaler, and W. J. Waalewijn, "Calculating Track Thrust with Track Functions," *Phys. Rev. D* **88** (2013) 034030, arXiv:1306.6630 [hep-ph].

[196] M. Jaarsma, Y. Li, I. Moult, W. Waalewijn, and H. X. Zhu, "Renormalization Group Flows for Track Function Moments," arXiv:2201.05166 [hep-ph].

[197] Y. Li, I. Moult, S. S. van Velzen, W. J. Waalewijn, and H. X. Zhu, "Extending Precision Perturbative QCD with Track Functions," *Phys. Rev. Lett.* **128** no. 18, (2022) 182001, arXiv:2108.01674 [hep-ph].

[198] J. M. Campbell *et al.*, "Working Group Report: Quantum Chromodynamics," in *Community Summer Study 2013: Snowmass on the Mississippi*. 10, 2013. arXiv:1310.5189 [hep-ph].

[199] L. A. Harland-Lang, A. D. Martin, P. Motylinski, and R. S. Thorne, "Parton distributions in the LHC era: MMHT 2014 PDFs," *Eur. Phys. J. C* **75** no. 5, (2015) 204, arXiv:1412.3989 [hep-ph].

[200] S. Dulat, T.-J. Hou, J. Gao, M. Guzzi, J. Huston, P. Nadolsky, J. Pumplin, C. Schmidt, D. Stump, and C. P. Yuan, "New parton distribution functions from a global analysis of quantum chromodynamics," *Phys. Rev. D* **93** no. 3, (2016) 033006, arXiv:1506.07443 [hep-ph].

[201] **H1, ZEUS** Collaboration, H. Abramowicz *et al.*, "Combination of measurements of inclusive deep inelastic $e^{\pm}p$ scattering cross sections and QCD analysis of HERA data," *Eur. Phys. J. C* **75** no. 12, (2015) 580, arXiv:1506.06042 [hep-ex].

[202] A. Accardi, L. T. Brady, W. Melnitchouk, J. F. Owens, and N. Sato, "Constraints on large-x parton distributions from new weak boson production and deep-inelastic scattering data," *Phys. Rev. D* **93** no. 11, (2016) 114017, arXiv:1602.03154 [hep-ph].

[203] S. Alekhin, J. Blümlein, S. Moch, and R. Placakyte, "Parton distribution functions, α_s, and heavy-quark masses for LHC Run II," *Phys. Rev. D* **96** no. 1, (2017) 014011, arXiv:1701.05838 [hep-ph].

[204] **NNPDF** Collaboration, R. D. Ball *et al.*, "Parton distributions from high-precision collider data," *Eur. Phys. J. C* **77** no. 10, (2017) 663, arXiv:1706.00428 [hep-ph].

[205] T.-J. Hou *et al.*, "New CTEQ global analysis of quantum chromodynamics with high-precision data from the LHC," *Phys. Rev. D* **103** no. 1, (2021) 014013, arXiv:1912.10053 [hep-ph].

[206] S. Bailey and L. Harland-Lang, "Differential Top Quark Pair Production at the LHC: Challenges for PDF Fits," *Eur. Phys. J. C* **80** no. 1, (2020) 60, arXiv:1909.10541 [hep-ph].

[207] S. Bailey, T. Cridge, L. A. Harland-Lang, A. D. Martin, and R. S. Thorne, "Parton distributions from LHC, HERA, Tevatron and fixed target data: MSHT20 PDFs," *Eur. Phys. J. C* **81** no. 4, (2021) 341, arXiv:2012.04684 [hep-ph].

[208] **NNPDF** Collaboration, R. D. Ball *et al.*, "The path to proton structure at 1% accuracy," *Eur. Phys. J. C* **82** no. 5, (2022) 428, arXiv:2109.02653 [hep-ph].

[209] **ATLAS** Collaboration, G. Aad *et al.*, "Determination of the parton distribution functions of the proton using diverse ATLAS data from pp collisions at $\sqrt{s} = 7$, 8 and 13 TeV," *Eur. Phys. J. C* **82** no. 5, (2022) 438, arXiv:2112.11266 [hep-ex].

[210] **PDF4LHC Working Group** Collaboration, R. D. Ball *et al.*, "The PDF4LHC21 combination of global PDF fits for the LHC Run III," *J. Phys. G* **49** no. 8, (2022) 080501, arXiv:2203.05506 [hep-ph].

[211] A. Accardi *et al.*, "A Critical Appraisal and Evaluation of Modern PDFs," *Eur. Phys. J. C* **76** no. 8, (2016) 471, arXiv:1603.08906 [hep-ph].

[212] K. Kovařík, P. M. Nadolsky, and D. E. Soper, "Hadronic structure in high-energy collisions," *Rev. Mod. Phys.* **92** no. 4, (2020) 045003, arXiv:1905.06957 [hep-ph].

[213] A. Courtoy, J. Huston, P. Nadolsky, K. Xie, M. Yan, and C. P. Yuan, "Parton distributions need representative sampling," arXiv:2205.10444 [hep-ph].

[214] J. Butterworth *et al.*, "PDF4LHC recommendations for LHC Run II," *J. Phys. G* **43** (2016) 023001, arXiv:1510.03865 [hep-ph].

[215] R. Abdul Khalek, S. Bailey, J. Gao, L. Harland-Lang, and J. Rojo, "Towards Ultimate Parton Distributions at the High-Luminosity LHC," *Eur. Phys. J. C* **78** no. 11, (2018) 962, arXiv:1810.03639 [hep-ph].

[216] H.-W. Lin *et al.*, "Parton distributions and lattice QCD calculations: a community white paper," *Prog. Part. Nucl. Phys.* **100** (2018) 107–160, arXiv:1711.07916 [hep-ph].

[217] M. Constantinou *et al.*, "Parton distributions and lattice-QCD calculations: Toward 3D structure," *Prog. Part. Nucl. Phys.* **121** (2021) 103908, arXiv:2006.08636 [hep-ph].

[218] T.-J. Hou, H.-W. Lin, M. Yan, and C. P. Yuan, "Impact of lattice $s(x) - \bar{s}(x)$ data in the CTEQ-TEA global analysis," arXiv:2204.07944 [hep-ph].

[219] P. C. Barry *et al.*, "Complementarity of experimental and lattice QCD data on pion parton distributions," arXiv:2204.00543 [hep-ph].

[220] M. Constantinou *et al.*, "Lattice QCD Calculations of Parton Physics," arXiv:2202.07193 [hep-lat].

[221] B. U. Musch, P. Hagler, J. W. Negele, and A. Schafer, "Exploring quark transverse momentum distributions with lattice QCD," *Phys. Rev. D* **83** (2011) 094507, arXiv:1011.1213 [hep-lat].

[222] B. U. Musch, P. Hagler, M. Engelhardt, J. W. Negele, and A. Schafer, "Sivers and Boer-Mulders observables from lattice QCD," *Phys. Rev. D* **85** (2012) 094510, arXiv:1111.4249 [hep-lat].

[223] M. Engelhardt, P. Hägler, B. Musch, J. Negele, and A. Schäfer, "Lattice QCD study of the Boer-Mulders effect in a pion," *Phys. Rev. D* **93** no. 5, (2016) 054501, arXiv:1506.07826 [hep-lat].

[224] B. Yoon, T. Bhattacharya, M. Engelhardt, J. Green, R. Gupta, P. Hägler, B. Musch, J. Negele, A. Pochinsky, and S. Syritsyn, "Lattice QCD calculations of nucleon transverse momentum-dependent parton distributions using clover and domain wall fermions," in *33rd International Symposium on Lattice Field Theory*. SISSA, 11, 2015. arXiv:1601.05717 [hep-lat].

[225] B. Yoon, M. Engelhardt, R. Gupta, T. Bhattacharya, J. R. Green, B. U. Musch, J. W. Negele, A. V. Pochinsky, A. Schäfer, and S. N. Syritsyn, "Nucleon Transverse Momentum-dependent Parton Distributions in Lattice QCD: Renormalization Patterns and Discretization Effects," *Phys. Rev. D* **96** no. 9, (2017) 094508, arXiv:1706.03406 [hep-lat].

[226] P. Shanahan, M. Wagman, and Y. Zhao, "Collins-Soper kernel for TMD evolution from lattice QCD," *Phys. Rev. D* **102** no. 1, (2020) 014511, arXiv:2003.06063 [hep-lat].

[227] **Lattice Parton** Collaboration, Q.-A. Zhang *et al.*, "Lattice-QCD Calculations of TMD Soft Function Through Large-Momentum Effective Theory," *Phys. Rev. Lett.* **125** no. 19, (2020) 192001, arXiv:2005.14572 [hep-lat].

[228] M. Schlemmer, A. Vladimirov, C. Zimmermann, M. Engelhardt, and A. Schäfer, "Determination of the Collins-Soper Kernel from Lattice QCD," *JHEP* **08** (2021) 004, arXiv:2103.16991 [hep-lat].

[229] Y. Li *et al.*, "Lattice QCD Study of Transverse-Momentum Dependent Soft Function," *Phys. Rev. Lett.* **128** no. 6, (2022) 062002, arXiv:2106.13027 [hep-lat].

[230] P. Shanahan, M. Wagman, and Y. Zhao, "Lattice QCD calculation of the Collins-Soper kernel from quasi-TMDPDFs," *Phys. Rev. D* **104** no. 11, (2021) 114502, arXiv:2107.11930 [hep-lat].

[231] J.-W. Chen, H.-W. Lin, and J.-H. Zhang, "Pion generalized parton distribution from lattice QCD," *Nucl. Phys. B* **952** (2020) 114940, arXiv:1904.12376 [hep-lat].

[232] C. Alexandrou, K. Cichy, M. Constantinou, K. Hadjiyiannakou, K. Jansen, A. Scapellato, and F. Steffens, "Unpolarized and helicity generalized parton distributions of the proton within lattice QCD," *Phys. Rev. Lett.* **125** no. 26, (2020) 262001, arXiv:2008.10573 [hep-lat].

[233] H.-W. Lin, "Nucleon Tomography and Generalized Parton Distribution at Physical Pion Mass from Lattice QCD," *Phys. Rev. Lett.* **127** no. 18, (2021) 182001, arXiv:2008.12474 [hep-ph].

[234] H.-W. Lin, "Nucleon helicity generalized parton distribution at physical pion mass from lattice QCD," *Phys. Lett. B* **824** (2022) 136821, arXiv:2112.07519 [hep-lat].

[235] M. Anselmino, A. Mukherjee, and A. Vossen, "Transverse spin effects in hard semi-inclusive collisions," *Prog. Part. Nucl. Phys.* **114** (2020) 103806, arXiv:2001.05415 [hep-ph].

[236] M. Burkardt, "Transverse force on quarks in deep-inelastic scattering," *Phys. Rev. D* **88** (2013) 114502, arXiv:0810.3589 [hep-ph].

[237] **CLAS** Collaboration, M. Mirazita *et al.*, "Beam Spin Asymmetry in Semi-Inclusive Electroproduction of Hadron Pairs," *Phys. Rev. Lett.* **126** no. 6, (2021) 062002, arXiv:2010.09544 [hep-ex].

[238] T. B. Hayward *et al.*, "Observation of Beam Spin Asymmetries in the Process $ep \to e^{'}\pi^{+}\pi^{-}X$ with CLAS12," *Phys. Rev. Lett.* **126** (2021) 152501, arXiv:2101.04842 [hep-ex].

[239] A. Courtoy, A. Miramontes, H. Avakian, M. Mirazita, and S. Pisano, "Extraction of the higher-twist parton distribution $e(x)$ from CLAS data," arXiv:2203.14975 [hep-ph].

[240] R. Abdul Khalek *et al.*, "Snowmass 2021 White Paper: Electron Ion Collider for High Energy Physics," in *2022 Snowmass Summer Study*. 3, 2022. arXiv:2203.13199 [hep-ph].

[241] M. Boglione and A. Simonelli, "Kinematic regions in the $e^{+}e^{-} \to h\,X$ factorized cross section in a 2-jet topology with thrust," *JHEP* **02** (2022) , arXiv:2109.11497 [hep-ph].

[242] M. Boglione and A. Simonelli, "Factorization of $e^{+}e^{-} \to H\,X$ cross section, differential in z_h, P_T and thrust, in the 2-jet limit," *JHEP* **02** (2021) 076, arXiv:2011.07366 [hep-ph].

[243] M. Boglione and A. Simonelli, "Universality-breaking effects in $e^{+}e^{-}$ hadronic production processes," *Eur. Phys. J. C* **81** no. 1, (2021) 96, arXiv:2007.13674 [hep-ph].

[244] **ATLAS** Collaboration, G. Aad *et al.*, "Measurement of the Lund Jet Plane Using Charged Particles in 13 TeV Proton-Proton Collisions with the ATLAS Detector," *Phys. Rev. Lett.* **124** no. 22, (2020) 222002, arXiv:2004.03540 [hep-ex].

[245] D. d'Enterria, K. J. Eskola, I. Helenius, and H. Paukkunen, "Confronting current NLO parton fragmentation functions with inclusive charged-particle spectra at hadron colliders," *Nucl. Phys. B* **883** (2014) 615–628, arXiv:1311.1415 [hep-ph].

[246] S. Albino *et al.*, "Parton fragmentation in the vacuum and in the medium," arXiv:0804.2021 [hep-ph].

[247] A. Accardi, F. Arleo, W. K. Brooks, D. D'Enterria, and V. Muccifora, "Parton Propagation and Fragmentation in QCD Matter," *Riv. Nuovo Cim.* **32** no. 9-10, (2009) 439–554, arXiv:0907.3534 [nucl-th].

[248] *Proceedings, Parton Radiation and Fragmentation from LHC to FCC-ee: CERN, Geneva, Switzerland, November 22-23, 2016*. 1, 2017. arXiv:1702.01329 [hep-ph].

[249] V. A. Khoze and T. Sjostrand, "Color correlations and multiplicities in top events," *Phys. Lett. B* **328** (1994) 466–476, arXiv:hep-ph/9403394.

[250] S. Argyropoulos and T. Sjöstrand, "Effects of color reconnection on $t\bar{t}$ final states at the LHC," *JHEP* **11** (2014) 043, arXiv:1407.6653 [hep-ph].

[251] J. R. Christiansen and T. Sjöstrand, "Color reconnection at future e^{+} e^{-} colliders," *Eur. Phys. J. C* **75** no. 9, (2015) 441, arXiv:1506.09085 [hep-ph].

[252] T. Sjostrand and V. A. Khoze, "On Color rearrangement in hadronic W+ W- events," *Z. Phys. C* **62** (1994) 281–310, arXiv:hep-ph/9310242.

[253] **ALEPH, DELPHI, L3, OPAL, LEP Electroweak** Collaboration, S. Schael *et al.*, "Electroweak Measurements in Electron-Positron Collisions at W-Boson-Pair Energies at LEP," *Phys. Rept.* **532** (2013) 119–244, `arXiv:1302.3415 [hep-ex]`.

[254] **FCC** Collaboration, A. Abada *et al.*, "FCC Physics Opportunities: Future Circular Collider Conceptual Design Report Volume 1," *Eur. Phys. J. C* **79** no. 6, (2019) 474.

[255] M. Cepeda *et al.*, "Report from Working Group 2: Higgs Physics at the HL-LHC and HE-LHC," *CERN Yellow Rep. Monogr.* **7** (2019) 221–584, `arXiv:1902.00134 [hep-ph]`.

[256] **FCC** Collaboration, A. Abada *et al.*, "FCC-hh: The Hadron Collider: Future Circular Collider Conceptual Design Report Volume 3," *Eur. Phys. J. ST* **228** no. 4, (2019) 755–1107.

[257] **FCC** Collaboration, A. Abada *et al.*, "FCC Physics Opportunities: Future Circular Collider Conceptual Design Report Volume 1," *Eur. Phys. J. C* **79** no. 6, (2019) 474.

[258] M. L. Mangano *et al.*, "Physics at a 100 TeV pp Collider: Standard Model Processes," `arXiv:1607.01831 [hep-ph]`.

[259] J. Rojo, "Parton Distributions at a 100 TeV Hadron Collider," *PoS* **DIS2016** (2016) 275, `arXiv:1605.08302 [hep-ph]`.

[260] V. S. Fadin, E. A. Kuraev, and L. N. Lipatov, "On the Pomeranchuk Singularity in Asymptotically Free Theories," *Phys. Lett. B* **60** (1975) 50–52.

[261] L. N. Lipatov, "Reggeization of the Vector Meson and the Vacuum Singularity in Nonabelian Gauge Theories," *Sov. J. Nucl. Phys.* **23** (1976) 338–345.

[262] E. A. Kuraev, L. N. Lipatov, and V. S. Fadin, "The Pomeranchuk Singularity in Nonabelian Gauge Theories," *Sov. Phys. JETP* **45** (1977) 199–204.

[263] I. I. Balitsky and L. N. Lipatov, "The Pomeranchuk Singularity in Quantum Chromodynamics," *Sov. J. Nucl. Phys.* **28** (1978) 822–829.

[264] K. J. Golec-Biernat and M. Wusthoff, "Saturation effects in deep inelastic scattering at low Q**2 and its implications on diffraction," *Phys. Rev. D* **59** (1998) 014017, `arXiv:hep-ph/9807513`.

[265] L. Lukaszuk and B. Nicolescu, "A Possible interpretation of p p rising total cross-sections," *Lett. Nuovo Cim.* **8** (1973) 405–413.

[266] E. Martynov and B. Nicolescu, "Odderon effects in the differential cross-sections at Tevatron and LHC energies," *Eur. Phys. J. C* **79** no. 6, (2019) 461, `arXiv:1808.08580 [hep-ph]`.

[267] A. Breakstone *et al.*, "A Measurement of $\bar{p}p$ and pp Elastic Scattering in the Dip Region at $\sqrt{s}$ = 53-GeV," *Phys. Rev. Lett.* **54** (1985) 2180.

[268] S. Erhan *et al.*, "Comparison of $\bar{p}p$ and pp Elastic Scattering With $0.6 - \text{GeV}^{<} t < 2.1 - \text{GeV}^2$ at the CERN ISR," *Phys. Lett. B* **152** (1985) 131–134.

[269] **UA4** Collaboration, D. Bernard *et al.*, "Large T Elastic Scattering at the CERN SPS Collider at $\sqrt{s}$ = 630-GeV," *Phys. Lett. B* **171** (1986) 142–144.

[270] **UA4** Collaboration, M. Bozzo *et al.*, "Elastic Scattering at the CERN SPS Collider Up to a Four Momentum Transfer of 1.55-GeV**2," *Phys. Lett. B* **155** (1985) 197–202.

[271] E. Nagy *et al.*, "Measurements of Elastic Proton Proton Scattering at Large Momentum Transfer at the CERN Intersecting Storage Rings," *Nucl. Phys. B* **150** (1979) 221–267.

[272] **LHCb** Collaboration, R. Aaij *et al.*, "Prompt charm production in pp collisions at sqrt(s)=7 TeV," *Nucl. Phys. B* **871** (2013) 1–20, `arXiv:1302.2864 [hep-ex]`.

[273] **LHCb** Collaboration, R. Aaij *et al.*, "Measurements of prompt charm production cross-sections in pp collisions at $\sqrt{s} = 13$ TeV," *JHEP* **03** (2016) 159, `arXiv:1510.01707 [hep-ex]`. [Erratum: JHEP 09, 013 (2016), Erratum: JHEP 05, 074 (2017)].

[274] **LHCb** Collaboration, R. Aaij *et al.*, "Measurements of prompt charm production cross-sections in pp collisions at $\sqrt{s} = 5$ TeV," *JHEP* **06** (2017) 147, `arXiv:1610.02230 [hep-ex]`.

[275] **LHCb** Collaboration, R. Aaij *et al.*, "Study of Z Bosons Produced in Association with Charm in the Forward Region," *Phys. Rev. Lett.* **128** no. 8, (2022) 082001, `arXiv:2109.08084 [hep-ex]`.

[276] S. J. Brodsky, A. Kusina, F. Lyonnet, I. Schienbein, H. Spiesberger, and R. Vogt, "A review of the intrinsic heavy quark content of the nucleon," *Adv. High Energy Phys.* **2015** (2015) 231547, `arXiv:1504.06287 [hep-ph]`.

[277] V. Bertone, R. Gauld, and J. Rojo, "Neutrino Telescopes as QCD Microscopes," *JHEP* **01** (2019) 217, `arXiv:1808.02034 [hep-ph]`.

[278] A. Garcia, R. Gauld, A. Heijboer, and J. Rojo, "Complete predictions for high-energy neutrino propagation in matter," *JCAP* **09** (2020) 025, `arXiv:2004.04756 [hep-ph]`.

[279] R. Gauld, J. Rojo, L. Rottoli, S. Sarkar, and J. Talbert, "The prompt atmospheric neutrino flux in the light of LHCb," *JHEP* **02** (2016) 130, `arXiv:1511.06346 [hep-ph]`.

[280] **PROSA** Collaboration, M. V. Garzelli, S. Moch, O. Zenaiev, A. Cooper-Sarkar, A. Geiser, K. Lipka, R. Placakyte, and G. Sigl, "Prompt neutrino fluxes in the atmosphere with PROSA parton distribution functions," *JHEP* **05** (2017) 004, `arXiv:1611.03815 [hep-ph]`.

[281] **IceCube** Collaboration, R. Abbasi *et al.*, "The IceCube high-energy starting event sample: Description and flux characterization with 7.5 years of data," *Phys. Rev. D* **104** (2021) 022002, `arXiv:2011.03545 [astro-ph.HE]`.

[282] J. Gao, L. Harland-Lang, and J. Rojo, "The Structure of the Proton in the LHC Precision Era," *Phys. Rept.* **742** (2018) 1–121, `arXiv:1709.04922 [hep-ph]`.

[283] R. A. Khalek, J. J. Ethier, E. R. Nocera, and J. Rojo, "Self-consistent determination of proton and nuclear PDFs at the Electron Ion Collider," *Phys. Rev. D* **103** no. 9, (2021) 096005, `arXiv:2102.00018 [hep-ph]`.

[284] **NuTeV** Collaboration, M. Tzanov *et al.*, "Precise measurement of neutrino and anti-neutrino differential cross sections," *Phys. Rev. D* **74** (2006) 012008, `arXiv:hep-ex/0509010`.

[285] **NOMAD** Collaboration, O. Samoylov *et al.*, "A Precision Measurement of Charm Dimuon Production in Neutrino Interactions from the NOMAD Experiment," *Nucl. Phys. B* **876** (2013) 339–375, `arXiv:1308.4750 [hep-ex]`.

[286] **NuTeV** Collaboration, M. Goncharov *et al.*, "Precise Measurement of Dimuon Production Cross-Sections in ν_μ Fe and $\overline{\nu}_\mu$ Fe Deep Inelastic Scattering at the Tevatron.," *Phys. Rev. D* **64** (2001) 112006, `arXiv:hep-ex/0102049`.

[287] **CHORUS** Collaboration, E. Eskut *et al.*, "The CHORUS experiment to search for muon-neutrino –> tau-neutrino oscillation," *Nucl. Instrum. Meth. A* **401** (1997) 7–44.

[288] W.-C. Chang and J.-C. Peng, "Flavor Structure of the Nucleon Sea," *Prog. Part. Nucl. Phys.* **79** (2014) 95–135, arXiv:1406.1260 [hep-ph].

[289] P. M. Nadolsky, H.-L. Lai, Q.-H. Cao, J. Huston, J. Pumplin, D. Stump, W.-K. Tung, and C. P. Yuan, "Implications of CTEQ global analysis for collider observables," *Phys. Rev. D* **78** (2008) 013004, arXiv:0802.0007 [hep-ph].

[290] S. Alekhin, J. Blumlein, L. Caminadac, K. Lipka, K. Lohwasser, S. Moch, R. Petti, and R. Placakyte, "Determination of Strange Sea Quark Distributions from Fixed-target and Collider Data," *Phys. Rev. D* **91** no. 9, (2015) 094002, arXiv:1404.6469 [hep-ph].

[291] S. Alekhin, J. Blümlein, and S. Moch, "Strange sea determination from collider data," *Phys. Lett. B* **777** (2018) 134–140, arXiv:1708.01067 [hep-ph].

[292] F. Faura, S. Iranipour, E. R. Nocera, J. Rojo, and M. Ubiali, "The Strangest Proton?," *Eur. Phys. J. C* **80** no. 12, (2020) 1168, arXiv:2009.00014 [hep-ph].

[293] G. Bevilacqua, M. V. Garzelli, A. Kardos, and L. Toth, "W + charm production with massive c quarks in PowHel," *JHEP* **04** (2022) 056, arXiv:2106.11261 [hep-ph].

[294] **CMS** Collaboration, V. Khachatryan *et al.*, "Observation of Long-Range Near-Side Angular Correlations in Proton-Proton Collisions at the LHC," *JHEP* **09** (2010) 091, arXiv:1009.4122 [hep-ex].

[295] **CMS** Collaboration, S. Chatrchyan *et al.*, "Observation of Long-Range Near-Side Angular Correlations in Proton-Lead Collisions at the LHC," *Phys. Lett. B* **718** (2013) 795–814, arXiv:1210.5482 [nucl-ex].

[296] **ATLAS** Collaboration, G. Aad *et al.*, "Observation of Associated Near-Side and Away-Side Long-Range Correlations in $\sqrt{s_{NN}}$=5.02 TeV Proton-Lead Collisions with the ATLAS Detector," *Phys. Rev. Lett.* **110** no. 18, (2013) 182302, arXiv:1212.5198 [hep-ex].

[297] **ALICE** Collaboration, B. Abelev *et al.*, "Long-range angular correlations on the near and away side in p-Pb collisions at $\sqrt{s_{NN}} = 5.02$ TeV," *Phys. Lett. B* **719** (2013) 29–41, arXiv:1212.2001 [nucl-ex].

[298] **LHCb** Collaboration, R. Aaij *et al.*, "Measurements of long-range near-side angular correlations in $\sqrt{s_{\text{NN}}} = 5$TeV proton-lead collisions in the forward region," *Phys. Lett. B* **762** (2016) 473–483, arXiv:1512.00439 [nucl-ex].

[299] **ATLAS** Collaboration, M. Aaboud *et al.*, "Evidence for light-by-light scattering in heavy-ion collisions with the ATLAS detector at the LHC," *Nature Phys.* **13** no. 9, (2017) 852–858, arXiv:1702.01625 [hep-ex].

[300] **CMS** Collaboration, A. M. Sirunyan *et al.*, "Evidence for light-by-light scattering and searches for axion-like particles in ultraperipheral PbPb collisions at $\sqrt{s_{\text{NN}}} = 5.02$ TeV," *Phys. Lett. B* **797** (2019) 134826, arXiv:1810.04602 [hep-ex].

[301] A. Dainese, M. Mangano, A. B. Meyer, A. Nisati, G. Salam, and M. A. Vesterinen, "Report on the Physics at the HL-LHC, and Perspectives for the HE-LHC," CERN Yellow Report CERN-2019-007, CERN, 2019. https://cds.cern.ch/record/2703572.

[302] ATLAS Collaboration, "A Radiation-Hard Zero Degree Calorimeter for ATLAS in the HL-LHC era," 2021. https://cds.cern.ch/record/2781150.

[303] Y. Bashan, Z. Citron, B. Cole, M. Grosse Perdekamp, A. Hase, T. Koeth, C. Lantz, S. Lascio, R. Longo, D. MacLean, A. Mignerey, Y. Moyal, M. Murray, M. Nickel, M. Phipps, S. Popescu, N. Santiago, A. Sickles, S. Shenkar, P. Steinberg, L. Sudit, A. Tate, Q. Wang, and S. Yang, "A Run 4 Zero Degree Calorimeter for CMS," tech. rep., CERN, Geneva, Nov, 2021. https://cds.cern.ch/record/2791533. This is a joint project with the ATLAS heavy ion group.

[304] CMS Collaboration, "A MIP Timing Detector for the CMS Phase-2 Upgrade," tech. rep., CERN, Geneva, Mar, 2019. https://cds.cern.ch/record/2667167.

[305] C. ALICE, "Letter of intent for ALICE 3: A next generation heavy-ion experiment at the LHC," tech. rep., CERN, Geneva, Mar, 2022. https://cds.cern.ch/record/2803563.

[306] **PHENIX** Collaboration, A. Adare *et al.*, "An Upgrade Proposal from the PHENIX Collaboration," arXiv:1501.06197 [nucl-ex].

[307] **ATLAS** Collaboration, G. Aad *et al.*, "Observation of a Centrality-Dependent Dijet Asymmetry in Lead-Lead Collisions at $\sqrt{s_{NN}} = 2.77$ TeV with the ATLAS Detector at the LHC," *Phys. Rev. Lett.* **105** (2010) 252303, arXiv:1011.6182 [hep-ex].

[308] **CMS** Collaboration, S. Chatrchyan *et al.*, "Observation and studies of jet quenching in PbPb collisions at nucleon-nucleon center-of-mass energy = 2.76 TeV," *Phys. Rev. C* **84** (2011) 024906, arXiv:1102.1957 [nucl-ex].

[309] **CMS** Collaboration, S. Chatrchyan *et al.*, "Jet momentum dependence of jet quenching in PbPb collisions at $\sqrt{s_{NN}} = 2.76$ TeV," *Phys. Lett. B* **712** (2012) 176–197, arXiv:1202.5022 [nucl-ex].

[310] **CMS** Collaboration, S. Chatrchyan *et al.*, "Studies of jet quenching using isolated-photon+jet correlations in PbPb and *pp* collisions at $\sqrt{s_{NN}} = 2.76$ TeV," *Phys. Lett. B* **718** (2013) 773–794, arXiv:1205.0206 [nucl-ex].

[311] **CMS** Collaboration, A. M. Sirunyan *et al.*, "Study of jet quenching with isolated-photon+jet correlations in PbPb and pp collisions at $\sqrt{s_{\mathrm{NN}}} = 5.02$ TeV," *Phys. Lett. B* **785** (2018) 14–39, arXiv:1711.09738 [nucl-ex].

[312] **ATLAS** Collaboration, M. Aaboud *et al.*, "Measurement of photon–jet transverse momentum correlations in 5.02 TeV Pb + Pb and *pp* collisions with ATLAS," *Phys. Lett. B* **789** (2019) 167–190, arXiv:1809.07280 [nucl-ex].

[313] **CMS** Collaboration, A. M. Sirunyan *et al.*, "Study of Jet Quenching with Z + jet Correlations in Pb-Pb and *pp* Collisions at $\sqrt{s}_{NN} = 5.02$ TeV," *Phys. Rev. Lett.* **119** no. 8, (2017) 082301, arXiv:1702.01060 [nucl-ex].

[314] **ATLAS** Collaboration, G. Aad *et al.*, "Measurement of the jet radius and transverse momentum dependence of inclusive jet suppression in lead-lead collisions at $\sqrt{s_{NN}}$= 2.76 TeV with the ATLAS detector," *Phys. Lett. B* **719** (2013) 220–241, arXiv:1208.1967 [hep-ex].

[315] **ATLAS** Collaboration, G. Aad *et al.*, "Measurements of the Nuclear Modification Factor for Jets in Pb+Pb Collisions at $\sqrt{s_{\mathrm{NN}}} = 2.76$ TeV with the ATLAS Detector," *Phys. Rev. Lett.* **114** no. 7, (2015) 072302, arXiv:1411.2357 [hep-ex].

[316] **CMS** Collaboration, V. Khachatryan *et al.*, "Measurement of inclusive jet cross sections in *pp* and PbPb collisions at $\sqrt{s_{NN}} = 2.76$ TeV," *Phys. Rev. C* **96** no. 1, (2017) 015202, arXiv:1609.05383 [nucl-ex].

[317] **ATLAS** Collaboration, M. Aaboud *et al.*, "Measurement of the nuclear modification factor for inclusive jets in Pb+Pb collisions at $\sqrt{s_{\mathrm{NN}}} = 5.02$ TeV with the ATLAS detector," *Phys. Lett. B* **790** (2019) 108–128, arXiv:1805.05635 [nucl-ex].

[318] **CMS** Collaboration, A. M. Sirunyan *et al.*, "First measurement of large area jet transverse momentum spectra in heavy-ion collisions," *JHEP* **05** (2021) 284, arXiv:2102.13080 [hep-ex].

[319] **ALICE** Collaboration, J. Adam *et al.*, "Measurement of jet suppression in central Pb-Pb collisions at $\sqrt{s_{\mathrm{NN}}} = 2.76$ TeV," *Phys. Lett. B* **746** (2015) 1–14, arXiv:1502.01689 [nucl-ex].

[320] **CMS** Collaboration, V. Khachatryan *et al.*, "Measurement of transverse momentum relative to dijet systems in PbPb and pp collisions at $\sqrt{s_{\mathrm{NN}}} = 2.76$ TeV," *JHEP* **01** (2016) 006, arXiv:1509.09029 [nucl-ex].

[321] **CMS** Collaboration, S. Chatrchyan *et al.*, "Modification of Jet Shapes in PbPb Collisions at $\sqrt{s_{NN}} = 2.76$ TeV," *Phys. Lett. B* **730** (2014) 243–263, arXiv:1310.0878 [nucl-ex].

[322] **CMS** Collaboration, S. Chatrchyan *et al.*, "Measurement of Jet Fragmentation in PbPb and pp Collisions at $\sqrt{s_{NN}} = 2.76$ TeV," *Phys. Rev. C* **90** no. 2, (2014) 024908, arXiv:1406.0932 [nucl-ex].

[323] **ATLAS** Collaboration, G. Aad *et al.*, "Measurement of inclusive jet charged-particle fragmentation functions in Pb+Pb collisions at $\sqrt{s_{NN}} = 2.76$ TeV with the ATLAS detector," *Phys. Lett. B* **739** (2014) 320–342, arXiv:1406.2979 [hep-ex].

[324] **CMS** Collaboration, A. M. Sirunyan *et al.*, "Measurement of the Splitting Function in *pp* and Pb-Pb Collisions at $\sqrt{s_{_{\mathrm{NN}}}} = 5.02$ TeV," *Phys. Rev. Lett.* **120** no. 14, (2018) 142302, arXiv:1708.09429 [nucl-ex].

[325] **CMS** Collaboration, A. M. Sirunyan *et al.*, "Jet Shapes of Isolated Photon-Tagged Jets in Pb-Pb and pp Collisions at $\sqrt{s_{\mathrm{NN}}} = 5.02$ TeV," *Phys. Rev. Lett.* **122** no. 15, (2019) 152001, arXiv:1809.08602 [hep-ex].

[326] **ATLAS** Collaboration, G. Aad *et al.*, "Medium-Induced Modification of Z-Tagged Charged Particle Yields in $Pb + Pb$ Collisions at 5.02 TeV with the ATLAS Detector," *Phys. Rev. Lett.* **126** no. 7, (2021) 072301, arXiv:2008.09811 [nucl-ex].

[327] **ATLAS** Collaboration, M. Aaboud *et al.*, "Measurement of jet fragmentation in Pb+Pb and *pp* collisions at $\sqrt{s_{NN}} = 5.02$ TeV with the ATLAS detector," *Phys. Rev. C* **98** no. 2, (2018) 024908, arXiv:1805.05424 [nucl-ex].

[328] **CMS** Collaboration, A. M. Sirunyan *et al.*, "Observation of Medium-Induced Modifications of Jet Fragmentation in Pb-Pb Collisions at $\sqrt{s_{NN}} = 5.02$ TeV Using Isolated Photon-Tagged Jets," *Phys. Rev. Lett.* **121** no. 24, (2018) 242301, arXiv:1801.04895 [hep-ex].

[329] **CMS** Collaboration, A. M. Sirunyan *et al.*, "Measurement of the groomed jet mass in PbPb and pp collisions at $\sqrt{s_{\mathrm{NN}}} = 5.02$ TeV," *JHEP* **10** (2018) 161, arXiv:1805.05145 [hep-ex].

[330] **ALICE** Collaboration, S. Acharya *et al.*, "Exploration of jet substructure using iterative declustering in pp and Pb–Pb collisions at LHC energies," *Phys. Lett. B* **802** (2020) 135227, arXiv:1905.02512 [nucl-ex].

[331] **ALICE** Collaboration, S. Acharya *et al.*, "Medium modification of the shape of small-radius jets in central Pb-Pb collisions at $\sqrt{s_{\rm NN}} = 2.76$ TeV," *JHEP* **10** (2018) 139, arXiv:1807.06854 [nucl-ex].

[332] **CMS** Collaboration, A. M. Sirunyan *et al.*, "Measurement of quark- and gluon-like jet fractions using jet charge in PbPb and pp collisions at 5.02 TeV," *JHEP* **07** (2020) 115, arXiv:2004.00602 [hep-ex].

[333] **CMS** Collaboration, A. M. Sirunyan *et al.*, "Using Z Boson Events to Study Parton-Medium Interactions in Pb-Pb Collisions," *Phys. Rev. Lett.* **128** no. 12, (2022) 122301, arXiv:2103.04377 [hep-ex].

[334] CMS Collaboration, "Performance of jet quenching measurements in pp and PbPb collisions with CMS at the HL-LHC," CMS Physics Analysis Summary CMS-PAS-FTR-18-025, CERN, 2018. http://cds.cern.ch/record/2651892.

[335] **ATLAS** Collaboration, "Projections for ATLAS Measurements of Jet Modifications in Pb+Pb Collisions in LHC Runs 3 and 4,".

[336] **sPHENIX** Collaboration, C. A. Aidala *et al.*, "Design and Beam Test Results for the sPHENIX Electromagnetic and Hadronic Calorimeter Prototypes," *IEEE Trans. Nucl. Sci.* **65** no. 12, (2018) 2901–2919, arXiv:1704.01461 [physics.ins-det].

[337] B. Z. Kopeliovich, I. K. Potashnikova, I. Schmidt, and M. Siddikov, "Survival of charmonia in a hot environment," *Phys. Rev. C* **91** no. 2, (2015) 024911, arXiv:1409.5147 [hep-ph].

[338] S. Aronson, E. Borras, B. Odegard, R. Sharma, and I. Vitev, "Collisional and thermal dissociation of J/ψ and Υ states at the LHC," *Phys. Lett. B* **778** (2018) 384–391, arXiv:1709.02372 [hep-ph].

[339] X. Du, R. Rapp, and M. He, "Color Screening and Regeneration of Bottomonia in High-Energy Heavy-Ion Collisions," *Phys. Rev. C* **96** no. 5, (2017) 054901, arXiv:1706.08670 [hep-ph].

[340] **CMS** Collaboration, A. M. Sirunyan *et al.*, "Measurement of the $B^{\pm}$ Meson Nuclear Modification Factor in Pb-Pb Collisions at $\sqrt{s_{NN}} = 5.02$ TeV," *Phys. Rev. Lett.* **119** no. 15, (2017) 152301, arXiv:1705.04727 [hep-ex].

[341] **CMS** Collaboration, A. M. Sirunyan *et al.*, "Measurement of $\rm B^0_s$ meson production in pp and PbPb collisions at $\sqrt{s_{\rm NN}} = 5.02$ TeV," *Phys. Lett. B* **796** (2019) 168–190, arXiv:1810.03022 [hep-ex].

[342] **ALICE** Collaboration, S. Acharya *et al.*, "Measurement of $\rm D^0$, $\rm D^+$, $\rm D^{*+}$ and $\rm D^+_s$ production in Pb-Pb collisions at $\sqrt{s_{\rm NN}} = 5.02$ TeV," *JHEP* **10** (2018) 174, arXiv:1804.09083 [nucl-ex].

[343] **CMS** Collaboration, A. M. Sirunyan *et al.*, "Nuclear modification factor of $\rm D^0$ mesons in PbPb collisions at $\sqrt{s_{\rm NN}} = 5.02$ TeV," *Phys. Lett. B* **782** (2018) 474–496, arXiv:1708.04962 [nucl-ex].

[344] **ALICE** Collaboration, J. Adam *et al.*, "Transverse momentum dependence of D-meson production in Pb-Pb collisions at $\sqrt{s_{\rm NN}} = 2.76$ TeV," *JHEP* **03** (2016) 081, arXiv:1509.06888 [nucl-ex].

[345] **ALICE** Collaboration, S. Acharya *et al.*, "Measurement of beauty and charm production in pp collisions at $\sqrt{s} = 5.02$ TeV via non-prompt and prompt D mesons," *JHEP* **05** (2021) 220, arXiv:2102.13601 [nucl-ex].

[346] **CMS** Collaboration, A. M. Sirunyan *et al.*, "Studies of Beauty Suppression via Nonprompt D^0 Mesons in Pb-Pb Collisions at $Q^2 = 4$ GeV^2," *Phys. Rev. Lett.* **123** no. 2, (2019) 022001, arXiv:1810.11102 [hep-ex].

[347] **CMS** Collaboration, A. M. Sirunyan *et al.*, "Measurement of prompt and nonprompt J/ψ production in pp and pPb collisions at $\sqrt{s_{\mathrm{NN}}} = 5.02\,\mathrm{TeV}$," *Eur. Phys. J. C* **77** no. 4, (2017) 269, arXiv:1702.01462 [nucl-ex].

[348] **ATLAS** Collaboration, M. Aaboud *et al.*, "Prompt and non-prompt J/ψ and ψ(2S) suppression at high transverse momentum in 5.02 TeV Pb+Pb collisions with the ATLAS experiment," *Eur. Phys. J. C* **78** no. 9, (2018) 762, arXiv:1805.04077 [nucl-ex].

[349] **CMS** Collaboration, S. Chatrchyan *et al.*, "Indications of suppression of excited Υ states in PbPb collisions at $\sqrt{S_{NN}} = 2.76$ TeV," *Phys. Rev. Lett.* **107** (2011) 052302, arXiv:1105.4894 [nucl-ex].

[350] **CMS** Collaboration, S. Chatrchyan *et al.*, "Suppression of non-prompt J/ψ, prompt J/ψ, and Y(1S) in PbPb collisions at $\sqrt{s_{NN}} = 2.76$ TeV," *JHEP* **05** (2012) 063, arXiv:1201.5069 [nucl-ex].

[351] **CMS** Collaboration, S. Chatrchyan *et al.*, "Observation of Sequential Upsilon Suppression in PbPb Collisions," *Phys. Rev. Lett.* **109** (2012) 222301, arXiv:1208.2826 [nucl-ex]. [Erratum: Phys.Rev.Lett. 120, 199903 (2018)].

[352] **CMS** Collaboration, V. Khachatryan *et al.*, "Suppression of $\Upsilon(1S), \Upsilon(2S)$ and $\Upsilon(3S)$ production in PbPb collisions at $\sqrt{s_{\mathrm{NN}}} = 2.76$ TeV," *Phys. Lett. B* **770** (2017) 357–379, arXiv:1611.01510 [nucl-ex].

[353] **ATLAS** Collaboration, G. Aad *et al.*, "Measurement of the centrality dependence of J/ψ yields and observation of Z production in lead–lead collisions with the ATLAS detector at the LHC," *Phys. Lett. B* **697** (2011) 294–312, arXiv:1012.5419 [hep-ex].

[354] **ALICE** Collaboration, B. Abelev *et al.*, "J/ψ suppression at forward rapidity in Pb-Pb collisions at $\sqrt{s_{NN}} = 2.76$ TeV," *Phys. Rev. Lett.* **109** (2012) 072301, arXiv:1202.1383 [hep-ex].

[355] **CMS** Collaboration, V. Khachatryan *et al.*, "Measurement of Prompt $\psi(2S) \to J/\psi$ Yield Ratios in Pb-Pb and $p-p$ Collisions at $\sqrt{s_{NN}} = 2.76$ TeV," *Phys. Rev. Lett.* **113** no. 26, (2014) 262301, arXiv:1410.1804 [nucl-ex].

[356] **ALICE** Collaboration, J. Adam *et al.*, "Differential studies of inclusive J/ψ and ψ(2S) production at forward rapidity in Pb-Pb collisions at $\sqrt{s_{\mathrm{NN}}} = 2.76$ TeV," *JHEP* **05** (2016) 179, arXiv:1506.08804 [nucl-ex].

[357] CMS Collaboration, "Open heavy flavor and quarkonia in heavy ion collisions at HL-LHC," CMS Physics Analysis Summary CMS-PAS-FTR-18-024, CERN, 2018. http://cds.cern.ch/record/2650897.

[358] CMS Collaboration, "Predictions on the precision achievable for small system flow observables in the context of HL-LHC," CMS Physics Analysis Summary CMS-PAS-FTR-18-026, CERN, 2018. http://cds.cern.ch/record/2650773.

[359] **ATLAS** Collaboration, "Projections for ATLAS Measurements of Bulk Properties of Pb+Pb, p+Pb, and pp Collisions in LHC Runs 3 and 4,".

[360] **LHCb** Collaboration, R. Aaij *et al.*, "Observation of Multiplicity Dependent Prompt $\chi_{c1}(3872)$ and $\psi(2S)$ Production in pp Collisions," *Phys. Rev. Lett.* **126** no. 9, (2021) 092001, arXiv:2009.06619 [hep-ex].

[361] **CMS** Collaboration, A. M. Sirunyan *et al.*, "Evidence for X(3872) in Pb-Pb Collisions and Studies of its Prompt Production at $\sqrt{s_{NN}}$=5.02 TeV," *Phys. Rev. Lett.* **128** no. 3, (2022) 032001, arXiv:2102.13048 [hep-ex].

[362] CMS Collaboration, "Constraining nuclear parton distributions with heavy ion collisions at the HL-LHC with the CMS experiment," CMS Physics Analysis Summary CMS-PAS-FTR-18-027, CERN, 2018. http://cds.cern.ch/record/2652030.

[363] T. Carli, D. Clements, A. Cooper-Sarkar, C. Gwenlan, G. P. Salam, F. Siegert, P. Starovoitov, and M. Sutton, "A posteriori inclusion of parton density functions in NLO QCD final-state calculations at hadron colliders: The APPLGRID Project," *Eur. Phys. J. C* **66** (2010) 503–524, arXiv:0911.2985 [hep-ph].

[364] T. Kluge, K. Rabbertz, and M. Wobisch, "FastNLO: Fast pQCD calculations for PDF fits," in *14th International Workshop on Deep Inelastic Scattering*, pp. 483–486. 9, 2006. arXiv:hep-ph/0609285.

[365] Z. Bern, L. J. Dixon, F. Febres Cordero, S. Höche, H. Ita, D. A. Kosower, and D. Maitre, "Ntuples for NLO Events at Hadron Colliders," *Comput. Phys. Commun.* **185** (2014) 1443–1460, arXiv:1310.7439 [hep-ph].

[366] K. Cranmer *et al.*, "Publishing statistical models: Getting the most out of particle physics experiments," *SciPost Phys.* **12** (2022) 037, arXiv:2109.04981 [hep-ph].

[367] X.-L. Meng, "Statistical paradises and paradoxes in big data (I): Law of large populations, big data paradox, and the 2016 US presidential election," *The Annals of Applied Statistics* **12** no. 2, (2018) 685.

[368] L. T. Brady, A. Accardi, W. Melnitchouk, and J. F. Owens, "Impact of PDF uncertainties at large x on heavy boson production," *JHEP* **06** (2012) 019, arXiv:1110.5398 [hep-ph].

[369] A. Greljo, S. Iranipour, Z. Kassabov, M. Madigan, J. Moore, J. Rojo, M. Ubiali, and C. Voisey, "Parton distributions in the SMEFT from high-energy Drell-Yan tails," *JHEP* **07** (2021) 122, arXiv:2104.02723 [hep-ph].

[370] A. V. Manohar, "Effective field theories," *Lect. Notes Phys.* **479** (1997) 311–362, arXiv:hep-ph/9606222.

[371] I. Brivio and M. Trott, "The Standard Model as an Effective Field Theory," *Phys. Rept.* **793** (2019) 1–98, arXiv:1706.08945 [hep-ph].

[372] S. Iranipour and M. Ubiali, "A new generation of simultaneous fits to LHC data using deep learning," *JHEP* **05** (2022) 032, arXiv:2201.07240 [hep-ph].

[373] D. Liu, C. Sun, and J. Gao, "Machine learning of log-likelihood functions in global analysis of parton distributions," arXiv:2201.06586 [hep-ph].

[374] S. Carrazza, C. Degrande, S. Iranipour, J. Rojo, and M. Ubiali, "Can New Physics hide inside the proton?," *Phys. Rev. Lett.* **123** no. 13, (2019) 132001, arXiv:1905.05215 [hep-ph].

[375] **ZEUS** Collaboration, H. Abramowicz *et al.*, "Limits on contact interactions and leptoquarks at HERA," *Phys. Rev. D* **99** no. 9, (2019) 092006, arXiv:1902.03048 [hep-ex].

[376] **CMS** Collaboration, A. Tumasyan *et al.*, "Measurement and QCD analysis of double-differential inclusive jet cross sections in proton-proton collisions at $\sqrt{s} = 13$ TeV," *JHEP* **02** (2022) 142, arXiv:2111.10431 [hep-ex].

[377] R. Boughezal, F. Petriello, and D. Wiegand, "Removing flat directions in standard model EFT fits: How polarized electron-ion collider data can complement the LHC," *Phys. Rev. D* **101** no. 11, (2020) 116002, arXiv:2004.00748 [hep-ph].

[378] R. Boughezal, F. Petriello, and D. Wiegand, "Disentangling Standard Model EFT operators with future low-energy parity-violating electron scattering experiments," *Phys. Rev. D* **104** no. 1, (2021) 016005, arXiv:2104.03979 [hep-ph].

[379] C. Baldenegro, A. Bellora, S. Fichet, G. von Gersdorff, M. Pitt, and C. Royon, "Searching for anomalous top quark interactions with proton tagging and timing detectors at the LHC," arXiv:2205.01173 [hep-ph].

[380] C. Baldenegro, S. Fichet, G. von Gersdorff, and C. Royon, "Probing the anomalous $\gamma\gamma\gamma$Z coupling at the LHC with proton tagging," *JHEP* **06** (2017) 142, arXiv:1703.10600 [hep-ph].

[381] S. Fichet, G. von Gersdorff, B. Lenzi, C. Royon, and M. Saimpert, "Light-by-light scattering with intact protons at the LHC: from Standard Model to New Physics," *JHEP* **02** (2015) 165, arXiv:1411.6629 [hep-ph].

[382] S. Fichet, G. von Gersdorff, O. Kepka, B. Lenzi, C. Royon, and M. Saimpert, "Probing new physics in diphoton production with proton tagging at the Large Hadron Collider," *Phys. Rev. D* **89** (2014) 114004, arXiv:1312.5153 [hep-ph].

[383] S. Fichet, G. von Gersdorff, and C. Royon, "Measuring the Diphoton Coupling of a 750 GeV Resonance," *Phys. Rev. Lett.* **116** no. 23, (2016) 231801, arXiv:1601.01712 [hep-ph].

[384] S. Fichet, G. von Gersdorff, and C. Royon, "Scattering light by light at 750 GeV at the LHC," *Phys. Rev. D* **93** no. 7, (2016) 075031, arXiv:1512.05751 [hep-ph].

[385] E. Chapon, C. Royon, and O. Kepka, "Anomalous quartic W W gamma gamma, Z Z gamma gamma, and trilinear WW gamma couplings in two-photon processes at high luminosity at the LHC," *Phys. Rev. D* **81** (2010) 074003, arXiv:0912.5161 [hep-ph].

[386] O. Kepka and C. Royon, "Anomalous $WW\gamma$ coupling in photon-induced processes using forward detectors at the LHC," *Phys. Rev. D* **78** (2008) 073005, arXiv:0808.0322 [hep-ph].

[387] C. Baldenegro, S. Hassani, C. Royon, and L. Schoeffel, "Extending the constraint for axion-like particles as resonances at the LHC and laser beam experiments," *Phys. Lett. B* **795** (2019) 339–345, arXiv:1903.04151 [hep-ph].

[388] C. Baldenegro, S. Fichet, G. von Gersdorff, and C. Royon, "Searching for axion-like particles with proton tagging at the LHC," *JHEP* **06** (2018) 131, arXiv:1803.10835 [hep-ph].

[389] A. J. Larkoski, F. Maltoni, and M. Selvaggi, "Tracking down hyper-boosted top quarks," arXiv:1503.03347 [hep-ph].

[390] H.-M. Chang, M. Procura, J. Thaler, and W. J. Waalewijn, "Calculating track-based observables for the lhc," *Physical Review Letters* **111** no. 10, (Sep, 2013) . http://dx.doi.org/10.1103/PhysRevLett.111.102002.

[391] B. T. Elder and J. Thaler, "Aspects of track-assisted mass," *Journal of High Energy Physics* **2019** no. 3, (Mar, 2019) . http://dx.doi.org/10.1007/JHEP03(2019)104.

[392] M. Spannowsky and M. Stoll, "Tracking new physics at the lhc and beyond," *Physical Review D* **92** no. 5, (Sep, 2015) . http://dx.doi.org/10.1103/PhysRevD.92.054033.

[393] **ATLAS** Collaboration, "Jet mass reconstruction with the ATLAS Detector in early Run 2 data,".

[394] L. Gouskos, A. Sung, and J. Incandela, "Search for stop scalar quarks at FCC-hh," tech. rep., CERN, Geneva, Oct, 2018. https://cds.cern.ch/record/2642475.

[395] M. Aleksa *et al.*, "Calorimeters for the FCC-hh," arXiv:1912.09962 [physics.ins-det].

[396] **GEANT4** Collaboration, S. Agostinelli *et al.*, "GEANT4–a simulation toolkit," *Nucl. Instrum. Meth. A* **506** (2003) 250–303.

[397] **CALICE** Collaboration, G. Eigen *et al.*, "Characterisation of different stages of hadronic showers using the CALICE Si-W ECAL physics prototype," *Nucl. Instrum. Meth. A* **937** (2019) 41–52, arXiv:1902.06161 [physics.ins-det].

[398] T. Han, Y. Ma, and K. Xie, "High energy leptonic collisions and electroweak parton distribution functions," *Phys. Rev. D* **103** no. 3, (2021) L031301, arXiv:2007.14300 [hep-ph].

[399] . Energy Frontier Topical Group 08, 09, "Physics Beyond the Standard Model at Energy Frontier,". Snowmass 2021 Community Study.

[400] R. K. Ellis, B. Heinemann, J. de Blas, M. Cepeda, C. Grojean, F. Maltoni, A. Nisati, E. Petit, R. Rattazzi, W. Verkerke, J. D'Hondt, K. Redlich, A. Andronic, F. Siklér, N. Armesto, D. Boer, D. d'Enterria, T. Galatyuk, T. Gehrmann, K. Kirch, U. Klein, J.-P. Lansberg, G. P. Salam, G. Schnell, J. Stachel, T. Pierog, H. Wittig, U. Wiedemann, B. Gavela, A. Zoccoli, S. Malvezzi, A. Teixeira, J. Zupan, D. Aloni, A. Ceccucci, A. Dery, M. Dine, S. Fajfer, S. Gori, G. Hiller, G. Isidori, Y. Kuno, A. Lusiani, Y. Nir, M.-H. Schune, M. Sozzi, S. Paul, C. Pena, S. Bentvelsen, M. Zito, A. De Roeck, T. Schwetz, B. Fleming, F. Halzen, A. Haungs, M. Kowalski, S. Mertens, M. Mezzetto, S. Pascoli, B. Sathyaprakash, N. Serra, G. F. Giudice, P. Sphicas, J. Alcaraz Maestre, C. Doglioni, G. Lanfranchi, M. D'Onofrio, M. McCullough, G. Perez, P. Roloff, V. Sanz, A. Weiler, A. Wulzer, S. Asai, M. Carena, B. Döbrich, J. Jaeckel, G. Krnjaic, J. Monroe, K. Petridis, C. Weniger, C. Biscari, L. Rivkin, P. Burrows, F. Zimmermann, M. Benedikt, P. Campana, E. Gschwendtner, E. Jensen, M. Lamont, W. Leemans, L. Rossi, D. Schulte, M. Seidel, V. Shiltsev, S. Stapnes, A. Yamamoto, X. Lou, B. Vachon, R. Jones, E. Leogrande, I. Bird, S. Campana, A. Cattai, D. Contardo, C. Da Via, F. Forti, M. Girone, M. Kasemann, L. Linssen, F. Sefkow, G. Stewart, H. Abramowicz, and R. Forty, "Physics Briefing Book: Input for the European Strategy for Particle Physics Update 2020," Tech. Rep. CERN-ESU-004, Geneva, Oct, 2019. arXiv:1910.11775. http://cds.cern.ch/record/2691414. 254 p.

[401] R. K. Ellis *et al.*, "Physics Briefing Book: Input for the European Strategy for Particle Physics Update 2020," arXiv:1910.11775 [hep-ex].

[402] D. Buttazzo, R. Franceschini, and A. Wulzer, "Two Paths Towards Precision at a Very High Energy Lepton Collider," *JHEP* **05** (2021) 219, arXiv:2012.11555 [hep-ph].

[403] P. Draper and H. Rzehak, "A Review of Higgs Mass Calculations in Supersymmetric Models," *Phys. Rept.* **619** (2016) 1–24, arXiv:1601.01890 [hep-ph].

[404] K. Harigaya, K. Ichikawa, A. Kundu, S. Matsumoto, and S. Shirai, "Indirect Probe of Electroweak-Interacting Particles at Future Lepton Colliders," *JHEP* **09** (2015) 105, arXiv:1504.03402 [hep-ph].

[405] **ATLAS** Collaboration, "Snowmass White Paper Contribution: Physics with the Phase-2 ATLAS and CMS Detectors,".

[406] B. A. Dobrescu and F. Yu, "Coupling-Mass Mapping of Dijet Peak Searches," *Phys. Rev. D* **88** no. 3, (2013) 035021, arXiv:1306.2629 [hep-ph]. [Erratum: Phys.Rev.D 90, 079901 (2014)].

[407] B. A. Dobrescu and F. Yu, "Dijet and electroweak limits on a Z' boson coupled to quarks," arXiv:2112.05392 [hep-ph].

[408] C. Aime *et al.*, "Muon Collider Physics Summary," arXiv:2203.07256 [hep-ph].

[409] T. Han, P. Langacker, Z. Liu, and L.-T. Wang, "Diagnosis of a New Neutral Gauge Boson at the LHC and ILC for Snowmass 2013," arXiv:1308.2738 [hep-ph].

[410] J. de Blas, Y. Du, C. Grojean, J. Gu, V. Miralles, M. E. Peskin, J. Tian, M. Vos, and E. Vryonidou, "Global SMEFT Fits at Future Colliders," in *2022 Snowmass Summer Study*. 6, 2022. arXiv:2206.08326 [hep-ph].

[411] R. M. Harris, E. G. Guler, and Y. Guler, "Sensitivity to Dijet Resonances at Proton-Proton Colliders," in *2022 Snowmass Summer Study*. 2, 2022. arXiv:2202.03389 [hep-ex].

[412] **ATLAS** Collaboration, "Prospects for searches for heavy Z' and W' bosons in fermionic final states with the ATLAS experiment at the HL-LHC,".

[413] **CMS** Collaboration, "Sensitivity projections for a search for new phenomena at high dilepton mass for the LHC Run 3 and the HL-LHC,".

[414] T. Suehara, "Two-fermion final states at International Linear Collider," in *2022 Snowmass Summer Study*. 3, 2022. arXiv:2203.07272 [hep-ph].

[415] C. Helsens, D. Jamin, M. L. Mangano, T. G. Rizzo, and M. Selvaggi, "Heavy resonances at energy-frontier hadron colliders," *Eur. Phys. J. C* **79** (2019) 569, arXiv:1902.11217 [hep-ph].

[416] T. Han, T. Li, and X. Wang, "Axion-Like Particles at High Energy Muon Colliders – A White paper for Snowmass 2021," in *2022 Snowmass Summer Study*. 3, 2022. arXiv:2203.05484 [hep-ph].

[417] A. Hook, S. Kumar, Z. Liu, and R. Sundrum, "High Quality QCD Axion and the LHC," *Phys. Rev. Lett.* **124** no. 22, (2020) 221801, arXiv:1911.12364 [hep-ph].

[418] L. Di Luzio, M. Giannotti, E. Nardi, and L. Visinelli, "The landscape of QCD axion models," *Phys. Rept.* **870** (2020) 1–117, arXiv:2003.01100 [hep-ph].

[419] K. J. Kelly, S. Kumar, and Z. Liu, "Heavy axion opportunities at the DUNE near detector," *Phys. Rev. D* **103** no. 9, (2021) 095002, arXiv:2011.05995 [hep-ph].

[420] P. Agrawal *et al.*, "Feebly-interacting particles: FIPs 2020 workshop report," *Eur. Phys. J. C* **81** no. 11, (2021) 1015, arXiv:2102.12143 [hep-ph].

[421] E. Gurpinar Guler, Y. Guler, and R. M. Harris, "Mass distributions of dijet resonances from excited quarks at proton-proton colliders," arXiv:2205.02781 [hep-ph].

[422] T. Han, S. Mukhopadhyay, and X. Wang, "Electroweak Dark Matter at Future Hadron Colliders," *Phys. Rev. D* **98** no. 3, (2018) 035026, arXiv:1805.00015 [hep-ph].

[423] J. F. Klamka, "The CLIC potential for new physics," Tech. Rep. CLICdp-Conf-2021-009, CERN, Geneva, Nov, 2021. https://cds.cern.ch/record/2790402/.

[424] M. T. N. n. Pardo de Vera, M. Berggren, and J. List, "Chargino production at the ILC," in *International Workshop on Future Linear Colliders*. 2, 2020. arXiv:2002.01239 [hep-ph].

[425] M. Saito, R. Sawada, K. Terashi, and S. Asai, "Discovery reach for wino and higgsino dark matter with a disappearing track signature at a 100 TeV *pp* collider," *Eur. Phys. J. C* **79** no. 6, (2019) 469, arXiv:1901.02987 [hep-ph].

[426] R. Capdevilla, F. Meloni, R. Simoniello, and J. Zurita, "Hunting wino and higgsino dark matter at the muon collider with disappearing tracks," *JHEP* **06** (2021) 133, arXiv:2102.11292 [hep-ph].

[427] **CHARM** Collaboration, F. Bergsma *et al.*, "A Search for Decays of Heavy Neutrinos in the Mass Range 0.5-GeV to 2.8-GeV," *Phys. Lett. B* **166** (1986) 473–478.

[428] R. Abela, M. Daum, G. H. Eaton, R. Frosch, B. Jost, P. R. Kettle, and E. Steiner, "Search for an Admixture of Heavy Neutrino in Pion Decay," *Phys. Lett. B* **105** (1981) 263–266. [Erratum: Phys.Lett.B 106, 513 (1981)].

[429] T. Yamazaki *et al.*, "Search for Heavy Neutrinos in Kaon Decay," *Conf. Proc. C* **840719** (1984) 262.

[430] **E949** Collaboration, A. V. Artamonov *et al.*, "Search for heavy neutrinos in $K^+ \to \mu^+ \nu_H$ decays," *Phys. Rev. D* **91** no. 5, (2015) 052001, arXiv:1411.3963 [hep-ex]. [Erratum: Phys.Rev.D 91, 059903 (2015)].

[431] G. Bernardi *et al.*, "FURTHER LIMITS ON HEAVY NEUTRINO COUPLINGS," *Phys. Lett. B* **203** (1988) 332–334.

[432] **NuTeV, E815** Collaboration, A. Vaitaitis *et al.*, "Search for neutral heavy leptons in a high-energy neutrino beam," *Phys. Rev. Lett.* **83** (1999) 4943–4946, arXiv:hep-ex/9908011.

[433] A. G. Vaitaitis, *Search for neutral heavy leptons in a high-energy neutrino beam*. PhD thesis, Columbia U., 2000.

[434] **CMS** Collaboration, A. M. Sirunyan *et al.*, "Search for heavy neutral leptons in events with three charged leptons in proton-proton collisions at $\sqrt{s} = 13$ TeV," *Phys. Rev. Lett.* **120** no. 22, (2018) 221801, arXiv:1802.02965 [hep-ex].

[435] **DELPHI** Collaboration, P. Abreu *et al.*, "Search for neutral heavy leptons produced in Z decays," *Z. Phys. C* **74** (1997) 57–71. [Erratum: Z.Phys.C 75, 580 (1997)].

[436] **ATLAS** Collaboration, G. Aad *et al.*, "Search for heavy neutral leptons in decays of W bosons produced in 13 TeV pp collisions using prompt and displaced signatures with the ATLAS detector," *JHEP* **10** (2019) 265, arXiv:1905.09787 [hep-ex].

[437] **CMS** Collaboration, A. Tumasyan *et al.*, "Search for long-lived heavy neutral leptons with displaced vertices in proton-proton collisions at $\sqrt{s}$ =13 TeV," arXiv:2201.05578 [hep-ex].

[438] E. Izaguirre and B. Shuve, "Multilepton and Lepton Jet Probes of Sub-Weak-Scale Right-Handed Neutrinos," *Phys. Rev. D* **91** no. 9, (2015) 093010, arXiv:1504.02470 [hep-ph].

[439] M. Drewes and J. Hajer, "Heavy Neutrinos in displaced vertex searches at the LHC and HL-LHC," *JHEP* **02** (2020) 070, arXiv:1903.06100 [hep-ph].

[440] S. Pascoli, R. Ruiz, and C. Weiland, "Heavy neutrinos with dynamic jet vetoes: multilepton searches at $\sqrt{s} = 14$, 27, and 100 TeV," *JHEP* **06** (2019) 049, arXiv:1812.08750 [hep-ph].

[441] M. Drewes, J. Hajer, J. Klaric, and G. Lanfranchi, "NA62 sensitivity to heavy neutral leptons in the low scale seesaw model," *JHEP* **07** (2018) 105, arXiv:1801.04207 [hep-ph].

[442] P. Ballett, T. Boschi, and S. Pascoli, "Heavy Neutral Leptons from low-scale seesaws at the DUNE Near Detector," *JHEP* **03** (2020) 111, arXiv:1905.00284 [hep-ph].

[443] **FASER** Collaboration, A. Ariga *et al.*, "FASER's physics reach for long-lived particles," *Phys. Rev. D* **99** no. 9, (2019) 095011, arXiv:1811.12522 [hep-ph].

[444] **SHiP** Collaboration, C. Ahdida *et al.*, "Sensitivity of the SHiP experiment to Heavy Neutral Leptons," *JHEP* **04** (2019) 077, arXiv:1811.00930 [hep-ph].

[445] D. Gorbunov, I. Krasnov, Y. Kudenko, and S. Suvorov, "Heavy Neutral Leptons from kaon decays in the SHiP experiment," *Phys. Lett. B* **810** (2020) 135817, arXiv:2004.07974 [hep-ph].

[446] D. Curtin *et al.*, "Long-Lived Particles at the Energy Frontier: The MATHUSLA Physics Case," *Rept. Prog. Phys.* **82** no. 11, (2019) 116201, arXiv:1806.07396 [hep-ph].

[447] G. Aielli *et al.*, "Expression of interest for the CODEX-b detector," *Eur. Phys. J. C* **80** no. 12, (2020) 1177, arXiv:1911.00481 [hep-ex].

[448] J. Alimena *et al.*, "Searches for Long-Lived Particles at the Future FCC-ee," arXiv:2203.05502 [hep-ex].

[449] Y.-F. Shen, J.-N. Ding, and Q. Qin, "Monojet search for heavy neutrinos at future Z-factories," *Eur. Phys. J. C* **82** no. 5, (2022) 398, arXiv:2201.05831 [hep-ph].

[450] S. Bay Nielsen, "Prospects of Sterile Neutrino Search with the FCC-ee," Master's thesis, Copenhagen U., 2017.

[451] S. Antusch, E. Cazzato, and O. Fischer, "Sterile neutrino searches at future e^-e^+, pp, and e^-p colliders," *Int. J. Mod. Phys. A* **32** no. 14, (2017) 1750078, arXiv:1612.02728 [hep-ph].

[452] K. Mekala, J. Reuter, and A. F. Żarnecki, "Heavy neutrinos at future linear e^+e^- colliders," *JHEP* **06** (2022) 010, arXiv:2202.06703 [hep-ph].

[453] S. Antusch, E. Cazzato, and O. Fischer, "Displaced vertex searches for sterile neutrinos at future lepton colliders," *JHEP* **12** (2016) 007, arXiv:1604.02420 [hep-ph].

[454] S. Antusch, O. Fischer, and A. Hammad, "Lepton-Trijet and Displaced Vertex Searches for Heavy Neutrinos at Future Electron-Proton Colliders," *JHEP* **03** (2020) 110, arXiv:1908.02852 [hep-ph].

[455] P. Li, Z. Liu, and F.-F. Lyu, "Heavy Neutral Leptons at Muon Colliders," arXiv:in progress [hep-ph].

[456] I. Esteban, M. C. Gonzalez-Garcia, M. Maltoni, T. Schwetz, and A. Zhou, "The fate of hints: updated global analysis of three-flavor neutrino oscillations," *JHEP* **09** (2020) 178, arXiv:2007.14792 [hep-ph].

[457] L. Canetti, M. Drewes, and M. Shaposhnikov, "Matter and Antimatter in the Universe," *New J. Phys.* **14** (2012) 095012, arXiv:1204.4186 [hep-ph].

[458] E. K. Akhmedov, V. A. Rubakov, and A. Y. Smirnov, "Baryogenesis via neutrino oscillations," *Phys. Rev. Lett.* **81** (1998) 1359–1362, arXiv:hep-ph/9803255.

[459] T. Asaka and M. Shaposhnikov, "The νMSM, dark matter and baryon asymmetry of the universe," *Phys. Lett. B* **620** (2005) 17–26, arXiv:hep-ph/0505013.

[460] A. Pilaftsis and T. E. J. Underwood, "Resonant leptogenesis," *Nucl. Phys. B* **692** (2004) 303–345, arXiv:hep-ph/0309342.

[461] M. Drewes, Y. Georis, and J. Klarić, "Mapping the Viable Parameter Space for Testable Leptogenesis," *Phys. Rev. Lett.* **128** no. 5, (2022) 051801, arXiv:2106.16226 [hep-ph].

[462] N. Sabti, A. Magalich, and A. Filimonova, "An Extended Analysis of Heavy Neutral Leptons during Big Bang Nucleosynthesis," *JCAP* **11** (2020) 056, arXiv:2006.07387 [hep-ph].

[463] A. Boyarsky, M. Ovchynnikov, O. Ruchayskiy, and V. Syvolap, "Improved big bang nucleosynthesis constraints on heavy neutral leptons," *Phys. Rev. D* **104** no. 2, (2021) 023517, arXiv:2008.00749 [hep-ph].

[464] A. M. Abdullahi *et al.*, "The Present and Future Status of Heavy Neutral Leptons," in *2022 Snowmass Summer Study*. 3, 2022. arXiv:2203.08039 [hep-ph].

[465] A. M. Abdullahi *et al.*, "The Present and Future Status of Heavy Neutral Leptons," arXiv:2203.08039 [hep-ph].

[466] G. Jungman, M. Kamionkowski, and K. Griest, "Supersymmetric dark matter," *Phys. Rept.* **267** (1996) 195–373, arXiv:hep-ph/9506380.

[467] M. Cirelli, N. Fornengo, and A. Strumia, "Minimal dark matter," *Nucl. Phys. B* **753** (2006) 178–194, arXiv:hep-ph/0512090.

[468] M. Cirelli and A. Strumia, "Minimal Dark Matter: Model and results," *New J. Phys.* **11** (2009) 105005, arXiv:0903.3381 [hep-ph].

[469] **Planck** Collaboration, N. Aghanim *et al.*, "Planck 2018 results. VI. Cosmological parameters," *Astron. Astrophys.* **641** (2020) A6, arXiv:1807.06209 [astro-ph.CO]. [Erratum: Astron.Astrophys. 652, C4 (2021)].

[470] K. M. Belotsky, M. Y. Khlopov, S. V. Legonkov, and K. I. Shibaev, "Effects of new long-range interaction: Recombination of relic heavy neutrinos and antineutrinos," *Grav. Cosmol.* **11** (2005) 27–33, arXiv:astro-ph/0504621.

[471] J. Hisano, S. Matsumoto, M. Nagai, O. Saito, and M. Senami, "Non-perturbative effect on thermal relic abundance of dark matter," *Phys. Lett. B* **646** (2007) 34–38, arXiv:hep-ph/0610249.

[472] M. Cirelli, A. Strumia, and M. Tamburini, "Cosmology and Astrophysics of Minimal Dark Matter," *Nucl. Phys. B* **787** (2007) 152–175, arXiv:0706.4071 [hep-ph].

[473] H. An, M. B. Wise, and Y. Zhang, "Effects of Bound States on Dark Matter Annihilation," *Phys. Rev. D* **93** no. 11, (2016) 115020, arXiv:1604.01776 [hep-ph].

[474] A. Mitridate, M. Redi, J. Smirnov, and A. Strumia, "Cosmological Implications of Dark Matter Bound States," *JCAP* **05** (2017) 006, arXiv:1702.01141 [hep-ph].

[475] E. Del Nobile, M. Nardecchia, and P. Panci, "Millicharge or Decay: A Critical Take on Minimal Dark Matter," *JCAP* **04** (2016) 048, arXiv:1512.05353 [hep-ph].

[476] T. Han, Z. Liu, L.-T. Wang, and X. Wang, "WIMPs at High Energy Muon Colliders," *Phys. Rev. D* **103** no. 7, (2021) 075004, arXiv:2009.11287 [hep-ph].

[477] T. Han, Z. Liu, L.-T. Wang, and X. Wang, "WIMP Dark Matter at High Energy Muon Colliders −A White Paper for Snowmass 2021," in *2022 Snowmass Summer Study*. 3, 2022. arXiv:2203.07351 [hep-ph].

[478] S. Bottaro, A. Strumia, and N. Vignaroli, "Minimal Dark Matter bound states at future colliders," *JHEP* **06** (2021) 143, arXiv:2103.12766 [hep-ph].

[479] S. Bottaro, D. Buttazzo, M. Costa, R. Franceschini, P. Panci, D. Redigolo, and L. Vittorio, "Closing the window on WIMP Dark Matter," *Eur. Phys. J. C* **82** no. 1, (2022) 31, arXiv:2107.09688 [hep-ph].

[480] S. Bottaro, D. Buttazzo, M. Costa, R. Franceschini, P. Panci, D. Redigolo, and L. Vittorio, "The last Complex WIMPs standing," arXiv:2205.04486 [hep-ph].

[481] K. Black, T. Bose, Y. Chen, S. Dasu, H. Jia, D. Pinna, V. Sharma, N. Venkatasubramanian, and C. Vuosalo, "Prospects for Heavy WIMP Dark Matter Searches at Muon Colliders," in *2022 Snowmass Summer Study*. 5, 2022. arXiv:2205.10404 [hep-ex].

[482] M. Low and L.-T. Wang, "Neutralino dark matter at 14 TeV and 100 TeV," *JHEP* **08** (2014) 161, arXiv:1404.0682 [hep-ph].

[483] X. Cid Vidal *et al.*, "Report from Working Group 3: Beyond the Standard Model physics at the HL-LHC and HE-LHC," *CERN Yellow Rep. Monogr.* **7** (2019) 585–865, arXiv:1812.07831 [hep-ph].

[484] **CMS** Collaboration, "Search for dark matter in final states with a Higgs boson decaying to a pair of b-jets and missing transverse momentum at the HL-LHC,".

[485] J. Kalinowski, T. Robens, and A. F. Zarnecki, "New Physics with missing energy at future lepton colliders - Snowmass White Paper," in *2022 Snowmass Summer Study*. 3, 2022. arXiv:2203.07913 [hep-ph].

[486] D. Abercrombie *et al.*, "Dark Matter benchmark models for early LHC Run-2 Searches: Report of the ATLAS/CMS Dark Matter Forum," *Phys. Dark Univ.* **27** (2020) 100371, arXiv:1507.00966 [hep-ex].

[487] A. Boveia *et al.*, "Recommendations on presenting LHC searches for missing transverse energy signals using simplified s-channel models of dark matter," *Phys. Dark Univ.* **27** (2020) 100365, arXiv:1603.04156 [hep-ex].

[488] A. Albert *et al.*, "Recommendations of the LHC Dark Matter Working Group: Comparing LHC searches for dark matter mediators in visible and invisible decay channels and calculations of the thermal relic density," *Phys. Dark Univ.* **26** (2019) 100377, arXiv:1703.05703 [hep-ex].

[489] A. Albert *et al.*, "Displaying dark matter constraints from colliders with varying simplified model parameters," arXiv:2203.12035 [hep-ph].

[490] A. Boveia *et al.*, "Summarizing experimental sensitivities of collider experiments to dark matter models and comparison to other experiments," in *2022 Snowmass Summer Study*. 6, 2022. arXiv:2206.03456 [hep-ph].

[491] **CMS** Collaboration, V. Khachatryan *et al.*, "Search for narrow resonances in dijet final states at $\sqrt{s} = 8$ TeV with the novel CMS technique of data scouting," *Phys. Rev. Lett.* **117** no. 3, (2016) 031802, arXiv:1604.08907 [hep-ex].

[492] **ATLAS** Collaboration, M. Aaboud *et al.*, "Search for low-mass dijet resonances using trigger-level jets with the ATLAS detector in pp collisions at $\sqrt{s} = 13$ TeV," *Phys. Rev. Lett.* **121** no. 8, (2018) 081801, arXiv:1804.03496 [hep-ex].

[493] B. Batell, A. Freitas, A. Ismail, and D. Mckeen, "Probing Light Dark Matter with a Hadrophilic Scalar Mediator," *Phys. Rev. D* **100** no. 9, (2019) 095020, arXiv:1812.05103 [hep-ph].

[494] B. Batell, A. Freitas, A. Ismail, D. McKeen, and M. Rai, "Renormalizable models of flavor-specific scalars," *Phys. Rev. D* **104** no. 11, (2021) 115032, arXiv:2107.08059 [hep-ph].

[495] T. G. Rizzo, "Portal Matter and Dark Sector Phenomenology at Colliders," in *2022 Snowmass Summer Study*. 2, 2022. arXiv:2202.02222 [hep-ph].

[496] D. Egana-Ugrinovic, S. Homiller, and P. Meade, "Light Scalars and the Koto Anomaly," *Phys. Rev. Lett.* **124** no. 19, (2020) 191801, arXiv:1911.10203 [hep-ph].

[497] M. J. Strassler and K. M. Zurek, "Echoes of a hidden valley at hadron colliders," *Phys. Lett. B* **651** (2007) 374–379, arXiv:hep-ph/0604261.

[498] K. R. Dienes and B. Thomas, "More is Different: Non-Minimal Dark Sectors and their Implications for Particle Physics, Astrophysics, and Cosmology - 13 Take-Away Lessons for Snowmass 2021," in *2022 Snowmass Summer Study*. 3, 2022. arXiv:2203.17258 [hep-ph].

[499] E. Bernreuther, F. Kahlhoefer, M. Krämer, and P. Tunney, "Strongly interacting dark sectors in the early Universe and at the LHC through a simplified portal," *JHEP* **01** (2020) 162, arXiv:1907.04346 [hep-ph].

[500] J. M. Cline, W. Huang, and G. D. Moore, "Challenges for models with composite states," *Phys. Rev. D* **94** no. 5, (2016) 055029, arXiv:1607.07865 [hep-ph].

[501] H. Mies, C. Scherb, and P. Schwaller, "Collider constraints on dark mediators," *JHEP* **04** (2021) 049, arXiv:2011.13990 [hep-ph].

[502] Y. Bai and P. Schwaller, "Scale of dark QCD," *Phys. Rev. D* **89** no. 6, (2014) 063522, arXiv:1306.4676 [hep-ph].

[503] G. Albouy *et al.*, "Theory, phenomenology, and experimental avenues for dark showers: a Snowmass 2021 report," arXiv:2203.09503 [hep-ph].

[504] S. Kulkarni, A. Maas, S. Mee, M. Nikolic, J. Pradler, and F. Zierler, "Low-energy effective description of dark $Sp(4)$ theories," arXiv:2202.05191 [hep-ph].

[505] P. Asadi, E. D. Kramer, E. Kuflik, G. W. Ridgway, T. R. Slatyer, and J. Smirnov, "Accidentally Asymmetric Dark Matter," *Phys. Rev. Lett.* **127** no. 21, (2021) 211101, arXiv:2103.09822 [hep-ph].

[506] B. Batell, J. L. Feng, and S. Trojanowski, "Detecting Dark Matter with Far-Forward Emulsion and Liquid Argon Detectors at the LHC," *Phys. Rev. D* **103** no. 7, (2021) 075023, arXiv:2101.10338 [hep-ph].

[507] S. Foroughi-Abari, F. Kling, and Y.-D. Tsai, "Looking forward to millicharged dark sectors at the LHC," *Phys. Rev. D* **104** no. 3, (2021) 035014, arXiv:2010.07941 [hep-ph].

[508] B. Fleming, I. Shipsey, M. Demarteau, J. Fast, *et al.*, "Basic research needs for high energy physics detector research and development: Report of the office of science workshop on basic research needs for hep detector research and development: December 11-14, 2019," (12, 2019) . https://www.osti.gov/biblio/1659761.

[509] **Muon Collider** Collaboration, N. Bartosik *et al.*, "Simulated Detector Performance at the Muon Collider," in *2022 Snowmass Summer Study*. 3, 2022. arXiv:2203.07964 [hep-ex].

[510] M. R. Hoeferkamp *et al.*, "Novel Sensors for Particle Tracking: a Contribution to the Snowmass Community Planning Exercise of 2021," arXiv:2202.11828 [physics.ins-det].

[511] C. Vernieri *et al.*, "Monolithic Active Pixel Sensors on CMOS technologies," in *2022 Snowmass Summer Study*. 3, 2022. arXiv:2203.07626 [physics.ins-det].

[512] P. Barletta, M. Cerullo, C. Haber, S. E. Holland, J. Muth, and B. Sekely, "Fast Timing With Silicon Carbide Low Gain Avalanche Detectors," arXiv:2203.08554 [physics.ins-det].

[513] I. Pezzotti *et al.*, "Dual-Readout Calorimetry for Future Experiments Probing Fundamental Physics," arXiv:2203.04312 [physics.ins-det].

[514] S. Jindariani *et al.*, "Promising Technologies and R&D Directions for the Future Muon Collider Detectors," in *2022 Snowmass Summer Study*. 3, 2022. arXiv:2203.07224 [physics.ins-det].

[515] D. Acosta *et al.*, "Review of opportunities for new long-lived particle triggers in Run 3 of the Large Hadron Collider," arXiv:2110.14675 [hep-ex].

[516] A. V. Kotwal, "A fast method for particle tracking and triggering using small-radius silicon detectors," *Nucl. Instrum. Meth. A* **957** (2020) 163427, arXiv:1910.14149 [physics.ins-det].

[517] S. V. Chekanov, A. V. Kotwal, C. H. Yeh, and S. S. Yu, "Physics potential of timing layers in future collider detectors," *JINST* **15** no. 09, (2020) P09021, arXiv:2005.05221 [physics.ins-det].

[518] D. Ally, L. Carpenter, T. Holmes, L. Lee, and P. Wagenknecht, "Strategies for Beam-Induced Background Reduction at Muon Colliders," arXiv:2203.06773 [physics.ins-det].

[519] J. M. Campbell *et al.*, "Event Generators for High-Energy Physics Experiments," in *2022 Snowmass Summer Study*. 3, 2022. arXiv:2203.11110 [hep-ph].

[520] "MC4EIC: Monte Carlo Event Simulation for the EIC.". https://indico.bnl.gov/event/13298.

[521] S. Badger *et al.*, "Machine Learning and LHC Event Generation," arXiv:2203.07460 [hep-ph].

[522] **ATLAS** Collaboration, "ATLAS HL-LHC Computing Conceptual Design Report,".

[523] CMS Collaboration, "Offline and Computing Public Results, Approved HL-LHC resource projections (November 2021)." https://twiki.cern.ch/twiki/bin/view/CMSPublic/CMSOfflineComputingResults.

[524] **HSF Physics Event Generator WG** Collaboration, S. Amoroso *et al.*, "Challenges in Monte Carlo Event Generator Software for High-Luminosity LHC," *Comput. Softw. Big Sci.* **5** no. 1, (2021) 12, arXiv:2004.13687 [hep-ph].

[525] **HSF Physics Event Generator WG** Collaboration, E. Yazgan *et al.*, "HL-LHC Computing Review Stage-2, Common Software Projects: Event Generators," arXiv:2109.14938 [hep-ph].

[526] EF community, "Comments on EF vision," 2022. https://snowmass21.org/_media/energy/efcommunityinput.pdf.